UiT The Arctic University of Norway

Faculty of Biosciences, Fisheries and Economics

Department of Arctic and Marine Biology

Microbial diversity and ecology in the coastal Arctic seasonal ice zone

Diversity and interactions of bacteria, archaea, and algae in Svalbard fjords and impacts of terrestrial freshwater inputs

Tobias Reiner Vonnahme

A dissertation for the degree of Philosophiae Doctor – November 2020

“Nothing is too wonderful to be true if it be consistent with the laws of nature.”

— Michael Faraday

Preface

"Shall we educate ourselves in what is known, and then casting away all we have acquired, turn to ignorance for aid to guide us among the unknown?" (**Michael Faraday**)

This quote summarizes what I see as fascinating in natural sciences. We start learning how the world works, but the more we learn the more we realize how much we do not know. At some point, we even realize that what we think we know might not be true. This is where I see the role of science starting. Besides curiosity and knowledge, I see some stubbornness and an open mind as crucial attributes for a scientist. On a daily basis, using the knowledge we have to find gaps worth exploring is important, but only after momentarily forgetting what we believe to be true and exploring hypotheses conflicting with everything we learned, can substantial progress be possible. This may eventually lead to paradigm changes, which bring knowledge forward. Thus, most motivating for me are discussions with colleagues who do not believe that my hypotheses are valid, or telling me that "this is not how it works". I believe that it is not only important to create new knowledge, but also to convey the knowledge to non-experts in the field. Simply bridging different disciplines may already allow changing the knowledge in people's minds and lead to new discoveries.

With a background in marine microbiology, my first realization when coming to Tromsø was the dismissal of bacteria and archaea when discussing biogeochemical cycles and food webs. In strong contrast to my previous institute, it appeared that the Arctic is driven by zooplankton and algae with little importance of anything smaller. Thus, one major aim of my time in Tromsø was to change this perception by giving talks about the importance of marine bacteria and eventually showing the importance of bacteria-algae interactions via modelling approaches. Further on, I started working on subglacial upwelling, a novel and exciting topic developing rapidly during my time in Tromsø. Ignorant of the knowledge that substantial subglacial upwelling requires deep tidewater glacier fronts and glacial surface melt (as I was told later on), I did my first fieldwork in winter in a sea ice-covered fjord affected by a glacier barely reaching the fjord. If working on subglacial upwelling in a system where subglacial upwelling should not have any substantial effects on the fjord ecology had any meaning, can be decided after reading paper IV. Eventually, I was introduced to the FreshFate project working on land-ocean interactions, another example where bridging disciplines was crucial to making sense of our findings and for understanding microbial and biogeochemical dynamics in coastal systems.

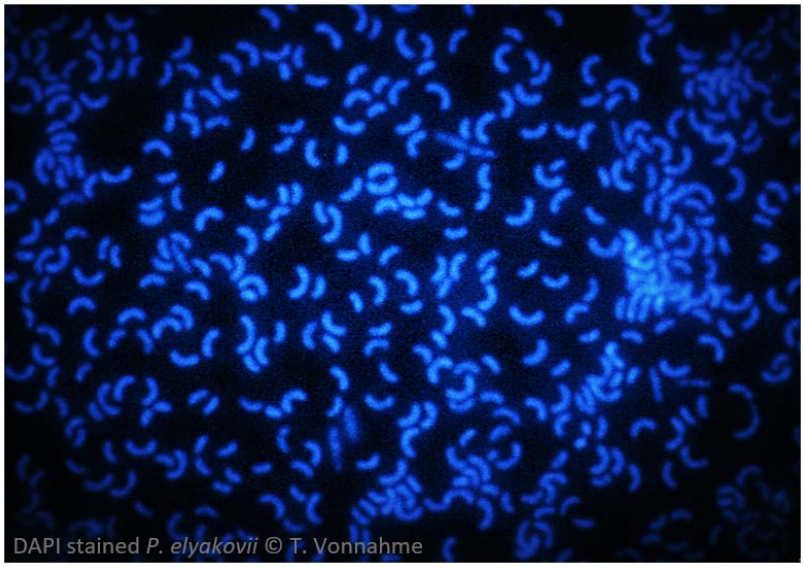

More than fifty billion (50000000000) bacteria and archaea

gave their lives for this PhD thesis.

Summary. The Arctic sea ice zone is one of the fastest changing systems worldwide due to climate change. The ocean is warming, leading to decreasing **sea ice** thickness and extent, with direct implications for ocean stratification, mixing, and primary production. On land, glaciers are melting, permafrost is thawing, and **river runoff** is increasing which is ultimately also affecting the Arctic Ocean. In fact, the Arctic Ocean contributes only 1% of the ocean volume while receiving 10% of the global riverine inputs, showing that the Arctic is highly influenced by terrestrial inputs. Together with freshwater, large amounts of dissolved organic matter (DOM), nutrients, and sediments are transported into the ocean, though amounts vary considerably seasonally. Melting **glaciers** can contribute additional freshwater, often rich in silicate and iron, with the potential to increase primary production via subglacial upwelling at marine terminating glaciers. Overall, terrestrial freshwater inputs can have strong impacts on the microbial food web; bacteria and archaea can feed on the organic matter, algae can benefit from nutrient inputs or, inversely, be limited by light absorbing sediments. At the same time, marine microbes are crucial for the entire food web and **carbon cycle**. Marine **algae** are the main source of organic matter in the oceans contributing to about 50% of the global primary production. About 50% of this organic carbon is channeled through heterotrophic **bacteria** and **archaea.** Phytoplankton blooms trigger reoccurring bacterial succession patterns of diverse communities capable of degrading various organic compounds. Nutrients (e.g. ammonium) can be recycled during the degradation process, fueling **regenerated primary production**, which may, at times, contribute up to 95% of the total production. Overall, terrestrial inputs have strong impacts on Arctic marine systems where bacteria and algae are tightly connected through a variety of interactions. The aims of this PhD thesis are i) to summarize the current knowledge about microbial ecology in the Arctic seasonal ice zone, ii) to study the effects of **terrestrial inputs** from rivers and glaciers on the microbial food web over different seasons, and iii) to dive into **algae-bacteria interactions** with a focus on the importance of regenerated production.

Our main study sites were located in **Svalbard fjord** systems, which are affected by land- and marine-terminating glaciers and some tundra-dominated catchments. In Billefjorden, we studied the impacts of subglacial upwelling on the carbon cycle and microbial communities. It had been suggested, that ecosystems in sea ice covered fjords in winter/spring are not influenced by **subglacial upwelling** processes. However, we were able to provide evidence that subglacial upwelling is present, leading to increased surface water nutrients, a stratified surface layer, and

brackish sea ice. We provided also first data, showing that winter/spring subglacial upwelling has substantial consequences for microbial communities and carbon cycling. Microbial communities were significantly different at the tidewater glacier front compared to a sea-ice edge reference site. The upwelling influenced ice algal community (dominated by cryptophytes and *Leptocylindrus sp.*) differed substantially from those in typical first-year ice systems. The phytoplankton primary production was two orders of magnitude higher at the glacier site compared to the reference site, due to upwelling related nutrient inputs (approx. 3-fold) and potentially also stratification and a thinner snow cover. In an Isfjorden system study, we investigated the impacts of **river runoff** during the spring freshet and late summer on bacterial and archaeal communities with detailed considerations of environmental drivers. We found significant differences between bacterial communities during the spring freshet and late summer, mainly controlled by the concentrations and properties of DOM, nutrient concentrations, and fjord hydrography. Combined with the Billefjorden study, we found a distinct bacterial succession following the algal spring bloom with similar patterns and taxa observed in other northern marine systems. We performed an experimental study using **cultures** of spring bloom algae (*Chaetoceros socialis*) and associated bacteria from Van Mijenfjorden and recreated major algal spring bloom dynamics, starting with the exponential phase mostly driven by new production leading into the stationary phase with growth maintained by regenerated production also under silicate limitations. I used the experimental data to extend a commonly used dynamic algal growth **model** improving the modeling of multi-nutrient limitations and bacterial remineralization and discussed the importance of these dynamics in ecosystem scale models. In conclusion, the work within this thesis demonstrates that photo- and heterotrophic microbial communities and functions are highly regulated by environmental constraints in the coastal seasonal ice zones, which need to be considered when evaluating climate change impacts in the Arctic.

Sammendrag. Den arktiske issonen er en av de raskest skiftende systemene på grunn av klimaendringer. Klimaet og havet varmes opp, og dette fører til redusert havistykkelse og -utbredelse, med direkte påvirkning for stratifisering, marin blanding, og primærproduksjon. På land smelter isbreer, permafrosten tiner, og elvavrenning øker, som til slutt også påvirker Polhavet. Polhavet har bare 1% av havvolumet mens det mottar 10% av globale elveinngangen, som viser at Polhavet er sterkt påvirket av terrestriske innganger. I tillegg til ferskvann importeres store mengder oppløst organisk materialer (DOM), næringsstoffer og sedimenter til havet med store sesongavhengige variasjoner. Smeltevannsutslipp under havoverflaten ved marinterminerende brefronter kan bidra ytterligere tilførsel av ferskvann som ofte er rikt på silikat og jern, noe som kan øke primærproduksjonen i området. Samlet sett kan terrestrisk ferskvannstilførsel ha sterk innvirkning på det mikrobielle næringsnettet; bakterier og arkea kan leve av og omdanne det organiske stoffet, alger kan dra nytte av næringstilskuddet eller være begrenset av lysabsorberende sediment. Samtidig er marine mikrober avgjørende for hele næringsnettet og karbonsyklusen. Marine alger er den viktigste kilden til organisk materiale i havet og bidrar til omtrent 50 % av den globale primærproduksjonen. Cirka 50 % av dette organiske karbonet omdannes av heterotrofiske bakterier og arkea som utløser gjentatte suksesjonsmønstre fra forskjellige organismer som kan nedbryte forskjellige organiske forbindelser. Under nedbrytingen kan næringsstoffer resirkuleres og gi næring til regenerert primærproduksjon, som noen ganger kan tilsvare opptil 95 % av den totale produksjonen. Samlet sett har terrestriske tilførsler sterk innvirkning på arktiske marine systemer der bakterier og alger er tett forbundet gjennom en rekke interaksjoner. Målet med denne doktorgradsavhandlingen er i) å oppsummere den nåværende kunnskapen om mikrobiell økologi i den arktiske issonen, ii) å studere effekten av terrestriske tilførsler fra elver og isbreer på det mikrobielle næringsnettet over forskjellige årstider, og iii) å utforske interaksjoner mellom alger og bakterier.

Våre hovedundersøkelsessteder er lokalisert i Svalbard-fjordsystemer, som er påvirket av isbreer som avsluttes på land eller i havet og noen nedslagsfelt dominert av tundra. I Billefjorden studerte vi innvirkningen av subglasial oppstrømning på karbonsyklusen og mikrobielle samfunn i og under sjøis. Vinter og vår har tidligere ikke blitt ansett som viktige for prosesser tilknyttet subglasial oppstrømning. Likevel klarte vi å vise at subglasial oppstrømning er til stede og at det fører til økt konsentrasjon av næringsstoffer, et lagdelt overflatelag, og sjøis med lav permeabilitet. Vi viste for første gang at vinter- / vår subglasial

oppstrømning har betydelige konsekvenser for mikrobielle samfunn og karbonsyklusen. Det var betydelige forskjeller i mikrobielle samfunn, spesielt i sjøis med alger som var atypiske for arktiske havisystemer (kryptofytter, *Leptocylindrus*) ved brefronten. Fytoplankton primærproduksjon ble betydelig (100 ganger) økt ved brefronten på grunn av tilskudd av næringsstoffer (ca. 3 ganger), men også på grunn av stratifisering og et tynnere snødekke. I Isfjorden-systemet studerte vi innvirkningene av avrenning fra elven i løpet av våren og på sensommeren på bakterie- og arkea samfunn, med detaljerte hensyn til miljømessige drivere, som DOM og inngang av næringssalter og fjordhydrografi. Vi fant signifikante forskjeller mellom bakteriesamfunn i løpet av våren og sensommeren, hovedsakelig kontrollert av konsentrasjonene og egenskapene til DOM, næringssaltkonsentrasjoner og fjordhydrografi. Sammen med Billefjorden-studien fant vi en tydelig bakteriesuksesjon etter våroppblomstringen med lignende mønstre og taksa observert i andre systemer. Vi fikk kulturer av våroppblomstrende alger og tilknyttede bakterier fra Van Mijenfjorden og gjenskapt våroppblomstringsdynamikk fra den eksponentielle fasen, hovedsakelig drevet av ny produksjon til den stasjonære fasen, bare opprettholdt av regenerert produksjon også under silikatbegrensninger. Vi brukte dette eksperimentet til å utvide en kjent modell for å representere begrensninger med flere næringsstoffer og bakteriell remineralisering, og for å diskutere hvor betydelig det er å inkludere disse dynamikkene i økosystemskalamodeller. Oppsummert viser arbeidet i denne oppgaven at samfunnet og funksjoner av foto- og heterotrofe mikroorganismer er sterk regulert av miljøet som DOM, næringssalter, lys, og hydrografi, som skal vurderes når man vurderer påvirkningen av klimaendringer i Arktis.

Acknowledgements

First of all, I want to thank my main supervisor Rolf Gradinger and the PIs of ArcticSIZE for giving me the opportunity to work in the seasonal ice zone with the freedom to work on any topic that I was excited about. I was able to develop and try out new methods, follow controversial ideas, and develop and test hypotheses that I was personally interested in. Besides the opportunity to do this open PhD, I am grateful for all the valuable discussions of my plans, data, and ideas with my supervisor team including Dick van Oevelen, Tron Frede Thingstad, and Geir Johnsen. Eventually, I got also enormous support from colleagues of all kind of fields helping me to discuss study designs, to analyze samples, develop new methods, discuss the data and discuss the papers. This freedom and multidisciplinary support allowed me to follow a large number of research questions and to get involved in a large number of projects, exceeding the scope of this PhD by far.

I am grateful to Amanda Poste and Maeve McGovern to include me into the TerrACE and FreshFate projects. It started with simply taking additional samples for each other and ended in a collaborative project with mutual fieldwork and exciting studies on microbial communities and activities in Isfjorden, which lead to one of the papers of this PhD. I also want to sincerely thank Lisa-Marie Delpech, a Master student that did an impressive job working on metabarcoding samples, including the implementation of a pipeline and writing up the paper. I was proud to be her supervisor. I am also thankful for the contribution of Sebastian Andersen, who will continue in the FreshFate project tackling questions that remained open, or developed during the work with Lisa-Marie.

I am very thankful to the team supporting the work on the modelling paper (paper III). The initial idea developed already during my Master in Bremen during a lab internship about dynamic phytoplankton modelling with Christoph Völker and Silke Thoms. Thanks to both I got introduced to the world of modelling with great feedback whenever I got stuck in Matlab. However, in order to go beyond reproducing published models and to develop something new, cultivation experiments were needed. Thus, I am extremely grateful to Martial Leroy who did a major part of the practical work for paper III resulting in an impressive Bachelor thesis. For analyzing the multitude of data I also want to thank Rodger Harvey for the DOC analyses, Elzbieta Anna Petelenz-Kurdziel and Ulrike Dietrich for the POC analyses, and Svein Kristiansen and Paul Dubourg for the nutrient analyses and the help with ammonium

measurements. During the final stages of the model development, I got invaluable support from Dick van Oevelen for various programming issues in R.

The Billefjorden project was one of the most exciting projects during my PhD. We developed the idea of a multidisciplinary study in a tidewater glacier influenced fjord during an algae taxonomy course in Drøbak in a team of PhD students including Christine Dybwad, Ulrike Dietrich, Fernanda de Miranda Vasconcelos, and Katharina Bading. Thanks to the Arctic Field Grant and support by the Czech Centre of Polar Ecology, we were actually able to secure funding and make this project happen. I am very grateful to everyone for this unique opportunity of being responsible of such an exciting project from the initial idea, funding applications, preparations, fieldwork, sample analyses and writing of the first manuscript. In the end, this work would not have been possible without the support of Josef Elster, Eva Hejdukova, Christine Dybwad, Ulrike Dietrich, Jan Pechar, Jiří Štojdl, Marie Šabacká, and Kjersti Kalhagen in the field; and Janne Søreide, Maja Hatlebakk, Christian Zoelly, Marek Brož, Stuart Thomson, Jason Roberts, and Tore Haukås for fieldwork preparation help.

As mentioned above, this PhD went further than the papers that are discussed in this thesis and I want to thank everyone involved. I am grateful to all co-authors of all the papers for their contributions criticisms and discussions during the preparations of the manuscripts. I also got a lot of help from many Master (Rose Marie Bank, Emma Persson, Martial Leroy, Lisa-Marie Delpech, Sebastian Andersen) and Bachelor students (Line Klausen) doing their theses with me with incredible dedication in the lab and field. I am extremely thankful for their help in the lab, interesting ideas and discussions, help in the field, and for often initiating the projects and publications of this PhD. I also acknowledge Melissa Brandner, Dolma Michellod, Gaute Lavik, Manuel Liebeke, Phillip Hach, and Claire Mourgues for the help in the lab. I am thankful for the meteorological data of Petuniabukta supplied by Kamil Laska. I also thank Julie Bitz-Thorsen and Kim Præbel for the help with the library preparation and sequencing. Finally, I thank Christiane Hassenrück and Owen Wangensteen for the help with bioinformatics and Jørn Dietze for the help with the Stallo HPC. I also want to thank Mette Marianne Svenning and Anne Grethe Hestnes for their support with the molecular work. Thanks to the crews of RV Kronprins Haakon, RV Helmer Hansen, and RV Hyas I was able to do an incredible amount of field work. I want to thank Frode Gerhardsen, who made it possible to start a time series in Ramfjorden with monthly sampling. I am grateful for every criticism and skepticism I got during my PhD, including reviewers, and colleagues after presentations, which helped to

improve my research and project designs. Since microbiology was an underrepresented field in my institute, I am grateful to the support and discussions of our small Arctic marine microbe group in the North, including Magdalena Wutkowska, Ulrike Dietrich, Brandon Hassett, and Marti Amargant.

I also want to thank the ARCTOS network for the interesting meetings and colloquia, which were extremely helpful for this PhD. Thanks to ARCTOS, I got to meet new friends and colleagues making a lot of the fieldwork easier or even possible. Thanks to the ForBIO, FILAMO, and NORBIS research schools, the APECS network, and IASC, I was able to attend exciting courses and meetings all over Norway and Europe.

Overall, this PhD was funded by the ArcticSIZE project - A research group on the productive Marginal Ice Zone at UiT (grant no. 01vm/h15). Fieldwork was funded by the individual Arctic Field Grants of the Svalbard Science forum for TV, UD, CD, and EH (project numbers: 282622 (TV, UD, CD), 282600 (TV), 296538 (EH), 281806 (UD)). The publication charges for the articles have been partly funded by a grant from the publication fund of UiT - The Arctic University of Norway and by the Alfred Wegener Institute. Additional financial support came from the TerrACE project; project number: 268458), the Fram Center Flagship “Fjord and Coast” grant (FreshFate; project number 132019), and the Svalbard Science Forum’s Arctic Field Grant (RIS number: 10914). Additional analyses were funded by individual grants allocated to Rodger Harvey, Kim Præbel, and the Max-Planck institute in Bremen.

Supervisors

Prof Dr Rolf Gradinger, Institute for Arctic and Marine Biology, UiT – The Arctic University of Norway, Tromsø, Norway

Dr Dick van Oevelen, Department of Estuarine and Delta Systems, NIOZ Royal Netherlands Institute for Sea Research, and Utrecht University, Texel, Yerseke, the Netherlands

Prof Dr Tron Frede Thingstad, Department of Biological Sciences, University of Bergen, Bergen, Norway

Prof Dr Geir Johnsen, Institute for Biology, NTNU – Norges teknisk-naturvitenskapelige universitet, Trondheim, Norway

List of papers

I) **Vonnahme, T. R.**, Dietrich, U., & Hassett, B. T. (2020). Progress in Microbial Ecology in Ice-Covered Seas. In YOUMARES 9-The Oceans: Our Research, Our Future (pp. 261-277). Springer, Cham., https://doi.org/10.1007/978-3-030-20389-4_14.

II) Delpech, L., **Vonnahme, T. R.**, McGovern, M., Gradinger, R., Præbel, K., Poste, A. (submitted). Terrestrial Inputs Shape Coastal Microbial Communities in a High Arctic Fjord (Isfjorden, Svalbard), in review by Frontiers in Microbiology.

III) **Vonnahme, T. R.**, Leroy, M., Thoms, S., van Oevelen, D., Harvey, H. R., Kristiansen, S., Gradinger, R., Dietrich, U. & Voelker, C. (submitted). Modelling Silicate–Nitrate-Ammonium co-limitation of algal growth and the importance of bacterial remineralisation based on an experimental Arctic coastal spring bloom culture study. Biogeosciences Discussions, 1-39, https://doi.org/10.5194/bg-2020-314.*

IV) **Vonnahme, T. R.**, Persson, E., Dietrich, U., Hejdukova, E., Dybwad, C., Elster, J., Chierci, M., Gradinger, R. (submitted). Subglacial upwelling in winter/spring increases under-ice primary production, The Cryosphere Discuss., https://doi.org/10.5194/tc-2020-326.*

* Submitted manuscripts in TC discussions and BGS discussions differ from the manuscripts in this PhD thesis, due to revisions based on reviewers' comments. The reviewers' comments can be found online in the interactive discussions under the given doi numbers.

Author contributions

	Paper I	Paper II	Paper III	Paper IV
Concept & idea	TRV, UD	TRV, LD, AP	TRV	TRV
Study design & methods	TRV, UD, BH	TRV, LD, AP, KP	TRV, CV, ML, ST, DvO, RH,, UD	TRV, UD, CD, EH, EP
Data gathering & interpretation	TRV, UD, BH	TRV, LD, AP, KP, MM	TRV, CV, ML, ST, DvO, RH, UD, SK	TRV, UD, CD, EP, EH, JE, MC
Manuscript preparation	TRV, UD, BH	TRV, LD, AP, KP, MM, RG	TRV, CV, ML, ST, DvO, RH, RG	TRV, CD, EP, EH, JE, MC, RG

Authors:

Tobias Reiner Vonnahme (TRV)
Ulrike Dietrich (UD)
Brandon Hassett (BH)
Lisa-Marie Delpech (LD)
Maeve McGovern (MM)
Rolf Gradinger (RG)
Kim Præbel (KP)
Amanda Poste (AP)
Martial Leroy (ML)
Dick van Oevelen (DvO)
Rodger Harvey (RH)
Svein Kristiansen (SK)
Christoph Voelker (CV)
Eva Hejdukova (EH)
Christine Dybwad (CD)
Josef Elster (JE)
Melissa Chierci (MC)
Silke Thoms (ST)

List of abbreviation

DOM – Dissolved organic matter

OM – Organic matter

DOC – Dissolved organic carbon

POC – particulate organic carbon

PON – particulate organic nitrogen

DIC – dissolved inorganic carbon

TA – total alkalinity

Chl – Chlorophyll a

PAR – photosynthetic active radiation

CTD – Conductivity, Temperature, Depth profiler

UIW – under (sea) ice water

SIZ – seasonal ice zone

DNA – deoxyribo nucleic acid

rRNA – ribosomal ribonucleic acid

OTU – operational taxonomic unit

SIP – stable isotope probing

FISH – Fluorescence in situ hybridization

ANOSIM – Analysis of similarity

ANOVA – Analysis of variance

NMDS – non-metric multidimensional scaling

Table of contents

1 Introduction

The Arctic Ocean, surrounded by land, is often considered a mediterranean sea with a long coastline, highly affected by land-ocean interactions (e.g. Østerhus et al., 2019). With climate change, the oceans, as well as land, are changing drastically with severe consequences for the marine ecosystem (reviewed by IPPC, 2019). On land, increasing temperatures lead to melting glaciers, thawing permafrost, and a longer melting season (e.g. Ding et al., 2019; IPPC, 2019). In the oceans, warming leads to retreating and thinning sea ice and changes in stratification (e.g. Lind et al., 2018; Polyakov et al., 2018; IPPC, 2019; Lannuzel et al., 2020). Besides increased temperatures, increased precipitation is also observed in the Arctic, leading to a thicker snow cover and increased freshwater runoff (e.g. Bintanja et al., 2020). These changes have direct implications for the flux of freshwater, nutrients, organic matter and organisms from land to sea (McGovern et al., 2020). In addition, indirect impacts via altered mixing and stratification patterns, and sea ice dynamics, have been described in the marine systems (IPPC, 2019). The first organisms affected are microbes, including bacteria, archaea, phytoplankton, and sea ice algae. They are controlled by the availability of light, nutrients, and organic matter, and by the stratification and circulation of the water column (e.g. Vincent, 2010). Microbes are key players shaping biogeochemical cycles, such as the carbon cycle with direct climate change feedbacks (Worden et al., 2015). They are also a major food source, ultimately sustaining the Arctic marine food web (Worden et al., 2015). For understanding how climate change will affect marine ecosystems in the future, it is crucial to understand the current shape of the microbial food web, including the impacts of land-ocean interactions. In addition, quantitative models accurately representing the dynamic bottom-up effects on marine microbes and interactions between secondary and primary producers are central for climate change predictions.

1.1 Land-Ocean interaction in the coastal Arctic

The coastal Arctic includes a variety of systems fed by different sources of freshwater and terrestrial matter. Large rivers with catchments reaching to sub-Arctic areas import large amounts of freshwater into the Arctic Ocean, mostly in Russia and North America (e.g. Holmes et al., 2012). Ice sheets and glaciers are important sources of freshwater in Greenland and high Arctic archipelagos with the capacity to change the global sea level (IPCC, 2019). Other regions in the European Arctic are influenced by smaller rivers with catchments in relatively moderate climates due to the warming effect of Atlantic water currents reaching up to western Svalbard.

In addition to freshwater inputs, ocean and land are tightly connected by seabirds feeding on marine organisms and fertilizing coastal (Kulinski et al. 2014) and terrestrial (Vonnahme et al., 2016) areas near their nesting sites with substantial amounts of nutrients.

1.1.1 Large rivers

In the Russian and American Arctic, large rivers, often originating far inland, enter the shelves in large estuaries introducing 10% of the global river inputs into a basin holding only about 1% of the global ocean volume (Holmes et al., 2012). The catchments are vast and mostly in tundra and taiga biomes with permafrost shaping the ground (Spencer et al., 2015). While the chemistry and hydrology can vary between rivers, some seasonal patterns seem to prevail in all large rivers. Overall, the large Arctic rivers are major sources of freshwater, DOM and nutrients to the Arctic Ocean with seasonal dynamics affecting the coastal microbial food web by stratification changes, light attenuation, nutrient inputs, and inputs of DOM with seasonally changing bioavailability (Holmes et al., 2012). A base flow is present throughout winter with high nutrient and low DOM concentrations, but the major volume of river runoff starts with the snowmelt during the spring freshet (Holmes et al., 2012). While nutrient concentrations decrease due to dilution and biological uptake, DOM concentrations and bioavailability are high (Holmes et al., 2012; Kaiser et al., 2017). Later in the season runoff decreases and is additionally fed by groundwater. During this time also the terrestrial active layer thickens and more ancient organic matter and nutrients can leach into freshwater, while the longer residence time of water in the watersheds allows for increased biodegradation of the organic matter until it reaches the coast (Kaiser et al., 2017). While permafrost may supply highly bioavailable DOM (Spencer et al., 2015), the summer runoff reaching the coast is often richer in more refractory organic matter (Kaiser et al., 2017). With climate change, the permafrost is thawing and the active layer thickening, leading to increased groundwater inputs, but also increased water retention in ponds and lakes (IPPC, 2019). Thereby the bioavailability of the DOM reaching the coast is decreasing due to terrestrial biodegradation (Kaiser et al., 2017). The impacts of these inputs on the coast include strongly stratified estuaries with high sediment load absorbing light, but also high concentrations of organic matter potentially feeding secondary producers. Permafrost thawing as well as increased precipitation in the Arctic have already led to increased runoff in both the Russian (10% between 1930 and 2002, Peterson et al., 2002), and American Arctic (McClelland et al., 2006).

1.1.2 Glacier influenced fjords

Freshwater inputs from Greenland and high Arctic archipelagos (e.g. Svalbard) are mostly fed by ice sheets and glaciers. The glaciers and ice sheets may either reach all the way to the coast (marine-terminating tidewater glaciers) or terminate on land and continue via smaller rivers (land-terminating glaciers). The two glacier types have substantially different impacts on the fjord hydrography and biogeochemistry (e.g. Hopwood et al., 2020).

Meltwater from **land-terminating glaciers** and snowmelt reaches the fjords via **smaller rivers**. These smaller rivers are fed primarily by **snowmelt** in spring and increasingly by **glacier melt** in summer. Similar to the large rivers, snowmelt in spring introduces large amounts of freshwater to the fjords. As for the large Arctic rivers, spring runoff is poor in nutrients, but rich in organic matter (McGovern et al., 2020; Fig. 1). Later in summer, the organic matter, sediment, and nutrient import into the fjord, as well as the impacts on the fjord hydrography are highly dependent on the catchment. Surface runoff from land-terminating glaciers may introduce some nutrients leached from the soil in the catchment area, remineralized in the tundra, or from the subglacial bedrock before entering the fjord (e.g. Hopwood et al., 2020; Kosek et al., 2019). Different bedrock geology may contribute different nutrients and sediments with different light absorbing properties to the fjord (Halbach et al., 2019). Organic matter in these rivers is typically considered more refractory compared to that of the large Arctic rivers due to its ancient origin (Dittmar & Kattner, 2003; Kim et al. 2011). High amounts of inorganic sediments are typical, leading to strong light attenuation close to the river outlets (McGovern et al., 2020; Fig. 1). However, terrestrial DOM may be more important in feeding and shaping bacterioplankton communities than previously thought, especially for rivers coming from tundra-covered catchments with short residence time of the runoff (e.g. Spencer et al., 2015; Kaiser et al., 2017). Once the rivers reach the fjord they lead to a strongly stratified brackish surface layer, inhibiting mixing with deeper water layers (Fig. 1). In early spring, this process can facilitate phytoplankton spring blooms, but later in summer, it also prevents deep mixing and the supply of fresh nutrients from the bottom water for primary production (Dittmar & Kattner, 2003; Hegseth et al., 2019). The changing magnitude and chemical composition of river inputs has most likely also strong impacts on bacterial communities and function, but only few small-scale studies gave first indications of these impacts (e.g. Bourgeois et al., 2016; Marquart et al., 2016; Garcia-Lopez et al., 2019; Kosek et al., 2019; Thomas et al., 2020).

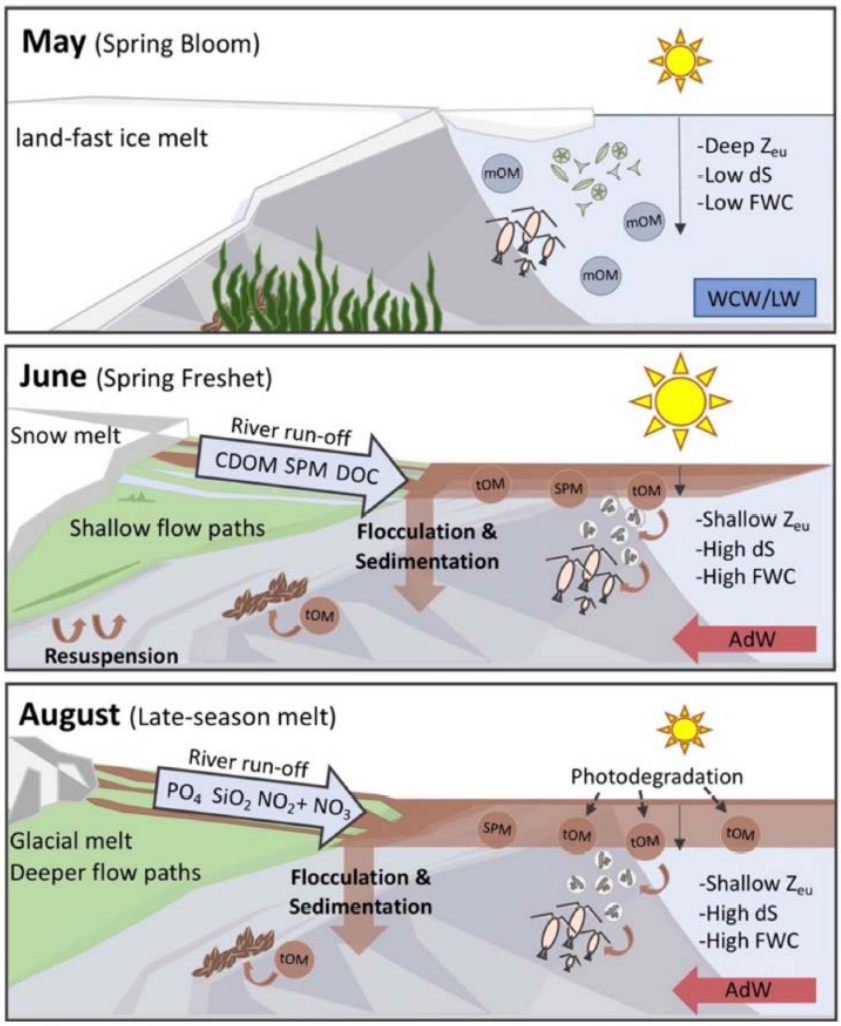

Fig 1. Impacts of river runoff on the coastal fjord systems in Isfjorden, Svalbard (Figure retrieved from McGovern et al., 2020; © CC BY 4.0). In **May**, land-fast ice melt (if present) is the only meltwater source. A spring bloom may develop, despite a deep euphotic layer (Z_{eu}), low stratification (dS), and low freshwater contribution (FWC). Marine organic matter (mOM) is dominating and the water consists mainly of local water (LW) and winter cooled water (WCW). In **June**, snow melt enters the fjord during the spring freshet including high concentrations of suspended particulate matter (SPM), dissolved organic carbon (DOC), and colored dissolved organic matter (cDOM) leading to high concentrations of terrestrial organic matter in the fjord (tOM) and a shallower Z_{eu}. Advected water (AdW), flocculation, sedimentation, and resuspension become more important. In **August**, river runoff is fed by glacier melt and deeper flow paths with high nutrient levels of phosphate (PO_4), silicate (SiO_2), nitrite (NO_2) and nitrate (NO_3).

Besides the surface runoff, marine-terminating **tidewater glaciers** also contribute to subglacial inputs of freshwater entering the fjord in deeper water layers leading to **subglacial upwelling** (reviewed by Hopwood et al., 2020; Fig. 2). During subglacial upwelling, deep nutrient-rich bottom water is entrained and transported to the surface via subglacial freshwater outflow with the capability to increase summer primary production, facilitating a productive marine ecosystem. In addition to the direct input of liquid freshwater, tidewater glaciers introduce freshwater via ice melt at the glacier front or via icebergs, which may lead to similar upwelling dynamics (Moon et al., 2018). In autumn, freshwater inputs, including subglacial outflows are commonly considered negligible. The brackish surface layer in the fjords, but also the cold glacier front, can facilitate sea ice production, even in otherwise warm fjord systems (e.g. Skogseth et al., 2020). In highly brackish surface waters, common near tidewater glacier fronts, the sea ice structure may be impacted through reduced brine volume fractions and thereby reduced inhabitable space and permeability (Fransson et al., 2020). The impacts of **brackish sea ice** on sea ice algae communities and production has been studied in sub-Arctic regions, such as the Baltic Sea (Granskog et al., 2003), but studies from high-Arctic fjords are scarce. Low ice algal primary production was found in Greenland fjords with high freshwater inputs, but this observation was explained by light limitation due to a thick snow cover, while limited sea ice permeability was not considered (e.g. Rysgaard et al., 2001; Leu et al., 2015). Studies on tidewater glacier melt in winter are scarce. In Greenland, freshwater inputs via basal ice melt at icebergs and glacier fronts, which are in contact with warm Atlantic water, have been observed (Moon et al., 2018). On Svalbard, glacially derived meltwater has been detected in spring with impacts on the sea ice physics (Fransson et al., 2020). However, to my knowledge, subglacial freshwater inputs have not been considered to have an impact on the fjord ecosystem, a paradigm I challenge in this PhD thesis.

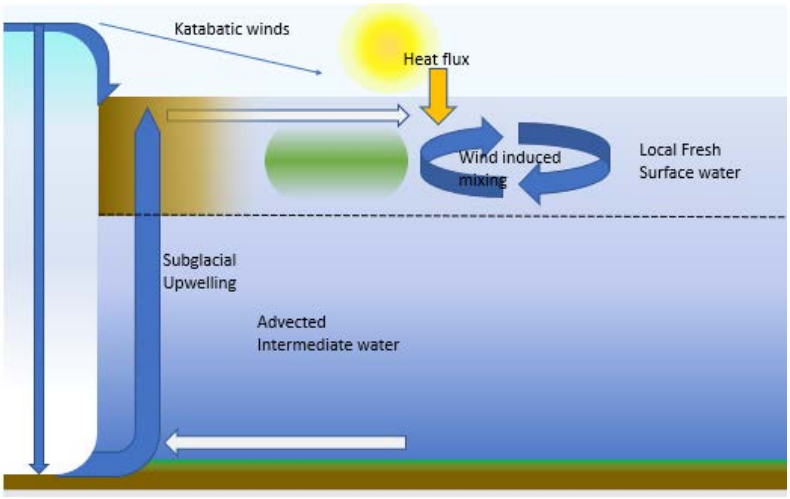

Fig 2: Summer circulation pattern in a tidewater glacier-influenced fjord (Figure retrieved from Vonnahme et al. in review, adapted after Meire et al. 2017). Thick light blue arrows indicate the water flow at the bottom and surface of the fjord. The thin blue arrow indicates the major wind direction and the orange arrow the main flux of heat. The dotted line indicates the halocline. The brown surface layer shows suspended sediments inhibiting light and the green layer phytoplankton.

With **climate change,** glaciers are melting at an accelerating rate, leading to increased runoff, capable of increasing the global sea level (IPPC, 2019). Tidewater glaciers are retreating onto land, and land-terminating glaciers are retreating to higher altitudes, leading to larger ice-free catchments (IPPC, 2019). The loss of tidewater glaciers has most severe implications for subglacial upwelling fueling summer primary production. Glaciers retreating further inland lead to changes in the properties of freshwater reaching the fjord via potential depletion of nutrients and degradation of labile DOM by land primary and secondary producers (Kosek et al., 2019).

The **Svalbard** archipelago is one of the fastest changing areas with sharp climatic gradients (Isaksen et al., 2016). The archipelago is influenced by warm Atlantic water reaching the Western coast and by cold Arctic water reaching the eastern coast (Fig. 3) leading to substantially different climates (Isaksen et al., 2016). The east coast is densely covered by glaciers and its marine waters typically covered in sea ice in winter, while the West coast is characterized by more glacier free areas (especially in Isfjorden) and sea ice formation limited to a few fjords (Fig. 3). Overall, Atlantic water inputs are increasing (Atlantification), introducing invasive taxa, altering stratification dynamics, and inhibiting sea ice formation

(Skogseth et al., 2020). As for the rest of the Arctic, freshwater runoff is increasing due to glacial melt and increased precipitation, especially in autumn (Adakudlu et al., 2019).

About 57% of Svalbard is covered by glaciers (Nuth et al., 2013, Fig. 3), which is about 10% of Arctic glacier ice outside the Greenland ice sheet (Schuler et al., 2020). 60% of these glaciers are marine terminating (Błaszczyk et al., 2009), with strong impacts on the fjord biogeochemistry (Halbach et al., 2019). Most of the glaciers are at low latitudes (Noël et al., 2020) and polythermal, which means that englacial and subglacial meltwater, can be present, even in winter (Hagen et al., 1993). This means that subglacial outflow may also be present and important in winter. Overall, Svalbard glaciers are losing mass due to climate change with estimates of about seven Gt a^{-1} (Schuler et al., 2020; Noël et al., 2020), which shows that impacts of glacial meltwater on fjord ecosystems are increasing, while subglacial upwelling at tidewater glaciers is decreasing.

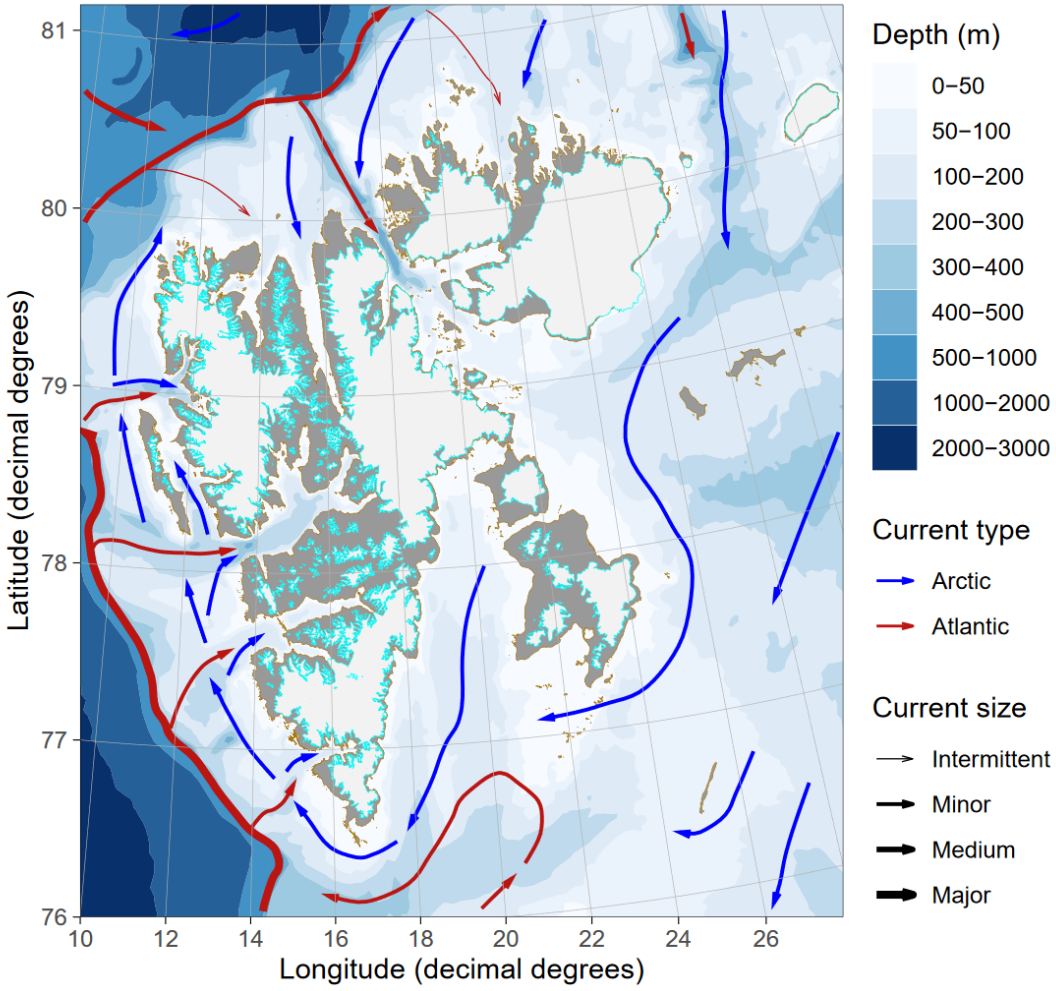

Fig. 3: Overview map of Svalbard with its bathymetry, main Ocean currents and glacier cover. Glacier margins are marked in cyan and land margins in brown. The map was created using the PlotSvalbard package in R (Vithakari 2019, Jakobsen et al. 2012)

Due to their good infrastructure, some Svalbard fjords are well studied and research on a high spatial and temporal scale is possible. At the same time, distances between considerably different systems are rather short, making it the perfect location to study impacts of climate change on coastal Arctic ecosystems. Research hotspots with long records are mostly available at the West coast, including Hornsund, Isfjorden, and Kongsfjorden.

1.2 Microbial ecology in the coastal Arctic sea ice zone

Marine microbes, including **algae**, **bacteria** and **archaea** are abundant in the global oceans and crucial as the base of the food web and for a range of functions controlling biogeochemical cycles (Worden et al., 2015). Overall, bacteria, algae, and archaea are controlled by a variety of environmental factors, such as light, nutrients and organic matter, but are also biologically

controlled, not only by grazing but also by a large diversity of interactions with each other (Worden et al., 2015). Due to their small size and undistinctive morphology most of these interactions are not obvious, but with advancing molecular methods, such as FISH and fluorescent stains it became possible to visualize specific taxa and organic matter otherwise indistinguishable, allowing to show spatial interactions and hypothesize about ecological interactions (Fig. 4).

Besides bacteria, archaea, and algae, other microbial groups can be important for the ecosystem. **Viruses** and phages are capable of terminating blooms and releasing intracellular compounds (viral shunt) including DOM and nutrients (Suttle et al., 2007; Zimmermann et al., 2019). **Fungi** were recently found to be surprisingly abundant in marine systems and we found fungi to be highly abundant with putative ecological roles similar to heterotrophic bacteria, including organic matter recycling and inorganic nutrient uptake, but also lysis of diatom cells (Hassett et al., 2019). During the polar night we also found protist grazers, such as heterotrophic dinoflagellates, ciliates, and choanoflagellates to be abundant and active in plankton communities around Svalbard and in a seasonally sea ice covered Norwegian fjord (Vonnahme et al., unpublished).

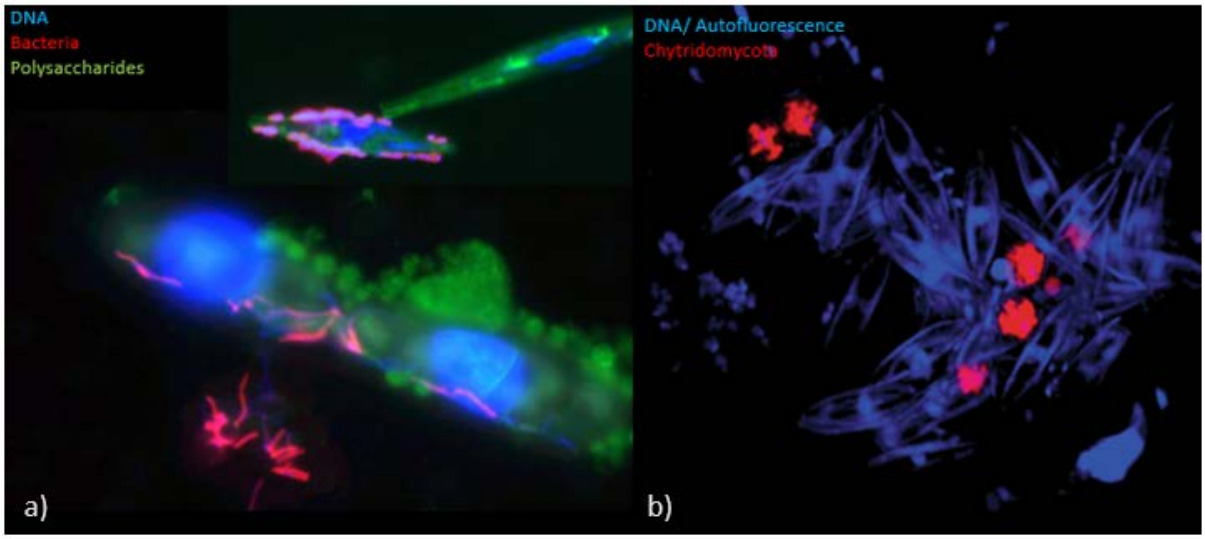

Fig 4. Visualisations of a) diatom (DAPI stained nucleus) – bacteria (CARD FISH stained) interactions via excreted polysaccharides (Lectine stained) by Vonnahme and Rapp (2016, unpublished), and b) Chytridomycota fungi (CARD FISH) and diatom (DAPI and blue autofluorscence) spatial organisation (Hassett et al., 2019, © copyright by co-authorship). Both pictures were taken with a confocal laser scanning microscope.

1.2.1 Algae in the coastal Arctic sea ice zone

The importance of phytoplankton and sea ice algae as primary producers is most apparent and well-studied in the context of ecosystem scale studies and models. At the base of the food web, photosynthetic algae fix CO_2 making the inorganic carbon available for a multitrophic food web. For doing so, they are mostly dependent on light and inorganic nutrients, which can both be limiting in marine systems, especially in polar seas. In addition, grazing pressure or viral lysis may suppress significant biomass accumulation.

In sea ice-free fjords in **spring**, inorganic nutrients are available from winter mixing, but light may be limiting during the polar night, or when negative net heat flux (out of the ocean into atmosphere) causes a lack of stratification, which leads to **phytoplankton** sinking faster out of the euphotic zone than it grows (Hegseth et al., 2019; Sverdrup 1953). As soon as the heat flux reverses and the water column starts stratifying, a phytoplankton spring bloom can start (Hegseth et al., 2019). Arctic coastal spring blooms are typically dominated by chain-forming centric diatoms (e.g. Eilertsen et al., 1989; von Quillfeldt 2000; Degerlund and Eilertsen, 2010; Fig. 5) such as *Chaeotoceros* spp.. In sea ice-covered systems, **sea ice algae** can form blooms within the bottom skeletal layer of sea ice, as soon as sufficient light reaches the bottom of the

ice (Leu et al., 2015; Fig. 5). Overall, sea ice algae are estimated to contribute 20% to the annual Barents Sea primary production (Hegseth, 1998). Arctic sea ice algae communities consist mostly of pennate diatoms with *Nitzschia frigida* often dominating the entire community (von Quillfeldt et al., 2009; Fig. 5). **Under-ice phytoplankton** blooms have been described in systems with thin or absent snow cover, leads (e.g. Arrigo et al., 2012; Assmy et al., 2017; Ardyna et al., 2020a,b), or in the presence of a stratified surface water layer (Lowry et al., 2017), but phytoplankton spring blooms are mostly following sea ice melt (Leu et al., 2015). Once the sea ice starts melting, sea ice algae melt out from the bottom and a phytoplankton bloom typically follows, fueled by high nutrient concentrations from winter mixing and a salinity-stratified water column, allowing phytoplankton to stay in the euphotic layer (freshwater input by sea ice melt, Hegseth et al., 2019). These ice edge blooms may be advected under the sea ice, explaining some of the observations of under-ice phytoplankton blooms (Johnsen et al., 2018; Ardyna et al., 2020a, b).

Later in the **summer** season, the water column becomes increasingly stratified with terrestrial freshwater inflow limiting vertical mixing, which keeps phytoplankton in the euphotic zone (Sverdrup, 1953; Fig. 5), but which is also inhibiting nutrient upwelling. Thus, Phytoplankton spring blooms are typically terminated after nutrients become limiting (typically nitrogen and/or silicon). If silicate is limiting, but inorganic nitrogen is still available, flagellates may form a secondary bloom. In particular, *Phaeocystsis pouchetii* has been described as an important spring bloom species dominant in the SIZ (Eilertsen et al. 1989; Ardyna et al., 2020a,b). Subglacial upwelling (Halbach et al., 2019; Hopwood et al., 2020) and bacterial ammonium regeneration (Spencer et al., 2015; Baer et al., 2017) may supply additional nutrients extending the bloom, but this process is often neglected or too simplified in ecosystem-scale models. After inorganic nitrogen becomes limiting, the bloom is terminated and phytoplankton communities are typically dominated by small flagellates (e.g. *Micromonas pusilla*) and ciliates (e.g. Cogieau et al., unpublished; Not et al., 2005). During this time, grazing is considered a major control on phytoplankton biomass (Owrid et al., 2000). Smaller flagellates are discussed to be dominant in summer, either due to their ability to use organic nitrogen sources, or due to their quick growth exceeding the grazing rates. At the ice edge, summer primary production may be highest due to a stratified and nutrient-rich surface layer left behind by the retreating ice edge. These ice-edge phytoplankton communities are often dominated by *Phaeocystis pouchetii* or *Chaetoceros socialis* (von Quillfeldt et al., 2009).

In **autumn**, freshwater inputs cease and the heat flux reverses, leading eventually to mixing of the water column. In some cases, this autumn mixing may trigger an autumn bloom if sufficient light is still available. This autumn bloom is often dominated by diatoms or dinoflagellates (e.g. Eilertsen et al., 1989; Fig. 5). Once the **polar night** starts, algae are light-limited, but they are still present and active as found in several recent studies (Kvernvik et al., 2018; Randelhoff et al., 2020). The communities are diverse, but often dominated by small flagellates and pennate diatoms (e.gt. Lizotte et al., 2003; Vader et al., 2015; Marquardt et al., 2015; Fig. 5). Algae may survive by reduced metabolic activities, spore formation, heterotrophic carbon uptake, or feeding on intracellular storage compounds (Zhang et al., 1998; Johnsen et al., 2020). Their photosynthetic machinery stays often surprisingly intact, ready to start photosynthesis as soon as the light returns (Kvernvik et al., 2018; Randelhoff et al., 2020). Deep winter mixing may supply additional algae spores from the sediment to the surface water, making them available for the race for nutrients and light in spring. In fact, winter mixing has been described as crucial for allowing a strong spring bloom (Hegseth et al., 2019).

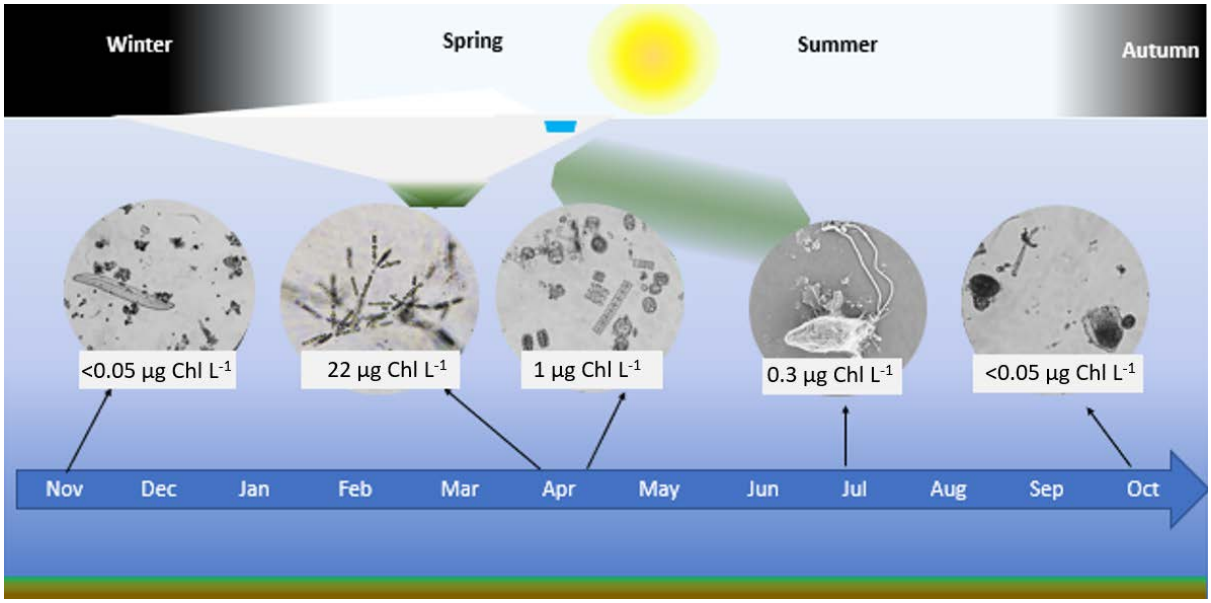

Fig 5. Seasonal cycle of sea ice formation, algae biomass (max. Chl values), and abundant taxa found under the light microscope in Billefjorden at the (ice edge) reference station (Fig. 7b, IE). The dominant taxa found were: ciliates, flagellates, pennate diatoms (November 2017) and *Nitzschia frigida* in sea ice (April 2019) and, in the water column, pennate and centric colony-forming diatoms in April 2019, flagellates in July 2018 and ciliates in October 2019. (Vonnahme et al. in review)

1.2.2 Bacteria and archaea in the coastal Arctic sea ice zone

The role of bacteria and archaea is substantial, but complex due to their vast diversity of metabolic functions affecting various intertwined biogeochemical cycles. Considering that about half of the global CO_2 fixation happens in the oceans (Field et al., 1998) and that half of that CO_2 is channeled through marine bacteria and archaea (Ducklow, 2000), their importance for the global carbon cycle becomes obvious. They also contribute to the highest abundances and diversity with strong spatial variations (Azam & Malfatti, 2007; Zorz et al., 2019). At the same time their importance is often neglected or too simplified in full ecosystem or modelling studies (e.g. Worden et al., 2015), potentially due to their small size, and need for specialized methods to study their abundances, diversity and functions. Their impact as heterotrophic secondary producers feeding higher trophic levels and regenerating nutrients is evaluated and implemented in some ecosystem models (e.g. Moore et al., 2004; Vichi et al., 2007; Wassmann et al., 2006), but often very simplified. Heterotrophic bacteria and archaea can use DOM as a carbon source building biomass and releasing inorganic nutrients, which can fuel regenerated primary production. However, DOM is a diverse pool of material, requiring a very diverse pool of metabolic pathways and taxa for its degradation and use (Azam & Malfatti, 2007). Considering the heterogeneous distribution of DOM, very localized bloom and bust scenarios have been described for bacterial activities (Azam & Malfatti, 2007). For the degradation of some DOM, complex consortia of different interdependent taxa are necessary (e.g. Chen et al., 2020). Consequently, the microbial community structure and metabolic functions are highly controlled by the organic matter present in the environment (Blanchet et al., 2017).

In coastal Arctic systems, the organic matter may come from land with differences based on the catchment properties and time of the year (e.g. Holmes et al., 2012; McGovern et al., 2020). In large catchments with long residence time in stationary reservoirs, the organic matter is often already degraded by terrestrial bacteria and archaea on the way to the coast (Spencer et al., 2015; Kaiser et al., 2017), leading to rather refractory DOM, despite their often labile source.

Another substantial source is DOM released by marine primary producers (Teeling et al., 2012; Muehlenbruch et al., 2018) or higher trophic levels (e.g. sloppy feeding, Shoemaker et al., 2019). This autochthonously produced DOM is typically more bioavailable, leading often to a bacterioplankton bloom associated to phytoplankton blooms with characteristic succession patterns (Teeling et al., 2016). Autochthonous DOM facilitates first the growth of fast-growing bacteria, such as Flavobacteriia, Gammaproteobacteria, and *Roseobacter* (Teeling et al., 2016).

After the first stage of degradation of the most bioavailable DOM (Kirchman et al., 1991), the bloom is typically followed by a characteristic succession of different bacteria species degrading increasingly refractory organic matter released by the algae or by other bacteria (Teeling et al., 2012; Teeling et al., 2016). Bacterioplankton succession and the important DOM compounds and enzymes involved have been studied in detail in the North Sea. A few studies in the Arctic show generally similar patterns with similar taxa involved (Sinha et al., 2018; Zorz et al., 2019). However, the amplitude of the population dynamics is typically higher and additional genera are involved (Bunse and Pinhassi, 2017). Due to the importance of ammonium regeneration, algae have also been found to farm a specific microbiome in their phycosphere, often specific to different algae species (Muehlenbruch et al., 2018). For understanding the role of a changing freshwater inputs and changing algae bloom dynamics, it is therefore important to also consider the diversity of organic matter and the diversity of bacterial and archaeal taxa needed to degrade it. Eventually, microbially reworked organic matter can become recalcitrant and unavailable for the marine food web (Jiao et al., 2010). Some biogeochemical models consider organic matter of different lability (van den Meersche et al., 2004), but considering the vast diversity of organic matter, metabolic pathways and bacterial diversity and interactions, this is still a limited approach.

Besides their importance for DOM recycling, bacteria and archaea are also crucial for various other processes. In the presence of oxygen, they can fix CO_2, not only with sunlight as energy source, but also with chemical reactions fueling the fixation of CO_2 (e.g. Nitrification). In the oxygenated pelagic part of the oceans, ammonia and nitrite oxidation (Nitrification) are the most important chemical reactions for chemoautotrophic CO_2 fixation, mostly driven by archaea (e.g. Yergeau et al., 2017). In fact, about 50% of the nitrate used for primary production is produced via nitrification, indicating its importance for the marine nitrogen cycle (Yool et al., 2007). Nitrification may also be an important part of the carbon cycle when photosynthesis is limited by light, such as during the polar night (Christman et al., 2011). This leads firstly to the decreased competition for ammonium with algae and secondly to decreased direct light inhibition of nitrification-related enzymes. Nitrification leads inevitably to NO_3 accumulation, which is more energy expensive for algae to assimilate and which is subject to denitrification (Nitrogen loss). Under anaerobic conditions, which may occur in sea ice or sediments, NO_3 can be converted to N_2, which is lost to the atmosphere via denitrification, or Anammox (e.g. Rysgaard et al., 2008). Other bacteria, including cyanobacteria (Diez et al., 2012) and

heterotrophs (Fernandez-Mendez et al., 2016) are capable of fixing atmospheric N_2 with the potential of resupplying 27.1% of the lost nitrogen back to the Arctic marine food web (Sipler et al., 2017). Some archaea can also oxidize methane as energy source, but need syntrophic bacteria for transferring the electrons (Reeburgh, 2007). Sulphate-reducing bacteria are one example of a taxonomic group of bacteria that can reduce sulphate with the electrons supplied by methane-oxidizing archaea allowing the overall reaction to be thermodynamically feasible. This symbiosis can be an important mechanism for retaining the potent greenhouse gas in marine sediments before it reaches the atmosphere (e.g. Reeburgh, 2007; Gruendger et al., 2019). Other potentially ecologically important functions discussed in the SIZ are dimethyl sulfide production, mercury methylation (Bowman et al., 2015), and vitamin B12 synthesis (Taylor and Sullivan, 2008). Overall, each of these processes has important implications for the biogeochemical cycles and ultimately for the marine food web. However, the limited understanding of the most basic question such as who is there, how many are there, and what are they doing makes it still challenging to consider them in full ecosystem studies and models.

1.2.3 Complexity of bacteria/archaea– algae interactions

As outlined above, discussion of the ecology of the individual microbial domains is limited without considering the multitude of interactions in the microbial food web. OM produced by algae is a major food source for bacteria, while nutrients released during the OM degradation allow regenerated production increasing the overall primary production substantially (Fig. 6). However, the interactions go far beyond that. Algae can become mixotrophic, feeding or parasitizing on bacteria and other algae especially under light and nutrient limitation (Stoecker et al., 2017). Bacteria can feed on dead algae in specific microenvironments such as marine snow, or the phycosphere, and may even cause their death (Worden et al., 2015; Fig. 6). Some bacteria and algae species live in tight symbiosis. For example, N_2 fixation by a unicellular cyanobacterium can be coupled with CO_2 fixation by a specific phytoplankton species (Martinez-Perez et al., 2016). Worden et al. (2014), give a more detailed review of the diversity of interactions in the microbial food web.

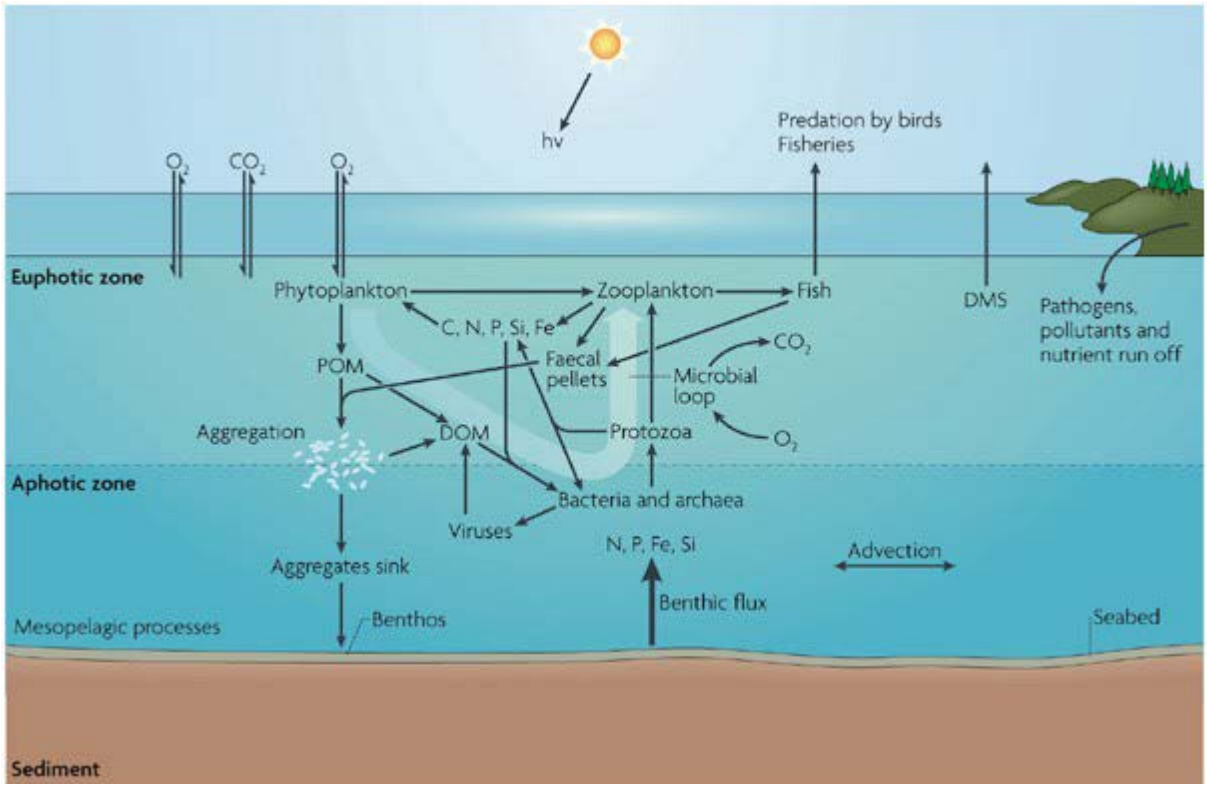

Fig 6. Conceptual summary of the microbial food web by Azam & Malfatti (2007; © copyright obtained under license number 4933041090830). Organic matter is given as particulate (POM) or dissolved (DOM).

2 Objectives

The thesis consists of a review on the current field of marine microbiology in the SIZ (paper I) and original research (paper II-IV) on the relevance of microbial processes in the coastal Arctic seasonal ice zone. Based on the review in paper I, I developed two main objectives as an umbrella for the entire thesis:

Firstly, I studied the effects of terrestrial freshwater inputs, which are expected to increase with climate change, on algae, bacteria and archaea diversity and functions. Secondly, I developed a dynamic model, integrating my own experimental studies with bacteria and algae under conditions similar to spring blooms, simple enough to be implemented in ecosystem-scale models, but complex enough to include crucial, but previously neglected processes.

Paper II studied the **bacterial** and **archaeal** diversity and potential role for biogeochemical cycles in Arctic land-ocean interfaces and the impacts of seasonal variation in organic matter, nutrient, and freshwater inputs. Paper III focused on the importance of bacteria for regenerated production and potential to extend phytoplankton spring blooms (addressed in paper III). The importance of **sea ice algae** and **phytoplankton** as primary producers building the base of the SIZ food web is overall well modelled. However, the thesis aims to advance the understanding of these key players by i) modelling bacteria-diatom interactions and the effects of multi-nutrient limitations (addressed in paper III), and by ii) studying their diversity and CO_2 fixation potential in a tidewater glacier influenced fjord (addressed in paper IV), which are both understudied fields of research. Paper IV focused in detail on **tidewater glaciers,** which are important for summer primary production. We evaluated the importance of subglacial freshwater outflow of tidewater glaciers in spring on a sea-ice covered fjord.

The following specific research questions and hypotheses were addressed:

1. What is the current state of knowledge regarding microbial ecology in the SIZ and which aspects are understudied? (I)
    a. Microbial ecology is still poorly represented in full ecosystem studies.
    b. Novel methods, such as –omics approaches allow a better understanding of SIZ microbes.
2. What are the impacts of freshwater inputs from land on the coastal microbial food web, diversity, and carbon cycle?
    a. Rivers supply terrestrially derived organic matter as potential food source shaping the marine microbial community structure. (II)
    b. Rivers and glaciers can transport specific bacteria into the fjord, but only few species can survive in the marine system. (II, IV)
    c. Subglacial upwelling is already important in spring and can increase under-ice phytoplankton primary production. (IV)
    d. Sea ice in freshwater-influenced systems is brackish and impermeable with negative consequences for sea ice algae. (IV)
3. What is the role of bacteria-algae interactions?
    a. Bacteria follow phytoplankton blooms in typical succession patterns with reoccurring taxa described from other succession studies. (II, IV)
    b. Spring blooms may be extended by length and total biomass production due to bacterial ammonia regeneration. (III)

3 Methods and own contribution to each paper

3.1 Review article

The first paper of the PhD is an extensive review of the current knowledge and technologies in microbial ecology in sea ice-covered oceans and future directions. The review was written as contribution to the YOUMARES conference proceedings in 2018 and had been peer-reviewed by two anonymous reviewers prior to acceptance. My contribution to the paper was the review of technological developments (ch. 14.2), diversity and biogeochemical functions of viruses, bacteria, and archaea (ch. 14.3.2, 14.3.4, 14,4,1,1, 14.4.1.2, & 14.4.1.3), and the seasonal changes in sea ice-covered seas (ch. 14.5). BH contributed with his expertise on marine fungi, and UD focused on algae diversity and biogeochemical functions as well as a general introduction to sea ice-covered seas. The review points out the importance of considering Arctic microbes for a whole ecosystem understanding, including modelling approaches, especially with the ongoing rapid climate change.

3.2 Field work

3.2.1 Sampling sites

Sampling for all research papers was done in Svalbard fjords (Fig. 7). Sampling included marine samples of sea ice, water, and sediments, but also terrestrial endmembers, such as river water, glacial runoff and glacier ice. Paper II focuses on the melting season in the Isfjorden fjord system with 95 samples of sediments, river water, and fjord water following gradients from terrestrially influenced systems to more open fjord systems. Samples were taken in June and August 2018, representing the spring freshet with snowmelt-fed rivers and the later melt season with mostly glacial meltwater-fed river inputs. The focus of this paper was to study the effects of river inputs on microbial communities. We investigated the microbial community structure via 16S rRNA metabarcoding and used a broad set of environmental metadata to discuss potential environmental controls. Paper IV focused in more detail on Billefjorden, a tidewater-influenced fjord connected to the larger Isfjorden including microbial diversity, carbon cycling, and physical and chemical processes in the fjord. Samples were taken in April 2018 and 2019, during a time with sea ice cover, no riverine inputs, but suspected subglacial meltwater inputs from the glacier Nordenskiöldbreen. Water and sea ice were sampled at three main stations (Fig. 7b); a marine reference site at the fast ice edge (ice edge, IE), and two different faces of Nordenskiöldbreen, one land-terminating (North Glacier, NG) and one marine

terminating (South Glacier, SG). Additional samples were taken from the glacier including subglacial meltwater, supraglacial meltwater (collected in summer), and glacier ice. The aim of this paper was to investigate the impacts of subglacial meltwater inputs on the microbial food web and carbon cycle. Algal and bacteria cultures (paper III) representative for Svalbard fjords were established with water samples from Van Mijenfjorden in April 2017. The aim of this paper was to recreate and model coastal Arctic spring bloom dynamics, with model organisms isolated from such a bloom. More details about the sites can be found in the corresponding papers.

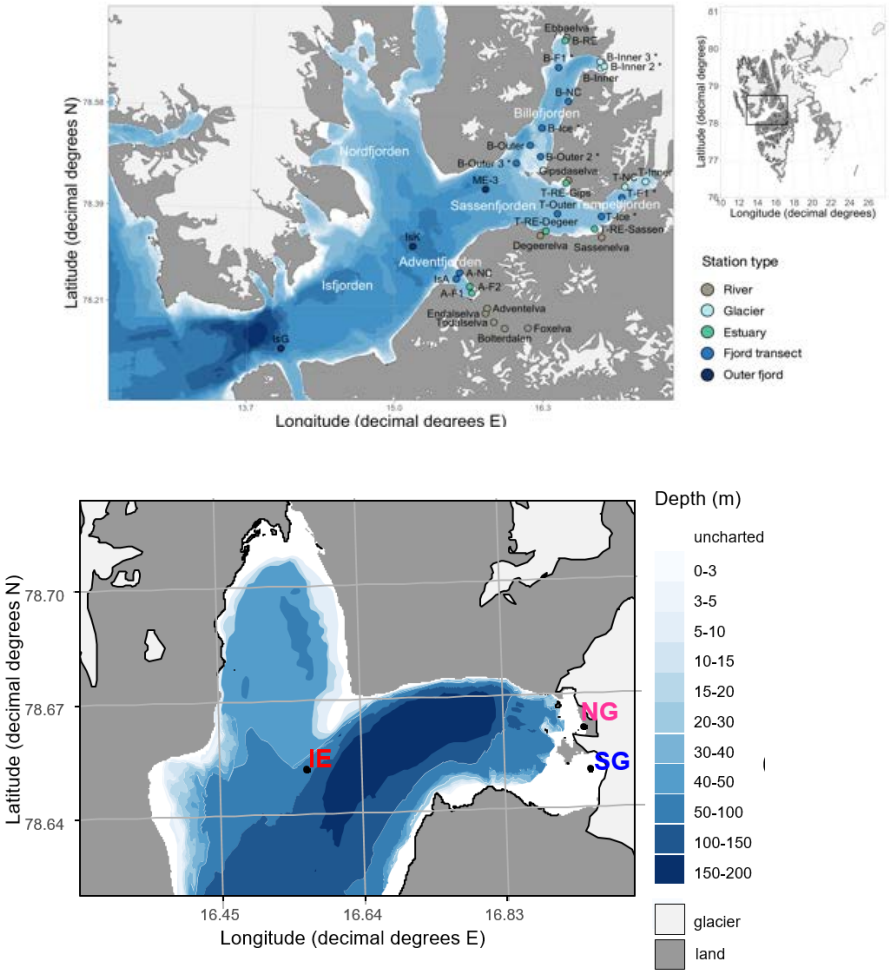

Fig 7. Sampling sites of Paper II (upper) and paper IV (lower). Further details about the stations are given in the papers.

3.2.2 Sampling methods

The sampling methods are described in detail in papers II-IV and Table 1, but a brief summary is given here. Water samples in Isfjorden (paper II) were taken from a small boat (PolarCirkel)

and samples were processed at UNIS. Samples in Billefjorden were processed in the field station of the Centre for Polar Ecology, and samples in Van Mijenfjorden were stored alive in an insulated bottle before transport to Tromsø for cultivation.

Seawater samples for paper II and IV were taken with a Niskin bottle or Ruttner water sampler at specific depths representing different water masses or light regimes.At locations covered with sea ice, water samples were taken through a hole in the ice. Under-ice water (UIW) for paper IV was taken with a pooter (tube connected to a vacuum pump). Water samples from glacial meltwater and rivers were directly taken in a sterile Whirl bag. Sea ice and glacier ice samples (paper IV) were taken using an ice corer. Sea ice samples were sectioned on site and either melted directly for nutrient and salinity measurements, or melted in sterile filtered water (ca 50% v/v dilution) for different biological parameters (chlorophyll, bacteria, algae, DNA).

Melted ice and water samples for paper IV, as well as culture samples for paper III, were prepared for the following analyses. Samples were sterile-filtered and frozen at -20 °C for nutrient and DOC analyses (papers III, IV). Bacteria samples were fixed in 2% (fin. conc.) Formaldehyde for 6-12 h before filtering onto polycarbonate filters (0.2 µm pore size) and stored frozen at -20 °C (papers III, IV). Algae samples were fixed in 1-2 % neutral Lugol solution and stored at 4 °C in brown borosilicate glass bottles (paper IV) or counted directly (paper III). Chlorophyll samples were filtered onto GF/F filters and stored dark and frozen at -20 °C (papers III, IV). POC/PON samples were filtered onto precombusted (5 h, 450 °C) GF/F filters and stored frozen at -20 °C (paper III). DNA samples were filtered onto 0.2 µm pore size Sterivex or polycarbonate filters and stored frozen at -20 °C (papers II, IV). DIC samples were filled air-free into Duran glass bottles, fixed in 2% $HgCl_2$ and stored cold at 4 °C (paper IV). For paper II an additional set of environmental parameters was measured by McGovern et al. (2020).

Temperature profiles in the sea ice were measured in pre-drilled holes in the ice cores immediately after ice coring and sea ice and snow thickness was measured on site (paper IV). Sediment samples were taken with a Van Veen grab, and the surface layer taken for further analyses (paper II). Phytoplankton samples were taken with a phytoplankton net (KC Denmark, 10 µm mesh size) haul from 35 m depth to the surface and fixed in Lugol as described above (papers II, IV). CTD profiles were taken with a Castaway or SAIV CTD (paper IV). Other

environmental data (paper IV) were obtained from meteorological stations in the area maintained by the Centre of Polar Ecology (Ceske Budejovice, Czech Republic).

Vertical fluxes of chlorophyll were measured (paper IV) using sediment traps at 1 m, 15 m and 25 m under the sea ice as described by Wiedmann et al. (2016) and left for about 1 day under the ice. Chlorophyll samples of the sediment trap tubes were obtained as described above. Primary production was estimated *in situ* in incubations with ^{14}C-labelled DIC (1 μCi ml^{-1}) for the same time period, attached to the rig of the sediment traps. After the incubations, the samples were filtered onto precombusted (5 h at 450°C) GF/F filters and excessive DIC removed via acidification with 37% HCl in a scintillation vial for about 12 h. The ^{14}C-DIC incubations included 2 dark (heterotrophic uptake) and 3 light (phototrophic uptake) incubations. Additional reciprocal transplant experiments were performed by incubating the communities from the IE or SG with the sterile filtered water from the same or the other station (50% v/v filtered seawater/unfiltered community). This experiment was performed to test for chemical effects of the water at two different stations on primary production, excluding effects of different light, temperatures, stratification, or community composition.

Table 1. Overview of the sampling types, location, season, sample types taken and parameters measured for the different research articles.

Paper #	II	III	IV
Sampling types	Field	Culture	Field
Location	Isfjorden	Van Mijenfjorden	Billefjorden
Season	summer	spring	winter/spring
Samples			
Sea ice			X
River	X		
Glacier			X
Fjord water	X	X	X
Sediments	X		
Communities and biomass			
Bacteria counts		X	X
Algae counts		X	X
16S rRNA	X		X
18S rRNA			X
Phytopigments	X	X	X
Biogeochemistry			
CTD	X		X
Sea ice physics			X
Turbidity	X		X
POC/PON	X	X	
DOC	X	X	
$Si(OH)_4$, NO_X, PO_4	X	X	X
NH_4	X	X	
Quantum yield (QY)		X	
DIC/TA			X
Light absorbance	X		
Fluxes			
Primary production			X
Vertical flux			X

3.3 Lab analyses

3.3.1 Environmental data

Detailed description for the different lab analyses can be found in the corresponding papers. A brief summary is given here. Bacteria samples were stained with DAPI for 7 min. after Porter et al. (1980), and embedded in Citifluor-Vectashield (3:1), before counting under an epifluorescence microscope (Leica DM LB2, Leica Microsystems, Germany) at 10x100 magnification (papers III, IV). Algae were counted alive in 2mL well plates (paper II), or fixed in neutral Lugol in Utermoehl settling chambers (paper IV) (Utermöhl, 1958) under an inverse microscope (Zeiss Primovert, Carl Zeiss AG, Germany) under 10 x 40 magnification. Algae and protist taxa were identified (papers III, IV) using the literature by Tomas (1997), and Throndsen et al. (2007). For more detailed molecular analyses of the microbial communities part of the 16S rRNA (v4) gene (bacteria and archaea) and 18S rRNA (v7) gene (eukaryotes)

were amplified (PCR) and sequenced (Illumina MiSeq PE; Wangensteen et al., 2018) after DNA extraction using a modified DNeasy® PowerSoil® kit as described in the manuscripts of this PhD thesis (papers II, IV). Chlorophyll was measured fluorometrically after extraction in 96% ethanol for about 12 h and measurement on a Turner Trilogy AU-10 fluorometer (Turner Designs, 2019) before and after acidification with a drop of 5 % HCl (papers III, IV) after Holm-Hansen and Riedmann (1978).

Nutrients, except ammonium, were measured colourimetrically on an autoanalyzer (QuAAtro 39, SEAL Analytical, Germany), using the instrument protocols: Q-068-05 Rev. 12 for nitrate (detection limit = 0.02 µmol L^{-1}), Q-068-05 Rev. 12 for nitrite (detection limit = 0.02 µmol L^{-1}), Q-066-05 Rev. 5 for silicate (detection limit = 0.07 µmol L^{-1}), and Q-064-05 Rev. 8 for phosphate (detection limit = 0.01 µmol L^{-1})(papers III, IV). Ammonium was measured manually after Solorzano (1969) on a spectrophotometer (Shimadzu UV-1201, detection limit = 0.01 µmol L^{-1})(paper III). POC and PON were measured on an elemental analyzer (Flash 2000 elemental analyzer, Thermo Fisher Scientific, Waltham, MA, USA; and Euro elemental analyzer, Hekatech) after drying and DIC removal via acidification in a desiccator with fuming (37%) HCl (Pella and Colombo, 1973)(paper III). For primary production estimates, the ^{14}C-DIC filters were submerged in the scintillation cocktail Ultima Gold™ and measured on a liquid scintillation counter (PerkinElmer Inc., Waltham, USA, Tri-Carb 2900TR) and PP was calculated after Parsons et al. (1984)(paper IV). DIC and TA were measured as described by Dickson et al. (2007) using a VINDTA (VINDTA 3C, Marianda, Germany) for titration (paper IV). DOC was measured by high temperature catalytic oxidation (HTCO) on a Shimadzu TOC-5000 total C analyzer as described by Burdige and Homstead (1994)(paper III). The photosynthetic quantum yield was measured on an Aquapen PA-C 100 (Photon Systems Instruments, Czech Republic)(paper III).

3.3.2 Cultivation of bacteria and algae

Phytoplankton and bacteria were cultured at 4 °C using different growth media and approaches. Diatoms were cultured using the dilution isolation method (Andersen et al., 2005) on F/2 medium (Guillard, 1975). This method provided pure cultures of *Nitzschia* sp., *Cylindrotheca* sp., *Porosira arctica*, and *Chaetoceros socialis*. *Chaetoceros socialis* was selected for further experiments due to its dominance in many phytoplankton blooms, quick growth, and survival of antibiotics treatment. The antibiotic treatment (penicillin and streptomycin) allowed obtaining an axenic culture, which was confirmed by incubation of the culture on LB Agar

plates, and DAPI staining followed by epifluorescence microscopy. Bacteria were isolated on LB Agar plates using the diatom cultures as inoculum in order to target heterotrophic bacteria associated with the diatom. After isolation of pure bacteria strains, the cultures were identified via Sanger sequencing of the 16S rRNA (V1-V9) gene at GENEWIZ and alignment with blastn (Altschul et al., 1990). This method provided pure cultures of *Pseudoaltermonas elyakovii* strain1, *Pseudoalteromonas elyakovii* strain2, *Pseudoalteromonas arctica*, *Pseudoalteromonas prydzensis*, and *Marinomonas primoryensis*. Both strains of *Pseudoaltermonas elyakovii* were used for further experiments due to their origin from the *C. socialis* culture and to account for inter-strain variability.

For paper II, a cultivation experiment was performed to study the response of *C. socialis* to nutrient limitation and the role of bacterial ammonium regeneration for its growth. For the experiment, *C. socialis* was grown in F/2 medium lacking nitrate, either axenic, or with addition of both *P. elyakovii* strains. The cultures were incubated at 4 °C, 100 μE m^{-2} s^{-1} PAR, in 96 200-mL cultivation bottles. Each day (with gaps on weekends), three bottles per treatment were sampled and processed for algae and bacteria cell counts, and measurements of POC/PON, chlorophyll a, DOC, photosynthetic quantum yield, and nutrients as described above. The experiment ran for 15 days covering the lag phase, exponential phase and stationary phase. The data were used to develop a dynamic quota-based model of algae physiology including Si N co-limitation, C excretion, and bacterial remineralization (See 3.4.2).

3.4 Computational analyses

3.4.1 Bioinformatics and statistics

All metabarcoding DNA sequences were analyzed on the UiT cluster Stallo to obtain OTU and taxonomy tables. Detailed descriptions of the programs and parameters used are given in the paper. Briefly, for paper II, 16S rRNA gene sequences were analyzed after Hassenrueck (2019) using SWARM (Mahe et al., 2015) for clustering and SINA (Pruesse et al., 2013) for alignment and taxonomic classification based on the Silva SSU non-redundant v138 database. For paper IV, sequences were analyzed after Atienza et al. (2020) based on OBITools v1.01.22 (Boyer et al., 2014). Clustering was done with SWARM for 18S rRNA and 16S rRNA sequences. 16S rRNA sequences were then classified using the RDP classifier and database (Wang et al., 2007) and 18S sequences using SINA aligner and the Silva SSU non-redundant v138 database.

The OTU and taxonomy tables were further analyzed in R as described in detail in papers II and IV. The different approaches, such as rarefaction, functional inference from taxonomy, and multivariate environmental correlations have their limitations and problems, which are addressed and discussed in detail in the related papers. Briefly, different groups were predefined based on the hypothesis of the papers and the vegan package was used to detect differences in alpha and beta diversity. Besides the taxonomic diversity, functional diversity was estimated using Tax4fun (Aßhauer et al., 2015) and key biogeochemical functional groups for cycling of C, P, Fe, Hg, Co, N, and S were studied for differences between the sites. For alpha diversity analyses, sequences were rarefied and rarefaction curves plotted (paper II). Different diversity indices were evaluated (number of OTUs, Chao1, Shannon-Wiener index, inverse Simpson index, number of singletons and doubletons, and evenness) to discuss differences in the rare and abundant biosphere and evenness or richness (paper II). Differences of alpha diversities in the predefined groups were tested using ANOVA. nMDS (papers II, IV) and RDA (paper II) ordination plots were created to visualize differences between the groups and potential environmental drivers. Significance of differences of communities between the sites was tested using ANOSIM (papers II, IV). Indicator OTUs were identified using the indicspecies package v1.7.9 (Caceres and Legendre, 2009)(paper II). The number of OTUs shared between the sites was calculated using the function vegdist (paper IV).

3.4.2 Dynamic modelling

A detailed description of the model and fitting routine is given in paper III. Briefly, for dynamic modelling in paper III, a dynamic quota-based model by Geider et al. (1998) was used as a baseline (G98), due to its wide use in ecosystem scale models and its strength in representing photoacclimation. I implemented the model in R and extended the model in order to represent silicate limitation, different kinetics of ammonium and nitrate uptake, carbon excretion, and bacterial remineralization, based on previous research. The aim was to keep the model as simple as possible while representing the cultivation experiment, which I consider representative for a typical Arctic coastal spring bloom. A detailed description of the model, model equations, and fitting routines is given in paper III. Differential equations were solved using the 2^{nd}-3^{rd} order runge-kutte method of the deSolve package (Soetart et al., 2010). Sensitivity analyses were done using the sensFun function, based on weighted residuals of model outputs vs measured data. Collinearity tests for estimating identifiability of parameter combinations were done with the collin function of the FME package (Soetart and Petzoldt, 2010). In case of significant

collinearity (collinearity index > 20), the more sensitive parameter was fitted. Parameters of the traditional G98 model were first fitted to the axenic experiment, before the additional parameters of the extended model were fitted to the bacteria-enriched experiment, while retaining the optimized parameter values of G98. All parameters were first fitted manually. The modfit function with a pseudorandom algorithm searching for a global optimum, followed by the Nelder-Mead algorithm searching for the local optimum was then used to check optimize the fits. In total, 15 parameters were fitted against 160 data points. The model cost was estimated via i) calculating the root of the sum of squares normalized by dividing the squares with the variance (Stow et al., 2009), ii) calculating the weighted residuals vs fitted data of the sensFUN function, and iii) graphical comparison with the experimental data.

3.4.3 Biogeochemical conversions

For discussing the carbon cycle with standardized units in paper IV, some biogeochemical conversions were necessary, which have some limitations but are useful in comparing the carbon cycles at the tidewater glacier influenced site with the marine reference site. Due to a broken elemental analyzer, the POC samples could not be analyzed and conversion from Chl to C was necessary. While the conversion factor depends highly on the physiological state and taxonomic composition, we used a conversion factor of 30 gC $gChl^{-1}$, an average value reported by Cloern et al. (1995), which is consistent with the average value measured in paper III during the exponential growth phase. Bacterial production can be estimated via dark DIC fixation in anapleurotic reactions, but typically, a biomass experiment is needed to obtain conversion factors for gDIC $gPOC^{-1}$ for a specific environment. Due to logistical limitations in the field we used the only reported conversion factor for marine microbes in deep-sea sediments of 190 mol POC (mol CO_2)$^{-1}$ (Molari et al., 2013). I am aware of the limitations and compared the estimate growth rates to other Arctic bacterioplankton studies. Bacteria biomass was estimated from cell counts based on a conversion factor of 20 fgC $cell^{-1}$ widely used for bacterioplankton (e.g. Posch et al., 2001).

3.5 FAIR Data

All data of this PhD thesis are archived in public data repositories with open access and permanent accession number following the FAIR (Findable, accessible, interoperable, reusable) data principles. Sequencing data were stored in the European Nucleotide archive (ENA) under the project accession numbers PRJEB40294 (paper IV) and PRJEB40446 (paper II).

Environmental data were stored at the UiT DATAVERSE archive under the doi numbers doi.org/10.18710/MTPR9E (paper IV) and doi.org/10.18710/VA4IU9 (paper III). Environmental data for paper II are given in, and published in an open access paper as part of the FreshFate project. Processed sequence data as OTU and taxonomy tables for paper II are archived at the UiT DATAVERSE (https://doi.org/10.18710/JDWLVA). Detailed descriptions of the fieldwork were stored in the Research in Svalbard database under RiS ID 10889. All papers of this PhD thesis are published or submitted in open access journals. Modelling codes and programs for paper III are available on github under https://github.com/tvonnahm/Dynamic-Algae-Bacteria-model.

4 Summary of the papers

4.1 Paper I: Progress in Microbial Ecology in Ice-Covered Seas

Microorganisms are key players in all marine ecosystems including ice-covered seas concerning biomass, primary and secondary production, and biogeochemical cycling of different elements. This review article first gives a summary of advances in microbiological and biogeochemical methods in the SIZ, before summarizing the current knowledge about microbial diversity, ecology, biogeochemical functions, and seasonality (See ch. 1.2 of this thesis; Fig. 8) and pointing out knowledge gaps and future directions. The gaps include the understanding of the diversity and biomass ("Who is there?") for key taxa in ice-covered seas, including the understudied group of marine fungi. Biomarker studies (e.g. sterols), omics studies (e.g. metabarcoding; See ch. 5.3.2 of this thesis, paper II), and the use of FISH are discussed as potential methods to fill these gaps. The importance of key biogeochemical processes, such as chemoautotrophy, cryptic carbon cycling and mixotrophy, are discussed. Omics approaches, sea ice *in situ* technologies, and isotope probing experiments are discussed as promising tools to detect the pathways and their importance for biogeochemical cycles (See ch. 5.3 of this thesis). The polar night is pointed out as an active and important season for microbial activities, which has only recently been considered biologically active (See ch. 5.1.1.5 of this thesis). The review concludes that understudied organisms, such as fungi, and various biogeochemical processes should be included in biogeochemical models (e.g. paper III) in order to forecast the effect of climate change on the ecosystem. The major points of this review are integrated throughout this PhD thesis and addressed in the related research papers.

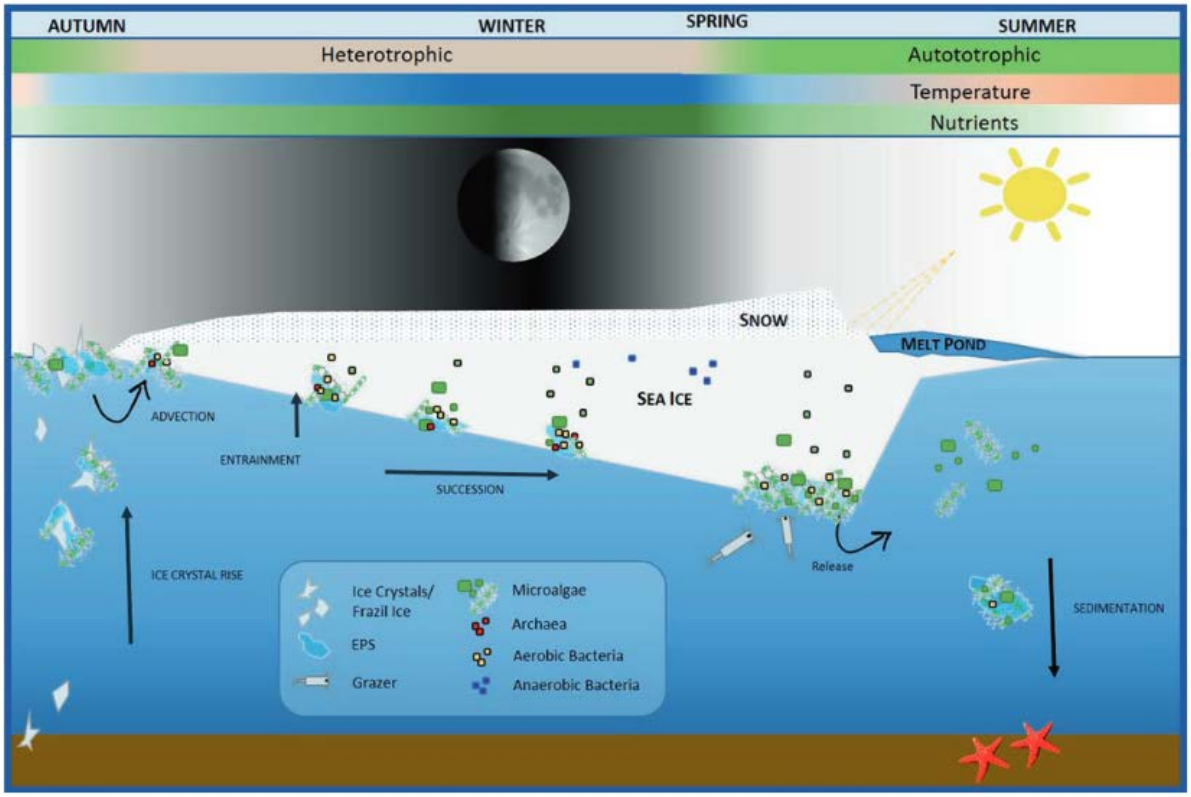

Fig 8. Summary of current knowledge on microbial ecology in the SIZ (Vonnahme et al., 2020). Sea ice is formed in autumn/winter and may incorporate microbes via rising ice crystals or advection through the ice. EPS may facilitate the attachment to the ice. During the polar night, sea ice algae are present, but the community is net heterotroph with mixotrophic algae playing a potentially important role. Later in winter/spring, anaerobic pockets may form allowing anaerobic bacteria to grow. In spring, sea ice algae are more dominant sustaining a sympagic food web before the sea ice algae bloom is terminated giving place to a phytoplankton bloom. During this time vertical export fluxes, feeding the benthic system increase.

4.2 Paper II: Terrestrial Inputs Shape Coastal Microbial Communities in a High Arctic Fjord

Coastal marine systems in the Arctic are affected by large amounts of freshwater inputs from rivers, which is increasing with climate change. These runoffs are changing with season, with snowmelt-dominated meltwater during the spring freshet, and glacier melt and permafrost thaw fed water later in summer. This study investigated bacterial and archaeal communities in the rivers, fjord water and fjord sediments using a 16S rRNA metabarcoding approach in the Isfjorden fjord system in early (June) and late (August) summer. We studied the effects of these different inputs and environmental controls on their communities and potential functions. The high spatial resolution of the samples showed, for the first time, robust and clear gradients from river to marine influenced communities, especially in late summer. Microbial communities were significantly different in later summer with a lower richness, potentially due to less input of river taxa, compared to early summer. The key environmental drivers were nutrient and organic matter inputs from the rivers. Potentially more labile organic matter favors copiotrophic taxa during the spring freshet, while more refractory organic matter and high nutrient inputs favor more cosmopolitan and oligotrophic taxa in late summer (Fig. 9). In contrast to earlier studies on large Arctic rivers, we suggest that river inputs have substantial impacts on microbial communities in Svalbard fjord mainly by providing DOM and nutrients available for bacterial production in the fjord. In addition, the stronger stratification in late summer was identified as important variable explaining the differences. In the late summer communities, Gammaproteobacteria, Verrucomirobiae, *SAR 11,* and other potential oligotrophs (OM60, SAR92) were more abundant, while the potential copiotrophic taxa Bacteroidia, *Octadecabacter* sp., and *Sulfitobacter* sp. were more abundant in June (Fig. 9). Careful considerations of the potential functions of the communities| indicated that the biogeochemical cycles of C, N, and S were potentially affected by the changes in river runoff, but further studies using activity measurements (See paper I) are needed to confirm and quantify these effects.

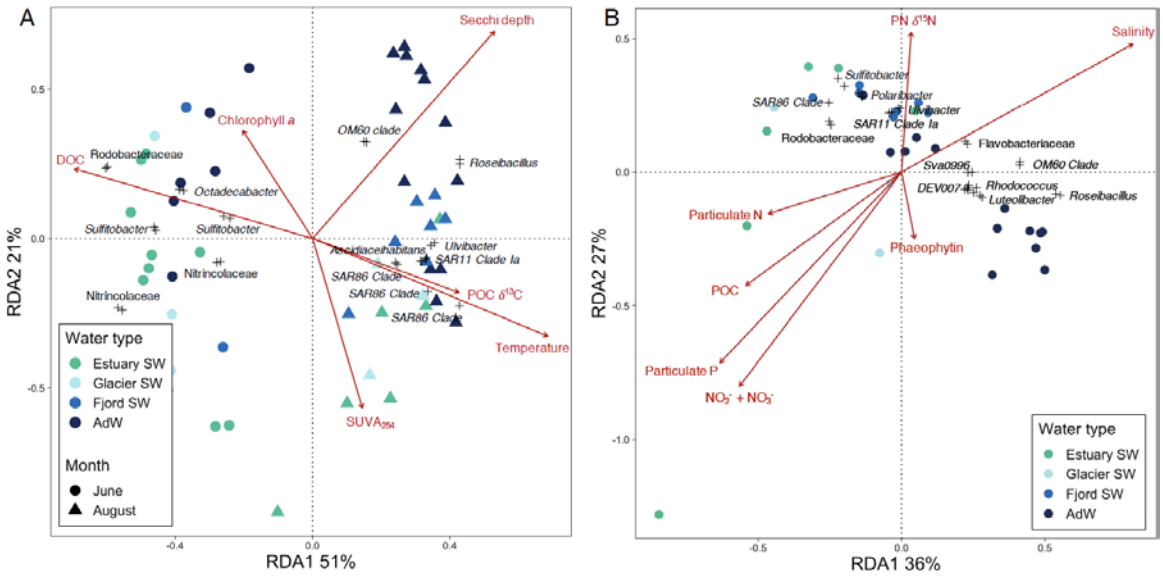

Fig 9. Results of the redundancy analyses, showing main differences between seasons and sites with the correlating indicator taxa (using the indicspecies packagae) and explanatory environmental variables of A) all data and B) August (Delpech et al., submitted).The clearest separation is between June and August communities (RDA1 axis) with a secondary gradient from estuaries to fjord and advected water (AdW) samples (RDA2 axis), which is, however, only significant in August (ANOSIM, $p<0.05$). June communities are driven by more DOC and Chlorophyll a, and lower temperatures and $\delta^{13}C$ POC. Marine communities are mostly driven by clearer water (deeper Secchi depth, higher UV light adsorption by aromatic compounds measured as $SUVA_{254}$). Further details are given in paper II.

4.3 Paper III: Modelling Silicate–Nitrate-Ammonium co-limitation of algal growth and the importance of bacterial remineralization based on an experimental Arctic coastal spring bloom culture study

In Arctic coastal ecosystems, primary production is typically highest during a pronounced spring bloom mostly dominated by diatoms (paper I, IV). The spring bloom is initiated once the water column stratifies, while high inorganic nutrient concentrations supplied via winter mixing fuel rapid growth. These blooms are typically terminated by inorganic nitrogen, and/or silicate limitation. Bacterial remineralization of DOM, originating either from primary production, or terrestrial inputs, can lead to ammonium regeneration and regenerated production extending the bloom. While these processes are generally well described, quantitative modelling of these dynamics has been challenging with detailed physiological models being too complex for ecosystem sale models. Full-scale ecosystem models are mostly too simplified, either neglecting the role of bacteria, or simplifying the different physiological responses of diatoms to Si or N limitation. We recreated typical spring bloom dynamics in a cultivation experiment with the model diatom *Chaetoceros socialis* and the model bacterium *Pseudoalteromonas elyakovii*. The experiment started with non-limiting nutrient concentrations. Under axenic conditions, the algal growth terminated after Si and N became both limiting, while reduced growth was enabled in the presence of bacteria supporting regenerated production (Fig. 10). In fact, 69% of the production in the presence of bacteria was estimated to be regenerated production. Based on this experiment we developed a dynamic model taking cellular C:N:Chl quotas, different responses to the different nutrient sources, and bacterial NH_4 remineralization into account. Our model reproduced the dynamics of the cultivation experiment well (Fig. 10), while keeping the complexity comparable to algae growth formulations in common ecosystem scale models. I suggest that accurate representation of bacterial remineralization and uncoupling of Si:N metabolism is crucial for modelling the impact of climate change on spring blooms via increased heterotrophic activities with increasing temperatures and terrestrial DOM inputs (paper II).

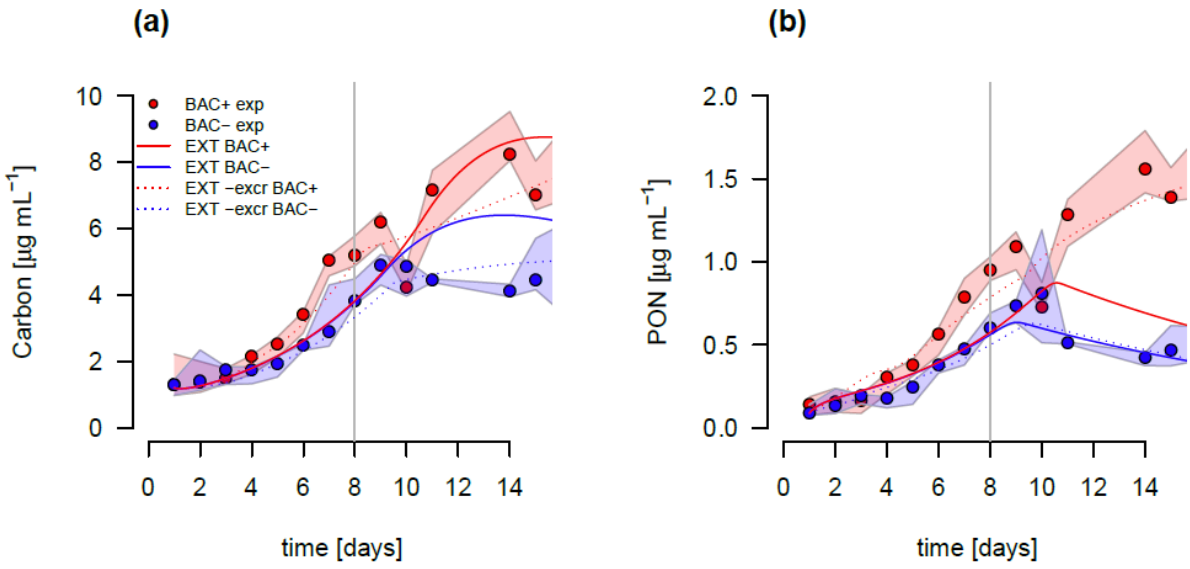

Fig 10. Experimental data on diatom growth as POC (a) and PON (b) changes under axenic (blue) and bacteria-enriched (red) conditions and the fit of our dynamic model (lines), showing model simulations with carbon excretion and without excretion. Circles show median values and shaded polygons show the total range of measured data (max and min). The solid lines show the model fit including DOM excretion by algae and the dotted line show the model fit without Dom excretion. Differences are small due to high concentrations of terrestrial DOM in the water used for the experiment (collected outside Tromsø). For further details, see paper III.

4.4 Paper IV: Subglacial upwelling in winter/spring increases under-ice primary production

Recently, subglacial upwelling was identified to supply nutrients via upwelling, leading to increased biological production near tidewater glacier fronts in summer. In winter and spring, this process has not been considered important due to the limited freshwater outflow. However, we hypothesized, that subglacial outflow is present in winter/spring, and that it is sufficient to increase primary production in a sea ice covered fjord as soon as sufficient light is available. We found indeed circumstantial evidence for subglacial upwelling, such as a brackish surface layer and sea ice, a turbidity peak at the halocline, glacial bacteria taxa under and in the sea ice, and icing in front of the land-terminating site of the glacier. We estimated a freshwater flux of roughly 1.1 m^3 m^{-2} $month^{-1}$ and an entrainment factor of 1.6 (1.6m^3 marine bottom water (m^3 subglacial freshwater)$^{-1}$), which is much lower than values reported in summer. However, in the fjord with slow tidal currents (0.1 cm s^{-1}), and wind mixing blocked by sea ice, the flux was sufficient to sustain a stratified 4 m thick surface layer under the sea ice with two orders of magnitude higher phytoplankton primary production at the glacier front, compared to a reference station near the sea ice edge (Fig. 11). The increased primary production was attributed to i) subglacial upwelling of nutrient rich bottom water, ii) direct silicate input with the meltwater, iii) increased light due to a thinner snow cover, potentially related to katabatic wind removal, and iv) a more stably stratified surface layer. Sea ice algae were negatively affected due to low brine volume fraction caused by the low salinity and thereby limited permeability and habitable place. Community structures of bacteria, archaea, algae and other eukaryotes were significantly different at the tidewater glacier-influenced site compared to the reference site. To my knowledge, this is the first study to show subglacial upwelling effects on spring carbon cycling and microbial communities.

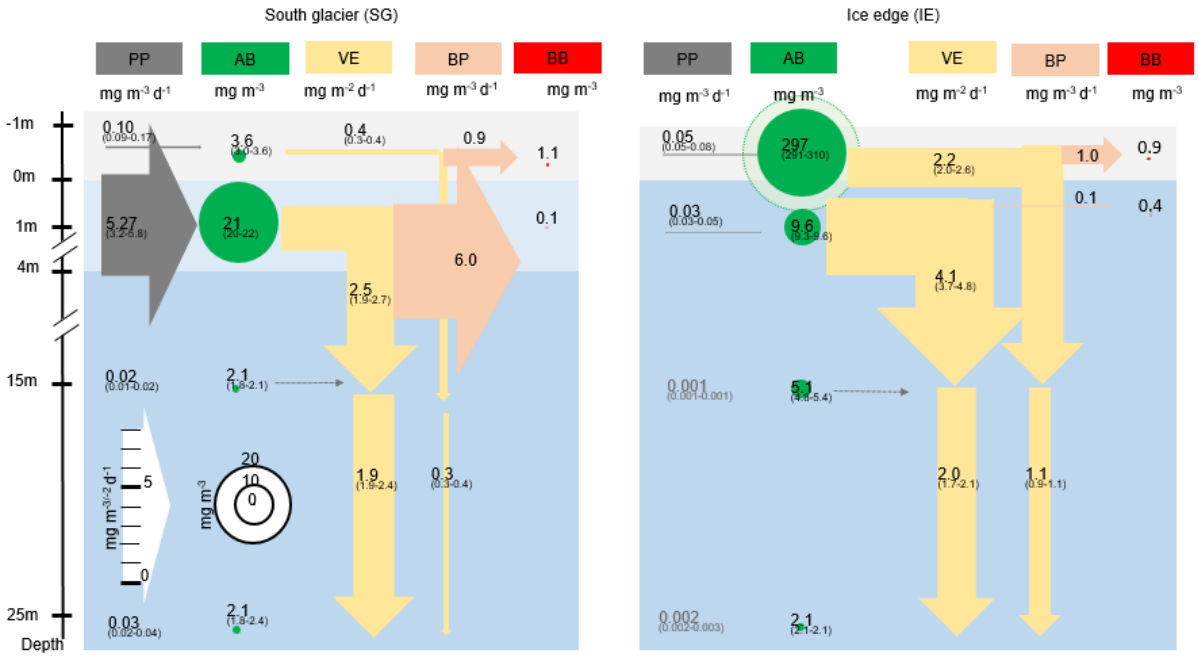

Fig 11. Differences of the biological carbon cycles between the tidewater glacier influenced South glacier site (SG) and the ice edge marine reference site (IE), in sea ice (grey layer), the 4 m thick stratified surface layer at SG (light blue), and the water column (blue). All values are in carbon units. Primary production (PP), Algae biomass (AB), vertical export (VE), bacterial production (BP), and bacterial biomass (BB) are given with their median values and min - max. The arrow thickness and circle diameters are scaled as shown in the legend under SG (Except for the light green circle for AB at IE, which is one order of magnitude higher). For details about the measurements, assumptions and conversions, see paper IV.

5 Synthesis of results and discussion

Detailed descriptions of the individual results and discussions can be found in the research papers (II-IV). Here, I take the opportunity to put the papers and their results into context to each other, giving a more complete picture about the seasonal cycle of land-ocean interactions and microbial ecology, bacteria-algae interactions, and methodological challenges. Where helpful, I include a few, yet, unpublished own data as support. I start with combining the results of all papers to describe seasonal dynamics in the coastal Arctic SIZ from spring to winter with a focus on land-ocean interactions and key taxa and potential environmental drivers. I continue with a detailed discussion about the role and fate of bacteria entering the fjords via rivers, which has only been discussed briefly in paper II and IV. I then continue to discuss bacteria-algae interactions, starting with the controls of bacteria by terrestrial inputs vs algae exudates with a detailed discussion of bacterial succession using data from Billefjorden. I then discuss the importance of bacteria for algae growth with a focus on regenerated production. Finally, I discuss some of the methodological challenges, such as; how to measure primary production? can metabarcoding replace classical taxonomy? and how to sample sea ice?

5.1 Land-ocean interaction in the coastal Arctic sea ice zone

The first objective of the practical part of this PhD thesis was to study the impacts of terrestrial freshwater inputs on the marine microbial food web. We studied the effects of subglacial outflows in winter/spring on a sea ice covered fjord (paper IV), the impacts of river runoff during the freshet in spring (paper II), and the impacts of glacier melt fed rivers in late summer (paper II). We show that all of these inputs are shaping the physicochemical environment of the fjord systems and thereby the microbial food web. We found freshwater input to be a major control on bacterial and algal communities, activities, and their biogeochemical potential and functions. These findings show that freshening of the Arctic will have severe effects on the marine food web, by altering carbon sources and fluxes into the microbial food web. In addition, climate feedbacks related to the balance of CO_2 fixation and respiration are likely.

5.1.1 Seasonal changes in the coastal Arctic sea ice zone

The PhD thesis studies coastal Arctic systems affected by terrestrial freshwater inputs at various seasons. This allows me to describe a full seasonal cycle of the effects of terrestrial freshwater inputs on the microbial food web. For completion, the following chapters also include some

discussion of, yet unpublished results of additional work in autumn/winter done during my PhD.

5.1.1.1 Sea ice covered fjords in winter/spring

From January to May, some Svalbard fjords are sea ice covered and therefor part of the seasonal ice zone. During this time, terrestrial inputs of freshwater have previously been considered negligible (Mortensen et al., 2013). The marine food web is considered to be mostly controlled by oceanographic and climatic forcing, leading to a characteristic phenology of heterotrophs dominating in winter, sea ice algae dominating in early spring, and subsequent phytoplankton blooms once the sea ice has melted (Leu et al., 2015). However, studies in other Arctic systems indicate that terrestrial inputs may be more prominent than has been often considered. A base flow of river water has been found in all large Arctic rivers with high concentrations of nutrients (Kaiser et al., 2017). Due to the polythermal base of most Svalbard glaciers (Hagen et al., 1993), subglacial outflow visible as proglacial icing has been described at several land-terminating glaciers on Svalbard (e.g. Hodgkins, 1997). Some studies based on physical oceanography found also inputs of glacial meltwater in Greenland (e.g. Moon et al., 2018) and in Tempelfjorden on Svalbard (Alkire et al., 2015; Fransson et al., 2020). In summer, subglacial upwelling is a major process adding nutrient-rich bottom water to the stratified surface layer (Halbach et al., 2019; Hopwood et al., 2020). These inputs have been described to increase primary production, feeding a productive marine food web including zooplankton, fish, and seabirds (Lydersen et al., 2014, Meire et al., 2016). Terrestrial freshwater inputs in winter/spring may be substantially less than in summer. However, I hypothesize that in systems with little other water exchange (e.g. advection, precipitation), such as sea ice covered fjords isolated by a shallow sill, even limited input especially from the subglacial system may still have a substantial impact on the microbial food web. We used Billefjorden as a case study to test if terrestrial inflow via subglacial meltwater is present and if it has any impacts on the microbial food web.

We found indeed various indications for subglacial outflow, rich in silicate, and the capability to pull 1.6 times as much nitrate-rich bottom water with it to the surface. These subglacial inputs contributed to a 4 m thick stratified surface layer under the sea ice with about 32 % of its volume originating from glacial ice melt. The sea ice structure is highly affected by the freshwater inputs leading to low brine volume fractions mostly below 5 %, a threshold under which sea ice is considered impermeable (e.g. Granskog et al., 2003). Overall, this finding is similar to

earlier studies in Greenland showing basal glacier and ice berg melt (Moon et al., 2018), and on Svalbard (Tempelfjorden) showing glacial melt affecting stratification and sea ice structure in Tempelfjorden (Fransson et al., 2020) with fall/winter subglacial upwelling as a major freshwater source (Alkire et al., 2015). Alkire et al. (2015) also attempted to measure subglacial freshwater inputs in Billefjorden, but found no evidence for glacial meltwater in the fjord. This can be explained by their sampling location at the northern mostly land-terminating site of the glacier front, where we did not find substantial freshwater inputs either. Based on circumstantial evidence, each of them not conclusive on its own, but supporting the same hypothesis, we concluded for the first time that meltwater is derived from persistent subglacial outflows in winter/spring (Fig. 12). However, for a solid conclusion if and how much subglacial upwelling is really happening in winter/spring, we need additional data from e.g. continuous *in situ* salinity measurements, ROV recordings and sampling directly at the glacier-fjord interface, or $\delta^{18}O$ measurements (e.g. Alkire et al., 2015).

We went one-step further than previous winter/spring studies and investigated the impacts of subglacial upwelling on the microbial food web and carbon cycle. To my knowledge, this is the first study that includes biological processes during this time of the year. We found substantial impacts on microbial communities and activities, affecting the entire carbon cycle (Fig. 11). Phytoplankton primary production was two orders of magnitude higher in the presence of subglacial upwelling (Fig. 11, 12). We attributed the increased production partly to the inputs of silicate and nitrate, which we clearly showed in a reciprocal transplant experiment (water chemistry increased primary production 3-fold; Fig. 12). However, water chemistry alone could not explain the full increase of primary production. In fact, under-ice phytoplankton blooms are often controlled by light (e.g. Leu et al., 2015, Ardyna et al., 2020a.b), or surface stratification (Lydersen et al., 2017), rather than nutrients. In our study, we found both, a stratified surface layer and a thinner snow cover (potentially thinner due to strong katabatic winds)(Fig. 12). This thinner snow layer would allow more light to reach the water column, while the stratified surface layer allows phytoplankton to stay longer in the euphotic zone (Sverdrup 1952; Lydersen et al., 2017). In the brackish sea ice, algae biomass and primary production was negatively affected, most likely due to the low brine volume fraction and permeability, inhibiting water and nutrient exchange with the water column and limiting inhabitable place (Granskog et al., 2003). Eukaryotic and prokaryotic communities were significantly different at the glacial meltwater influenced site. Most remarkable is the finding of sea ice algae

communities dominated by flagellates (*Thaumatomastix* sp., cyptophytes (*Hemiselmis* sp., Geminigeraceae)) and the centric diatom *Leptocylindrus* sp., all taxa typically not described as high-Arctic sea ice algae (Von Quillfeldt et al., 2009). Ongoing work found some of the same taxa abundant in brackish sea ice in a northern Norwegian fjord (Ramfjorden), indicating that they are preadapted to live in sea ice with low brine volumes and permeability independent of their geographical location.

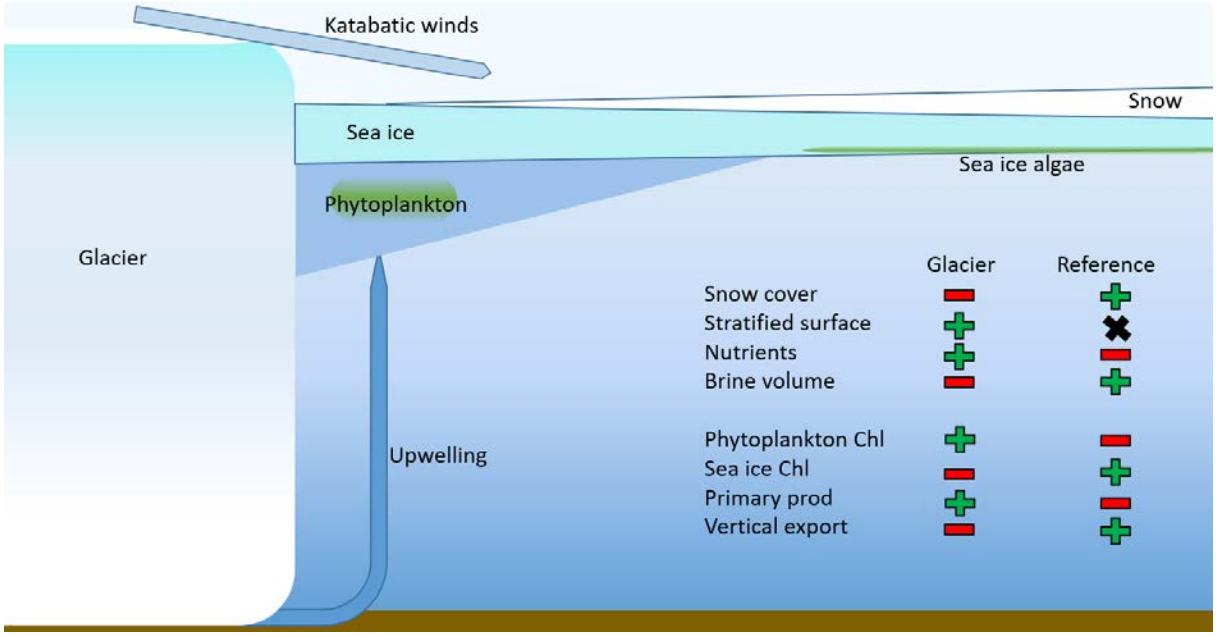

Fig 12. Summary of the impacts of subglacial upwelling on physicochemical sea ice and water properties and algae biomass, primary production and export. The blue arrows indicate the main suggested drivers: subglacial upwelling (dark blue), and katabatic winds (light blue). The red – shows lower values, the green + shows higher values, and the black X the absence of the measured variable.

5.1.1.2 The spring phytoplankton bloom

In higher latitudes, spring is the most productive time of the year with respect to primary production. Thus, many studies investigated dominant algae and bacteria taxa, physicochemical controls, and the phytoplankton phenology during this time of the year (von Quillfeldt, 2000; Leu et al., 2015; See paper I and Introduction). Briefly, nutrients supplied by winter mixing in combination with a stratifying water column allows rapid growth of phytoplankton mostly dominated by centric diatoms until nutrients are used up and the bloom is terminated (Sverdrup, 1953; Siegel et al., 2002; von Quillfeldt, 2000; Fig. 14). However, this paradigm has been

challenged and the spring bloom system may not be as simple with spring blooms observed in mixed water columns (Hegseth et al., 2019; Behrenfeld, 2010). Terrestrial inputs in spring may vary between being absent; over slow subglacial upwelling (5.1.1.1); to large amounts of meltwater during the freshet. The contribution of this PhD thesis is to improve current representations of diatom physiology and interactions with bacteria in biogeochemical models, from the onset of the spring bloom until nutrient depletion. For accurate parameter fitting and controlled environmental controls, we recreated typical spring bloom dynamics using a common spring-bloom diatom species and an associated bacteria species in a cultivation experiment. The model diatom *Chaetoceros socialis* (paper IV) and the model bacterium *Pseudoalteromonas* sp. (paper II) were also abundant in our field studies. In fact, *Chaetoceros socialis* was the single most abundant species in Ramfjorden in spring 2019 (Fig. 14). We fitted a widely used dynamic model of phytoplankton dynamics responding to varying nutrients and light by Geider et al. (1998) to the axenic experiment. We show some limitations of the model and provide extensions to include silicate-nitrate-ammonium co-limitation and bacterial regeneration of ammonium, which we identified as crucial processes needed to model phytoplankton spring blooms. The extended model gave a substantially better fit to the bacteria-enriched experiment (55% reduction of model cost), while keeping complexity low. We showed that bacterial regeneration of ammonium is needed to model an extended spring bloom based on regenerated production (f-ratio = 0.31) and we showed that diatoms respond differently to silicate or nitrogen limitations due to different physiological responses.

5.1.1.3 The spring freshet.

The highest amount of freshwater is reaching the fjords with snowmelt during the spring freshet (McGovern et al., 2020). Earlier studies on the large Arctic rivers (Holmes et al., 2012) and on Svalbard (MCGovern et al., 2020) showed that river water at this time of the year is rich in labile organic matter, and terrestrial POC, but rather poor in inorganic nutrients. The allochthonous DOC may be supplemented by autochthonous DOC produced by phytoplankton. In fact, phytoplankton spring blooms typically occur just before the freshet, as indicated by higher Chl a values in June. While the impacts of the spring freshet on coastal hydrography and chemistry is rather well studied (e.g. McGovern et al., 2020), the impacts of the riverine inputs on the microbial food web is poorly understood. The high spatial resolution of our study, including various rivers, estuaries and fjords in the Isfjorden system allowed detecting patterns of bacterial and archaeal communities typical for this part of the year. We identified DOC and

terrestrial derived POC to be major controls on spring communities. Mostly copiotrophic bacterial taxa (e.g. *Sulfitobacter* sp., *Octadecabacter* sp., Gammaproteobacteria) were dominating the communities during this period (Fig. 9; Fig. 13). These taxa have been discussed as efficient degraders of more labile OM responding to algae polysaccharide addition (Jain et al., 2020). We identified specific indicator taxa dominant in systems influenced by river inputs during the freshet which have also been described in other studies in similar systems (e.g. Bunse and Pinhassi, 2017; Sinha et al., 2018; Jain et al., 2020).

5.1.1.4 Summer river runoff

Later in summer, rivers are increasingly fed by glacier melt and permafrost thawing with associated substantial changes in the freshwater properties compared to the snowmelt phase. McGovern et al. (2020) found about 12 times higher concentrations of nutrients, lower sediment concentrations, and a higher fraction of potentially refractory organic matter (humic and aromatic substances) in the rivers of Isfjorden. During this time, the fjord surface layer is also strongly stratified with substantial impacts on the microbial food web (Fig. 13). The surface layer can act as a distinctive niche for microbes, but blocks also nutrient and DOM supply from deeper water layers. We found significant differences in microbial communities in different water masses in August, but not in June (Fig. 9). We also found more oligotrophic and cosmopolitan taxa potentially more adapted to the refractory organic matter and high surface temperature (e.g. SAR11, OM60, SAR92, + Verrucomicrobiae). Flagellates dominated algae communities in Billefjorden during this time (Vonnahme, unpublished data). Despite the increased nutrient concentrations in the river water, nutrient concentrations in Billefjorden stayed low, explaining the dominance of potential mixotrophs adapted to low-nutrient conditions.

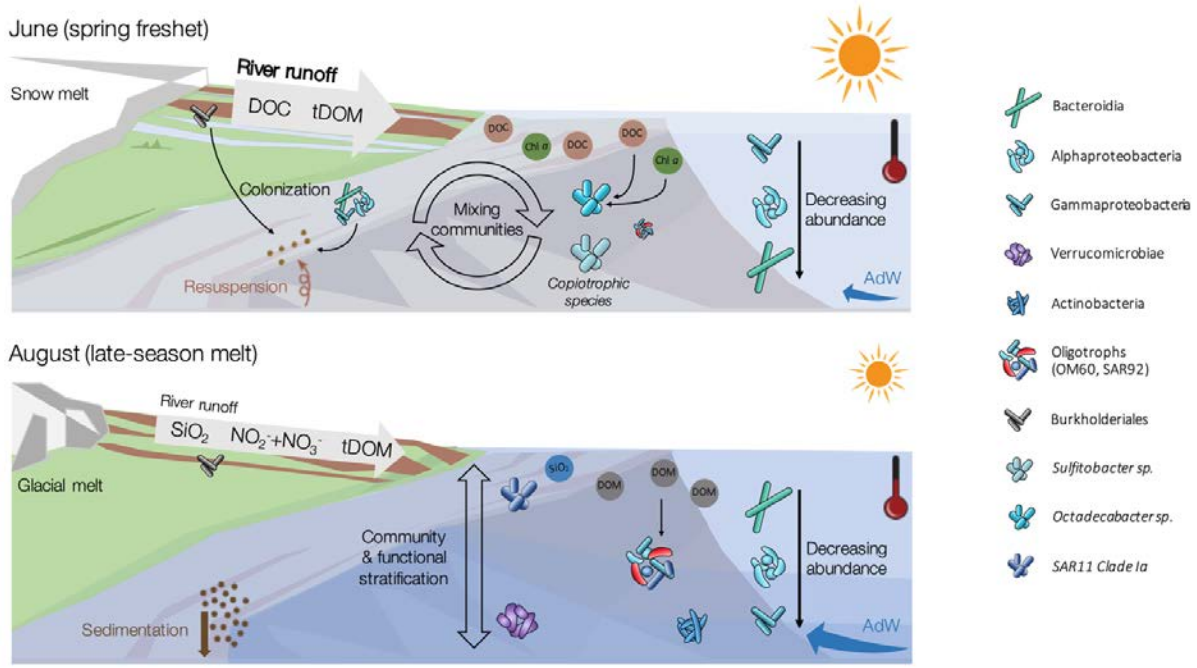

Fig 13. Summary of the environmental drivers associated with river runoff in June (freshet) and August (summer) and the different associated key taxa in the microbial communities in Isfjorden (Delpech et al., submitted, paper II).

5.1.1.5 Ongoing work on autumn and winter systems

While the autumn and the polar night are not part of the PhD thesis, I want to give a brief summary of ongoing work in this field to complete the synthesis of the seasonal cycle in the coastal Arctic SIZ. In autumn, freshwater inputs are decreasing, while the surface water cools down, leading to a weakening stratification and eventually mixing of the water column (e.g. Eilertsen and Taasen, 1984; Cottier et al., 2010; Carooppo et al., 2017). If the water column mixes while light is still available the input of nutrient rich bottom water may fuel an autumn bloom. In Ramfjorden, a northern Norwegian fjord, we found indeed an autumn bloom in September 2019, when temperatures and precipitation were low. However, in 2018, higher temperatures and more precipitation lead to a strongly stratified water column until December and no autumn bloom was detected. A weak mixing event in November allowed some increase in *Pseudo-nitzschia* sp., *Scripsiella* sp., and *Skeletonema* sp. abundances (Fig. 14), but Chlorophyll values were far below the other years.

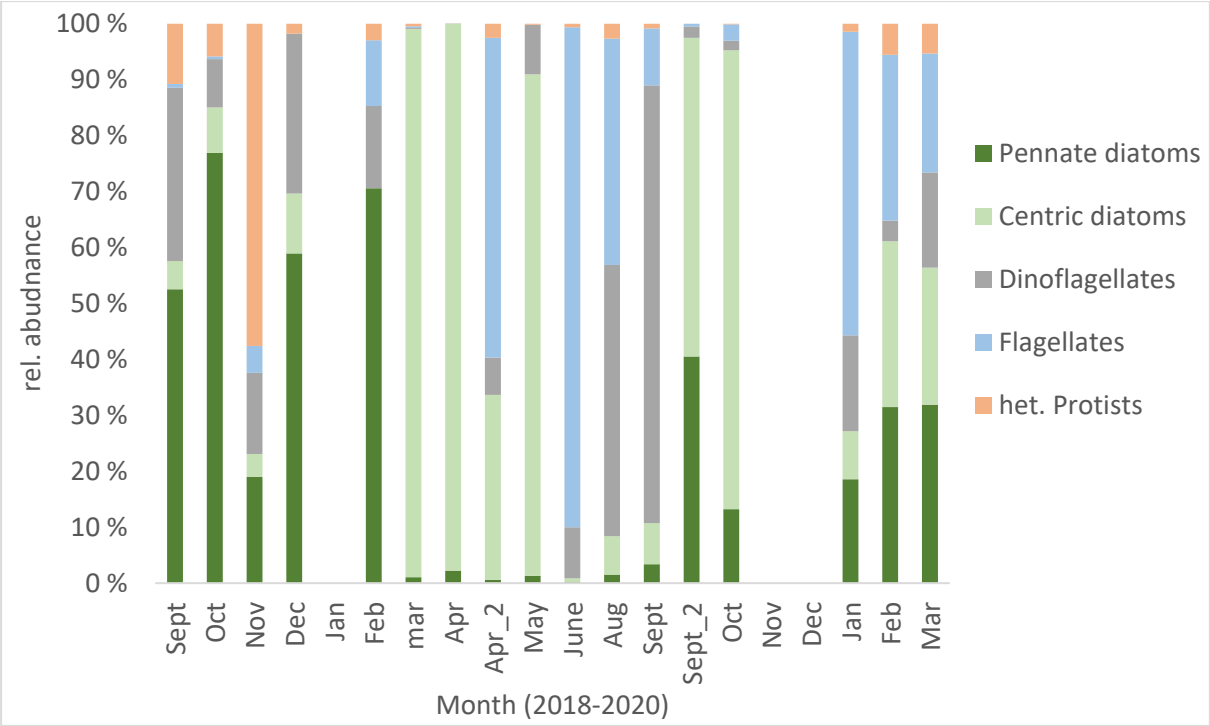

Fig 14. Microalgal community structures between September 2018 and March 2020 in Ramfjorden, counted from phytoplankton net hauls (10 µm mesh size) from 35 m to the surface in the entrance of the fjord. Counts from Sept to Feb 2018 by Line Klausen, Rose-Marie Bank and Tobias Vonnahme. All other counts by Tobias Vonnahme.

During the polar night, we took samples for 18S and 16S metabarcoding of DNA and cDNA around Svalbard in the Polar night and in Ramfjorden (Fig. 15). I found Dinophyceaea to be most dominant in the present communities (DNA, genomic sequencing) around Svalbard and in Ramfjorden during autumn and spring. During the polar night in Ramfjorden, the radiolarian group of Polycystina was most abundant. The same class has been found on Svalbard, but only at the West coast, indicating that this is a class either adapted to Atlantic water conditions, or advected to Svalbard with the West Spitsbergen current. The active communities around Svalbard (cDNA, ribosome sequencing) were significantly different from the present community, with Dinophyceaea being rare and Oligotrichae ciliates being most abundant. The substantial difference indicates that Dinoflagellates are most likely just surviving the polar night, while ciliates are thriving in it. This makes sense considering that most Dinoflagellates are mainly phototroph with the potential for mixotrophy (constitutive mixotrophs), while ciliates are mainly heterotroph with the potential for mixotrophy (non-constitutive mixotrophs) via kleptoplastidy (Mitra et al., 2016). Future metabarcoding studies should consider a similar

approach of combined metatranscriptomics and metagenomics. Only Billefjorden has Flabellinia, Centrohelea, and Intramacronucleata as additional dominant active classes, which are however, almost absent in the present community.

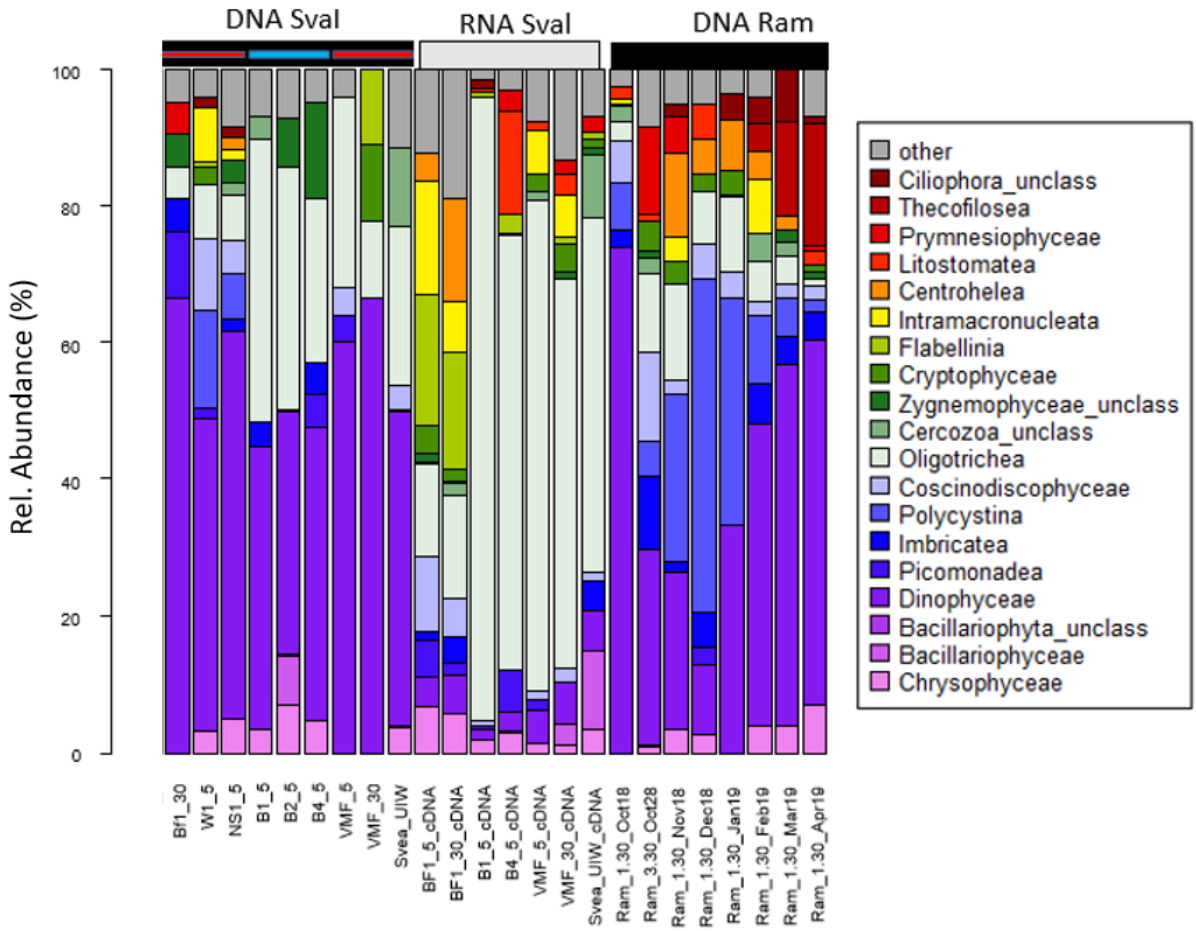

Fig. 15. Protist community structure on class level in the Polar night based on 18S Metabarcoding of DNA and RNA (transcribed to cDNA) samples around Svalbard (November 2017) and in Ramfjorden (September 2018 to April 2019). Red bars on top indicate West Svalbard samples and the blue bar East Svalbard samples.

During the polar night, we studied microbial communities and activities in the same northern Norwegian fjord and at different stations around Svalbard. As indicated by earlier studies, we found a diverse algal community in all stations, but activities were mostly heterotrophic (^{13}C labelled Glycine vs CO_2 uptake). However, some CO_2 has been fixed throughout the polar night in northern Norway, indicating the efficient use of low light levels. Different mechanisms of algal survival in the polar night have been discussed including, adaptation to extremely low light, spore formation, reduced activities, feeding on storage compound, and heterotrophic

carbon uptake (Zhang et al.,1998; Kvernvik et al., 2018; Johnsen et al., 2020). We found indeed CO_2 fixation under very low light in November in Ramfjorden. I hypothesize that heterotrophic carbon uptake is an important survival mechanism not only for certain specialized taxa as suggested by Johnsen et al. (2020), but for all microalgae including diatoms. I developed an experiment, where we tracked ^{13}C labelled glycine into algae sugar (e.g. sucrose, laminarin) and fatty acid biomarkers (Metabolomics SIP). On Svalbard, we were indeed capable of showing heterotrophic glycine uptake by algae, preferably in darkness, by tracking ^{13}C labelled glycine into sucrose as algae biomarker. Few studies attempted to measure heterotrophic carbon uptake in diatoms in the Antarctic and Arctic, using radiographic methods (Palmisano et al., 1985; Rivkin and Putt, 1987; Horner and Alexander, 1972), but only studies under complete darkness found substantial uptake (Rivkin and Putt, 1987), while studies in presence of light found heterotrophy in algae to be negligible (Horner and Alexander, 1972). To my knowledge, our metabolomics SIP experiment is the first study to show heterotrophic carbon uptake by algae as adaptation to darkness in the.

5.1.2 Allochthonous inputs of microbes

The dogma of microbial biogeography 'Everything is everywhere, but, the environment selects' by Baas Becking (1934) implies that a water sample, collected anywhere in the ocean, would allow to retrieve the entire global bacterial diversity, while the dominant community is governed by the environment. With advancing molecular methods, allowing a more detailed investigation of bacterial diversity, down to ecotypes defined by single nucleotide variances (e.g. Haro-Moreno et al., 2020), this dogma has been challenged widely (O'Malley, 2008; Livermore & Jones, 2015; Zorz et al., 2019). I hypothesize that bacteria communities may be distinctively different in environments, sufficiently different, such as rivers and fjords. However, I also suggest that terrestrial and river bacteria may be imported into the fjords, potentially inhabiting new suitable environments, which would partly support the dogma by Baas Becking (1934). However, I suggest that most taxa imported with river water do most likely not survive or grow due to their pre-adaptation to terrestrial and freshwater systems concerning salinity, organic matter availability, and oxygen (Waleron et al., 2007). In contrast to Baas Becking (1934), I thus hypothesize that bacterial taxa have a limited residence time under sub-optimal conditions. The imported taxa can however increase local diversity (as found in paper II) making coastal ecosystems more diverse. In addition, the strong seasonality in high

latitudes leads typically to a high bacterial diversity in a global context (e.g. Ladau et al., 2013). Thus, I argue that high latitude coastal systems may be prominent diversity hotspots.

Spatial proximity may allow the imported taxa to inhabit other suitable environments. The identity, fate and ecological function of these imported groups for the marine system were addressed in few previous studies with limited technologies, such as bacteria counts (Vallieres et al., 2008), or clone libraries (Waleron et al., 2007). Other studies had sampling designs limited by spatial and temporal resolution representing only one fjord with few samples (Garcia-Lopez et al., 2019), or only sediments, missing the terrestrial endmembers (Jørgensen et al., 2020).

We found evidence of riverine input of terrestrial bacteria during the freshet in June (paper II) in shared OTUs and estuarine community structures similar to rivers. The imported taxa belonged to the rare biosphere, indicating that they have little importance for the marine microbial food web. However, as shown in Fig. 15 the rare biosphere may well be part of the active community (based on cDNA sequencing of ribosomal RNA). Furthermore, sufficient OTUs were imported during the freshet to lead to a significant higher OTU richness, compared to late summer. Some functions related to these taxa, such as sulfate reduction, denitrification, and methane oxidation are typical in anoxic sediment and soil environments, but not likely, in the oxygenated water column, which indicates that the imported taxa were not only rare, but also inactive. While terrestrial microbes appear not to be relevant for marine plankton communities, we found a number of terrestrial taxa in marine sediments, not only in June but also in August. This finding indicates that terrestrial taxa may be transported to marine sediments and stay alive for at least several months. Marine sediments may also be similar enough to soil and permafrost environments to allow functions, such as denitrification, sulfate reduction, and methane oxidation to occur. The same hypothesis may be true for chemotrophic bacteria frozen into sea ice, experiencing anoxic conditions, or cyanobacteria thriving in melt ponds with low salinity and high light levels. However, further coupled activity-diversity studies, such as cDNA/DNA sequencing, or DNA-SIP are needed to confirm these hypotheses (e.g. Deng et al., 2018).

We also found a higher fraction of phototrophs and N_2 fixers, related to riverine inputs. These functions are possible in the oxygenated water column and may even give an advantage in the brackish nitrogen-depleted water column in June. An earlier study also found picocyanobacteria

from large Arctic rivers reaching the coastal environment, being viable but inactive under the conditions of the study (Waleron et al., 2007). This leads to the question if terrestrial derived cyanobacteria are also viable in our study and if they play any role in the marine food web. Cyanobacteria are also commonly found in melt ponds (Fernandez-Mendez et al., 2016) in the central Arctic Ocean opening the question if these taxa were initially imported by rivers, surviving in a dormant stage until the conditions were optimal (low salinity), which would be in agreement with Baas Becking's dogma (1934). Further activity measurements and stable isotope probing experiments, may clarify how active these taxa are. Detailed genetic population studies may additionally help to find out if some of the sediment, sea ice, and melt pond taxa originate from land and from which geographic region (e.g. Okazaki et al., 2020).

Our overall conclusion of paper II is that terrestrial taxa are introduced to the marine system, mainly during the spring freshet, but are likely not active in the marine water column as indicated by earlier studies. This finding is further supported by our finding that they are not detectable anymore in late summer. This conclusion may allow using terrestrial bacteria as a suitable marker for the origin of freshwater in fjord systems. In paper IV, we studied bacterial community structures of various fjord water and sea ice samples, including various terrestrial endmembers (glacier ice, subglacial outflow, supraglacial meltwater). At the sampling site most influenced by glacial meltwater inputs, we found a community similar to subglacial meltwater communities, supporting our hypothesis of subglacial meltwater as the main endmember for the freshwater detected on this site. Considering the disappearance of riverine taxa within months (paper II), we use the presence of subglacial bacteria in the water column and sea ice as supportive evidence for a consistent supply of subglacial meltwater in the weeks prior to the sampling. Using bacterial growth rates, we estimated a turnover of the freshwater in the range of weeks to months.

5.2 Bacteria – algae interactions

Interactions of bacterioplankton and algae are diverse and include the full spectrum of ecological interactions; competition, commensalism, mutualism, symbiosis, parasitism and predation (Worden et al. 2015). Bacteria can suppress algae growth by acting as pathogens or parasites, or by competition for inorganic nutrients, but bacteria can also be important for regeneration of nutrients via organic matter degradation, vitamin synthesis, or trace metal chelation and/or reduction (Croft et al., 2005; Sunda, 2012; Worden et al., 2015). For the global

carbon cycle these mutualistic interactions may be most relevant and thus the focus of this PhD thesis. I focused on the simplest interaction of bacteria remineralizing organic matter, either excreted by algae, or imported from land, releasing inorganic nutrients in the process (e.g. ammonium) that can be used by algae for extended growth.

5.2.1 Importance of autochthonous vs allochthonous DOM for bacteria

Paper II shows how DOM can shape microbial communities. During the freshet DOM is typically labile and available for bacteria production, while it becomes more refractory towards summer (McGovern et al., 2020) with a higher fraction likely already degraded on land, especially in the large Arctic rivers (Kaiser et al., 2017). On Svalbard, terrestrially derived DOM can be imported in large amounts (Kulinski et al., 2014; McGovern et al., 2020) but is often considered refractory due to its ancient origin from freshly deglaciated catchments (Kim et al., 2011). However, during the freshet phase, we found evidence for high terrestrial DOC and POC input ($\delta^{13}C$ POC signature) with low amounts of humic and aromatic substances, indicating high bioavailability. At the same time, we found higher levels of Chl, showing a spring phytoplankton bloom as a second source of labile organic matter. These high concentrations of likely bioavailable organic matter allowed copiotrophic bacteria taxa to dominate the communities. Later in summer, a lower DOC and terrestrial POC signature was detected and a high proportion of more refractory humic and aromatic substances were measured. This lead to a bacterial community with oligotrophic taxa becoming more dominant.

Under sea ice in Billefjorden, we found evidence for bacteria production controlled by primary production and algae biomass. We measured an order of magnitude higher bacterial production (based on dark carbon fixation) at the tidewater glacier front where primary production was two orders of magnitude higher and algae biomass two times higher. Considering the low amount of DOC in glacial meltwater (paper II), we do not consider subglacial meltwater as a major DOC source fueling this higher production, but the related increased algae primary production. In fact, sea ice algae and phytoplankton studies commonly find a coupling of primary and secondary production (e.g. Teeling et al., 2012, 2016). Hence, the tidewater freshwater outflow does not only affect primary production, but indirectly also bacterial production. For confirming these hypotheses, pulse chase SIP experiments may help where ^{13}C labelled DIC is tracked via algal primary production into bacteria biomass (e.g. van den Meersche et al., 2004).

5.2.2 Bacterioplankton succession after a spring bloom

Our studies of bacterioplankton communities, ranging from an early spring bloom in Billefjorden to summer communities in Isfjorden and yet unpublished data from autumn and winter allow a careful discussion of potential key taxa for coastal Arctic bacterioplankton successions. The results may help to identify key players for algae exudate degradation in the Arctic, or key taxa facilitated by river input rather than autochthonous production.

Some of the most extensive studies of bacterial succession after phytoplankton blooms were done in the North Sea (Teeling et al., 2012, 2016) in consecutive years. Teeling et al. (2012, 2016) found specific bacterial taxa feeding on specific algae exudates or metabolites by other bacteria in a successive pattern. Flavobacteriaceae (*Flavobacterium* sp., *Ulvibacter* sp., *Formosa* sp., *Polaribacter* sp.), Gammaproteobacteria (*Reinekea* sp., *SAR92*), and Alphaproteobacteria (*SAR11, Roseobacter* sp.) were found to be most abundant and tightly connected to phytoplankton blooms, capable of degrading specific algae exudates. Similarly extensive succession studies in the Arctic are rare, but point to the overall same taxonomic groups responsible with increasing amplitudes of population dynamics with latitude (Bunse and Pinhassi, 2017; Manna et al., 2020). In the Arctic, a range of additional taxa, such as Verrucomicrobiae, *Colwellia* sp., *Polaribacter* sp., *Formosa* sp., *Paraglaciecola* sp., *Lentimonas* sp., and Altermonoadacea, were abundant in spring (Bunse and Pinhassi, 2017; Sinha et al., 2018; Zorz et al., 2019). Many of these taxa also responded positively to addition of algal polysaccharides, making them candidates for key taxa in the Arctic succession (Jain et al., 2020). In a study in Nova Scotia, also Deltaproteobacteria, Cyanobacteria, and Verrucomicrobiae have been found to be abundant taxa, particularly in association with particles (Zorz et al., 2019). In general, similar bacteria taxa are associated with phytoplankton blooms in Antarctica with *Polaribacter*, *Collwellia*, and *Pseudoalteromonas* becoming abundant after incubation in phytodetritus, and Alphaproteobacteria becoming less abundant (Manna et al., 2020). Only *Idiomarina* is a genus, apparently important for phytodetritus degradation in the Antarctic study, which is not described as abundant in Arctic, or sub-Arctic studies.

In April (paper IV) and during the freshet in June (paper II), we found similar classes abundant in the phytoplankton and sea ice microbiome in Billefjorden as the studies mentioned above, but differences, as well as similarities in dominant genera (Fig. 16). Considering the high primary production, high algae biomass, and low vertical export at the tidewater glacier front,

we consider the April community at the glacier front representative for the early spring bloom phase. In agreement with the studies by Teeling et al. (2012, 2016) we found mostly Flavobacteriales, Gammaproteobacteria, and Alphaproteobacteria dominating the pelagic and sea ice microbiome (Fig. 16). On genus level, we found a clear dominance of *Flavobacterium* sp. and *Polaribacter* sp., comparable to the early bloom taxa described by Teeling et al. (2012, 2016). However, we also found high abundances of *Amphritea* sp., which appears to be another bacteria genus related to the early bloom stage not found in the North Sea or Kongsfjorden before. However, a potential primer or database bias cannot be excluded, especially considering that *Amphritea* sp. is also rare in the Isfjorden study using a slightly different bioinformatics pipeline.

The April samples at the sea ice edge represented a later stage of the bloom as indicated by lower primary production and higher vertical export. In these systems, we found increasing fractions of Flavobacteriaceae and Gammaproteobacteria and a decreasing fraction of Alphaproteobacteria (Fig. 16). The increased fraction of Gammaproteobacteria was related to *Polaribacter* sp., *Colwellia* sp. and Alteromonadales. Of these, only *Polaribacter* sp. had been described in the North Sea studies, while *Colwellia* sp. and Alteromonadadales are more important in Arctic and Antarctic successions (Jain et al., 2020; Sinha et al., 2018, Manna et al., 2020). *Pseudoalteromonas* sp. is in fact often found associated with algae blooms (e.g. Jain et al., 2020; Dadaglio et al., 2018; Manna et al., 2020) known to degrade a variety of algae exudates (e.g. Ma et al., 2008). As shown in our cultivation study (paper III) with *Pseudoalteromonas elyakovii*, this group is not only growing efficiently on diatom exudates, but has the potential to regenerate substantial amounts of ammonium leading to an extended diatom bloom sustained by regenerated production.

In June, we sampled presumably an even later stage after the phytoplankton spring bloom. Due to the high amount of freshwater inputs, it is difficult to differentiate the bacteria feeding on preprocessed algae exudates or allochthonous DOM imported with the rivers. The dominant taxa during this time were also typical spring classes belonging to Gammaproteobacteria, Alphaproteobacteria, Actinobacteria, and Flavobacteriales (including *Flavobacterium* sp. and *Formosa* sp.)(Fig. 16). Overall, Alphaproteobacteria and Actinobacteria became substantially more dominant compared to April. On family level, Rhodobacteracea (*Sulfitobacter* sp.) became most abundant. *Sulfitobacter* sp. is not described as dominant genus in the North Sea or Kongsfjorden spring bloom studies, but has been related to more open-ocean Arctic spring

blooms (Lee et al., 2019; Thomas et al., 2020). However, considering the high fraction of *Sulfitobacter* sp. in the rivers, and the finding *Sulfitobacter* sp. mostly associated with particles at Nova Scotia (Zorz et al., 2019), *Sulfitobacter* sp. is likely associated with riverine particle inputs rather than phytoplankton exudate degradation.

Later in summer, the community composition became more even (higher Pielou's evenness index) with Verrucomicrobiae becoming part of the dominant biosphere (Fig. 16). While Verrucomicrobiae are not dominating the North Sea study (Teeling et al., 2012, 2016), they reoccurred in other Svalbard fjords (Smeerenburgfjord, Kongsfjorden) with the potential to degrade specific polysaccharides (Cardman et al., 2014). In Nova Scotia, Verrucomicrobiae were also associated with particles (Zorz et al., 2019) indicating that they may also originate from riverine sediment inputs. In late summer, we found overall more oceanic and oligotrophic taxa (Jain et al., 2020) increasing in abundances (e.g. *SAR 11*), which is in overall agreement with the finding by Teeling et al. (2012, 2016), and Jain et al. (2020). Towards autumn and winter, evenness increased even more with the ammonia oxidizing Archaea (AOA) order Nitrosopumilales becoming part of the dominant biosphere. Earlier studies on nitrification during the polar night indicate that AOA are an important and active group during the polar night due to reduced light inhibition of the ammonia oxidases and reduced competition for ammonium with algae (Christman et al., 2011). Nitrosopumilales are, thus not directly part of the bacteria/archaea succession following the spring bloom, but reliant on the absence of active algae. They are, however indirectly dependent on algae exudates, by using ammonium, which may mostly be regenerated by other bacteria and archaea feeding on algae exudates.

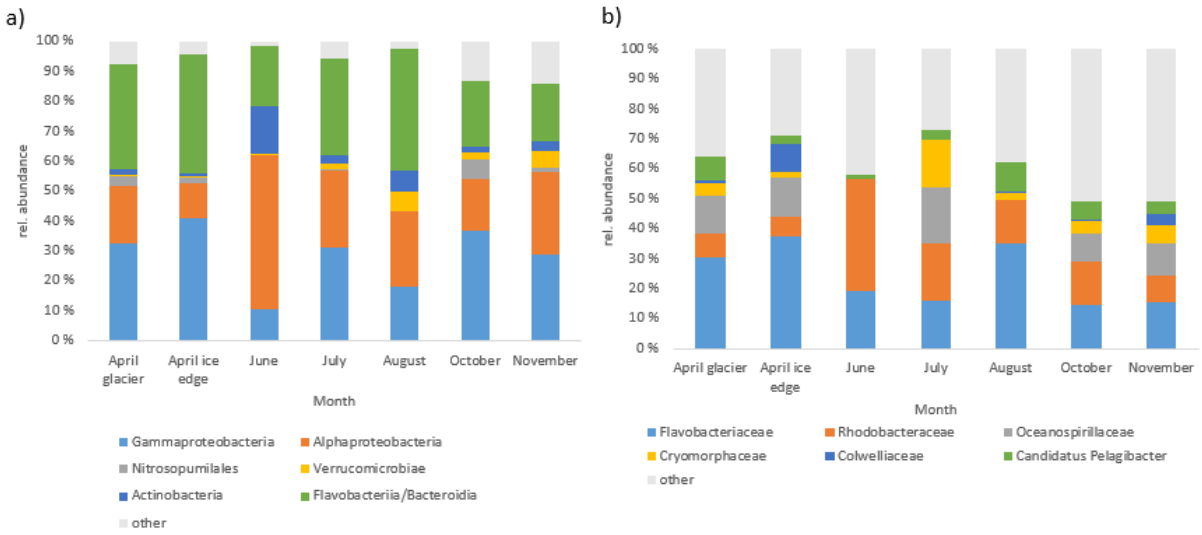

Fig. 16. Seasonal changes in the community structures of the most abundant bacterial and archaeal classes (a) and families (b) in Billefjorden. Data from April from paper IV, data from June and August from paper II and remaining data yet unpublished.

In conclusion, we found similar patterns of bacterial succession as in the North Sea, but some species important in the North Sea were rare in our study (e.g. *Roseobacter* sp.), and the other way round (e.g. *Sulfitobacter* sp.). Differences between temperate and polar bacterial communities are common, but temperate taxa appear to be increasingly imported to the Arctic via Ocean currents (Carter-Gates et al., 2020). Hence, Arctic succession patterns may become more similar to the North Sea in the future with increased Atlantification (Carter-Gates et al., 2020). However, some taxa (e.g. *Colwellia*, Alteromonadaceae) are related to algae degradation in the Arctic and Antarctic, indicating a higher importance of environmental conditions, compared to advection (Jain et al., 2029; Manna et al., 2020). Similar to the communities in Nova Scotia (Zorz et al., 2019) we found Gammaproteobacteria and Flavobacteria to dominate spring communities, but we found substantially less Alphaproteobacteria and Deltaproteobacteria. Spring and summer communities in Kongsfjorden were more comparable to our findings, but lacked the seasonal component and metadata indicating the stage pf the phytoplankton bloom and importance of terrestrial inputs. Considering the few comparable bacterioplankton succession studies in coastal Arctic systems, our findings add an important contribution to identifying potential key bacterial taxa succeeding the sea ice algae and phytoplankton spring blooms, especially for the taxa consistently found in other Arctic spring and summer studies. The important groups, even at relatively high taxonomic resolution

(genus), were consistent over different years in the North Sea and over several independent Arctic spring and summer studies, indicating that this reoccurring pattern also applies to the Arctic. With climate change, the conditions may lead to a bacterioplankton succession pattern more similar to the North Sea. However, after the spring freshet we found that allochthonous inputs of OM is an additional important factor shaping the microbial community, probably allowing some taxa to dominate that are feeding on allochthonous DOM. A succession of bacteria taxa degrading terrestrial OM is likely already starting on land (Spencer et al., 2015; Kaiser et al., 2017).

5.2.3 Importance of bacterial organic matter regeneration for algal growth

While algal organic matter production and excretion is important in shaping bacterioplankton communities and specific succession patterns, bacteria are also crucial for algae growth. A major role of bacteria is the remineralization of organic matter, thereby releasing metabolized DOM and phosphate, but also ammonium, a nitrogen source allowing regenerated algal production. In fact, about half of the CO_2 fixed by marine phytoplankton is estimated to channel through heterotrophic bacteria (Ducklow, 2000). The role of regenerated vs new production is an important question to understand global primary production and still a challenge in biogeochemical models that we tackled quantitatively in paper III. Regenerated production has been found to contribute up to 80 and 93% to the total primary production in post-bloom Arctic studies (Kristiansen et al., 1994; Simpson et al., 2013). Considering common underestimations of new production due to NO_3 originating from nitrification (Yool et al., 2007), the values may be even higher. Towards the end of spring blooms, new DIN inputs are highly limited due to the stratified water column inhibiting mixing, and riverine DIN being quickly consumed near the shore (Tank et al., 2012). However, even low rates of DOM regeneration have been found to sustain primary production using the high riverine silicate inputs in the coastal Arctic (Dittmar & Kattner, 2003). In fact, a major part of riverine nitrogen input, especially in the open ocean, has been related to regenerated DIN by bacterial DON degradation (Tank et al. 2012). Nevertheless, regenerated production is still not considered as separate process in many large ecosystem scale models (Azam and Malfatti, 2007; See model comparisons in paper III). Algae are recognized as key primary producers in all models, and regeneration of nutrients has been implemented in a few models. However, these models are highly simplified omitting key dynamics, such as algal carbon excretion and bacterial regeneration (as a function of DOM and

bacterial biomass), and different responses of algal growth on different nutrient limitations (e.g. silicate, nitrate, ammonium). Hence, we recreated typical spring bloom dynamics under controlled conditions in a cultivation experiment and developed a simple dynamic model representing these dynamics, while keeping complexity low. We show that models neglecting these dynamics would mostly underestimate primary production. Attempts to simplify models by bacteria-independent remineralization rates, a single nitrogen source, or threshold functions for different nutrient limitations, which are common in ecosystem scale models, would mostly misrepresent the late stages of spring blooms. While these simplified models may still be able to represent current algae bloom patterns, future predictions are challenging with increased heterotrophic activities related to increased temperatures, and changes in spring stratification (IPPC, 2019; Lannuzel et al., 2020).

Other important roles of bacteria, not represented in our model, include trace metal (e.g. iron, copper) reduction (e.g. Sunda, 2012) or chelation (e.g. Sunda, 2012; Gutierrez et al., 2012), or vitamin B12 synthesis (e.g. Croft et al., 2005). In fact, various trace metals and vitamin B12 can be limiting in different parts of the ocean (Moore et al., 2013) and only bacterial activities may allow the primary production currently observed in these systems to occur in presently measured rates. While these compounds are typically not limiting in Arctic coastal regions, mainly due to terrestrial inputs, and thus not implemented in our model, we showed the general importance to include bacterial production, regeneration, or transformation of limiting nutrients for estimating primary production accurately, especially towards the end of a bloom.

5.3 Methodological considerations

The following chapters discuss some of the methods used during this PhD thesis more critically focusing on not only their strength, but also their limitations and future directions. Parts of these chapters have been presented in paper I.

5.3.1 How do we measure primary production?

Photosynthetic primary production is the uptake of CO_2 into biomass with light energy, in the oceans mainly by eukaryotic algae. During this process, H_2O is oxidized to O_2. Consequently, primary production could be measured by changes in O_2 or DIC, or by tracking isotopically labelled C or O.

The most commonly used methods are described by Regaudie-de-Gioux et al. (2014) and include ^{14}C or ^{13}C labelled DIC incubations, Oxygen changes in light and dark incubations, and ^{18}O-H_2O incubations. ^{14}C labelled DIC tracking into biomass is a commonly used approach that we also used for paper IV with low detection limits and the potential to differentiate DOC and POC production (Steeman Nielsen, 1952). However, artifacts can be problematic in bottle incubations and during filtration and the use of radioactive isotopes comes with specific risks. An alternative is to track ^{13}C labelled DIC (used for our polar night study), which is not radioactive, but which comes with a higher detection limit (Slawyk et al., 1977). For both $^{13/14}C$ tracking experiment knowledge of the background concentration of DIC is required which comes with its own methodological challenges, such as gas free sampling, and fixation with very toxic chemicals (e.g. $HgCl_2$). Another typical approach is to measure O_2 changes in light and dark incubations, whereby the difference is considered the net primary production assuming equal respiration under light and dark conditions (Carpenter, 1965). Tracking of ^{18}O labelled H_2O into O_2 is another method used with the additional potential to also estimate respiration, but with problems related to the Mehler reaction and photorespiration (Bender et al., 1987).

However, inorganic carbon and oxygen are part of various other reactions, specifically respiration, making these approaches not as straightforward as they seem (Regaudie-de-Gioux et al., 2014). DIC can be released, or O_2 consumed either by algae themselves or by heterotrophs. Especially for the ^{18}O approach, it is estimated that about 20% of the O_2 is used by algae via the Mehler reaction and photorespiration (Bender et al., 1987). Furthermore, DIC can also be fixed by heterotrophs into the TCA cycle via anapleurotic reactions, or by chemoautotrophs using e.g. reduced metals or ammonium as electron donor. Dark DIC fixation is a process we used in paper IV to estimate bacterial production, and for the polar night study to estimate nitrification. Photosynthetic primary production is a direct function of light and thus, light needs to be controlled or measured for reasonable discussions of other environmental controls. Standardized production vs irradiance (PI) curves are often used to measure potential primary production under various light conditions. Eventually one main problem arises with any incubations in small volumes due to the changing environment and potentially changing communities and activities (bottle effect). Another problem is related to incubations times. The community has to be long enough exposed to the tracers to measure uptake, but not so long that the produced DOC or POC is used by other parts of the food web eventually releasing CO_2 again (cross-feeding).

Several methods have been developed to avoid the bottle effect, each with specific limitations. Primary production can be estimated via changes in the active fluorescence under illumination with different light intensities (Kolber and Falkowski, 1993), but the method was prone to uncertainties due to many assumptions and parameters needed and interference with colored DOM, which can absorb some of the light on its own (Regaudie-de-Gioux et al.,2014). Another approach is to measure oxygen gradients along boundary layers and calculate primary production based on the flux of oxygen along the diffusive boundary layer (used in Vonnahme et al. 2020). If currents are negligible, this method can estimate net primary production at surfaces of sediments, but not in the water column (e.g. Attard et al., 2016). Another method useful under sea ice (Long et al., 2012), or sediments (Attard et al., 2016) are eddy covariance measurements as described in ch. 5.3.3, which is however limited to sea ice bottom net primary production measurements and sensible to physical interferences during sea ice melt or formation (Long et al., 2012).

Often, the efficiency of the algae for primary production is of interest. A straightforward way is to normalize the measured primary production to algae biomass as carbon, chlorophyll, or cell numbers (See paper IV). For identifying the taxa responsible for the DIC uptake, isotopically labelled DIC can be tracked into specific taxa using autoradiography or stable isotope probing experiments (See ch. 5.1.1). Due to its radioactive properties, ^{14}C can be visualized on microscopic slides with a photosensitive cover allowing to couple microscopy with the detection of ^{14}C incorporation in specific organisms a method known as microautoradiography (Douglas, 1984). ^{13}C can be detected via mass spectrometry, and due to its stability, it can be used in a wider range of instruments unsuitable for radiotracers. A method similar to microautoradiography is the detection of stable isotopes via nanoscale secondary ion mass spectrometry (NanoSIMS), a method that allows to visualize microbial interactions including element exchange quantitatively (Musat et al., 2016). Other methods allow tracking the ^{13}C label into different biomarkers (stable isotope probing/ SIP), such as DNA or RNA, allowing to find exactly which taxa are taking up the DIC (with considerations of problems discussed in ch. 5.3.2) and if different time steps are used, which taxa are feeding on the phototrophs, or their exudates (Kreuzer-Martin, 2007). Tracking the ^{13}C label into metabolites, such as fatty acids (PLFA-SIP) and sugars has a lower taxonomic resolution but allows a quantitative estimate of primary production in different algal groups (Neufeld et al., 2007). Metabolomics-SIP is one of the methods we used in ongoing work to track ^{13}C-labelled DIC

and glycine into algae and bacteria biomarkers in order to quantify heterotrophic carbon uptake by algae in the polar night. ^{13}C-DIC-SIP has the same limitation as the ^{13}C-DIC primary production measurements and general bottle incubations as discussed above, in addition to the need for advanced mass spectrometry instruments.

5.3.2 Can Metabarcoding replace classical taxonomy?

High throughput sequencing technologies opened the door to read genetic information of a large number of organisms and samples in a short time. With the help of genetic markers specific for different taxa backed by a growing database, this tool has been used increasingly, to obtain taxonomic information of environmental samples, quickly, cost-efficient, without identifier bias and without the need for extensive prior expert knowledge of their morphology. For some taxa, such as flagellates, bacteria and archaea this is one of the few methods making it possible to get detailed taxonomic information at all. While it sounds like traditional taxonomy can be replaced by metabarcoding studies, there are limitations, biases and pitfalls, which still make cultivation, supplementary molecular methods, and morphological identifications necessary.

First of all, the method comes with a large number of biases, during i) DNA extraction, which has different efficiencies for different types of cell walls, ii) PCR primers targeting not all microbial taxa of interest equally, iii) bioinformatics processing with different filtering and clustering algorithms, and iv) classification relying on a database, which is still limited by the published reference sequences (reviewed by Nilsson et al., 2019). Shotgun metagenomics sequencing may overcome some of the limitations related to PCR and primer bias (Obiol et al., 2020), but overall, the outcome of both methods may lack important taxa or over-represent others, making comparisons between different studies rather speculative. If the differences are real or artifacts of the processing pipeline is often difficult to determine. Only comparisons of studies using the same pipeline and reference database are meaningful for detailed discussions, while comparisons between different studies should focus on general patterns and abundant taxonomic groups on high taxonomic levels.

Secondly, metabarcoding studies provide insights into microbial community compositions, but due to the biases mentioned above and inefficient DNA extractions varying with the type of sample, traditional metabarcoding studies are usually not quantitative. Some organisms have high copy numbers of the target gene (Prokopowich et al., 2003). Dinophyceae and Dictychophyceae, for example, are often over-represented in 18S metabarcoding studies (e.g.

Gran-Stadniczenko et al., 2019). Consequently, even compositionality is unreliable unless the gene copy numbers are considered. A combination of metabarcoding with microscopy is one powerful approach to tackle this challenge (Gran-Stadniczenko et al., 2019; Fig. 17). For algae, light microscopic counts can be used to estimate community structures on lower taxonomic resolution, while metabarcoding can give more insights into higher taxonomic resolution, especially for organisms not possible to differentiate via light microscopy (e.g. flagellates) as we did in paper IV (Fig. 17). A main issue remaining with this approach is the incomplete reference database preventing accurate genus or species level identifications. Thus, cultivation, identification, and sequencing of the barcode genes are still crucial to fill these gaps in the database, making future metabarcoding studies more reliable. Bacteria and archaea are mostly indistinguishable using morphology. Thus, FISH has become a common method to fluorescently-label specific bacterial and archaeal taxa, allowing accurate quantification under an epifluorescence microscope (Amann et al., 2001; Bakenhus et al., 2019). A combination of metabarcoding followed by probe design and FISH based on the results is a powerful tool to get a quantitative estimate of important taxa (Bakenhus et al., 2019), as we have also shown for Svalbard fungi in Hassett et al. (2019) and cold seep biofilms in Gruendger et al. (2019). However, also FISH comes with its limitations regarding signal strength, background fluorescence, and probe design (Zwirglmaier, 2005).

Thirdly, metabarcoding and microscopy give only information about the taxonomic composition, but little information about functionality, trophic modes, or activity. For questions such as; who is active? what are they capable of doing? and what are they actually doing? different approaches are needed. As shown in Fig. 15 about active (cDNA) vs present (DNA) communities around Svalbard, there can be a substantial mismatch on who is there, and who is active. Concerning functions, for some taxa some functional information may be stored in the reference database, but inference of functions from taxonomy only is highly unreliable and biased (See paper II) and can only point to general directions for future work. In the time of omics, complementing methods such as metatranscriptomics (used in the ongoing polar night study), metaproteomics (e.g. Teeling et al., 2012), metabolomics (used in the ongoing polar night study), or metafluxomics (Ghosh et al., 2014) can give additional information. Ultimately direct activity studies, such as isotope probing experiments (Deng et al., 2018), leading to metafluxomics (Ghosh et al., 2014) are needed for detailed investigations and modelling (metabolic pathway modelling) of processes happening in the microbial food web.

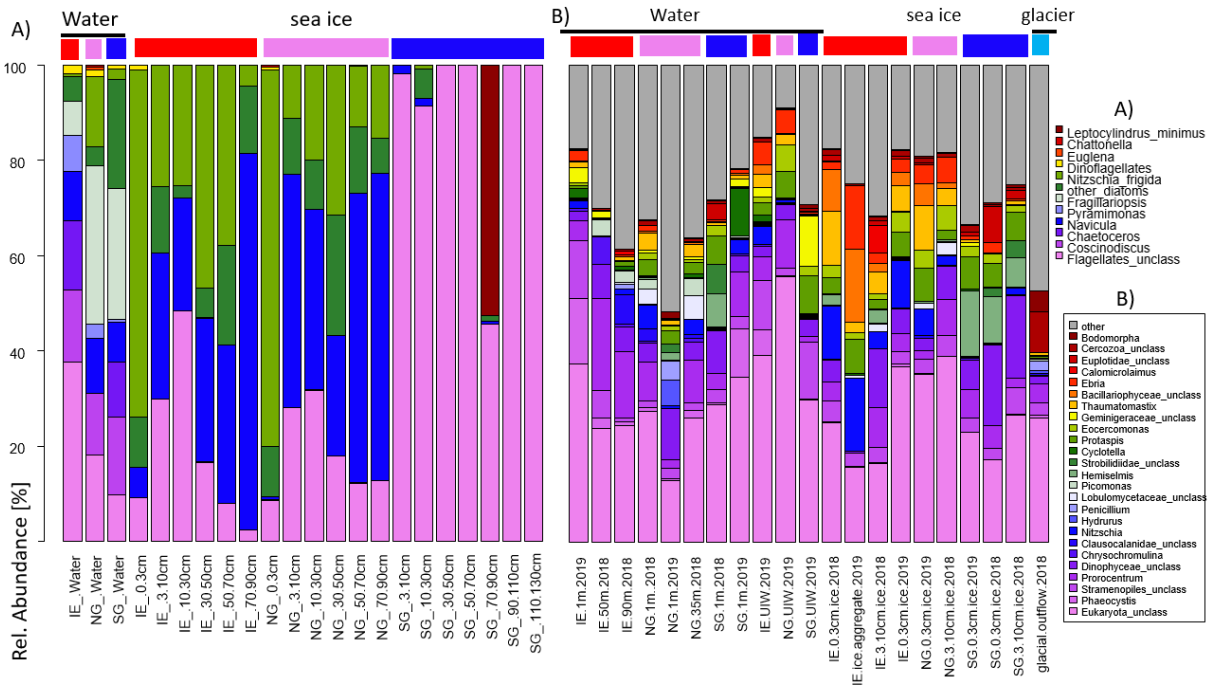

Fig 17. Comparison of microbial eukaryotic community structure at the highest reliable taxonomic resolution based on a) light microscopy and b) metabarcoding in Billefjorden (Paper IV). Red bars on top show IE samples, pink bars NG samples, and blue bars SG samples.

5.3.3 How do we take, process and incubate sea ice samples?

For understanding microbial ecology, diversity, and processes in the environment it is often necessary to remove samples and process them for further measurements or incubate them in conditions that may be different from the environment. Obviously, this may create artifacts and data may no longer representative for the environment. For several parameters and variables, standards have been developed, that are used in most studies and seem to allow some confidence that the data are representative for the environment and comparable between studies. The problems associated with *ex situ* and sampling artifacts are numerous and extend the scope of this chapter. Thus, we focus on a subset of challenges encountered during this PhD.

Particularly challenging is the processing of sea ice samples. Sea ice is a very heterogeneous habitat with fresh solid ice, and often very saline brine channels. First, sea ice cores may vary substantially in close proximity to each other and a nested sampling design is highly recommended (Miller et al., 2015). In our studies, we pooled several ice cores collected over a larger area to tackle this problem. Most methods for measuring biological and chemical parameters are developed for water samples, which mostly require melting of sea ice samples.

During the melting procedure, the salinity changes drastically, leading to hypotonic conditions and osmotic shock in organisms inhabiting the brine channels. The common approach to tackle this problem is the addition of sterile filtered seawater to prevent osmolysis, as we did for paper IV. This approach is commonly used and promising for cell counts, community analyses and Chl, POC, PON measurements. For brackish sea ice, this method may, however be problematic since the seawater below the sea ice may be more saline than the brine channels (e.g. Ramfjorden) and direct melt may be a better method (e.g. Kaartokallio, 2004). For activity measurements the seawater addition and melting approach is even more problematic. Melted sea ice has still a different salinity, and temperature, but more importantly different nutrient and DOM levels introduced with the melted solid ice and filtered seawater fractions diluting the brine fluid (e.g. Campbell et al., 2019). Another approach may be to extract the brine fluid via sack holes. However, sea ice organisms are known to produce extrapolymeric substances, which may stick to the ice, while the remaining brine fluid is extracted. Several alternatives have been developed that may give more accurate estimates, but are technologically challenging. One method tested was microsensor profiling using oxygen sensors frozen along a gradient from the water column into the sea ice to calculate potential respiration and production rates via diffusion estimates (Mock et al., 2002). However, this method has not been applied in the environment and may not consider deeper sea ice layers (Søgaard et al., 2010). In another *in situ* approach, ice core sections have been spiked with isotopically labelled DIC and reinserted into the ice (Mock and Gradinger, 1999), but problems arise with the distribution of tracer over the entire section and during filtrations for later measurements. Eddy covariance measurements (Measurement of oxygen concentrations and water currents) is another *in situ* method to estimate sea ice primary production, which allows to estimate net primary production, avoiding small scale patchiness (Long et al., 2012). However, this method does not separate respiration and production, it can be biased by physical processes related to sea ice growth or melt, and it is limited to the bottom layer of the ice (reviewed by Miller et al., 2012). Overall, incubations of melted sea ice, is still the most practical and widely used method (e.g. paper IV). For salinity and nutrient sampling direct melting appears to be suitable at first. However, some nutrients, in particular ammonium may be stored in algae and bacteria cells and may be released via osmolysis by direct melt (reviewed by Miller et al., 2012).

5.4 Context of other publications during the PhD

Besides the publications included in this PhD thesis, several additional papers were published during the time of my PhD, covering a broad area of topics in marine microbiology. In two papers, we studied the role of marine fungi. We first studied their diversity in the world oceans in a metaanalyses of published 18S rRNA metabarcoding and shotgun metagenomics datasets (Hassett et al., 2020). Secondly, we studied their diversity, biomass, and potential ecological role in detail in the plankton, sediment, and air East of Svalbard (Hassett et al., 2019). Ina global context, the group of Chytridomycota was most dominant in the Arctic Ocean. The same group also dominated fungi biomass East of Svalbard. This indicates that future studies of land-ocean interactions and algae-heterotrophs interactions should also consider this important group. Another paper describes a biofilm in sediments in a cold methane seep consisting of a consortium of methane oxidizing archaea and sulfate reducing bacteria (Gruendger et al., 2019). This study shows that this consortium often found in lower latitudes is also important in the Arctic, where it may have an even more important role in retaining the potent greenhouse gas methane before it can reach the atmosphere. Two other publications investigated the potential impacts of deep-sea mining on microbial communities and activities in deep-sea sediments. We found that disturbances of the active surface layer at 4 km depth have long-lasting effects for at least 50 years, keeping microbial activities and biomass low, thereby preventing also the recovery of higher trophic levels (Vonnahme et al., 2020). We also found distinctive bacterial and archaeal communities in manganese nodules that would be lost for geological time-scales if deep-sea mining would happen (Molari et al., 2020). Even though these studies were performed in the equatorial Pacific Ocean, they are relevant for the Arctic in two ways. Firstly, deep-sea mining is also discussed in Arctic regions with a similar loss of microbial communities after removal of polymetallic crusts. Secondly, the impacts discussed by Vonnahme et al., (2020) are very similar to bottom trawling. With a retreating sea ice edge, bottom trawling may become an increasing issue in the Arctic.

Papers published outside the PhD:

1. Hassett, B. T.*, **Vonnahme, T. R.***, Peng, X., Jones, E. G., & Heuzé, C. (2020). Global diversity and geography of planktonic marine fungi. Botanica Marina, 63(2), 121-139. (*equal contribution)

2. Hassett, B. T., Borrego, E. J., **Vonnahme, T. R.**, Rämä, T., Kolomiets, M. V., & Gradinger, R. (2019). Arctic marine fungi: biomass, functional genes, and putative ecological roles. The ISME journal, 13(6), 1484-1496.

3. Gründger, F., Carrier, V., Svenning, M. M., Panieri, G., **Vonnahme, T. R.**, Klasek, S., & Niemann, H. (2019). Methane-fuelled biofilms predominantly composed of methanotrophic ANME-1 in Arctic gas hydrate-related sediments. Scientific reports, 9(1), 1-10.

4. **Vonnahme, T. R.**, Molari, M., Janssen, F., Wenzhöfer, F., Haeckel, M., Titschack, J., & Boetius, A. (2020). Effects of a deep-sea mining experiment on seafloor microbial communities and functions after 26 years. Science Advances, 6(18), eaaz5922.

5. Molari, M., Janssen, F., **Vonnahme, T. R.**, Wenzhöfer, F., & Boetius, A. (2020). The contribution of microbial communities in polymetallic nodules to the diversity of the deep-sea microbiome of the Peru Basin (4130–4198 m depth). Biogeosciences, 17(12), 3203-3222.

6 Outlook

6.1 Impacts of river inputs on microbial communities

While the PhD thesis is representative for fjord systems with glacier-fed rivers, a large part of the Arctic consists of estuaries fed by larger rivers, with larger and farther-reaching catchment areas. Extrapolating our results to other Arctic rivers is speculative, but a similar approach could be powerful to understand the impact of these large rivers in similar detail. A design with a large set of environmental data including characterization of DOM and metagenomic samples on spatial gradients from land to ocean would be feasible and similarly powerful in other Arctic river systems.

In addition, the impacts on other microbial groups, such as fungi and algae could be investigated with the same design, using different primers, and potentially light microscopy as supplement. In fact, we are currently working on a similar study, based on 18S rRNA sequences and microscopic counts with the same set of samples in Isfjorden (paper II). Besides the community structure, we also showed evidence for impacts on biogeochemical cycles. However, functional inference from taxonomy is problematic, and direct activity measurements are needed to study the impacts of river inputs on the biogeochemical cycles. Hence, we are preparing another field campaign for summer 2021 focusing on studying the effects of river inputs on the carbon cycle, including bacteria, and primary production, metabolic efficiencies and standing stock biomass, similar to paper IV.

6.2 Impacts of tidewater glaciers on microbial communities and activities

We suggest that subglacial upwelling during the frozen part of the year is a widespread, yet overlooked process that would lead to underestimations of primary production in tidewater glacier influenced fjords, such as on Svalbard and Greenland. Further studies at different locations, with higher spatial and temporal resolution could help to quantify this process on Arctic-fjord carbon cycles, leading to potentially higher estimates of phytoplankton primary production and lower estimates of sea ice algae primary production in tidewater glacier influenced fjords. In particular, under-ice phytoplankton blooms have become increasingly recognized as important contributor to marine Arctic CO_2 fixation, albeit previously neglected in global carbon cycle models (Ardyna et al., 2020a, b). Our study suggests that this process is not limited to the previously described Arctic basin systems affected by melting sea ice (Lowry

et al., 2017), melt ponds (Arrigo et al., 2012), leads (Assmy et al., 2017), or sea ice edges (Mundy et al., 2009), but also important in tidewater glacier influenced fjords. The strong impact on the microbial food web has ultimately also consequences for higher trophic levels. We are currently working on a manuscript describing the seasonal dynamics of the ecosystem in Billefjorden, including zooplankton.

To my knowledge, impact of sea ice with very low brine volume and permeability on sea ice algae and production has previously not been studied in the high Arctic. Our study suggests that the dynamics and important taxa are similar to Baltic sea ice and comparisons on other aspects may be valid, too, but must be validated by more detailed field studies. During an ongoing study, we also found brackish sea ice in a northern Norwegian fjord (Ramfjorden) with similar impacts on algae communities. In Ramfjorden and many other Norwegian fjords, the freshwater may originate from a reduced base flow of rivers during winter (O'Sadnick et al., 2020). Considering that river runoff has also been found throughout winter in all large Arctic rivers (Holmes et al., 2012), brackish sea ice may be a dominant feature in the Arctic, highly affected by climate change. So far, brackish river sea ice has been described from Arctic river deltas in respect to its physical and chemical properties (e.g. Emmerton et al., 2008), but studies looking at the effects of the freshwater on Arctic sea ice algae are lacking.

6.3 Modelling algae – bacteria/fungi interactions

Our cultivation experiment with support from the field studies showed clearly that implementation of bacterial ammonium regeneration and different physiological responses to different nutrients is crucial for modelling the "end of bloom" scenarios. The next step would be to implement the extended model on a larger scale, including a full ecosystem and detailed physical compartment (e.g. SINMOD: Wassmann et al., 2006) and investigate the different predictions of primary production, compared to the original model. I hypothesize that our model will lead to higher estimates of future primary production due to the increased importance of heterotrophic processes with increasing temperatures leading to potentially increasing regenerated production. This would lead to the scenario of silicate-depleted but nitrogen-rich waters becoming more dominant in the future.

Similar experiments with additional variables as we did in paper III would help to extend the scope of the model from coastal Arctic systems to global marine systems. Specifically, other nutrients, such as iron and phosphate, and other important functional groups such as flagellates,

or cyanobacteria would be important for broadening the scope of the model. With climate change, community shifts from diatom to flagellate blooms have already been observed (e.g. Terrado et al., 2013; Lannuzel et al., 2020). Thus, it is important to consider competition between diatoms and flagellates especially under silicate limitation. In addition to bacteria, we found fungi to be important compartments of the heterotrophic microbial food web (Hassett et al., 2019). Hence, a similar cultivation experiment with fungi instead of bacteria could help to develop a model that includes this important group. I hypothesize, that fungi may have a similarly important role for regenerated production as bacteria.

References

6. Adakudlu, M., Andresen, J., Bakke, J., Beldring, S., Benestad, R., van der Bilt, W. (2019). Climate in Svalbard 2100. Available at: https://bora.uib.no/handle/1956/19136 [Accessed June 8,2020].
7. Alkire, M. B., Nilsen, F., Falck, E., Søreide, J., & Gabrielsen, T. M. (2015). Tracing sources of freshwater contributions to first-year sea ice in Svalbard fjords. Continental Shelf Research, 101, 85-97.
8. Altschul, S. F., Gish, W., Miller, W., Myers, E. W., & Lipman, D. J. (1990). Basic local alignment search tool. Journal of molecular biology, 215(3), 403-410.
9. Amann, R., Fuchs, B. M., & Behrens, S. (2001). The identification of microorganisms by fluorescence in situ hybridisation. Current opinion in biotechnology, 12(3), 231-236.
10. Andersen, R. A., and Kawachi, M. (2005). Microalgae isolation techniques. in: Algal culturing techniques, edited by: Andersen, R. A., Elsevier, 83.
11. Ardyna, M., Mundy, C. J., Mayot, N., Matthes, L. C., Oziel, L., Horvat, C., ... & Gale, M. (2020b). Under-ice phytoplankton blooms: shedding light on the'invisible'part of Arctic primary production. Frontiers in Marine Science, 7, 985.
12. Ardyna, M., Mundy, C. J., Mills, M. M., Oziel, L., Grondin, P. L., Lacour, L., ... & Babin, M. (2020a). Environmental drivers of under-ice phytoplankton bloom dynamics in the Arctic Ocean. Elem Sci Anth, 8(1).
13. Arrigo, K. R., Arrigo, K. R., Perovich, D. K., Pickart, R. S., Brown, Z. W., van Dijken, G. L., Lowry, K. E., Mills, M. M., Palmer, M. A., Balch, W. M., Bates, N. R., Benitez-Nelson, C. R., Brownlee, E., Frey, K. E., Laney, S. R., Mathis, J., Matsuoka, A., Mitchell, B. G., Moore, G. W. K., Reynolds, R. A., Sosik, H. A., Swift, J. H. (2014). Phytoplankton blooms beneath the sea ice in 695 the Chukchi Sea. Deep Sea Res. Part II Top. Stud. Oceanogr., 105, 1-16, https://org/10.1016/j.dsr2.2014.03.018.
14. Aßhauer, K. P., Wemheuer, B., Daniel, R., and Meinicke, P. (2015). Tax4Fun: predicting functional profiles from metagenomic 16S rRNA data. Bioinformatics 31, 2882–2884. doi:10.1093/bioinformatics/btv287.
15. Assmy, P., M. Fernández-Méndez, P. Duarte, A. Meyer, A. Randelhoff, C. J. Mundy, L. M. Olsen, H. M. Kauko, A. Bailey,and Chierici, M. (2017). Leads in Arctic pack ice enable early phytoplankton blooms below snow-covered sea ice. Scientific reports, 7, 705 40850.
16. Atienza, S., Guardiola, M., Præbel, K., Antich, A., Turon, X., and Wangensteen, O. S. (2020). DNA Metabarcoding of Deep-Sea Sediment Communities Using COI: Community Assessment, Spatio-Temporal Patterns and Comparison with 18S rDNA. Diversity, 12(4), 123, https://org/10.3390/d12040123.
17. Attard, K. M., Hancke, K., Sejr, M. K., & Glud, R. N. (2016). Benthic primary production and mineralization in a High Arctic fjord: in situ assessments by aquatic eddy covariance. Marine ecology progress series, 554, 35-50.
18. Azam, F., & Malfatti, F. (2007). Microbial structuring of marine ecosystems. Nature Reviews Microbiology, 5(10), 782-791.
19. Baer, S. E., Sipler, R. E., Roberts, Q. N., Yager, P. L., Frischer, M. E., & Bronk, D. A. (2017). Seasonal nitrogen uptake and regeneration in the western coastal Arctic. Limnology and Oceanography, 62(6), 2463-2479.

20. Behrenfeld, M. J. (2010). Abandoning Sverdrup's critical depth hypothesis on phytoplankton blooms. Ecology, 91(4), 977-989.
21. Bender, M., Grande, K., Johnson, K., Marra, J., Williams, P. J. L., Sieburth, J., ... & Hunt, C. (1987). A comparison of four methods for determining planktonic community production 1. Limnology and Oceanography, 32(5), 1085-1098, doi: 10.4319/lo.1987.32.5.1085.
22. Bintanja, R., van der Wiel, K., Van der Linden, E. C., Reusen, J., Bogerd, L., Krikken, F., & Selten, F. M. (2020). Strong future increases in Arctic precipitation variability linked to poleward moisture transport. Science advances, 6(7), eaax6869.
23. Blanchet, M., Pringault, O., Panagiotopoulos, C., Lefèvre, D., Charrière, B., Ghiglione, J. F., ... & Oriol, L. (2017). When riverine dissolved organic matter (DOM) meets labile DOM in coastal waters: changes in bacterial community activity and composition. Aquatic Sciences, 79(1), 27-43.
24. Błaszczyk, M., Jania, J. A., and Hagen, J. O. (2009). Tidewater glaciers of Svalbard: recent changes and estimates of calving fluxes. Pol. Polar Res. 30:85.
25. Bourgeois, S., Kerhervé, P., Calleja, M. Ll., Many, G., and Morata, N. (2016). Glacier inputs influence Terrestrial Inputs Shape Microbial Communities organic matter composition and prokaryotic distribution 775 in a high Arctic fjord (Kongsfjorden, Svalbard). Journal of Marine Systems 164, 112–127, doi:10.1016/j.jmarsys.2016.08.009.
26. Bowman, J. S. (2015). The relationship between sea ice bacterial community structure and biogeochemistry: a synthesis of current knowledge and known unknowns. Elem Sci Anth 3:000072. https://doi.org/10.12952/journal.elementa.000072
27. Boyer, F., Mercier, C., Bonin, A., Le Bras, Y., Taberlet, P., & Coissac, E. (2016). obitools: A unix-inspired software package for DNA metabarcoding. Molecular ecology resources, 16(1), 176-182.
28. Bunse, C., & Pinhassi, J. (2017). Marine bacterioplankton seasonal succession dynamics. Trends in microbiology, 25(6), 494-505.
29. Burdige, D.J., and Homstead, J. (1994). Fluxes of dissolved organi carbon from Chesapeake Bay sediments. Geochim. Cosmochim. Acta, 58, 3407-3424.
30. Baas-Becking, L. G. M. (1934). Geobiologie; of inleiding tot de milieukunde. WP Van Stockum & Zoon NV.
31. Cáceres, M. D., and Legendre, P. (2009). Associations between species and groups of sites: indices and statistical inference. Ecology 90, 3566–3574. doi:10.1890/08-1823.1.
32. Campbell, K., Mundy, C. J., Juhl, A. R., Dalman, L. A., Michel, C., Galley, R. J., ... & Rysgaard, S. (2019). Melt procedure affects the photosynthetic response of sea ice algae. Frontiers in Earth Science, 7, 21.
33. Cardman, Z., Arnosti, C., Durbin, A., Ziervogel, K., Cox, C., Steen, A. D., & Teske, A. (2014). Verrucomicrobia are candidates for polysaccharide-degrading bacterioplankton in an arctic fjord of Svalbard. Applied and environmental microbiology, 80(12), 3749-3756.
34. Caroppo, C., P. Pagliara, F. Azzaro, S. Miserocchi, M. Azzaro (2017). Late summer phytoplankton blooms in the changing polar environment of the Kongsfjorden (Svalbard, arctic). Cryptogam. Algol., 38, 53-72, 10.7872/crya/v38.iss1.2017.53
35. Carpenter, J. H. (1965). The accuracy of the Winkler method for dissolved oxygen analysis. Limnol. Oceanogr. 10, 135–140. doi: 10.4319/lo.1965.10.1.0135

36. Carter-Gates, M., Balestreri, C., Thorpe, S.E., Cottier, F., Baylays, A., Bibbys, T. S., Moores, C. M., & Schroeder, D. C. (2020). Implications of increasing Atlantic influence for Arctic microbial community structure. Sci Rep 10, 19262
37. Chen, J., Li, H., Zhang, Z., He, C., Shi, Q., Jiao, N., & Zhang, Y. (2020). DOC dynamics and bacterial community succession during long-term degradation of Ulva prolifera and their implications for the legacy effect of green tides on refractory DOC pool in seawater. Water Research, 185, 116268.
38. Christman, G. D., Cottrell, M. T., Popp, B. N., Gier, E., & Kirchman, D. L. (2011). Abundance, diversity, and activity of ammonia-oxidizing prokaryotes in the coastal Arctic Ocean in summer and winter. Appl. Environ. Microbiol., 77(6), 2026-2034.
39. Cloern, J. E., Grenz, C., and Vidergar-Lucas, L. (1995). An empirical model of the phytoplankton chlorophyll: carbon ratio-the conversion factor between productivity and growth rate. Limnol. Oceanogr., 40(7), 1313-1321, https://org/10.4319/lo.1995.40.7.1313.
40. Cottier, F. R., Nilsen, F., Skogseth, R., Tverberg, V., Skarðhamar, J., & Svendsen, H. (2010). Arctic fjords: a review of the oceanographic environment and dominant physical processes. Geological Society, London, Special Publications, 344(1), 35-50.
41. Croft, M. T., Lawrence, A. D., Raux-Deery, E., Warren, M. J., & Smith, A. G. (2005). Algae acquire vitamin B 12 through a symbiotic relationship with bacteria. Nature, 438(7064), 90-93.
42. Dadaglio, L., Dinasquet, J., Obernosterer, I., & Joux, F. (2018). Differential responses of bacteria to diatom-derived dissolved organic matter in the Arctic Ocean. Aquatic Microbial Ecology, 82(1), 59-72.
43. Degerlund, M., and Eilertsen, H. C. (2010). Main species characteristics of phytoplankton spring blooms in NE Atlantic and Arctic waters (68–80 N). Estuaries Coast, 33, 242-269.
44. Deng, W., Peng, L., Jiao, N., & Zhang, Y. (2018). Differential incorporation of one-carbon substrates among microbial populations identified by stable isotope probing from the estuary to South China Sea. Scientific reports, 8(1), 1-12.
45. Dickson, A. G., Sabine, C. L., and Christian, J. R. (2007). Guide to best practices for ocean CO2 measurements. PICES Special Publication 3.
46. Díez, B., Bergman, B., Pedrós-Alió, C., Antó, M., & Snoeijs, P. (2012). High cyanobacterial nifH gene diversity in Arctic seawater and sea ice brine. Environmental microbiology reports, 4(3), 360-366.
47. Ding, Y., Zhang, S., Zhao, L., Li, Z., & Kang, S. (2019). Global warming weakening the inherent stability of glaciers and permafrost. Science Bulletin, 64(4), 245-253.
48. Dittmar, T., & Kattner, G. (2003). The biogeochemistry of the river and shelf ecosystem of the Arctic Ocean: a review. Marine chemistry, 83(3-4), 103-120.
49. Douglas, D. J. (1984). Microautoradiography-based enumeration of photosynthetic picoplankton with estimates of carbon-specific growth rates. Marine ecology progress series. Oldendorf, 14(2), 223-228.
50. Ducklow, H.W. (2000) Bacterial production and biomass in the oceans D.L. Kirchman (Ed.), Microbial Ecology of the Oceans, John Wiley and Sons, pp. 85-120
51. Eilertsen, H. C., & Taasen, J. P. (1984). Investigations on the plankton community of Balsfjorden, northern Norway. The phytoplankton 1976–1978. Environmental factors, dynamics of growth, and primary production. Sarsia, 69(1), 1-15.

52. Eilertsen, H. C., Taasen, J. P., and WesIawski, J. M. (1989). Phytoplankton studies in the fjords of West Spitzbergen: physical environment and production in spring and summer. J. Plankton Res., 11, 1245-1260.
53. Emmerton, C. A., Lesack, L. F., & Vincent, W. F. (2008). Nutrient and organic matter patterns across the Mackenzie River, estuary and shelf during the seasonal recession of sea-ice. Journal of Marine Systems, 74(3-4), 741-755.
54. Fernández-Méndez, M., Katlein, C., Rabe, B., Nicolaus, M., Peeken, I., Bakker, K., ... & Boetius, A. (2015). Photosynthetic production in the central Arctic Ocean during the record sea-ice minimum in 2012. Biogeosciences, 12(11), 3525-3549.
55. Field, C. B., Behrenfeld, M. J., Randerson, J. T., & Falkowski, P. (1998). Primary production of the biosphere: integrating terrestrial and oceanic components. science, 281(5374), 237-240.
56. Fransson, A., Chierici, M., Nomura, D., Granskog, M. A., Kristiansen, S., Martma, T., & Nehrke, G. (2020). Influence of glacial water and carbonate minerals on wintertime sea-ice biogeochemistry and the CO2 system in an Arctic fjord in Svalbard. Annals of Glaciology, 1-21.
57. Garcia-Descalzo, L., Garcia-Lopez, E., Postigo, M., Baquero, F., Alcazar, A., and Cid, C. (2013).Eukaryotic microorganisms in cold environments: examples from Pyrenean glaciers. Front. Microbiol. 4. doi:10.3389/fmicb.2013.00055.
58. Garcia-Lopez, E., Rodriguez-Lorente, I., Alcazar, P., & Cid, C. (2019). Microbial communities in coastal glaciers and tidewater tongues of Svalbard Archipelago, Norway. Frontiers in Marine Science, 5, 512.
59. Geider, R. J., Maclntyre, H. L., and Kana, T. M. (1998). A dynamic regulatory model of phytoplanktonic acclimation to light, nutrients, and temperature. Limnol. Oceanogr., 43, 679-694.
60. Ghosh, A., Nilmeier, J., Weaver, D., Adams, P. D., Keasling, J. D., Mukhopadhyay, A., ... & Martín, H. G. (2014). A peptide-based method for 13 C metabolic flux analysis in microbial communities. PLoS Comput Biol, 10(9), e1003827.
61. Grann-Meyer, E. (2020). Chrysochromulina leadbeateri-Understanding the Presumed Causal Agent Behind the Harmful Algal Bloom of 2019 (Master's thesis, UiT The Arctic University of Norway).
62. Granskog, M. A., Kaartokallio, H., & Shirasawa, K. (2003). Nutrient status of Baltic Sea ice: Evidence for control by snow-ice formation, ice permeability, and ice algae. Journal of Geophysical Research: Oceans, 108(C8).
63. Gran-Stadniczeñko, S., Egge, E., Hostyeva, V., Logares, R., Eikrem, W., & Edvardsen, B. (2019). Protist diversity and seasonal dynamics in Skagerrak plankton communities as revealed by metabarcoding and microscopy. Journal of Eukaryotic Microbiology, 66(3), 494-513.
64. Gründger, F., Carrier, V., Svenning, M. M., Panieri, G., Vonnahme, T. R., Klasek, S., & Niemann, H. (2019). Methane-fuelled biofilms predominantly composed of methanotrophic ANME-1 in Arctic gas hydrate-related sediments. Scientific reports, 9(1), 1-10.
65. Guillard, R.L.L. (1975). Culture of phytoplankton for feeding marine invertebrates. in: Culture of Marine Invertebrates Animals, edited by: Smith, W.L., Chanley, M.H., Plenum Press, New York, 29–60.
66. Gutierrez, T., Biller, D. V., Shimmield, T., & Green, D. H. (2012). Metal binding properties of the EPS produced by Halomonas sp. TG39 and its potential in enhancing trace element bioavailability to eukaryotic phytoplankton. Biometals, 25(6), 1185-1194.

67. Hagen, J. O., Liestøl, O., Roland, E., and Jørgensen, T. (1993). Glacier Atlas of Svalbard and Jan Mayen. Oslo: Norwegian Polar Institute.
68. Halbach, L., Vihtakari, M., Duarte, P., Everett, A., Granskog, M. A., Hop, H., ... & Pramanik, A. (2019). Tidewater glaciers and bedrock characteristics control the phytoplankton growth environment in a fjord in the arctic. Frontiers in Marine Science, 6, 254.
69. Haro‐Moreno, J. M., Rodriguez‐Valera, F., Rosselli, R., Martinez‐Hernandez, F., Roda‐Garcia, J. J., Gomez, M. L., ... & López‐Pérez, M. (2020). Ecogenomics of the SAR11 clade. Environmental microbiology, 22(5), 1748-1763.
70. Hassenrück, C. (2019). R and bash scripts for sequence processing of amplicon and shotgun sequencing data. Available at: https://github.com/chassenr/NGS/tree/master/AMPLICON.
71. Hassett, B. T., Borrego, E. J., Vonnahme, T. R., Rämä, T., Kolomiets, M. V., & Gradinger, R. (2019). Arctic marine fungi: biomass, functional genes, and putative ecological roles. The ISME journal, 13(6), 1484-1496.
72. Hassett, B. T., Vonnahme, T. R., Peng, X., Jones, E. G., & Heuzé, C. (2020). Global diversity and geography of planktonic marine fungi. Botanica Marina, 63(2), 121-139.
73. Hegseth, E. N. (1998). Primary production of the northern Barents Sea. Polar Research, 17(2), 113-123. https://doi.org/10.1111/j.1751-8369.1998.tb00266.x
74. Hegseth, E. N., Assmy, P., Wiktor, J. M., Wiktor, J., Kristiansen, S., Leu, E., ... & Cottier, F. (2019). Phytoplankton seasonal dynamics in Kongsfjorden, Svalbard and the adjacent shelf. In The Ecosystem of Kongsfjorden, Svalbard (pp. 173-227). Springer, Cham.
75. Holmes, R. M., Coe, M. T., Fiske, G. J., Gurtovaya, T., McClelland, J. W., Shiklomanov, A. I., ... & Zhulidov, A. V. (2013). Climate change impacts on the hydrology and biogeochemistry of Arctic rivers. Climatic Change and Global Warming of Inland Waters, 1-26.
76. Holm-Hansen, O., & Riemann, B. (1978). Chlorophyll a determination: Improvements in methodology. Oikos, 30(3), 438–447. https://doi.org/10.2307/3543338
77. Hopwood, M. J., Carroll, D., Dunse, T., Hodson, A., Holding, J. M., Iriarte, J. L., ... & Chierici, M. (2020). How does glacier discharge affect marine biogeochemistry and primary production in the Arctic?. The Cryosphere, 14, 1347-1383.
78. Horner, R., & Alexander, V. (1972). Algal populations in Arctic Sea ice: An investigation of heterotrophy. Limnology and Oceanography, 17(3), 454-458.
79. Intergovernmental Panel on Climate Change (IPCC). (2019). Special Report on the Ocean and Cryosphere in a Changing Climate.
80. Isaksen, K., Nordli, Ø, Førland, E. J., Łupikasza, E., Eastwood, S., and Niedźwiedź, T. (2016). Recent warming on Spitsbergen—Influence of atmospheric circulation and sea ice cover. J. Geophys. Res. Atmosph. 121, 913–911. doi: 10.1002/2016JD025606
81. Jain, A., Krishnan, K. P., Begum, N., Singh, A., Thomas, F. A., & Gopinath, A. (2020). Response of bacterial communities from Kongsfjorden (Svalbard, Arctic Ocean) to macroalgal polysaccharide amendments. Marine Environmental Research, 155, 104874.
82. Jakobsson, M., Mayer, L., Coakley, B., Dowdeswell, J. A., Forbes, S., Fridman, B., ... & Schenke, H. W. (2012). The international bathymetric chart of the Arctic Ocean (IBCAO) version 3.0. Geophysical Research Letters, 39(12). Jiao, N., Herndl, G. J., Hansell, D. A., Benner, R., Kattner, G., Wilhelm, S. W., ... & Azam, F. (2010). Microbial production of recalcitrant dissolved organic matter: long-term carbon storage in the global ocean. Nature Reviews Microbiology, 8(8), 593-599.

83. Johnsen, G., Leu, E., & Gradinger, R. (2020). Marine Micro-and Macroalgae in the Polar Night. In POLAR NIGHT Marine Ecology (pp. 67-112). Springer, Cham.
84. Johnsen, G., Norli, M., Moline, M., Robbins, I., von Quillfeldt, C., Sørensen, K., ... & Berge, J. (2018). The advective origin of an under-ice spring bloom in the Arctic Ocean using multiple observational platforms. Polar biology, 41(6), 1197-1216.
85. Jørgensen, B. B., Laufer, K., Michaud, A. B., & Wehrmann, L. M. (2020). Biogeochemistry and microbiology of high Arctic marine sediment ecosystems—Case study of Svalbard fjords. Limnology and Oceanography.
86. Kaiser, K., Canedo-Oropeza, M., McMahon, R., & Amon, R. M. (2017). Origins and transformations of dissolved organic matter in large Arctic rivers. Scientific reports, 7(1), 1-11.
87. Kim, J. H., Peterse, F., Willmott, V., Kristensen, D. K., Baas, M., Schouten, S., & Sinninghe Damsté, J. S. (2011). Large ancient organic matter contributions to Arctic marine sediments (Svalbard). Limnology and Oceanography, 56(4), 1463-1474.
88. Kirchman, D. L., Suzuki, Y., Garside, C., & Ducklow, H. W. (1991). High turnover rates of dissolved organic carbon during a spring phytoplankton bloom. Nature, 352(6336), 612-614.ology and Oceanography, 49(3), 862-878.
89. Kolber, Z., & Falkowski, P. G. (1993). Use of active fluorescence to estimate phytoplankton photosynthesis in situ. Limnology and Oceanography, 38(8), 1646-1665.
90. Kosek, K., Luczkiewicz, A., Kozioł, K., Jankowska, K., Ruman, M., & Polkowska, Ż. (2019). Environmental characteristics of a tundra river system in Svalbard. Part 1: Bacterial abundance, community structure and nutrient levels. Science of The Total Environment, 653, 1571-1584.
91. Kreuzer-Martin, H. W. (2007). Stable isotope probing: linking functional activity to specific members of microbial communities. Soil Science Society of America Journal, 71(2), 611-619.
92. Kristiansen, S., Farbrot, T., & Wheeler, P. A. (1994). Nitrogen cycling in the Barents Sea–Seasonal dynamics of new and regenerated production in the marginal ice zone. Limnology and Oceanography, 39(7), 1630-1642.
93. Kuliński, K., Kędra, M., Legeżyńska, J., Gluchowska, M., & Zaborska, A. (2014). Particulate organic matter sinks and sources in high Arctic fjord. Journal of Marine Systems, 139, 27-37.
94. Kvernvik, A. C., Hoppe, C. J. M., Lawrenz, E., Prášil, O., Greenacre, M., Wiktor, J. M., & Leu, E. (2018). Fast reactivation of photosynthesis in arctic phytoplankton during the polar night1. Journal of phycology, 54(4), 461-470.
95. Kaartokallio, H. (2004). Food web components, and physical and chemical properties of Baltic Sea ice. Marine Ecology Progress Series, 273, 49-63.
96. Ladau, J., Sharpton, T. J., Finucane, M. M., Jospin, G., Kembel, S. W., O'dwyer, J., ... & Pollard, K. S. (2013). Global marine bacterial diversity peaks at high latitudes in winter. The ISME journal, 7(9), 1669-1677.
97. Lannuzel, D., Tedesco, L., Van Leeuwe, M., Campbell, K., Flores, H., Delille, B., ... & Brown, K. (2020). The future of Arctic sea-ice biogeochemistry and ice-associated ecosystems. Nature Climate Change, 1-10.
98. Lee, J., Kang, S. H., Yang, E. J., Macdonald, A. M., Joo, H. M., Park, J., ... & Kim, S. S. (2019). Latitudinal Distributions and Controls of Bacterial Community Composition during the Summer of 2017 in Western Arctic Surface Waters (from the Bering Strait to the Chukchi Borderland). Scientific reports, 9(1), 1-10, .doi:10.1038/s41598-019-53427-4.

99. Leu, E., Mundy, C. J., Assmy, P., Campbell, K., Gabrielsen, T. M., Gosselin, M., ... & Gradinger, R. (2015). Arctic spring awakening–Steering principles behind the phenology of vernal ice algal blooms. Progress in Oceanography, 139, 151-170.
100. Lind, S., Ingvaldsen, R. B., & Furevik, T. (2018). Arctic warming hotspot in the northern Barents Sea linked to declining sea-ice import. Nature climate change, 8(7), 634-639.
101. Lizotte, M.P. (2003). The microbiology of sea ice. In: Thomas DN, Dieckmann GS (eds.). Sea ice: an introduction to its physics, chemistry, biology and geology (pp184-210). Blackwell Sci, Oxford.
102. Long, M. H., Koopmans, D., Berg, P., Rysgaard, S., Glud, R. N., & Søgaard, D. H. (2012). Oxygen exchange and ice melt measured at the ice-water interface by eddy correlation. Biogeosciences, 9(6).
103. Lowry, K. E., Pickart, R. S., Selz, V., Mills, M. M., Pacini, A., Lewis, K. M., Joy-Warren, H., Nobre, C., van Dijken, G. L., Grondin, P., Ferland, J., and Arrigo, K. R. (2018). Under-ice phytoplankton blooms inhibited by spring convective mixing in refreezing leads. J Geophys Res Oceans, 123(1), 90-109, https://org/10.1002/2016JC012575.
104. Lydersen, C., Assmy, P., Falk-Petersen, S., Kohler, J., Kovacs, K. M., Reigstad, M., Stehen, H., Strøm, H., Sundfjord, A., Varpe, Ø., Walczowski, W., Weslawski, K. M., and Zajaczkowski, M. (2014). The importance of tidewater glaciers for marine mammals and seabirds in Svalbard, Norway. J Marine Sys, 129, 452-471, https://org/10.1016/j.jmarsys.2013.09.006.
105. Ma, L. Y., Chi, Z. M., Li, J., and Wu, L. F. (2008). Overexpression of alginate lyase of Pseudoalteromonas elyakovii in Escherichia coli, purification, and characterization of the recombinant alginate lyase. World J. Microbiol. Biotechnol., 24, 89-96.
106. Mahé, F., Rognes, T., Quince, C., de Vargas, C., and Dunthorn, M. (2015). Swarmv2: Highly-scalable and high-resolution amplicon clustering. PeerJ 3, e1420. doi:10.7717/peerj.1420.
107. Manna, V., Malfatti, F., Banchi, E., Cerino, F., De Pascale, F., Franzo, A., ... & Celussi, M. (2020). Prokaryotic response to phytodetritus-derived organic material in epi-and mesopelagic Antarctic waters. Frontiers in Microbiology, 11, 1242.
108. Marquardt, M., Vader, A., Stübner, E. I., Reigstad, M., and Gabrielsen, T. M. (2016). Strong Seasonality of Marine Microbial Eukaryotes in a High-Arctic Fjord (Isfjorden, in West Spitsbergen, Norway). Appl. Environ. Microbiol. 82, 1868–1880. doi:10.1128/AEM.03208-15.
109. Martínez-Pérez, C., Mohr, W., Löscher, C. R., Dekaezemacker, J., Littmann, S., Yilmaz, P., ... & LaRoche, J. (2016). The small unicellular diazotrophic symbiont, UCYN-A, is a key player in the marine nitrogen cycle. Nature Microbiology, 1(11), 1-7.
110. Martin-Jézéquel, V., Hildebrand, M., and Brzezinski, M. A. (2000). Silicon Metabolism in Diatoms : Implications for Growth. J. Phycol., 36, 821–840.
111. McClelland, J.W., Holmes, R.M., Peterson, B.J., and Stieglitz, M. (2004). Increasing riverdischarge in the Eurasian Arctic: Consideration of dams, permafrost thaw, and fires aspotential agents of change.J. Geophys. Res.—Atmos.,109, D18102, doi: 18110.11029/12004JD004583
112. McGovern, M., Pavlov, A. K., Deininger, A., Granskog, M., Leu, E. S., Søreide, J., & Poste, A. (2020). Terrestrial Inputs Drive Seasonality in Organic Matter and Nutrient Biogeochemistry in a High Arctic Fjord System (Isfjorden, Svalbard).

113. Meire, L., Mortensen, J., Rysgaard, S., Bendtsen, J., Boone, W., Meire, P., and Meysman, F. J. (2016). Spring bloom dynamics in a 820 subarctic fjord influenced by tidewater outlet glaciers (Godthåbsfjord, SW Greenland). J Geophys Res Biogeosci, 121(6), 1581-1592, https://org/10.1002/2015JG003240.
114. Miller, L. A., Fripiat, F., Else, B. G., Bowman, J. S., Brown, K. A., Collins, R. E., ... & Meiners, K. M. (2015). Methods for biogeochemical studies of sea ice: The state of the art, caveats, and recommendations.
115. Mitra, A., Flynn, K. J., Tillmann, U., Raven, J. A., Caron, D., Stoecker, D. K., ... & Wilken, S. (2016). Defining planktonic protist functional groups on mechanisms for energy and nutrient acquisition: incorporation of diverse mixotrophic strategies. Protist, 167(2), 106-120.
116. Mock, T., & Gradinger, R. (1999). Determination of Arctic ice algal production with a new in situ incubation technique. Marine Ecology Progress Series, 177, 15-26.
117. Mock, T., Dieckmann, G. S., Haas, C., Krell, A., Tison, J. L., Belem, A. L., ... & Thomas, D. N. (2002). Micro-optodes in sea ice: a new approach to investigate oxygen dynamics during sea ice formation. Aquatic microbial ecology, 29(3), 297-306.
118. Molari, M., Janssen, F., Vonnahme, T. R., Wenzhöfer, F., & Boetius, A. (2020). The contribution of microbial communities in polymetallic nodules to the diversity of the deep-sea microbiome of the Peru Basin (4130–4198 m depth). Biogeosciences, 17(12), 3203-3222.
119. Molari, M., Manini, E., and Dell'Anno, A. (2013). Dark inorganic carbon fixation sustains the functioning of benthic deep-sea ecosystems. Global Biogeochem Cycles, 27(1), 212-221, https://org/10.1002/gbc.20030.
120. Moon, T., Sutherland, D. A., Carroll, D., Felikson, D., Kehrl, L., and Straneo, F. (2018). Subsurface iceberg melt key to Greenland fjord freshwater budget. Nat Geosci, 11(1), 49-54, https://org/10.1038/s41561-017-0018-z.
121. Moore, C. M., Mills, M. M., Arrigo, K. R., Berman-Frank, I., Bopp, L., Boyd, P. W., ... & Jickells, T. D. (2013). Processes and patterns of oceanic nutrient limitation. Nature geoscience, 6(9), 701-710.
122. Mortensen, J., Bendtsen, J., Motyka, R. J., Lennert, K., Truffer, M., Fahnestock, M., & Rysgaard, S. (2013). On the seasonal freshwater stratification in the proximity of fast-flowing tidewater outlet glaciers in a sub-Arctic sill fjord. Journal of Geophysical Research: Oceans, 118(3), 1382-1395.
123. Mundy, C. J., Gosselin, M., Ehn, J., Gratton, Y., Rossnagel, A., Barber, D. G., Martin, J., Tremblay, J., Palmer, M., Arrigo, K. R., Darnis, G., Fortier, L., Else, B., Papakyriokou, T. (2009). Contribution of under ice primary production to an ice-edge upwelling phytoplankton bloom in the Canadian Beaufort Sea. Geophys. Res. Lett, 36(17), https://org/10.1029/2009GL038837.
124. Musat, N., Musat, F., Weber, P. K., & Pett-Ridge, J. (2016). Tracking microbial interactions with NanoSIMS. Current opinion in biotechnology, 41, 114-121.
125. Mühlenbruch, M., Grossart, H. P., Eigemann, F., & Voss, M. (2018). Mini-review: Phytoplankton-derived polysaccharides in the marine environment and their interactions with heterotrophic bacteria. Environmental microbiology, 20(8), 2671-2685.
126. Neufeld, J. D., Dumont, M. G., Vohra, J., & Murrell, J. C. (2007). Methodological considerations for the use of stable isotope probing in microbial ecology. Microbial Ecology, 53(3), 435-442.

127. Nilsson, R. H., Larsson, K.-H., Taylor, A. F. S., Bengtsson-Palme, J., Jeppesen, T. S., Schigel, D., Kennedy, P., Picard, K., Glöckner, F. O., Tedersoo, L., Saar, I., Kõljalg, U., & Abarenkov, K. (2019). The UNITE database for molecular identification of fungi: Handling dark taxa and parallel taxonomic classifications. Nucleic Acids Research, 47(D1), D259–D264. https://doi.org/10.1093/nar/gky1022

128. Noël, B., Jakobs, C. L., van Pelt, W. J. J., Lhermitte, S., Wouters, B., Kohler, J., ... & van den Broeke, M. R. (2020). Low elevation of Svalbard glaciers drives high mass loss variability. Nature Communications, 11(1), 1-8.

129. Not, F., Massana, R., Latasa, M., Marie, D., Colson, C., Eikrem, W., Pedros-Alio, C., Valot, D. & Simon, N. (2005). Late summer community composition and abundance of photosynthetic picoeukaryotes in Norwegian and Barents Seas. Limnology and Oceanography, 50(5), 1677-1686.

130. Nuth, C., Gilbert, A., Köhler, A., McNabb, R., Schellenberger, T., Sevestre, H., ... & Kääb, A. (2019). Dynamic vulnerability revealed in the collapse of an Arctic tidewater glacier. Scientific reports, 9(1), 1-13.

131. O'Malley, M. A. (2008). 'Everything is everywhere: but the environment selects': ubiquitous distribution and ecological determinism in microbial biogeography. Studies in History and Philosophy of Science Part C: Studies in History and Philosophy of Biological and Biomedical Sciences, 39(3), 314-325.

132. O'Sadnick, M., Petrich, C., Brekke, C., & Skarðhamar, J. Ice extent in sub-arctic fjords and coastal areas from 2001 to 2019 analyzed from MODIS imagery. Annals of Glaciology, 1-17.

133. Obiol, A., Giner, C. R., Sánchez, P., Duarte, C. M., Acinas, S. G., & Massana, R. (2020). A metagenomic assessment of microbial eukaryotic diversity in the global ocean. Molecular Ecology Resources, 20(3).

134. Okazaki, Y., Fujinaga, S., Salcher, M. M., Callieri, C., Tanaka, A., Kohzu, A., ... & Nakano, S. I. (2020). Microdiversity and phylogeographic diversification of bacterioplankton in pelagic freshwater systems revealed through long-read amplicon sequencing. bioRxiv.

135. Owrid, G., Socal, G., Civitarese, G., Luchetta, A., Wiktor, J., Nöthig, E. M., Andreassen, I, Schauer, U. & Strass, V. (2000). Spatial variability of phytoplankton, nutrients and new production estimates in the waters around Svalbard. Polar Research, 19(2), 155-171.

136. Palmisano, A. C., Kottmeier, S. T., Moe, R. L., & Sullivan, C. W. (1985). Sea ice microbial communities. IV. The effect of light perturbation on microalgae at the ice-seawater interface in McMurdo Sound, Antarctica. Marine ecology progress series. Oldendorf, 21(1), 37-45.

137. Parsons, T. R., Maita, Y. and Lalli, C. M. (1984). A Manual of Chemical and Biological Methods for Seawater Analysis. Pergamon Press, Toronto.

138. Pella E, Colombo B. (1973). Study of carbon, hydrogen and nitrogen determination by combustion-gas chromatography. Microchim Acta. 61, 697–719.

139. Peterson, B. J., Holmes, R. M., McClelland, J. W., Vörösmarty, C. J., Lammers, R. B., Shiklomanov, A. I., ... & Rahmstorf, S. (2002). Increasing river discharge to the Arctic Ocean. science, 298(5601), 2171-2173.

140. Polyakov, I. V., Pnyushkov, A. V., & Carmack, E. C. (2018). Stability of the arctic halocline: a new indicator of arctic climate change. Environmental Research Letters, 13(12), 125008.

141. Porter, K. G., and Feig, Y. S. (1980). The use of DAPI for identifying and counting aquatic microfloral. Limnol Oceanogr, 25, 943–850 948, https://wiley.com/10.4319/lo.1980.25.5.0943.
142. Posch, T., Loferer-Krößbacher, M., Gao, G., Alfreider, A., Pernthaler, J., & Psenner, R. (2001). Precision of bacterioplankton biomass determination: a comparison of two fluorescent dyes, and of allometric and linear volume-to-carbon conversion factors. Aquatic Microbial Ecology, 25(1), 55-63.
143. Prokopowich, C. D., Gregory, T. R. & Crease, T. J. (2003). The correlation between rDNA copy number and genome size in eukaryotes. Genome, 46:48–50.
144. Pruesse, E., Peplies, J., and Glöckner, F. O. (2012). SINA: accurate high-throughput multiple sequence alignment of ribosomal RNA genes. Bioinformatics 28, 1823–1829. doi:10.1093/bioinformatics/bts252.
145. Quast, C., Pruesse, E., Yilmaz, P., Gerken, J., Schweer, T., Yarza, P., ... & Glöckner, F. O. (2012). The SILVA ribosomal RNA gene database project: improved data processing and web-based tools. Nucleic acids research, 41(D1), D590-D596. R Core Team (2020). R: A language and environment for statistical computing. R Foundation for Statistical Computing, Vienna, Austria Available at: https://www.R-project.org/.
146. Reeburgh, W. S. (2007). Oceanic methane biogeochemistry. Chemical reviews, 107(2), 486-513.
147. Regaudie-de-Gioux, A., Lasternas, S., Agustí, S., & Duarte, C. M. (2014). Comparing marine primary production estimates through different methods and development of conversion equations. Frontiers in Marine Science, 1, 19.
148. Rivkin, R. B., & Putt, M. (1987). Heterotrophy and photoheterotrophy by Antarctic microalgae: ligh-dependent incorporation of amino acids and glucose. Journal of Phycology, 23(3), 442-452.
149. Rysgaard, S., Glud, R. N., Sejr, M. K., Blicher, M. E., & Stahl, H. J. (2008). Denitrification activity and oxygen dynamics in Arctic sea ice. Polar Biology, 31(5), 527-537.
150. Rysgaard, S., Kühl, M., Glud, R. N., & Hansen, J. W. (2001). Biomass, production and horizontal patchiness of sea ice algae in a high-Arctic fjord (Young Sound, NE Greenland). Marine Ecology Progress Series, 223, 15-26.
151. Schuler, T. V., Kohler, J., Elagina, N., Hagen, J. O. M., Hodson, A. J., Jania, J. A., ... & Pohjola, V. A. (2020). Reconciling Svalbard glacier mass balance. Frontiers in Earth Science, 8, 156.
152. Shoemaker, K. M., Duhamel, S., & Moisander, P. H. (2019). Copepods promote bacterial community changes in surrounding seawater through farming and nutrient enrichment. Environmental microbiology, 21(10), 3737-3750.
153. Siegel, D. A., Doney, S. C., & Yoder, J. A. (2002). The North Atlantic spring phytoplankton bloom and Sverdrup's critical depth hypothesis. science, 296(5568), 730-733.
154. Simpson, K. G., Tremblay, J. É., Brugel, S., & Price, N. M. (2013). Nutrient dynamics in the western Canadian Arctic. II. Estimates of new and regenerated production over the Mackenzie Shelf and Cape Bathurst Polynya. Marine Ecology Progress Series, 484, 47-62.
155. Sinha, R. K., Krishnan, K. P., & Kerkar, S. (2018). Population dynamics of bacterioplanktonic component associated with the phytoplankton biomass in Kongsfjorden, an Arctic fjord. CURRENT SCIENCE, 115(9), 1690.

156. Sipler, R. E., Gong, D., Baer, S. E., Sanderson, M. P., Roberts, Q. N., Mulholland, M. R., & Bronk, D. A. (2017). Preliminary estimates of the contribution of Arctic nitrogen fixation to the global nitrogen budget. Limnology and Oceanography Letters, 2(5), 159-166.
157. Skogseth, R., Olivier, L. L., Nilsen, F., Falck, E., Fraser, N., Tverberg, V., Ledang, A. B., Vader, A., Jonassen, M. O., Søreide, J., Cottier, F., Berge, J., Ivanov, B. V., and Falk Petersen, S. (2020). Variability and decadal trends in the Isfjorden (Svalbard) ocean climate and circulation-an indicator for climate change in the European Arctic. Prog Oceanogr, 187, 102394, https://org/10.1016/j.pocean.2020.102394.
158. Slawyk, G., Collos, Y., and Auclair, J.-C. (1977). The use of the 13C and 15N isotopes for the simultaneous measurement of carbon and nitrogen turnover rates in marine phytoplankton. Limnol. Oceanogr. 22, 925–932. doi: 10.4319/lo.1977.22.5.0925
159. Soetaert, K., Petzoldt, T. (2010). Inverse Modelling, Sensitivity and Monte Carlo Analysis in R Using Package FME. J Stat Softw, 33, 1–28, doi: 10.18637/jss.v033.i03.
160. Soetaert, K., Petzoldt, T., and Setzer, R. W. (2010). Solving Differential Equations in R: Package deSolve. J Stat Softw, 33, 1548- 585 7660, doi: 10.18637/jss.v033.i09.
161. Solorzano, L. (1969). Determination of ammonia in natural waters by the phenolhypochlorite method. Limnology and oceanography, 14(5), 799-801.
162. Spencer, R. G., Mann, P. J., Dittmar, T., Eglinton, T. I., McIntyre, C., Holmes, R. M., ... & Stubbins, A. (2015). Detecting the signature of permafrost thaw in Arctic rivers. Geophysical Research Letters, 42(8), 2830-2835.
163. Steeman Nielsen, E. (1952). The use of radioactive carbon (14C) for measuring production in the sea. J. Cons. Perm. Int. Explor. Mer. 18, 117–140. doi: 10.1093/icesjms/18.2.117
164. Stoecker, D. K., Hansen, P. J., Caron, D. A., & Mitra, A. (2017). Mixotrophy in the marine plankton. Annual Review of Marine Science, 9, 311-335.
165. Stow, C. A., Jolliff, J., McGillicuddy Jr, D. J., Doney, S. C., Allen, J. I., Friedrichs, M. A., Kenneth, A. R., and Wallhead, P. (2009). Skill assessment for coupled biological/physical models of marine systems. J Mar Syst, 76, 4-15.
166. Sunda, W. (2012). Feedback interactions between trace metal nutrients and phytoplankton in the ocean. Frontiers in microbiology, 3, 204.
167. Suttle, C. A. (2007). Marine viruses—major players in the global ecosystem. *Nature Reviews Microbiology*, *5*(10), 801-812.
168. Sverdrup, H. U. (1953). On conditions for the vernal blooming of phytoplankton. J. Cons. Int. Explor. Mer, 18(3), 287-295.
169. Søgaard, D. H., Kristensen, M., Rysgaard, S., Glud, R. N., Hansen, P. J., & Hilligsøe, K. M. (2010). Autotrophic and heterotrophic activity in Arctic first-year sea ice: seasonal study from Malene Bight, SW Greenland. Marine Ecology Progress Series, 419, 31-45, https://doi.org/10.3354/meps08845.
170. Tank, S. E., Manizza, M., Holmes, R. M., McClelland, J. W., & Peterson, B. J. (2012). The processing and impact of dissolved riverine nitrogen in the Arctic Ocean. Estuaries and Coasts, 35(2), 401-415.
171. Taylor, G. T., & Sullivan, C. W. (2008). Vitamin B12 and cobalt cycling among diatoms and bacteria in Antarctic sea ice microbial communities. Limnology and Oceanography, 53(5), 1862-1877.

172. Teeling, H., Fuchs, B. M., Becher, D., Klockow, C., Gardebrecht, A., Bennke, C. M., ... & Weber, M. (2012). Substrate-controlled succession of marine bacterioplankton populations induced by a phytoplankton bloom. Science, 336(6081), 608-611.
173. Teeling, H., Fuchs, B. M., Bennke, C. M., Krueger, K., Chafee, M., Kappelmann, L., ... & Lucas, J. (2016). Recurring patterns in bacterioplankton dynamics during coastal spring algae blooms. elife, 5, e11888.
174. Terrado, R., Scarcella, K., Thaler, M., Vincent, W. F., & Lovejoy, C. (2013). Small phytoplankton in Arctic seas: vulnerability to climate change. Biodiversity, 14(1), 2-18.
175. Thomas, F. A., Sinha, R. K., & Krishnan, K. P. (2020). Bacterial community structure of a glacio-marine system in the Arctic (Ny-Ålesund, Svalbard). Science of The Total Environment, 718, 135264.
176. Throndsen, J., Hasle, G. R., & Tangen, K. (2007). Phytoplankton of Norwegian coastal waters. Almater Forlag AS.
177. Tomas, C. R. (1997). Identifying Marine Phytoplankton, Elsevier, San Diego.
178. Utermöhl, H. (1958). Methods of collecting plankton for various purposes are discussed. SIL Commun 1953-1996. 9, 1–38, https://doi.org/10.1080/05384680.1958.11904091.
179. Vader, A., Marquardt, M., Meshram, A. R., & Gabrielsen, T. M. (2015). Key Arctic phototrophs are widespread in the polar night. Polar Biology, 38(1), 13-21.
180. Vallières, C., Retamal, L., Ramlal, P., Osburn, C. L., & Vincent, W. F. (2008). Bacterial production and microbial food web structure in a large arctic river and the coastal Arctic Ocean. Journal of Marine Systems, 74(3-4), 756-773.
181. Van den Meersche, K., Middelburg, J. J., Soetaert, K., Van Rijswijk, P., Boschker, H. T., & Heip, C. H. (2004). Carbon-nitrogen coupling and algal-bacterial interactions during an experimental bloom: Modeling a 13C tracer experiment. Limn
182. Vihtakari, M. (2020). PlotSvalbard: PlotSvalbard - Plot research data from Svalbard on maps. R package version 0.9.2. https://github.com/MikkoVihtakari/PlotSvalbard.
183. Vincent, W. F. (2010). Microbial ecosystem responses to rapid climate change in the Arctic. The ISME journal, 4(9), 1087-1090.
184. Von Quillfeldt, C. H. (2000). Common diatom species in Arctic spring blooms: their distribution and abundance. Botanica Marina, 43(6), 499-516.
185. Von Quillfeldt, C.H., Hegseth, E.N., Jonhsen, G., Sakshaug, E., Syvertsen, E.E. (2009). Ice algae. In: Sakshaug, E., Johnsen, G., Kovacs, K.M. (Eds.), Ecosystem Barents Sea (pp. 285–302). Trondheim. Tapir Academic Press.
186. Vonnahme, T. R., Devetter, M., Žárský, J. D., Šabacká, M., & Elster, J. (2016). Controls on microalgal community structures in cryoconite holes upon high Arctic glaciers, Svalbard. *Biogeosciences, 13*, 659-674.
187. Vonnahme, T. R., Molari, M., Janssen, F., Wenzhöfer, F., Haeckel, M., Titschack, J., & Boetius, A. (2020). Effects of a deep-sea mining experiment on seafloor microbial communities and functions after 26 years. Science Advances, 6(18), eaaz5922.
188. Vonnahme, T.R., Dietrich, O., (in review), Life on the sea and shelf seas. Food web in the sea, in: Polar Ecology, edited by: Dietrich, O.

189. Waleron, M., Waleron, K., Vincent, W. F., & Wilmotte, A. (2007). Allochthonous inputs of riverine picocyanobacteria to coastal waters in the Arctic Ocean. FEMS microbiology ecology, 59(2), 356-365.
190. Wang, Q., Garrity, G. M., Tiedje, J. M., and Cole, J. R. (2007). Naive Bayesian Classifier for Rapid Assignment of rRNA Sequences into the New Bacterial Taxonomy. Appl Environ Microbiol. 73(16), 5261-7, https://org/ 10.1128/AEM.00062-07.
191. Wangensteen, O. S., Palacín, C., Guardiola, M., and Turon, X. (2018). DNA metabarcoding of littoral hard-bottom communities: high diversity and database gaps revealed by two molecular markers. PeerJ, 6, e4705, https://org/10.7717/peerj.4705.
192. Wassmann, P., Slagstad, D., Riser, C. W., and Reigstad, M. (2006). Modelling the ecosystem dynamics of the Barents Sea including the marginal ice zone: II. Carbon flux and interannual variability. J Mar Syst, 59, 1-24.
193. Wiedmann, I., Reigstad, M., Marquardt, M., Vader, A., and Gabrielsen, T. M. (2016). Seasonality of vertical flux and sinking particle 895 characteristics in an ice-free high arctic fjord—Different from subarctic fjords?. J Marine Sys, 154, 192-205, https://org/10.1016/j.jmarsys.2015.10.003.
194. Worden, A. Z., Follows, M. J., Giovannoni, S. J., Wilken, S., Zimmerman, A. E., & Keeling, P. J. (2015). Rethinking the marine carbon cycle: factoring in the multifarious lifestyles of microbes. Science, 347(6223).
195. Yergeau, E., Michel, C., Tremblay, J., Niemi, A., King, T. L., Wyglinski, J., ... & Greer, C. W. (2017). Metagenomic survey of the taxonomic and functional microbial communities of seawater and sea ice from the Canadian Arctic. Scientific reports, 7, 42242.
196. Yool, A., Martin, A. P., Fernández, C., & Clark, D. R. (2007). The significance of nitrification for oceanic new production. *Nature*, *447*(7147), 999-1002.
197. Zhang, Q., Gradinger, R., & Spindler, M. (1998). Dark survival of marine microalgae in the high Arctic (Greenland Sea). Polarforschung, 65(3), 111-116.
198. Zimmerman, A. E., Howard-Varona, C., Needham, D. M., John, S. G., Worden, A. Z., Sullivan, M. B., ... & Coleman, M. L. (2019). Metabolic and biogeochemical consequences of viral infection in aquatic ecosystems. Nature Reviews Microbiology, 1-14.
199. Zorz, J., Willis, C., Comeau, A. M., Langille, M. G., Johnson, C. L., Li, W. K., & LaRoche, J. (2019). Drivers of regional bacterial community structure and diversity in the Northwest Atlantic Ocean. Frontiers in microbiology, 10, 281.
200. Zwirglmaier, K. (2005). Fluorescence in situ hybridisation (FISH)–the next generation. FEMS Microbiology Letters, 246(2), 151-158.
201. Østerhus, S., Woodgate, R., Valdimarsson, H., Turrell, B., Steur, L. D., Quadfasel, D., ... & Jónsson, S. (2019). Arctic Mediterranean exchanges: A consistent volume budget and trends in transports from two decades of observations. Ocean Science, 15(2), 379-399.

Progress in Microbial Ecology in Ice-Covered Seas

14

Tobias R. Vonnahme, Ulrike Dietrich, and Brandon T. Hassett

Abstract

Sea ice seasonally covers 10% of the earth's oceans and shapes global ocean chemistry. The unique physical processes associated with sea ice growth and development shape the associated biological diversity and ecosystem function. Microbes make up the base of all marine food webs and the overwhelming majority of biomass in the sea ice ecosystem. Despite their biomass, microbial processes are not fully integrated into marine ecosystem models. Recent applications of novel molecular biology technologies to studies of marine ecology have elucidated numerous microbial-mediated processes interfaced by previously unknown organisms and processes. These discoveries are yielding more in-depth studies on the relevance of mixotrophy, the ecology of fungi, and the interplay between major microbial clades. In ecosystem studies, the basis of the food web is frequently neglected even though the accessibility of energy, recycling of nutrients, and parasitism are crucial factors shaping the environment for grazers and higher trophic levels. In this review, we focus on the species composition, abundance, and functions of microalgae, bacteria, archaea, fungi, and viruses in the sea ice-covered seas throughout the year. A strong emphasis will be put on advances in molecular methods that empower scientists to further investigate microorganisms in more detail. Since microbes make up the majority of all oceanic biomass, we believe that it is impossible to accurately forecast the biological fate of polar marine ecosystems without placing a proportional emphasis on microbes relative to their biomass.

Keywords

Mixotrophy · Autotrophy · Heterotrophy · Omics · Fungi

T. R. Vonnahme (✉) · U. Dietrich (✉) · B. T. Hassett
UiT- The Arctic University of Norway, Tromsø, Norway
e-mail: tobias.vonnahme@uit.no; Ulrike.dietrich@uit.no

14.1 Introduction

Sea ice seasonally covers approximately 10% of the global ocean surface and is responsible for altering global ocean chemistry. The main ice-covered marine ecosystems are found in the Arctic Ocean, the Southern Ocean, and the Baltic Sea. Within the polar marine ecosystems, sea ice formation and subsequent coverage influence light transmittance that seasonally governs under-ice primary production and the associated heterotrophic biological community. Specifically, sea ice can support 50% of total primary productivity in permanently ice-covered ecosystems (Gosselin et al. 1997; Fernández-Méndez et al. 2015) and constitutes a habitat and feeding ground for various organisms. It provides microhabitats for microalgae, chemoautotrophic and heterotrophic bacteria, archaea, viruses, fungi, and multicellular organisms (Bluhm et al. 2018) that inhabit the hypersaline brine channels (Hunt et al. 2016). The sea ice habitat is characterized by strong gradients in temperature, salinity, nutrients, and light. The small-scale spatial distribution of sea ice-associated (sympagic) biota is determined to a large extent by these physical properties (Krembs et al. 2011). Organisms within the brine channels are exposed to extreme temperatures from 0 °C in summer to below −15 °C in winter with associated brine salinities ranging from 0 to over 200 (Gradinger 2001). Most of the biomass within brine channels is localized near the warmer ice-water interface, where temperatures are about −1.8 °C, the brine-volume fraction is greatest, and a continuous exchange of nutrients from the water below takes place.

The two major ice types found in polar environments provide different habitat characteristics (e.g., thickness, ice bulk salinities, age, and albedo), relevant for the associated biological processes (Weeks and Ackley 1986). Multiyear ice (MYI) persists at least one melting season, whereas first-year ice (FYI) follows a seasonal pattern of ice formation and melt. On average, the surface salinity of FYI is typically around 10–12, whereas MYI typically has surface salinities

S. Jungblut et al. (eds.), *YOUMARES 9 - The Oceans: Our Research, Our Future*,
https://doi.org/10.1007/978-3-030-20389-4_14

that approach 0 (Weeks and Ackley 1986). FYI is often structurally less complex, characterized by greater light penetration through the ice that is prone to an earlier onset of seasonal melt (Moline et al. 2008). Contrasting studies between FYI and MYI indicate that FYI hosts a higher number of organisms, but a less rich microbial community. Changes within the ice biological system might have cascading effects on the ice-associated ecosystem (Secretariat of Arctic Council 2017).

The open water in sea ice-covered seas is a special system in itself. At the marginal ice zone or in open leads, a system with high levels of light and nutrients may support ice edge phytoplankton blooms dominated by different species compared to sea ice (Assmy et al. 2017). With climate change, these areas are expected to increase, changing the microbial community structure in sea-ice covered seas (Oziel et al. 2017). The consequences for higher trophic levels and carbon export are a topic of recent studies. In the Arctic and Antarctic, a large part of the ocean is ice-free during the polar night. The absence of light challenges the pelagic microbial food web due to a lack of photosynthetic primary production. Nevertheless, microbes have been found to be active throughout the polar night and different biogeochemical cycles may be dominant (Zhang et al. 2003; Berge et al. 2015; Nguyen et al. 2015).

The polar marine environment is in a state of rapid transition with tremendous changes in the abiotic environment. In the Arctic Ocean, air and surface-layer temperatures are increasing faster than the global average (Serreze and Francis 2006; Holding et al. 2015) and is driving the replacement of MYI with thinner FYI (Maslanik et al. 2011; Perovich et al. 2014; Barber et al. 2015). This replacement has contributed to an earlier onset of seasonal ice melt, an increased duration of ice melt (Stroeve et al. 2014), and persistent open water conditions in the seasonal ice zone (Lange et al. 2016). A strong reduction in overall Arctic sea ice extent occurred over the last two decades, with the lowest summer minimum ice extent in 2012 (3.61×10^6 km^2), which had been 18% below the previous low of 2007 (Beitler 2012). In contrast to the Arctic, the Antarctic is characterized by a large extent of seasonally forming ice that grows from 4×10^6 km^2 in summer to approximately 19×10^6 km^2 in late winter (Cavalieri et al. 1999). Specifically during autumn, the surface of the ocean surrounding the Antarctic continent begins to freeze, forming sea ice of about 0.4 m thickness (up to 1 m; Worby et al. 2001). Overall, the ice extent in the Antarctic has been much less impacted compared to the Arctic. In the Antarctic Peninsula and Bellinghausen Sea region, the ice-free summer season is extended by three months, whereas in the western Ross Sea region, the ice-free season is shortened by two months (Lange et al. 2016). Due to strong wind events, large quantities of heat are extracted from the surface ocean, facilitating rapid formation of frazil ice (Eicken 2003).

The Baltic Sea is one of the world's largest brackish water basins with a surface area of 422,000 km^2 and a mean depth of only 55 m. Surface salinities vary from 9 in the southern part to below 1 in the innermost parts (Voipio 1981). Annually, sea ice covers about 40% of the Baltic Sea (Kaartokallio et al. 2007). Even though the seasonal ice of the Baltic Sea has many similarities with the seasonal ice in the polar areas, fresher water results in sea ice with lower bulk salinities and smaller brine channels, despite the comparably high temperatures (Meiners et al. 2002). Low brine volumes reduce the rate of seawater exchange across the ice-water interface that affects rates of nutrient replenishment, convective heat transport, and desalination processes (Lytle and Ackley 1996). Due to milder climate in the Baltic Sea region, snow and freeze-melt cycles occur throughout winter, leading to a greater contribution (up to 35%) of sea ice mass in the form of metamorphic snow (Granskog et al. 2006). The high dissolved organic matter (DOM) content in Baltic Sea water and ice leads to different chemical characteristics and causes increased absorption of solar radiation at shorter wavelengths than are utilized for photosynthesis (Granskog et al. 2006). During early winter most of the Baltic Sea is ice free and below the Arctic Circle, where daylight is available for photosynthesis throughout the year in contrast to the polar night in polar regions. As a result, the microbial community differs considerably from polar sea ice environments.

14.2 Advances in Microbial Ecology

Advances in marine microbial ecology are driven by methodological advances in understanding both, the environment, as well as the biological taxa that inhabit the environment. Microbial methodology and associated observations advanced marginally from the late 1800s during Nansen's First Fram Expedition to the 1960s and 1970s, where light microscopy and cultivation-based studies of microbes shaped science's understanding of microbial ecology (e.g., Hobbie et al. 1977; reviewed by Baross and Morita 1978). With advancing resolution in microscopy, it was possible to get a better understanding of microbial diversity and abundances that has now ushered in the -omics era. These microbial methodologies have evolved in parallel with in situ technologies. Early approaches measured primary production in slices of an ice core incubated in surrounding ice (Mock and Gradinger 1999). Since these early studies, technological advancements have allowed for in situ measurements of primary production; oxygen microsensors have been used successfully in artificial sea ice experiments to measure in situ ecosystem production (Mock et al. 2002). However, the standard method is to still work on melted sea ice, which may be an underestimation of primary production (Søgaard et al.

2010). Stable- and radioisotope incubations allowed estimates of microbial activities and associated organic matter utilization. The future of methods for studying biogeochemistry in sea ice may be in situ technologies (reviewed by Miller et al. 2015). Methods for water sampling and biogeochemical studies have been similar to traditional work in other pelagic systems.

The application of molecular fingerprinting methods (e.g., denaturing gradient gel electrophoresis, restriction fragment length polymorphism), clone library sequencing, and in recent years, metagenomics have generated a detailed understanding of microbial phylogeny, taxonomy, and more recently, function and ecology in the seasonal ice zone. Amplicon-based sequencing of the taxonomically informative small ribosomal subunit became a standard genetic barcode, which allowed the identification of microbial taxa down to the level of ecotypes. Advancing sequencing technologies are generating more sequence reads at a lower cost, affording high spatial and temporal resolution of microbial (primarily bacterial) communities and subsequent investigation of their connectivity, seasonal successions, and biogeography (e.g., Brown and Bowman 2001; Brinkmeyer et al. 2003; Collins et al. 2010; Hatam et al. 2016; Yergeau et al. 2017; Rapp et al. 2018). Novel sequencing tools, such as the Nanopore MinION have the potential to be used for in-field sequencing, and have been used in remote polar regions (e.g., Johnson et al. 2017), but not yet in sea ice. Novel sequencing technologies are evolving in parallel with bioinformatic tools that can identify small, yet significant community differences. When used together, these novel sequencing technologies and bioinformatic tools are yielding novel ecological insights that are, in turn, shifting sciences' understanding of microbial community complexity. Consequently, there is an emerging trend away from the traditional 97% to 98% similarity cutoff that defines microbial taxa toward network- and nucleotide entropy-based clustering methods (e.g., Rapp et al. 2018).

Recent studies are focusing more on full genome, metagenomic shotgun sequencing approaches. Approaches, which simultaneously generate taxonomic and functional gene information. So far, only several studies have applied metagenomic shotgun sequencing to sea ice samples (e.g., Bowman et al. 2014; Yergeau et al. 2017), but the potential to elucidate complex polar microbial ecology questions is generally unrealized. Metagenomic sequencing efforts have demonstrated bacterial-mediated chemical cycling in frost flowers (Bowman et al. 2014) and the importance of select photoreceptors in Antarctic and Arctic sea ice (Koh et al. 2010; Vader et al. 2018). With increasing throughput of sequence generation and decreasing costs, deep sequencing (i.e., sequencing the same locus multiple times) of the environment should allow comparative studies of full metagenomes to describe the metabolic potential (including uncultured strains) and strain level microbial diversity (e.g., Delmont et al. 2017) in sea ice ecosystems.

Other -omics studies that target byproducts of protein synthesis and secondary metabolism are rare in sea ice. While metagenomics can demonstrate the genetic potential of microbes, RNA-based studies, such as metatranscriptomics, can show whether the genes are expressed. For example, Koh et al. (2010) and Vader et al. (2018) showed that the genes for proteorhodopsin are actively transcribed in Antarctic and Arctic sea ice, indicating an active phototrophic bacterial community. Interdisciplinary research with biochemists identified the functions of translated proteins and ascribed a functional purpose for gene products used in survival and metabolism in sea ice (reviewed by Feller and Gerday 2003; Feng et al. 2014). Metaproteomics is not only possible for cultured bacteria, but can be used for understanding the biochemical functions of the in situ community (Junge et al. 2019). Ultimately, combined -omics studies are important for a thorough understanding of microbial ecology and biogeochemistry (Junge et al. 2019). In cultures, the potential to combine proteomics and genomics has already been shown to help understanding key genes for a life in subzero temperatures (Feng et al. 2014). To date, metaproteomics and metabolomics studies of the whole community have yet to be applied to studies of sea ice.

Ribosomal gene sequencing data have been used to develop fluorescently labeled nucleotide probes that target taxonomically informative genetic loci, namely, fluorescence in situ hybridization (FISH) (Pernthaler et al. 2002). The application of FISH has informed analyses of spatial interactions and abundances of specific taxa, without the known biases associated with DNA sequencing (De Corte et al. 2013), nonspecific fluorescent stains (e.g., 4′,6-diamidino-2-phenylindole), or cultivation (e.g., Brinkmeyer et al. 2003; Baer et al. 2015). Combined with isotope probing methods, catalyzed reporter deposition-FISH (CARD-FISH) has been used to identify microbial taxa responsible for the uptake of specific organic compounds (e.g., Alonso-Sáez et al. 2008; Nikrad et al. 2012). Consequently, CARD-FISH is a robust method that should be used to supplement DNA sequencing analysis. Only a few of the metabolic capacities mentioned in this chapter have been measured and a common limitation is still the separation of biogeochemical rate measurements and investigations of the genetic potential of communities, or organisms. Studies coupling the function, activity, and diversity of bacteria are lacking in sea ice systems, but their potential has been shown in other marine systems. RNA stable isotope probing is one recent method, which could be used to overcome these limitations. For example, Fortunato and Huber (2016) coupled stable isotope probing with metatranscriptomics to identify taxa and pathways involved in chemolithotrophic processes at hydrothermal vents. Methods for visualization of radioisotope (Microautoradiography,

(Nierychlo et al. 2016) or stable isotope (Nanoscale secondary ion mass spectrometry, Gao et al. 2016) enrichments in single cells coupled to CARD-FISH could be another method to quantify biogeochemical fluxes of certain taxonomic groups.

One of the major applications of novel ecological data is the incorporation into ecosystem models. Despite the increasing computational power, the representation of microbial interactions in ecosystem models is still rudimentary. For example, bacterial activities are often hidden in functions for organic matter remineralization and respiration (e.g., Tedesco et al. 2010; Wassmann et al. 2010; Vancoppenolle and Tedesco 2017). A recent ecosystem model in the Baltic Sea started realizing for the first time the importance of bacteria beyond nutrient remineralization. Specifically, aerobic and anaerobic bacterial taxa were separately considered, both as crucial for remineralization processes and for generating anaerobic conditions linked to algal production (Tedesco et al. 2017). Linking metabolic pathway models, bacterial functions (such as denitrification and nitrogen fixation), and viral lysis may further improve the accuracy of models with increasing data availability and computational power. In most ecosystem models and discussions, the role of sea ice bacteria and archaea is seen in the heterotrophic aerobic remineralization of DOM (e.g., Tedesco et al. 2010; Wassmann et al. 2010; Vancoppenolle and Tedesco 2017).

14.3 Sea Ice-Associated Microorganisms

The base of polar food webs is comprised of microbial organisms allied to multiple clades of life. Polar organisms are well adapted to the seasonality of light, nutrient/food availability, and cold temperatures. Additional challenges arise for ice-associated biota, with extreme cold temperatures, highly variable salinities and only temporary existence of their habitat (Meier et al. 2014). The balance between producers and consumers seasonally shifts with light availability which drives taxa-specific abundances. Diatoms and other microalgae (haptophytes, prasinophytes, dinoflagellates) are some of the most common eukaryotic producers that support a diverse heterotrophic community of prokaryotes, fungi, and fungal-like organisms, ciliates, and larger multicellular organisms. These organisms are all presumably susceptible to viral infection, which can rapidly shunt organic material into the available dissolved organic material pool. Together, these organisms cycle carbon and exchange genes that maintain ecosystem function and support the feeding needs of higher trophic levels.

14.3.1 Microalgae

The microalgae community in polar sea ice is dominated by diatoms that comprise the most biomass and greatest species richness, including up to 170 species predominated by *Nitzschia* sp., *Thalassiosira* sp., *Fragilariopsis* sp., and *Navicula* sp. (Arrigo 2010). Pennate diatoms dominate the spring ice algal bloom in Arctic FYI, as well as in Antarctic sea ice due to the nutrient-rich Southern Ocean (Arrigo et al. 2014). Sea ice associated phytoplankton blooms are often dominated by aggregates of *Phaeocystis* sp., capable of producing large biomasses and drawing down large amounts of nutrients (Assmy et al. 2017). Other algae groups in the pico- and nanoplankton-size fraction contribute substantially to the pelagic and sympagic winter community. *Micromonas* sp., *Cyanobacteria*, and *Ostreococcus* sp. have been found to be abundant phytoplankton species in the polar night (Joli et al. 2017; Amargant Arumí 2018) but only constitute a small fraction of the biomass during spring and summer (Riedel et al. 2008; Niemi et al. 2011; Vader et al. 2018) and therefore have not been studied in more detail until recently. Still, reliable identification and quantification of pico- and nanosized eukaryotes are lacking (Piwosz et al. 2013) or are purely based on sequencing (Vader et al. 2018).

As a consequence of the lower water salinity and corresponding small-sized brine ice channels, the Baltic Sea ice is dominated by smaller protists (Kaartokallio et al. 2007). In early spring, centric diatoms dominate under-ice biomass. These centric diatoms are supplemented by large contributions of *Melosira arctica* and the cyanobacterium *Aphanizomenon* sp. that can predominate abundances in the brine channels (Majaneva et al. 2017). In contrast to Arctic and Antarctic sea ice communities, dinoflagellates and green algae contribute to a large fraction of the biomass in Baltic Sea ice and open water (Kaartokallio et al. 2007; Piiparinen et al. 2010). Furthermore, the surface-layer algal biomass can significantly contribute to the overall sea ice algal biomass (Meiners et al. 2002; Piiparinen et al. 2010). So far, the knowledge of species composition and distribution is limited, and there is only little known on the overwintering of cyanobacteria, which are typical for the Baltic Sea (Laamanen 1996).

14.3.2 Bacteria

The most common orders found in sea ice are *Alteromonadales* (*Gammaproteobacteria*) and *Flavobacteriales* (*Bacteroidetes*) with the most common genera *Pseudoalteromonas*, *Colwellia*, *Shewanella*, *Flavobacterium*, and *Polaribacter* (Bowman et al. 2012, 2014; Boetius et al. 2015; Yergeau et al. 2017). Rarer phyla are the *Alphaproteobacteria*, *Betaproteobacteria*,

Actinobacteria, and *Firmicutes* (Bowman et al. 2012, 2014; Boetius et al. 2015; Yergeau et al. 2017). Archaea are mainly found in autumn and winter; they consist primarily of the genus *Nitrosopumilus*, known for its nitrification capability (Brinkmeyer et al. 2003; Collins et al. 2010). However, most studies are biased toward sampling in summer and spring, but a few studies in winter indicate differences in communities (Collins et al. 2010). On the operational taxonomic unit (OTU) level (97% cutoff), there seem to be no endemic species for sea ice in certain ice zones so far (reviewed by Deming and Collins 2017), but further studies focusing on strain variability may find differences. It has been shown that the bacterial OTUs are more variable in seasonal sea ice and more related to temperate communities compared to MYI (Hatam et al. 2016). Several bacteria found are known to be psychrophilic (e.g., Feng et al. 2014), and a large fraction could be cultured (up to 60%, Junge et al. 2002). The bacterial and archaeal communities in the water column of sea ice systems are significantly different with *Nitrosopumilus* sp., *Pelagibacter* sp., *Flavobacteriales* sp., and *Oceanosprillaceae* sp. as dominating taxa (e.g., Bowman et al. 2012, 2014; Yergeau et al. 2017), indicating a strong selection of potentially endemic sea ice bacteria.

14.3.3 Fungi

Fungi are eukaryotic, spore-bearing, heterotrophic organisms that secrete extracellular enzymes used for interfacing symbiosis and facilitating osmotrophy. Within this ecological definition, fungi are a polyphyletic functional group that include the *Labyrinthulomycota*, *Mesomycetozoea*, *Oomycota*, select *Amoebozoa*, the True Fungi, and several additional clades. True Fungi are distinct from ecological fungi (fungal-like organisms) by possessing cell walls made of chitin and forming a molecular monophyletic clade among the opisthokonts. The True Fungi include many prominent mycelial-producing members, such as the *Ascomycota*, *Basidiomycota*, and *Mucoromycota*, as well as reduced zoosporic varieties, such as the *Blastocladiomycota*, *Chytridiomycota*, and *Neocallimastigomycota*. In this review, fungi are explored within their ecological definition, unless otherwise noted. The often inconspicuous morphology of fungi has challenged the easy identification and subsequent integration of mycological data into ecosystem ecology. As a result, the relevance of fungi remains unrealized in ecosystem modeling efforts globally. Historical culturing-based studies have resulted in the description of hundreds of marine fungal species (Johnson and Sparrow 1961; Kohlmeyer and Kohlmeyer 2013), whose global distribution remains largely unexplored. The more-recent application of molecular methods to studies of marine ecosystem ecology helps to circumvent challenges associated with visual classification and have identified an abundant and dynamic fungal community in subseafloor sediment (Orsi et al. 2013), in association with pelagic marine snow (Bochdansky et al. 2017), in coastal marine habitats (Ueda et al. 2015; Picard 2017) as parasites of phytoplankton (Hanic et al. 2009; Lepelletier et al. 2014; Hassett and Gradinger 2016; Jephcott et al. 2016; Scholz et al. 2017a, b) and metazoans (Polglase 1980; Mclean and Porter 1982; Bower 1987; Shields 1990; Rahimian 1998). Relative to lower latitudes, knowledge of Arctic marine fungi is considerably less developed, in part due to the logistical constraints and inaccessibility of sampling sites. The state of ecological knowledge on Arctic marine True Fungi has largely centered on establishing presence-absence data, supplemented with baselines of diversity and richness, currently estimated at several hundred species (Rämä et al. 2017), with a low success rate of culturing (Bubnova and Nikitin 2017). DNA sequence-based analysis identified overlapping True Fungi taxa from the Bering Sea region and Svalbard, demonstrating a broad distribution of fungal taxa across the Arctic Ocean (Hassett et al. 2017) that are selectively predominated by the *Chytridiomycota* (Terrado et al. 2011; Hassett and Gradinger 2016) and comprise a novel, uncharacterized branch of life (Comeau et al. 2016; Hassett et al. 2017). The diversity and distribution of Arctic marine fungal-like organisms is currently unknown and unreported in assessments of unicellular eukaryotic biodiversity (Poulin et al. 2011).

14.3.4 Viruses

Historically, the study of viral diversity was limited by the co-cultivation of the virus and its host (Borriss et al. 2003; Wells and Deming 2006b). Sea ice viruses are cold-adapted (Luhtanen et al. 2018) and may be less host-specific than in more temperate regions (Wells and Deming 2006b). Cultivated viruses only include *Siphoviridae* and *Myoviridae* as sea ice-specific taxa (Borriss et al. 2003; Wells and Deming 2006a; Sencilo et al. 2015). With increasing -omic efforts, more viruses could be found indicating a higher diversity than previously thought, and taxa such as *Podoviridae*, *Nodaviridae* (RNA), *Iridoviridae* (DNA), and *Caudovirales* have been detected (Allen et al. 2017).

14.4 General Ecology of Sea Ice-Associated Microbes

14.4.1 Autotrophy

14.4.1.1 Photoautotrophy

The activity of the microbial food web follows the fixation of carbon and its subsequent turnover into the DOM pool

(Arrigo and Thomas 2004). While sea ice algal annual primary production rates are generally low compared to the phytoplankton fraction, they are often the main source of fixed carbon for higher trophic levels in ice-covered seas. During winter, ice algae are of special importance, when other sources of food are lacking (Lizotte 2003). Chlorophyll *a* (Chl *a*) concentrations in sea ice vary by region, ice type and season and covers a range somewhat typical for oceanic values up to the highest concentrations found in aquatic environments (Arrigo 2010). In the Arctic**,** the balance between annual phytoplankton to ice algal primary production differs regionally. In the northern Barents Sea, ice algae account for about 20% of total primary production (Hegseth 1998), whereas in more heavily ice-covered areas like the Central Arctic Ocean, ice algae can contribute more than 50% to the total primary production (Gosselin et al. 1997). Chl *a* concentrations vary between 22 mg m^{-2} in Allen Bay, Nunavut, during spring (Campbell et al. 2014) and 0.3–8 mg m^{-2} in the Central Arctic in summer (Fernández-Méndez et al. 2015). In ice-covered waters of the Antarctic, sea ice algae account for up to 25% of total annual primary production (Arrigo and Thomas 2004). Chl *a* concentrations vary from 1 to 50 mg m^{-2} in the Weddel Sea region (Ackley et al. 1979), whereas sea ice attached to the coast of Antarctica (fast ice) accumulates biomass of up to 2120 mg m^{-2} (Arrigo and Sullivan 1992). On average, under sufficient light intensities for photosynthesis, Chl *a* concentrations exceed 200 mg m^{-2} during spring and summer (Palmisano and Sullivan 1983; Trenerry et al. 2002). In contrast, productivity by sea ice algae in the Baltic Sea is much lower, contributing about 10% to the primary production during the ice-covered season (Haecky et al. 1999). Average Chl *a* values range between 0.2 and 5.5 mg m^{-2} (Haecky et al. 1999; Kaartokallio 2001, 2004).

Based on sequencing results and detection of photopigments, sea ice and sea ice-associated bacteria have also been speculated to be capable of photoautotrophic carbon fixation (Petri and Imhoff 2001; Koh et al. 2011, 2012; Boetius et al. 2015). Despite their high abundance in other cold environments, such as glaciers (Vonnahme et al. 2016), phototrophic cyanobacteria and anoxygenic phototrophs (e.g., purple sulfur bacteria, Chloroflexi) are not as abundant as eukaryotic sea ice algae, but are frequently detected in the Arctic (Petri and Imhoff 2001; Boetius et al. 2015; Yergeau et al. 2017) and Antarctic (Koh et al. 2011, 2012). Their pigments (phycobiliproteins and bacteriochlorophyll), as well as their genes (e.g., 16S rRNA genes), have been found (Cottrell and Kirchman 2009; Koh et al. 2012; Boetius et al. 2015). However, a proof of their phototrophic activity in sea ice is, yet, lacking. Cyanobacteria are more abundant in the snow layer of sea ice suggesting aeolian origin in the Antarctic (Koh et al. 2012). It appears that cyanobacteria are more abundant in fresher systems, such as melt ponds and the Baltic Sea (Petri and Imhoff 2001; Rintala et al. 2014) and that they become more abundant in winter (Cottrell and Kirchman 2009). In the water column, anoxygenic phototrophs may contribute to up to around 15% of the bacterial communities in the Arctic, which is 1000 times more than cyanobacteria such as *Synechococcus* sp. and may indicate a high importance of this pathway in addition to photosynthesis by sea ice algae (Cottrell and Kirchman 2009). In contrast to cyanobacteria, anoxygenic phototrophs appear to be more abundant in summer (Cottrell and Kirchman 2009). Proteorhodopsin, a pigment for using light energy to create a proton motive force, which can be used for energy production, or nutrient transport, is commonly found in seasonal sea ice in the Arctic and Antarctic and can be seen as another way of phototrophic carbon fixation by *Alphaproteobacteria*, *Gammaproteobacteria*, and *Flavobacterium* (Koh et al. 2010, 2012; Yergeau et al. 2017). A combination of these alternative photosynthetic pathways using different wavelengths efficiently may be an important component of the primary production in the seasonal ice zones, but their phototrophic activity has not been quantified in sea ice, yet.

14.4.1.2 Chemoautotrophy

In the water column, chemoautotrophy (inorganic carbon uptake, using chemical energy), appears to be an important autotrophic carbon acquisition process. During nitrification, ammonium is used as energy source, which delivers energy during reduction to nitrite and nitrate for inorganic carbon fixation. The ammonium originates commonly from primary production by sea ice algae and phytoplankton. The nitrate produced via nitrification can be used as recycled inorganic nitrogen for primary production. Archaea constitute a large fraction of potential nitrifiers in the water column, with significantly higher abundances than in sea ice (Yergeau et al. 2017). Nitrifying bacteria appear to be important in coastal areas of the Arctic seasonal ice zone, potentially due to a high supply of ammonium from the bottom water (Damashek et al. 2017). Nitrifying taxa have also been found in deeper stations, but nitrifying archaea are more abundant (e.g., Yergeau et al. 2017). Other autotrophic pathways have not been described yet and are rather unlikely due to the lack of sources for reduced ions in sea ice.

Aerobic bacterial production may become high enough to leave anoxic pockets in the sea ice, where anaerobic processes become energetically favorable. Denitrification and anaerobic ammonia oxidation (Anammox) rates comparable to sediments have been measured in sea ice, reducing the overall nitrogen availability for primary production (Rysgaard and Glud 2004; Rysgaard et al. 2008). New production of nitrogen is possible via upwelling from nutrient-rich bottom waters, bacterial recycling of organic matter, or N_2 fixation. So far, the *nifH* gene for nitrogen fixation has been detected in Arctic seasonal sea ice connected to a

diverse group of cyanobacteria (Diez et al. 2012). The potential for nitrogen fixation has also been found in the central Arctic Ocean, but the genes are mainly related to heterotrophic bacteria indicating different communities for N_2 fixation in the Arctic (Fernández-Méndez et al. 2016). However, the importance of nitrogen fixation in sea ice remains unclear until nitrogen fixation has been measured directly or the gene expression has been assessed via omics approaches. Nitrogen fixation measurements from open water in the seasonal ice zone suggest that 27.1% of the nitrogen lost via denitrification can be resupplied via nitrogen fixation (Sipler et al. 2017).

14.4.1.3 Others

Other biogeochemical cycles have been discovered in metagenomic and metatranscriptomic datasets (reviewed by Bowman 2015), indicating the potential for mercury cycling and dimethyl sulfide (DMS) production (Bowman et al. 2014), hydrocarbon degradation (Gerdes et al. 2005), and vitamin B12 synthesis (Taylor and Sullivan 2008) in and under sea ice, all processes which can effect primary production in sea ice-covered seas.

14.4.2 Mixotrophy

Mixotrophy in algae is the combination of a heterotrophic (phagotrophic and/or osmotrophic) and phototrophic nutritional mode within a single cell (Sanders 1991). The awareness of the importance of mixotrophic behavior in aquatic systems has increased tremendously (Hansen 2011) and has been reported to be widespread among flagellate algal groups such as dinoflagellates, prymnesiophytes, and cryptophytes in the marine system (Ballen-Segura et al. 2017). Many bloom-forming algal species have been recognized to be mixotrophs causing an increased interest in this field. The potential benefits of particle ingestion include the acquisition of organic carbon, energy, major nutrients, vitamins, and trace metals (Caron et al. 1993). Mixotrophy is particularly beneficial when there is a limitation in inorganic nutrients (Unrein et al. 2014) or light availability (Hansen 2011). Under oligotrophic conditions, flagellated algae can account for up to 80% of total bacterial grazing (Unrein et al. 2007; Sanders and Gast 2012). Predation by flagellated algae is among the primary mortality factors of prokaryotes in planktonic communities, constituting an important selective pressure (Ballen-Segura et al. 2017).

The Arctic nanoplankton species *Micromonas pusilla* is abundant in polar waters throughout the year and was identified as being independent of the availability of light based on a mixotrophic life style (Unrein et al. 2007; Sanders and Gast 2012). Under thick ice cover in the Canadian Arctic, *Micromonas* sp. contributed up to 93% of autotrophic cell abundance (Sherr et al. 1997). *Micromonas pusilla* ingests higher rates of fluorescently labeled bacteria at oligotrophic conditions, but only if exposed to light. This suggests that the ingestion supplemented nitrogen and/or phosphorus supply to allow for balanced growth when photosynthesis rate is high (McKie-Krisberg and Sanders 2014). In the dark, the tested strain would take up less fluorescently labeled bacteria, which points to an osmotrophic uptake of carbon and energy.

Although the potential importance of mixotrophy within the sea ice community has been recognized, comparably few studies have focused on this environment. Facultative heterotrophy and energy storage have been suggested to be the main processes enabling winter survival in sea ice (Syvertsen 1991; Zhang et al. 2003). Piwosz et al. (2013) found bacterial cells in the food vacuoles of picoeukaryotes from various trophic groups in FYI of the Arctic. Phagotrophic ingestion was investigated in mixotrophic nanoflagellates (MNF) of Antarctic sea ice during spring where they comprised 5–10% of the autotrophic nanoflagellates (Moorthi et al. 2009). Mixotrophy has been proposed to be an important mode of winter survival in sea ice algae. However, Horner and Alexander (1972) only found low uptake rates of organic substances by sea ice diatoms. Osmotrophy is widespread among pennate and centric diatoms from Antarctic and Arctic marine environments. The uptake rate of organic material is dependent on solar radiation and shows great interspecific variability (Ruiz-González et al. 2012). Algae are able to take up a variety of organic substrates such as pyruvate, acetate, lactate, ethanol, saturated fatty acids, glycerol, urea, and amino acids (Parker et al. 1961; Lewin and Hellebust 1976; Amblard 1991; Bronk et al. 2007). Ruiz-Gonzáles et al. (2012) concluded that osmotrophy together with phagotrophy suggest that algae may play a more diverse role in aquatic biogeochemical cycles than only supplying heterotrophs with photosynthetically fixed organic matter.

14.4.3 Cryptic Carbon Cycling and Underrepresented Microbes

Both ecological and phylogenetic fungi are prominent parasites of cyanobacteria, macro-algae, and animals that also biogeochemically cycle nutrients and degrade recalcitrant molecules. Fungal-like organisms in the *Oomycota* have been reported as parasites on algae in the Canadian Arctic (Küpper et al. 2016) and have been observed in the Norwegian Sea and Svalbard region (Fig. 14.1). The detection of fungi on Arctic marine bird feathers (Singh et al. 2016) and in association with driftwood (Rämä et al. 2014) suggests additional ecological niches occupied by the fungi that currently remain unexplored. Arctic members of the *Labyrinthulomycota* can exceed 10^5 cells L^{-1} (Naganuma

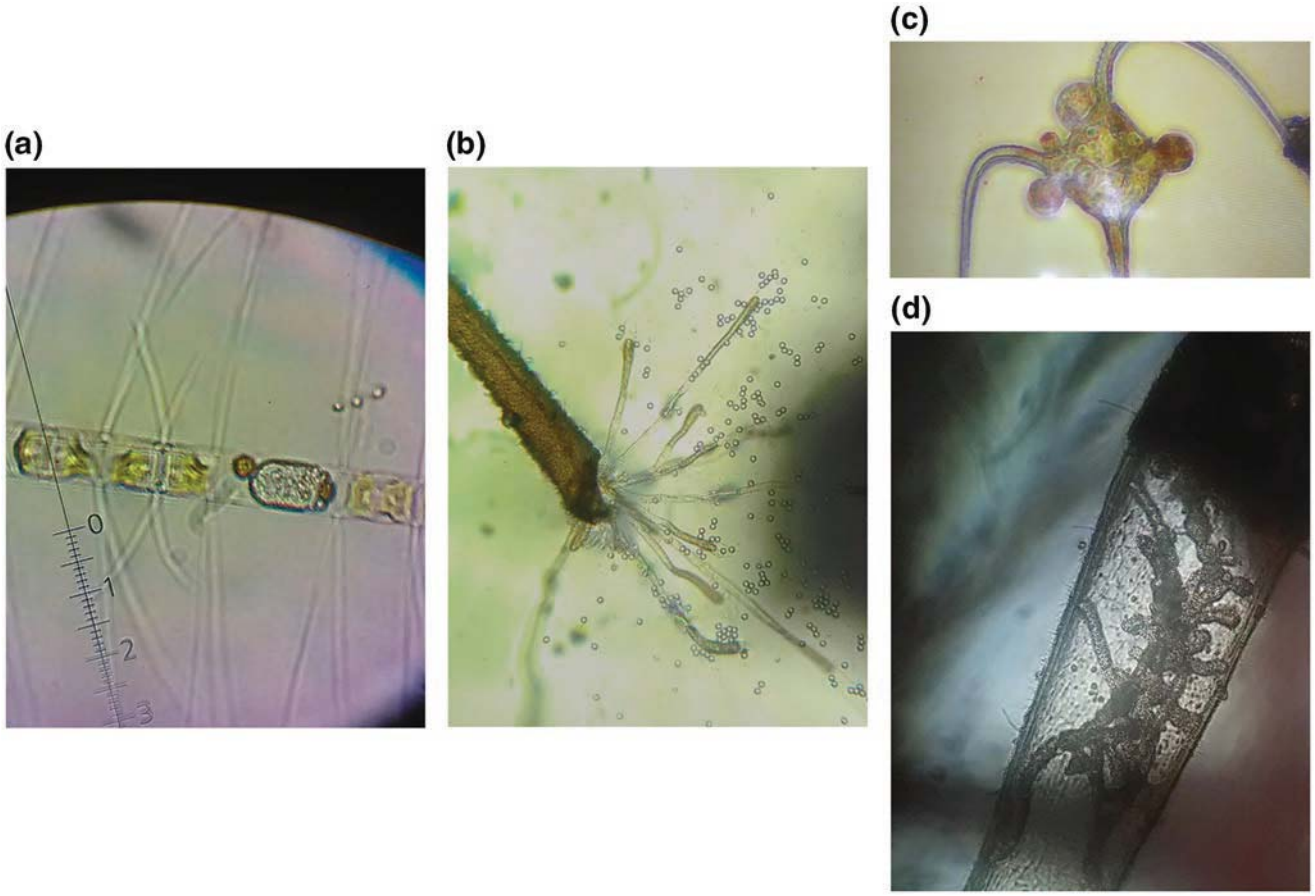

Fig. 14.1 Unidentified fungi and fungal-like pathogens. (**a**) A probable oomycete pathogen of *Chaetoceros* sp. captured in southern Norway (Drøbak). (**b**) A probable oomycete pathogen (*Saprolegnia* sp.) fruiting at the tip of benthic red macro-algae (image from samples collected in Drøbak by the authors). (**c**) Unknown pathogen parasitizing the dinoflagellate *Tripos* sp. in a Tromsø fjord (photo provided by Richard Ingebrigtsen, UiT). (**d**) Unknown pathogen with extensive branching inside a benthic red algae. (Image from Drøbak)

et al. 2006) and are capable of degrading pine pollen (Hassett and Gradinger 2018), suggesting that these organisms might be seasonally important in degradative processes. Members of the *Mesomycetozoea* (namely, the genus *Ichthyophonus*) primarily exist as parasites of Arctic fish (Klimpel et al. 2006) but whose abundance, distribution, and relevance to other ecosystem processes remain unknown.

Ecologically, the Arctic marine *Chytridiomycota* are seasonally abundant parasites that can infect approximately 1% of all diatoms in the near-shore sea ice environment (Hassett and Gradinger 2016) and 25% of a single diatom species (Hassett et al. 2017). Specifically, the *Chytridiomycota* parasitize light-stressed diatoms within sea ice brine channels (Horner and Schrader 1982; Hassett and Gradinger 2016). True Fungi have been reported in sea ice as far north as the North Pole (Bachy et al. 2011) and across the Western Arctic (Hassett et al. 2017). Beyond these observations, there is little information detailing the sea ice ecology of Fungi and fungal-like organisms. Seawater advection into sea ice and entrainment processes of particulates (Eicken et al. 2005; Gradinger et al. 2009) suggest that many fungi and fungal-like organisms observed in sediments and seawater are likely present in sea ice. However, little to no known specific empirical evidence exists to suggest this phenomenon.

Viruses play an important role in nutrient recycling via the viral shunt. Especially in winter and autumn, viral lysis is known to be the most important mortality factor for bacteria (Krembs et al. 2002b). Besides, viruses may have important roles for horizontal gene transfer. In an extensive virome study by Allen et al. (2017), a diverse virus community was found, including viruses with photosystem genes. Data mining of published metagenomes and metatranscriptomes revealed similar patterns of evolutionary important genes (e.g., photosystem) in viruses. The sea ice metagenome from Cottrell and Kirchman (2012), for example, showed cyanophages, synechococcus phages, and prochlorococcus phages with photosystem genes in their genome. The high bacterial density in sea ice, the close spatial connection, and low host specificity may allow a rather quick evolution via viral gene transfer compared to other systems. This may help to develop

hypotheses on the evolution of life and life on other planets, such as Europa. With further studies of transposons in metagenome assembled genomes, these hypotheses can be developed and tested further.

14.5 Seasonal Cycle in Ice-Covered Seas

Sea ice-covered systems are characterized by highly seasonal variabilities of temperature and light. In sea ice, brine channels spatially constrain biota and increase interactions between consumers (bacteria and fungi) and primary producers. Therefore, the sea ice habitat is more comparable to biofilms and processes taking place within biofilms (Krembs et al. 2000). Ice algae and bacteria release extracellular polymeric substances (EPS) that protect cells from high salinities and low temperatures, foster the adhesion to surfaces, and alter the microstructure and corresponding desalination processes of sea ice (Krembs et al. 2011). Thus, sympagic microalgae and bacteria can cause physical changes to their immediate environment, improving sea ice habitability (Krembs et al. 2002a, 2011). Concentration and chemical composition of EPS significantly differed in response to gradients in temperature and salinity in Antarctic sea ice and simulated sea ice formation experiments with cultures of the bi-polar diatom *Fragilariopsis cylindrus* (Aslam et al. 2018). Under combined conditions of low temperature and high salinity, the relative contribution of EPS to total carbohydrates and their monosaccharide composition changed significantly, both in the field and lab. Increased concentrations of uronic acids and mannose at low temperatures increase the stiffness of EPS gels (Aslam et al. 2012), needed to produce protective cell coatings as observed in natural sea ice brines.

The initial colonization stage during sea ice formation is followed by a low-productive, heterotrophic winter stage, dominated by pelagic organisms (Fig. 14.2) (Grossmann and Gleitz 1993; Joli et al. 2017; Amargant Arumí 2018). Biomass accumulation follows the seasonal increase in solar radiation during winter-spring transition. The sea ice algal bloom is terminated either by nutrient depletion or sea ice melt in late spring/early summer. At the ice edge phytoplankton blooms of *Phaeocystis* sp. may contribute to high primary production (Assmy et al. 2017). The post-bloom stage is dominated again by heterotrophic processes in the sea ice and water column (Haecky et al. 1999; Kaartokallio 2004).

14.5.1 Autumn

In autumn, sea ice starts forming as frazil ice, which can form at the surface or in deeper water layers (Petrich and Eicken 2010). During ice formation, larger particles, such as eukaryotes or sediment particles, can be transported to the water surface and incorporated into the ice. Ice formation begins in autumn when there are still substantial microbial populations left over in surface waters from the preceding spring bloom (Arrigo and Thomas 2004). As the frazil crystals rise to the surface, particles such as microalgae, heterotrophic protists, and bacteria are scavenged (Garrison et al. 1989). During wave movement, the frazil ice may further act as a sieve, concentrating biomass from the water column (Reimnitz et al. 1993; Weissenberger and Grossmann 1998). This process is thought to select for sticky bacteria, diatoms and organisms attached to larger organisms or particles (Grossmann and Dieckmann 1994; Weissenberger and Grossmann 1998). Another concentration process is the brine exclusion during the ice formation, concentrating nutrients, salts, and organisms in small and densely packed brine channels (reviewed by Deming and Collins 2017). The brine channels are very rich in nutrients and organic matter but may limit bacterial and algal activities at low temperatures and high salinities, which may fluctuate greatly. Thus, the organisms that are concentrated into the ice are further selected by their capability to survive or grow in the extreme physical conditions (Grossmann and Dieckmann 1994). Survival may be enhanced by EPS production or cryoprotectants and changes in biochemical structures to withstand osmotic shock and freezing (Krembs et al. 2011). Studies in the autumn are rare, but the overall bacterial production is low compared to the rest of the year and exceeds that by microalgae (Grossmann and Dieckmann 1994). Grazing seems to be a minor impact, while viruses and phages are enriched 10–100 times (e.g., Gowing et al. 2002; Collins and Deming 2011). Knowledge on bacterial and algal diversity and functions are rare, but the community structures seem to differ from the other seasons and are more similar to the seawater below the newly forming sea ice (Collins et al. 2010). Archaea and oligotrophic bacteria (e.g., OM182) become more dominant, while *Alteromonadales* become less abundant (Collins et al. 2010). Throughout the winter, large centric diatoms are gradually reduced, shifting to a dominance of small pennate species such as *Fragilariopsis* sp. (Lizotte 2003). A water column bloom may start due to the nutrient upwelling after autumn storms which are increasingly abundant with the effects of climate change and retreating sea ice (Ardyna et al. 2014).

14.5.2 Winter

In winter, the temperature in sea ice drops and the brine volume may decrease giving little space for eukaryotes and high concentrations of DOM for bacteria (reviewed by Deming and Collins 2017). Absence of light, extreme salinities, and cold temperatures challenge the microbial survival and

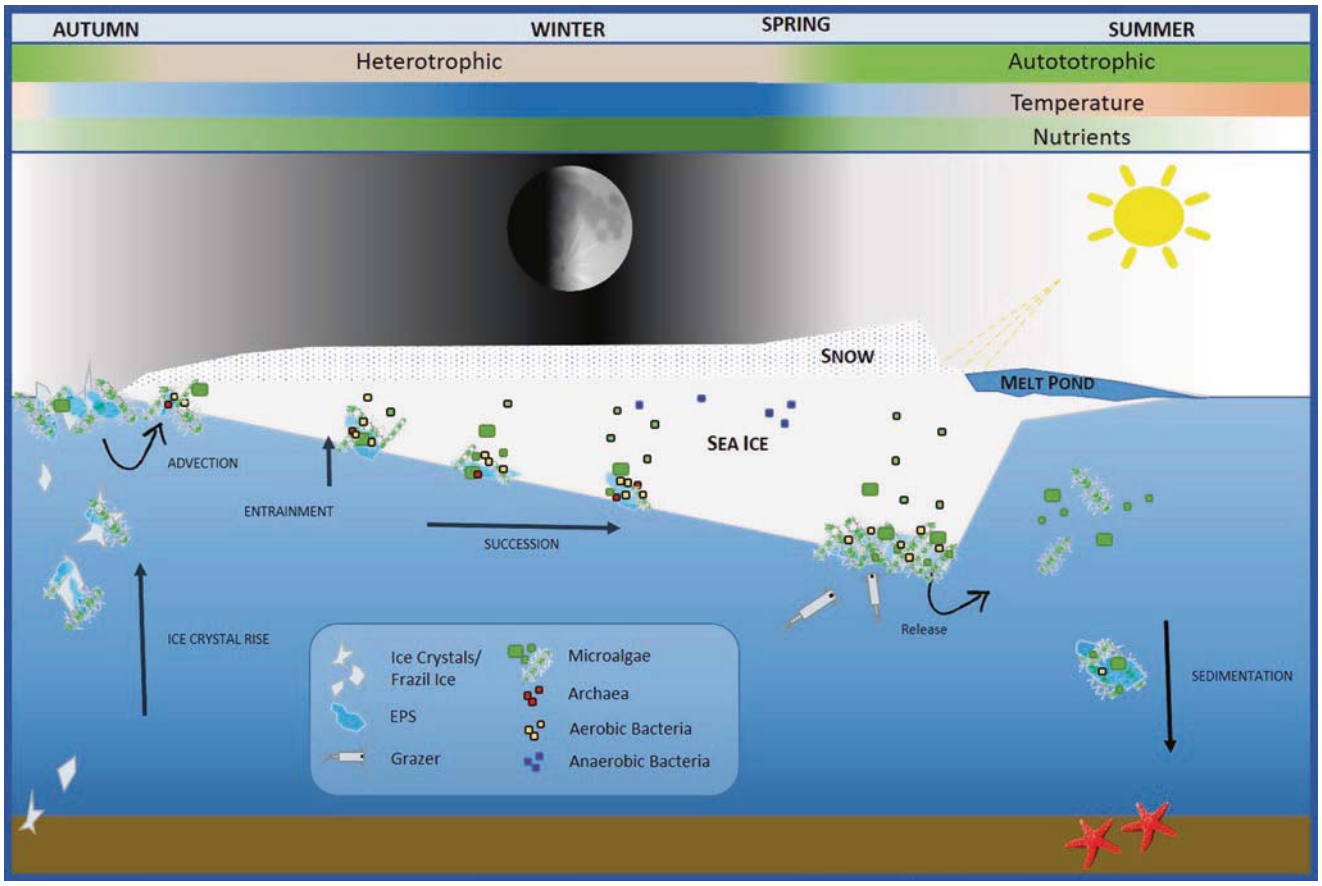

Fig. 14.2 Sea ice and microbial dynamics in the seasonal ice zone. Figure produced based on references in the text

activities. Grazers are mostly absent in winter and bacterial mortality is mainly caused by viral lysis (Krembs et al. 2002a). Overall, bacterial production is low, but certain bacteria are active allowing viruses to produce (Wells and Deming 2006a, b). Up to 86% of winter sea ice bacteria have been found to be active in FISH counts and 4% showed respiration during 5-Cyano-2,3-ditolyl tetrazolium chloride staining (Junge et al. 2004). Bacterial activity is crucial for surviving the harsh conditions, ion transporters have to be active and the membranes intact to compensate for large osmotic differences between the brine water and cell interior transportation of ions and compatible solutes (Collins and Deming 2013). EPS has been found in winter sea ice, which can be important as cryoprotectant and which is mostly produced by bacteria due to the low abundances of eukaryotic algae (Krembs et al. 2002b, 2011). As in autumn, heterotrophic bacterial production is higher than primary production, making the system net heterotroph (Kottmeier and Sullivan 1987). Little is known about the community structure, but the community becomes more similar to typical heterotrophic sea ice communities. Archaea appear more abundant in winter and autumn sea ice, compared to spring and summer indicating their potential importance for autotrophic nitrification (Brinkmeyer et al. 2003; Collins et al. 2010). The microalgal winter diversity in the Beaufort Sea is similar to spring with pennate diatoms dominating, and *Nitzschia frigida* being the most abundant species (Niemi et al. 2011). The dominance of pennate diatoms during the spring algal bloom indicates a competitive advantage, due to their high production rates of EPS and potential for heterotrophy as survival strategies (Niemi et al. 2011). In the water column, picophytoplankton becomes dominant with *Micromonas* sp., *Ostreococcus* sp., and cyanobacteria as main phototrophic organisms (Vader et al. 2015; Joli et al. 2017; Amargant Arumí 2018). In the absence of light, mixotrophic pathways may be important for their survival and explain their dominance (Sanders and Gast 2012; Vader et al. 2015). Nitrifier abundances based on bacterial and archaea amoA genes in the Arctic water column may become 30–115 times more abundant in winter indicating that nitrification may be an important autotrophic process (Christman et al. 2011).

14.5.3 Spring

With the returning sun and increasing temperatures in spring, microbial activities generally increase. At the bottom of the ice, sea ice algae may form blooms supporting bacterial production. The under-ice production is generally higher than in autumn and winter but only about 10% of sea ice algal production (Deming and Collins 2017). In the upper ice layers, bacterial activity is still increasing to levels higher than algal primary production (Gradinger and Zhang 1997). The production can be fueled by degradation of cryoprotectants (e.g., EPS) which are not needed anymore, or by old organic matter (Collins and Deming 2013; Arrigo et al. 2014; Firth et al. 2016). Overall, the system may become net heterotrophic and even anoxic, allowing denitrification and annamox to play a role (Rysgaard et al. 2008; Rysgaard and Glud 2004). In oxygenated zones, bacteria play an important role in recycling nutrients from organic matter into ammonium and eventually into nitrate (e.g., Rysgaard et al. 2008). Viral concentrations increase, but viral lysis is a minor mortality factor of bacterial mortality, while microzooplankton grazing becomes more important (Maranger et al. 1994; Piwosz et al. 2013). The community structure changes toward a community with significantly less archaea and more representatives of the *Alteromonadales* clade (Collins et al. 2010), indicating a system in favor of faster-growing heterotrophic bacteria. Primary production in the water column is limited by light absorbed through the sea ice.

14.5.4 Summer

In summer, the sea ice starts melting from the bottom releasing concentrated organic matter and algal biomass. Large algae aggregate together with their bacterial community may sink to the bottom seeding sediment communities and feeding deep-sea animals (Rapp et al. 2018). In the deep central basins, this process may be a permanent loss, while seeding of new sea ice with the sediment communities is possible down to depth of about 30 m. With a retreating seasonal ice zone toward the central Arctic Ocean, this may become problematic. The communities are dominated by *Flavobacteriia* and *Gammaproteobacteria*, but *Flavobacteriia* are only a minor fraction in sediment associated communities and autumn communities (Collins et al. 2010; Rapp et al. 2018). Archaea are mostly absent (Collins et al. 2010). The water column becomes more heterotrophic with increased bacterial production with decreasing phytoplankton biomass (Kirchman et al. 2009) and a community shift toward heterotrophs and mixotrophs (e.g., Stoecker et al. 2014).

14.5.5 Climate Change Effects

Changes in sea ice properties are forecasted to drive climate feedback loops and impact biological processes, such as element cycling (Holding et al. 2015; Tremblay et al. 2015). As sea ice melting starts earlier in the year, habitat loss occurs before solar radiation is sufficient for algal productivity and growth in the high Arctic (Arrigo et al. 2008) and near the Antarctic Peninsula. Sea ice algae are an important high-quality energy source for grazers in early spring and can seed the pelagic phytoplankton bloom. A shift or loss of the sea ice bloom is forecasted to change the productivity of the system and negatively affect the reproduction success of highly synchronized grazers like *Calanus glacialis* (Søreide et al. 2010), krill (Hoshiai et al. 1987), and of calanoid copepods such as *Acartia bifilosa* (Werner and Auel 2004) in the Arctic, Antarctic, and Baltic, respectively. In addition, the nutrient and light conditions in which sea ice algae thrive induce the synthesis of polyunsaturated fatty acids, a crucial constituent of the diet of grazers, especially during winter (Nichols et al. 1999; Arrigo and Thomas 2004). Increased light intensities reduce the nutritional value of ice-associated (sympagic) microalgae (Leu et al. 2010). Due to warming, the water column may become more stratified (Tremblay et al. 2015), reducing the vertical supply of nutrients to the euphotic zone. On the other hand, a longer ice-free period might counteract stratification through re-mixing of nutrients by wind and storms, but only minor effects on vertical mixing could be observed (Toole et al. 2010; Lincoln et al. 2016). Extended ice-free periods and thinner sea ice in the Arctic increases light availability to pelagic and sympagic microalgae, enhancing annual primary production (Wassmann et al. 2011). The community structure may shift to more pelagic algae species, such as *Phaeocystis* sp. (Assmy et al. 2017). However, the overall consequences of sea ice retreat on primary production remain under debate (Arrigo et al. 2014; Tremblay et al. 2015).

14.6 Conclusions

Knowledge on the distribution and abundance of sea ice protists is crucial to understand and foresee possible changes in microbial communities that potentially have great impacts on food webs of the ice-covered oceans. Even though -omics provide thorough insights into species composition and processes, one should not neglect the importance of assessing their respective abundances. New methods have the potential to shed more light onto the functions of sea ice microorganisms. However, one should not overlook the limitations and restrictions when it comes to sea ice sampling. Melting of sea ice material exposes organisms to changes in physical and chemical conditions, to which microorganisms might

react instantaneously. Good care needs to be taken to manipulate the community as little as possible. In the future, the development of good practices and standards is crucial to ensure intercomparable observations of ice biota and properties. A strong seasonality in the seasonal ice zone determines the community structures and functions of the sea ice ecosystem and the associated water column. With climate change, some of the annual processes change (e.g., timing of ice formation), while others will stay the same (length of the polar night). This will eventually change the communities and functions in sea ice, as we know it now. We believe that a focus on microbes, and a proportional representation of their activity (relative to their biomass contributions) in ecosystem models will help to forecast the biological fate of polar marine ecosystems under forecasted climate change scenarios.

Appendix

This article is related to the YOUMARES 9 conference session no. 17: "Bridging disciplines in the seasonal ice zone (SIZ)." The original Call for Abstracts and the abstracts of the presentations within this session can be found in the Appendix "Conference Sessions and Abstracts", Chapter "13 Bridging disciplines in the seasonal ice zone (SIZ)", of this book.

References

Ackley SF, Buck KR, Taguchi S (1979) Standing crop of algae in the sea ice of the Weddell Sea Region. Deep-Sea Res I 26:269–281. https://doi.org/10.1016/0198-0149(79)90024-4

Allen LZ, McCrow JP, Ininbergs K et al (2017) The Baltic Sea virome: diversity and transcriptional activity of DNA and RNA viruses. Msystems 2:e00125–e00116. https://doi.org/10.1128/mSystems.00125-16

Alonso-Sáez L, Sanchez O, Gasol JM et al (2008) Winter-to-summer changes in the composition and single-cell activity of near-surface Arctic prokaryotes. Environ Microbiol 10:2444–2454. https://doi.org/10.1111/j.1462-2920.2008.01674.x

Amargant Arumí M (2018) Arctic marine microbial ecology during the Svalbard Polar Night. Master thesis, UiT Norges arktiske universitet

Amblard C (1991) Carbon heterotrophic activity of microalgae and cyanobacteria – ecological significance. Ann Biol-Paris 30:6–107

Ardyna M, Babin M, Gosselin M et al (2014) Recent Arctic Ocean sea ice loss triggers novel fall phytoplankton blooms. Geophys Res Lett 41:6207–6212. https://doi.org/10.1002/2014gl061047

Arrigo KR (2010) Marine microalgae in Antarctic sea ice. Integr Comp Biol 50:E5–E5

Arrigo KR, Sullivan CW (1992) The influence of salinity and temperature covariation on the photophysiological characteristics of Antarctic sea ice microalgae. J Phycol 28:746–756. https://doi.org/10.1111/j.0022-3646.1992.00746.x

Arrigo KR, Thomas DN (2004) Large scale importance of sea ice biology in the Southern Ocean. Antarct Sci 16:471–486. https://doi.org/10.1017/S0954102004002263

Arrigo KR, van Dijken G, Pabi S (2008) Impact of a shrinking Arctic ice cover on marine primary production. Geophys Res Lett 35:L19603. https://doi.org/10.1029/2008GL035028

Arrigo KR, Perovich DK, Pickart RS et al (2014) Phytoplankton blooms beneath the sea ice in the Chukchi Sea. Deep-Sea Res II 105:1–16. https://doi.org/10.1016/j.dsr2.2014.03.018

Aslam SN, Strauss J, Thomas DN et al (2018) Identifying metabolic pathways for production of extracellular polymeric substances by the diatom *Fragilariopsis cylindrus* inhabiting sea ice. ISME J 12:1237–1251. https://doi.org/10.1038/s41396-017-0039-z

Aslam SN, Cresswell-Maynard T, Thomas DN et al (2012) Production and characterization of the intra- and extracellular carbohydrates and polymeric substances (EPS) of three sea-ice diatom species, and evidence for a cryoprotective role for EPS. J Phycol 48:1494–1509. https://doi.org/10.1111/jpy.12004

Assmy P, Fernández-Méndez M, Duarte P et al (2017) Leads in Arctic pack ice enable early phytoplankton blooms below snow-covered sea ice. Sci Rep 7:40850. https://doi.org/10.1038/srep40850

Bachy C, Lopez-Garcia P, Vereshchaka A et al (2011) Diversity and vertical distribution of microbial eukaryotes in the snow, sea ice and seawater near the North Pole at the end of the polar night. Front Microbiol 2:106. https://doi.org/10.3389/fmicb.2011.00106

Baer SE, Connelly TL, Bronk DA (2015) Nitrogen uptake dynamics in landfast sea ice of the Chukchi Sea. Polar Biol 38:781–797. https://doi.org/10.1007/s00300-014-1639-y

Ballen-Segura M, Felip M, Catalan J (2017) Some mixotrophic flagellate species selectively graze on archaea. Appl Environ Microbiol 83:e02317–e02316. https://doi.org/10.1128/AEM.02317-16

Barber DG, Hop H, Mundy CJ et al (2015) Selected physical, biological and biogeochemical implications of a rapidly changing Arctic Marginal Ice Zone. Prog Oceanogr 139:122–150. https://doi.org/10.1016/j.pocean.2015.09.003

Baross J, Morita R (1978) Microbial life at low temperatures: ecological aspects. In: Kushner DJ (ed) Microbial life in extreme environments. Academic Press, London, pp 9–71

Beitler J (2012) Arctic sea ice extent settles at record seasonal minimum. National Snow and Ice Data Center. http://nsidc.org/arcticseaicenews/2012/09/arctic-sea-ice-extent-settles-at-record-seasonal-minimum/. Accessed 1 Feb 2016

Berge J, Daase M, Renaud P et al (2015) Unexpected levels of biological activity during the polar night offer new perspectives on a warming Arctic. Curr Biol 25:2555–2561. https://doi.org/10.1016/j.cub.2015.08.024

Bluhm BA, Hop H, Vihtakari M et al (2018) Sea ice meiofauna distribution on local to pan-Arctic scales. Ecol Evol 8:2350–2364. https://doi.org/10.1002/ece3.3797

Bochdansky AB, Clouse MA, Herndl GJ (2017) Eukaryotic microbes, principally fungi and labyrinthulomycetes, dominate biomass on bathypelagic marine snow. ISME J 11:362–373. https://doi.org/10.1038/ismej.2016.113

Boetius A, Anesio AM, Deming JW et al (2015) Microbial ecology of the cryosphere: sea ice and glacial habitats. Nat Rev Microbiol 13:677–690. https://doi.org/10.1038/nrmicro3522

Borriss M, Helmke E, Hanschke R et al (2003) Isolation and characterization of marine psychrophilic phage-host systems from Arctic sea ice. Extremophiles 7:377–384. https://doi.org/10.1007/s00792-003-0334-7

Bower SM (1987) *Labyrinthuloides haliotidis* n.sp (Protozoa, Labyrinthomorpha), a pathogenic parasite of small juvenile abalone in a British-Columbia mariculture facility. Can J Zool 65:1996–2007. https://doi.org/10.1139/z87-304

Bowman JS (2015) The relationship between sea ice bacterial community structure and biogeochemistry: a synthesis of current knowledge and known unknowns. Elem Sci Anth 3:000072. https://doi.org/10.12952/journal.elementa.000072

Bowman JS, Rasmussen S, Blom N et al (2012) Microbial community structure of Arctic multiyear sea ice and surface seawater by 454 sequencing of the 16S RNA gene. ISME J 6:11–20

Bowman JS, Berthiaume CT, Armbrust EV et al (2014) The genetic potential for key biogeochemical processes in Arctic frost flowers and young sea ice revealed by metagenomic analysis. FEMS Microbiol Ecol 89:376–387. https://doi.org/10.1111/1574-6941.12331

Brinkmeyer R, Knittel K, Jurgens J et al (2003) Diversity and structure of bacterial communities in Arctic versus Antarctic pack ice. Appl Environ Microbiol 69:6610–6619. https://doi.org/10.1128/Aem.69.11.6610-6619.2003

Bronk DA, See JH, Bradley P et al (2007) DON as a source of bioavailable nitrogen for phytoplankton. Biogeosciences 4:283–296. https://doi.org/10.5194/bg-4-283-2007

Brown MV, Bowman JP (2001) A molecular phylogenetic survey of sea-ice microbial communities (SIMCO). FEMS Microbiol Ecol 35:267–275. https://doi.org/10.1016/S0168-6496(01)00100-3

Bubnova EN, Nikitin DA (2017) Fungi in bottom sediments of the Barents and Kara Seas. Russ J Mar Biol 43:400–406. https://doi.org/10.1134/S1063074017050029

Campbell K, Mundy CJ, Barber DG et al (2014) Remote estimates of ice algae biomass and their response to environmental conditions during spring melt. Arctic 67:375–387. https://doi.org/10.14430/arctic4409

Caron DA, Sanders RW, Lim EL et al (1993) Light-dependent phagotrophy in the freshwater mixotrophic chrysophyte *Dinobryon cylindricum*. Microb Ecol 25:93–111. https://doi.org/10.1007/BF00182132

Cavalieri DJ, Parkinson CL, Gloersen P et al (1999) Deriving long-term time series of sea ice cover from satellite passive-microwave multisensor data sets. J Geophys Res Oceans 104:15803–15814. https://doi.org/10.1029/1999jc900081

Christman GD, Cottrell MT, Popp BN et al (2011) Abundance, diversity, and activity of ammonia-oxidizing prokaryotes in the Coastal Arctic Ocean in summer and winter. Appl Environ Microbiol 77:2026–2034. https://doi.org/10.1128/Aem.01907-10

Collins RE, Deming JW (2011) Abundant dissolved genetic material in Arctic sea ice Part II: viral dynamics during autumn freeze-up. Polar Biol 34:1831–1841. https://doi.org/10.1007/s00300-011-1008-z

Collins RE, Deming JW (2013) An inter-order horizontal gene transfer event enables the catabolism of compatible solutes by *Colwellia psychrerythraea* 34H. Extremophiles 17:601–610. https://doi.org/10.1007/s00792-013-0543-7

Collins RE, Rocap G, Deming JW (2010) Persistence of bacterial and archaeal communities in sea ice through an Arctic winter. Environ Microbiol 12:1828–1841. https://doi.org/10.1111/j.1462-2920.2010.02179.x

Comeau AM, Vincent WF, Bernier L et al (2016) Novel chytrid lineages dominate fungal sequences in diverse marine and freshwater habitats. Sci Rep 6:30120. https://doi.org/10.1038/srep30120

Cottrell MT, Kirchman DL (2009) Photoheterotrophic microbes in the Arctic Ocean in summer and winter. Appl Environ Microbiol 75:4958–4966. https://doi.org/10.1128/Aem.00117-09

Cottrell MT, Kirchman DL (2012) Virus genes in Arctic marine bacteria identified by metagenomic analysis. Aquat Microb Ecol 66:107–116. https://doi.org/10.3354/ame01569

Damashek J, Pettie KP, Brown ZW et al (2017) Regional patterns in ammonia-oxidizing communities throughout Chukchi Sea waters from the Bering Strait to the Beaufort Sea. Aquat Microb Ecol 79:273–286. https://doi.org/10.3354/ame01834

De Corte D, Sintes E, Yokokawa T et al (2013) Comparison between MICRO-CARD-FISH and 16S rRNA gene clone libraries to assess the active versus total bacterial community in the coastal Arctic. Environ Microbiol Rep 5:272–281. https://doi.org/10.1111/1758-2229.12013

Delmont TO, Kiefl E, Kilinc O et al (2017) The global biogeography of amino acid variants within a single SAR11 population is governed by natural selection. BioRxiv 170639. https://doi.org/10.1101/170639

Deming JW, Collins RE (2017) Sea ice as a habitat for bacteria, archaea and viruses. In: Thomas ND (ed) Sea ice. Wiley, New York, pp 326–351

Diez B, Bergman B, Pedros-Alio C et al (2012) High cyanobacterial nifH gene diversity in Arctic seawater and sea ice brine. Environ Microbiol Rep 4:360–366. https://doi.org/10.1111/j.1758-2229.2012.00343.x

Eicken H (2003) From the microscopic, to the macroscopic, to the regional scale: growth, microstructure and properties of sea ice. In: Thomas DN, Dieckmann GS (eds) Sea ice: an introduction to its physics, chemistry, biology and geology. Blackwell Sci, Oxford, pp 22–81

Eicken H, Gradinger R, Gaylord A et al (2005) Sediment transport by sea ice in the Chukchi and Beaufort Seas: increasing importance due to changing ice conditions? Deep-Sea Res II 52:3281–3302. https://doi.org/10.1016/j.dsr2.2005.10.006

Feller G, Gerday C (2003) Psychrophilic enzymes: hot topics in cold adaptation. Nat Rev Microbiol 1:200–208. https://doi.org/10.1038/nrmicro773

Feng S, Powell SM, Wilson R et al (2014) Extensive gene acquisition in the extremely psychrophilic bacterial species *Psychroflexus torquis* and the link to sea-ice ecosystem specialism genome. Biol Evol 6:133–148. https://doi.org/10.1093/gbe/evt209

Fernández-Méndez M, Katlein C, Rabe B et al (2015) Photosynthetic production in the central Arctic Ocean during the record sea-ice minimum in 2012. Biogeosciences 12:3525–3549. https://doi.org/10.5194/bg-12-3525-2015

Fernández-Méndez M, Turk-Kubo KA, Buttigieg PL et al (2016) Diazotroph diversity in the sea ice, melt ponds, and surface waters of the Eurasian Basin of the Central Arctic Ocean. Front Microbiol 7:1884. https://doi.org/10.3389/fmicb.2016.01884

Firth E, Carpenter SD, Sorensen HL et al (2016) Bacterial use of choline to tolerate salinity shifts in sea-ice brines. Elem Sci Anth 4:000120. https://doi.org/10.12952/journal.elementa.000120

Fortunato CS, Huber JA (2016) Coupled RNA-SIP and metatranscriptomics of active chemolithoautotrophic communities at a deep-sea hydrothermal vent. ISME J 10:1925–1938. https://doi.org/10.1038/ismej.2015.258

Gao DW, Huang XL, Tao Y (2016) A critical review of NanoSIMS in analysis of microbial metabolic activities at single-cell level. Crit Rev Biotechnol 36:884–890. https://doi.org/10.3109/07388551.2015.1057550

Garrison DL, Close AR, Reimnitz E (1989) Algae concentrated by frazil ice – evidence from laboratory experiments and field measurements. Antarct Sci 1:313–316. https://doi.org/10.1017/S0954102089000477

Gerdes B, Brinkmeyer R, Dieckmann G et al (2005) Influence of crude oil on changes of bacterial communities in Arctic sea-ice. FEMS Microbiol Ecol 53:129–139. https://doi.org/10.1016/j.femsee.2004.11.010

Gosselin M, Levasseur M, Wheeler PA et al (1997) New measurements of phytoplankton and ice algal production in the Arctic Ocean. Deep Sea Res II 44:1623–1644. https://doi.org/10.1016/S0967-0645(97)00054-4

Gowing MM, Riggs BE, Garrison DL et al (2002) Large viruses in Ross Sea late autumn pack ice habitats. Mar Ecol Prog Ser 241:1–11. https://doi.org/10.3354/meps241001

Gradinger RR (2001) Adaptation of Arctic and Antarctic ice metazoa to their habitat. Zool-Anal Complex Sy 104:339–345. https://doi.org/10.1078/0944-2006-00039

Gradinger RR, Zhang Q (1997) Vertical distribution of bacteria in Arctic sea ice from the Barents and Laptev Seas. Polar Biol 17:448–454. https://doi.org/10.1007/s003000050139

Gradinger RR, Kaufman MR, Bluhm BA (2009) Pivotal role of sea ice sediments in the seasonal development of near-shore Arctic fast ice biota. Mar Ecol Prog Ser 394:49–63. https://doi.org/10.3354/meps08320

Granskog M, Kaartokallio H, Kuosa H et al (2006) Sea ice in the Baltic Sea – a review. Estuar Coast Shelf Sci 70:145–160. https://doi.org/10.1016/j.ecss.2006.06.001

Grossmann S, Gleitz M (1993) Microbial responses to experimental sea-ice formation – implications for the establishment of Antarctic sea-ice communities. J Exp Mar Biol Ecol 173:273–289. https://doi.org/10.1016/0022-0981(93)90058-V

Grossmann S, Dieckmann GS (1994) Bacterial standing stock, activity, and carbon production during formation and growth of sea-ice in the Weddell Sea, Antarctica. Appl Environ Microbiol 60:2746–2753

Haecky P, Jonson S, Andersson A (1999) Influence of sea ice on the composition of the spring phytoplankton bloom in the northern Baltic Sea. Polar Biol 20:1–8. https://doi.org/10.1007/s003000050270

Hanic LA, Sekimoto S, Bates SS (2009) Oomycete and chytrid infections of the marine diatom *Pseudo-nitzschia pungens* (Bacillariophyceae) from Prince Edward Island, Canada. Botany 87:1096–1105. https://doi.org/10.1139/B09-070

Hansen PJ (2011) The role of photosynthesis and food uptake for the growth of marine mixotrophic dinoflagellates. J Eukaryot Microbiol 58:203–214. https://doi.org/10.1111/j.1550-7408.2011.00537.x

Hassett BT, Gradinger RR (2016) Chytrids dominate arctic marine fungal communities. Environ Microbiol 18:2001–2009. https://doi.org/10.1111/1462-2920.13216

Hassett BT, Gradinger RR (2018) New species of saprobic Labyrinthulea (=Labyrinthulomycota) and the erection of a *gen. nov* to resolve molecular polyphyly within the Aplanochytrids. J Eukaryot Microbiol 65:475–483. https://doi.org/10.1111/jeu.12494

Hassett BT, Ducluzeau ALL, Collins RE et al (2017) Spatial distribution of aquatic marine fungi across the western Arctic and sub-arctic. Environ Microbiol 19:475–484. https://doi.org/10.1111/1462-2920.13371

Hatam I, Lange B, Beckers J et al (2016) Bacterial communities from Arctic seasonal sea ice are more compositionally variable than those from multi-year sea ice. ISME J 10:2543–2552. https://doi.org/10.1038/ismej.2016.4

Hegseth EN (1998) Primary production of the northern Barents Sea. Polar Res 17:113–123. https://doi.org/10.1111/j.1751-8369.1998.tb00266.x

Hobbie JE, Daley RJ, Jasper S (1977) Use of Nuclepore filters for counting bacteria by fluorescence microscopy. Appl Environ Microbiol 33:1225–1228

Holding JM, Duarte CM, Sanz-Martin M et al (2015) Temperature dependence of CO_2-enhanced primary production in the European Arctic Ocean. Nat Clim Chang 5:1079–1082. https://doi.org/10.1038/Nclimate2768

Horner R, Alexander V (1972) Algal populations in Arctic sea ice – investigation of heterotrophy. Limnol Oceanogr 17:454–458. https://doi.org/10.4319/lo.1972.17.3.0454

Horner R, Schrader GC (1982) Relative contributions of ice algae, phytoplankton, and benthic microalgae to primary production in near-shore regions of the Beaufort Sea. Arctic 35:485–503

Hoshiai T, Tanimura A, Watanabe K (edited by Hoshiai T) (1987) Ice algae as food of an Antarctic ice-associated copepod, *Paralabidocera antarctica* (IC Thompson). In: Proceedings of the NIPR Symposium on Polar Biology, Citeseer, pp 105–111

Hunt GL, Drinkwater KF, Arrigo K et al (2016) Advection in polar and sub-polar environments: impacts on high latitude marine ecosystems. Prog Oceanogr 149:40–81. https://doi.org/10.1016/j.pocean.2016.10.004

Jephcott TG, Alves-De-Souza C, Gleason FH et al (2016) Ecological impacts of parasitic chytrids, syndiniales and perkinsids on populations of marine photosynthetic dinoflagellates. Fungal Ecol 19:47–58. https://doi.org/10.1016/j.funeco.2015.03.007

Johnson TW, Sparrow FK (1961) Fungi in oceans and estuaries. Hafner Publishing, New York

Johnson SS, Zaikova E, Goerlitz DS et al (2017) Real-time DNA sequencing in the Antarctic dry valleys using the Oxford Nanopore sequencer. J Biomol Tech 28:2. https://doi.org/10.7171/jbt.17-2801-009

Joli N, Monier A, Logares R et al (2017) Seasonal patterns in Arctic prasinophytes and inferred ecology of *Bathycoccus* unveiled in an Arctic winter metagenome. ISME J 11:1372–1385. https://doi.org/10.1038/ismej.2017.7

Junge K, Imhoff F, Staley T et al (2002) Phylogenetic diversity of numerically important arctic sea-ice bacteria cultured at subzero temperature. Microbial Ecol 43:315–328. https://doi.org/10.1007/s00248-001-1026-4

Junge K, Eicken H, Deming JW (2004) Bacterial activity at −2 to −20 degrees C in Arctic wintertime sea ice. Appl Environ Microbiol 70:550–557. https://doi.org/10.1128/Aem.70.1.550-557.2004

Junge K, Cameron K, Nunn B (2019) Chapter 12 – diversity of psychrophilic bacteria in sea and glacier ice environments—insights through genomics, metagenomics, and proteomics approaches. In: Das S, Dash HR (eds) Microbial diversity in the genomic era. Academic Press, Cambridge, pp 197–216. https://doi.org/10.1016/B978-0-12-814849-5.00012-5

Kaartokallio H (2001) Evidence for active microbial nitrogen transformations in sea ice (Gulf of Bothnia, Baltic Sea) in midwinter. Polar Biol 24:21–28. https://doi.org/10.1007/s003000000169

Kaartokallio H (2004) Food web components, and physical and chemical properties of Baltic Sea ice. Mar Ecol Prog Ser 273:49–63. https://doi.org/10.3354/meps273049

Kaartokallio H, Kuosa H, Thomas DN et al (2007) Biomass, composition and activity of organism assemblages along a salinity gradient in sea ice subjected to river discharge in the Baltic Sea. Polar Biol 30:183–197. https://doi.org/10.1007/s00300-006-0172-z

Kirchman DL, Hill V, Cottrell MT et al (2009) Standing stocks, production, and respiration of phytoplankton and heterotrophic bacteria in the western Arctic Ocean. Deep-Sea Res II 56:1237–1248. https://doi.org/10.1016/j.dsr2.2008.10.018

Klimpel S, Palm HW, Busch MW et al (2006) Fish parasites in the Arctic deep-sea: poor diversity in pelagic fish species vs. heavy parasite load in a demersal fish. Deep-Sea Res I 53:1167–1181. https://doi.org/10.1016/j.dsr.2006.05.009

Koh EY, Atamna-Ismaeel N, Martin A et al (2010) Proteorhodopsin-bearing bacteria in Antarctic sea ice. Appl Environ Microbiol 76:5918–5925. https://doi.org/10.1128/Aem.00562-10

Koh EY, Phua W, Ryan KG (2011) Aerobic anoxygenic phototrophic bacteria in Antarctic sea ice and seawater. Env Microbiol Rep 3:710–716. https://doi.org/10.1111/j.1758-2229.2011.00286.x

Koh EY, Martin AR, McMinn A et al (2012) Recent advances and future perspectives in microbial phototrophy in Antarctic sea ice. Biology 1:542–556. https://doi.org/10.3390/biology1030542

Kohlmeyer J, Kohlmeyer E (2013) Marine mycology: the higher fungi. Elsevier, Amsterdam

Kottmeier ST, Sullivan CW (1987) Late winter primary production and bacterial production in sea ice and seawater west of the Antarctic Peninsula. Mar Ecol Prog Ser 36:287–298. https://doi.org/10.3354/meps036287

Krembs C, Gradinger R, Spindler M (2000) Implications of brine channel geometry and surface area for the interaction of sympagic organisms in Arctic sea ice. J Exp Mar Biol Ecol 243:55–80. https://doi.org/10.1016/S0022-0981(99)00111-2

Krembs C, Eicken H, Junge K et al (2002a) High concentrations of exopolymeric substances in Arctic winter sea ice: implications for the polar ocean carbon cycle and cryoprotection of

diatoms. Deep-Sea Res I 49:2163–2181. https://doi.org/10.1016/S0967-0637(02)00122-X

Krembs C, Tuschling K, von Juterzenka K (2002b) The topography of the ice-water interface – its influence on the colonization of sea ice by algae. Polar Biol 25:106–117. https://doi.org/10.1007/s003000100318

Krembs C, Eicken H, Deming JW (2011) Exopolymer alteration of physical properties of sea ice and implications for ice habitability and biogeochemistry in a warmer Arctic. Proc Natl Acad Sci USA 108:3653–3658. https://doi.org/10.1073/pnas.1100701108

Küpper FC, Peters AF, Shewring DM et al (2016) Arctic marine phytobenthos of northern Baffin Island. J Phycol 52:532–549. https://doi.org/10.1111/jpy.12417

Laamanen M (1996) Cyanoprokaryotes in the Baltic Sea ice and winter plankton. Algological Studies/Archiv für Hydrobiologie, Supplement Volumes 83:423–433

Lange BA, Katlein C, Nicolaus M et al (2016) Sea ice algae chlorophyll a concentrations derived from under-ice spectral radiation profiling platforms. J Geophys Res Oceans 121:8511–8534. https://doi.org/10.1002/2016jc011991

Lepelletier F, Karpov SA, Alacid E et al (2014) *Dinomyces arenysensis* gen. et sp nov (Rhizophydiales, Dinomycetaceae fam. nov.), a chytrid infecting marine dinoflagellates. Protist 165:230–244. https://doi.org/10.1016/j.protis.2014.02.004

Leu E, Wiktor J, Søreide JE et al (2010) Increased irradiance reduces food quality of sea ice algae. Mar Ecol Prog Ser 411:49–60. https://doi.org/10.3354/meps08647

Lewin J, Hellebust JA (1976) Heterotrophic nutrition of marine pennate diatom *Nitzschia angularis var affinis*. Mar Biol 36:313–320. https://doi.org/10.1007/Bf00389192

Lincoln BJ, Rippeth TP, Simpson JH (2016) Surface mixed layer deepening through wind shear alignment in a seasonally stratified shallow sea. J Geophys Res Oceans 121:6021–6034. https://doi.org/10.1002/2015jc011382

Lizotte MP (2003) The microbiology of sea ice. In: Thomas DN, Dieckmann GS (eds) Sea ice: an introduction to its physics, chemistry, biology and geology. Blackwell Sci, Oxford, pp 184–210

Luhtanen AM, Eronen-Rasimus E, Oksanen HM et al (2018) The first known virus isolates from Antarctic sea ice have complex infection patterns. Fems Microbiol Ecol 94:fiy028. https://doi.org/10.1093/femsec/fiy028

Lytle VI, Ackley SF (1996) Heat flux through sea ice in the western Weddell Sea: convective and conductive transfer processes. J Geophys Res Oceans 101:8853–8868. https://doi.org/10.1029/95jc03675

Majaneva M, Blomster J, Müller S et al (2017) Sea-ice eukaryotes of the Gulf of Finland, Baltic Sea, and evidence for herbivory on weakly shade-adapted ice algae. Eur J Protistol 57:1–15. https://doi.org/10.1016/j.ejop.2016.10.005

Maranger R, Bird DF, Juniper SK (1994) Viral and bacterial dynamics in Arctic sea-ice during the spring algal bloom near Resolute, Nwt, Canada. Mar Ecol Prog Ser 111:121–127. https://doi.org/10.3354/meps111121

Maslanik J, Stroeve J, Fowler C et al (2011) Distribution and trends in Arctic sea ice age through spring 2011. Geophys Res Lett 38:L13502. https://doi.org/10.1029/2011gl047735

Mclean N, Porter D (1982) The yellow-spot disease of *Tritonia diomedea* Bergh, 1894 (Mollusca, Gastropoda, Nudibranchia) – encapsulation of the thraustochytriaceous parasite by host amebocytes. J Parasitol 68:243–252. https://doi.org/10.2307/3281182

McKie-Krisberg ZM, Sanders RW (2014) Phagotrophy by the picoeukaryotic green alga Micromonas: implications for Arctic Oceans. ISME J 8:1953–1961. https://doi.org/10.1038/ismej.2014.16

Meier WN, Hovelsrud GK, van Oort BEH et al (2014) Arctic sea ice in transformation: a review of recent observed changes and impacts on biology and human activity. Rev Geophys 52:185–217. https://doi.org/10.1002/2013rg000431

Meiners K, Fehling J, Granskog MA et al (2002) Abundance, biomass and composition of biota in Baltic sea ice and underlying water (March 2000). Polar Biol 25:761–770. https://doi.org/10.1007/s00300-002-0403-x

Miller LA, Fripiat F, Else BGT et al (2015) Methods for biogeochemical studies of sea ice: the state of the art, caveats, and recommendations. Elem Sci Anth 3:000038. https://doi.org/10.12952/journal.elementa.000038

Mock T, Gradinger RR (1999) Determination of Arctic ice algal production with a new in situ incubation technique. Mar Ecol Prog Ser 177:15–26. https://doi.org/10.3354/meps177015

Mock T, Dieckmann GS, Haas C et al (2002) Micro-optodes in sea ice: a new approach to investigate oxygen dynamics during sea ice formation. Aquat Microb Ecol 29:297–306. https://doi.org/10.3354/ame029297

Moline MA, Karnovsky NJ, Brown Z et al (2008) High latitude changes in ice dynamics and their impact on polar marine ecosystems. Ann N Y Acad Sci 1134:267–319. https://doi.org/10.1196/annals.1439.010

Moorthi S, Caron DA, Gast RJ et al (2009) Mixotrophy: a widespread and important ecological strategy for planktonic and sea-ice nanoflagellates in the Ross Sea, Antarctica. Aquat Microb Ecol 54:269–277. https://doi.org/10.3354/ame01276

Naganuma T, Kimura H, Karimoto R et al (2006) Abundance of planktonic thraustochytrids and bacteria and the concentration of particulate ATP in the Greenland and Norwegian Seas. Polar Biosci 20:37–45

Nguyen D, Maranger R, Balague V et al (2015) Winter diversity and expression of proteorhodopsin genes in a polar ocean. ISME J 9:1835–1845. https://doi.org/10.1038/ismej.2015.1

Nichols D, Bowman J, Sanderson K et al (1999) Developments with Antarctic microorganisms: culture collections, bioactivity screening, taxonomy, PUFA production and cold-adapted enzymes. Curr Opin Biotechnol 10:240–246. https://doi.org/10.1016/S0958-1669(99)80042-1

Niemi A, Michel C, Hille K et al (2011) Protist assemblages in winter sea ice: setting the stage for the spring ice algal bloom. Polar Biol 34:1803–1817. https://doi.org/10.1007/s00300-011-1059-1

Nierychlo M, Nielsen JL, Nielsen PH (2016) Studies of the ecophysiology of single cells in microbial communities by (quantitative) microautoradiography and fluorescence in situ hybridization (MAR-FISH). In: McGenity TJ, Timmis KN, Nogales B (eds) Hydrocarbon and lipid microbiology protocols: ultrastructure and imaging. Springer, Berlin, pp 115–130. https://doi.org/10.1007/8623_2015_66

Nikrad MP, Cottrell MT, Kirchman DL (2012) Abundance and single-cell activity of heterotrophic bacterial groups in the Western Arctic Ocean in summer and winter. Appl Environ Microbiol 78:2402–2409. https://doi.org/10.1128/Aem.07130-11

Orsi W, Biddle JF, Edgcomb V (2013) Deep sequencing of subseafloor eukaryotic rRNA reveals active fungi across marine subsurface provinces. PLoS One 8:e56335. https://doi.org/10.1371/journal.pone.0056335

Oziel L, Neukermans G, Ardyna M et al (2017) Role for Atlantic inflows and sea ice loss on shifting phytoplankton blooms in the Barents Sea. J Geophys Res Oceans 122:5121–5139. https://doi.org/10.1002/2016jc012582

Palmisano AC, Sullivan CW (1983) Sea ice microbial communities (SIMCO) – distribution, abundance, and primary production of ice microalgae in McMurdo Sound, Antarctica in 1980. Polar Biol 2:171–177. https://doi.org/10.1007/Bf00448967

Parker BC, Bold HC, Deason TR (1961) Facultative heterotrophy in some chlorococcacean algae. Science 133:761–763. https://doi.org/10.1126/science.133.3455.761

Pernthaler A, Pernthaler J, Amann R (2002) Fluorescence in situ hybridization and catalyzed reporter deposition for the identification of marine bacteria. Appl Environ Microbiol 68:3094–3101. https://doi.org/10.1128/Aem.68.6.3094-3101.2002

Perovich D, Richter-Menge J, Polashenski C et al (2014) Sea ice mass balance observations from the North Pole Environmental Observatory. Geophys Res Lett 41:2019–2025. https://doi.org/10.1002/2014gl059356

Petri R, Imhoff JF (2001) Genetic analysis of sea-ice bacterial communities of the Western Baltic Sea using an improved double gradient method. Polar Biol 24:252–257. https://doi.org/10.1007/s003000000205

Petrich C, Eicken H (2010) Growth, structure and properties of sea ice. In: Thomas DN, Dieckmann SD (eds) Sea ice, 2nd edn. Wiley, Oxford, pp 23–77

Picard KT (2017) Coastal marine habitats harbor novel early-diverging fungal diversity. Fungal Ecol 25:1–13. https://doi.org/10.1016/j.funeco.2016.10.006

Piiparinen J, Kuosa H, Rintala JM (2010) Winter-time ecology in the Bothnian Bay, Baltic Sea: nutrients and algae in fast ice. Polar Biol 33:1445–1461. https://doi.org/10.1007/s00300-010-0771-6

Piwosz K, Wiktor JM, Niemi A et al (2013) Mesoscale distribution and functional diversity of picoeukaryotes in the first-year sea ice of the Canadian Arctic. ISME J 7:1461–1471. https://doi.org/10.1038/ismej.2013.39

Polglase JL (1980) A preliminary report on the thraustochytrid(s) and labyrinthulid(s) associated with a pathological condition in the Lesser octopus Eledone cirrhosa. Bot Mar 23:699–706. https://doi.org/10.1515/botm-1980-1106

Poulin M, Daugbjerg N, Gradinger RR et al (2011) The pan-Arctic biodiversity of marine pelagic and sea-ice unicellular eukaryotes: a first-attempt assessment. Mar Biodivers 41:13–28. https://doi.org/10.1007/s12526-010-0058-8

Rahimian H (1998) Pathology and morphology of *Ichthyophonus hoferi* in naturally infected fishes off the Swedish west coast. Dis Aquat Org 34:109–123. https://doi.org/10.3354/dao034109

Rämä T, Norden J, Davey ML et al (2014) Fungi ahoy! Diversity on marine wooden substrata in the high North. Fungal Ecol 8:46–58. https://doi.org/10.1016/j.funeco.2013.12.002

Rämä T, Hassett BT, Bubnova E (2017) Arctic marine fungi: from filaments and flagella to operational taxonomic units and beyond. Bot Mar 60:433–452. https://doi.org/10.1515/bot-2016-0104

Rapp JZ, Fernández-Méndez M, Bienhold C et al (2018) Effects of ice-algal aggregate export on the connectivity of bacterial communities in the central Arctic Ocean. Front Microbiol 9:1035. https://doi.org/10.3389/fmicb.2018.01035

Reimnitz E, Clayton JR, Kempema EW et al (1993) Interaction of rising frazil with suspended particles – tank experiments with applications to nature. Cold Reg Sci Technol 21:117–135. https://doi.org/10.1016/0165-232x(93)90002-P

Riedel A, Michel C, Gosselin M et al (2008) Winter-spring dynamics in sea-ice carbon cycling in the coastal Arctic Ocean. J Mar Syst 74:918–932. https://doi.org/10.1016/j.jmarsys.2008.01.003

Rintala JM, Piiparinen J, Blomster J et al (2014) Fast direct melting of brackish sea-ice samples results in biologically more accurate results than slow buffered melting. Polar Biol 37:1811–1822. https://doi.org/10.1007/s00300-014-1563-1

Ruiz-González C, Gali M, Sintes E et al (2012) Sunlight effects on the osmotrophic uptake of DMSP-Sulfur and leucine by polar phytoplankton. PLoS One 7:45545. https://doi.org/10.1371/journal.pone.0045545

Rysgaard S, Glud RN (2004) Anaerobic N-2 production in Arctic sea ice. Limnol Oceanogr 49:86–94. https://doi.org/10.4319/lo.2004.49.1.0086

Rysgaard S, Glud RN, Sejr MK et al (2008) Denitrification activity and oxygen dynamics in Arctic sea ice. Polar Biol 31:527–537. https://doi.org/10.1007/s00300-007-0384-x

Sanders RW (1991) Mixotrophic protists in marine and freshwater ecosystems. J Protozool 38:76–81. https://doi.org/10.1111/j.1550-7408.1991.tb04805.x

Sanders RW, Gast RJ (2012) Bacterivory by phototrophic picoplankton and nanoplankton in Arctic waters. FEMS Microbiol Ecol 82:242–253. https://doi.org/10.1111/j.1574-6941.2011.01253.x

Scholz B, Küpper FC, Vyverman W et al (2017a) Chytridiomycosis of marine diatoms-The role of stress physiology and resistance in parasite-host recognition and accumulation of defense molecules. Mar Drugs 15:26. https://doi.org/10.3390/md15020026

Scholz B, Vyverman W, Küpper FC et al (2017b) Effects of environmental parameters on chytrid infection prevalence of four marine diatoms: a laboratory case study. Bot Mar 60:419–431. https://doi.org/10.1515/bot-2016-0105

Secretariat of Arctic Council (2017) State of the arctic marine biodiversity report. Conservation of Arctic Flora and Fauna, Fairbanks

Sencilo A, Luhtanen AM, Saarijarvi M et al (2015) Cold-active bacteriophages from the Baltic Sea ice have diverse genomes and virus-host interactions. Environ Microbiol 17:3628–3641. https://doi.org/10.1111/1462-2920.12611

Serreze MC, Francis JA (2006) The Arctic amplification debate. Clim Chang 76:241–264. https://doi.org/10.1007/s10584-005-9017-y

Sherr EB, Sherr BF, Fessenden L (1997) Heterotrophic protists in the Central Arctic Ocean. Deep-Sea Res II 44:1665–1673. https://doi.org/10.1016/S0967-0645(97)00050-7

Shields JD (1990) *Rhizophydium littoreum* on the eggs of *Cancer anthonyi* – parasite or saprobe. Biol Bull 179:201–206. https://doi.org/10.2307/1541770

Singh SM, Tsuji M, Gawas-Sakhalker P et al (2016) Bird feather fungi from Svalbard. Arctic Polar Biol 39:523–532. https://doi.org/10.1007/s00300-015-1804-y

Sipler RE, Gong D, Baer SE et al (2017) Preliminary estimates of the contribution of Arctic nitrogen fixation to the global nitrogen budget. Limnol Oceanogr Lett 2:159–166. https://doi.org/10.1002/lol2.10046

Søgaard DH, Kristensen M, Rysgaard S et al (2010) Autotrophic and heterotrophic activity in Arctic first-year sea ice: seasonal study from Malene Bight, SW Greenland. Mar Ecol Prog Ser 419:31–45. https://doi.org/10.3354/meps08845

Søreide JE, Leu E, Berge J et al (2010) Timing of blooms, algal food quality and *Calanus glacialis* reproduction and growth in a changing Arctic. Glob Chang Biol 16:3154–3163. https://doi.org/10.1111/j.1365-2486.2010.02175.x

Stoecker DK, Weigel AC, Stockwell DA et al (2014) Microzooplankton: abundance, biomass and contribution to chlorophyll in the Eastern Bering Sea in summer. Deep-Sea Res II 109:134–144. https://doi.org/10.1016/j.dsr2.2013.09.007

Stroeve JC, Markus T, Boisvert L et al (2014) Changes in Arctic melt season and implications for sea ice loss. Geophys Res Lett 41:1216–1225. https://doi.org/10.1002/2013gl058951

Syvertsen EE (1991) Ice algae in the Barents Sea – types of assemblages, origin, fate and role in the ice-edge phytoplankton bloom. Polar Res 10:277–287. https://doi.org/10.1111/j.1751-8369.1991.tb00653.x

Taylor GT, Sullivan CW (2008) Vitamin B-12 and cobalt cycling among diatoms and bacteria in Antarctic sea ice microbial communities. Limnol Oceanogr 53:1862–1877. https://doi.org/10.4319/lo.2008.53.5.1862

Tedesco L, Vichi M, Haapala J et al (2010) A dynamic biologically active layer for numerical studies of the sea ice ecosystem. Ocean Model 35:89–104. https://doi.org/10.1016/j.ocemod.2010.06.008

Tedesco L, Miettunen E, An BW et al (2017) Long-term mesoscale variability of modelled sea-ice primary production in the northern Baltic Sea. Elem Sci Anth 5:29. https://doi.org/10.1525/elementa.223

Terrado R, Medrinal E, Dasilva C et al (2011) Protist community composition during spring in an Arctic flaw lead polynya. Polar Biol 34:1901–1914. https://doi.org/10.1007/s00300-011-1039-5

Toole JM, Timmermans ML, Perovich DK et al (2010) Influences of the ocean surface mixed layer and thermohaline stratification on Arctic sea ice in the central Canada Basin. J Geophys Res Oceans 115. https://doi.org/10.1029/2009jc005660

Tremblay JE, Anderson LG, Matrai P et al (2015) Global and regional drivers of nutrient supply, primary production and CO_2 drawdown in the changing Arctic Ocean. Prog Oceanogr 139:171–196. https://doi.org/10.1016/j.pocean.2015.08.009

Trenerry LJ, McMinn A, Ryan KG (2002) In situ oxygen microelectrode measurements of bottom-ice algal production in McMurdo Sound, Antarctica. Polar Biol 25:72–80. https://doi.org/10.1007/s003000100314

Ueda M, Nomura Y, Doi K et al (2015) Seasonal dynamics of culturable thraustochytrids (Labyrinthulomycetes, Stramenopiles) in estuarine and coastal waters. Aquat Microb Ecol 74:187–204. https://doi.org/10.3354/ame01736

Unrein F, Massana R, Alonso-Sáez L et al (2007) Significant year-round effect of small mixotrophic flagellates on bacterioplankton in an oligotrophic coastal system. Limnol Oceanogr 52:456–469. https://doi.org/10.4319/lo.2007.52.1.0456

Unrein F, Gasol JM, Not F et al (2014) Mixotrophic haptophytes are key bacterial grazers in oligotrophic coastal waters. ISME J 8:164–176. https://doi.org/10.1038/ismej.2013.132

Vader A, Marquardt M, Meshram AR et al (2015) Key Arctic phototrophs are widespread in the polar night. Polar Biol 38:13–21. https://doi.org/10.1007/s00300-014-1570-2

Vader A, Laughinghouse HD, Griffiths C et al (2018) Proton-pumping rhodopsins are abundantly expressed by microbial eukaryotes in a high-Arctic fjord. Environ Microbiol 20:890–902. https://doi.org/10.1111/1462-2920.14035

Vancoppenolle M, Tedesco L (2017) Numerical models of sea ice biogeochemistry. In: Thomas DN (ed) Sea ice. Wiley, New York, pp 492–515

Voipio A (1981) The Baltic Sea. Elsevier, Amsterdam

Vonnahme TR, Devetter M, Zarsky JD et al (2016) Controls on microalgal community structures in cryoconite holes upon high-Arctic glaciers, Svalbard. Biogeosciences 13:659–674. https://doi.org/10.5194/bg-13-659-2016

Wassmann P, Slagstad D, Ellingsen I (2010) Primary production and climatic variability in the European sector of the Arctic Ocean prior to 2007: preliminary results. Polar Biol 33:1641–1650. https://doi.org/10.1007/s00300-010-0839-3

Wassmann P, Duarte CM, Agusti S et al (2011) Footprints of climate change in the Arctic marine ecosystem. Glob Chang Biol 17:1235–1249. https://doi.org/10.1111/j.1365-2486.2010.02311.x

Weeks WF, Ackley SF (1986) The growth, structure, and properties of sea ice. In: Untersteiner N (ed) The geophysics of sea ice. Springer US, Boston, pp 9–164. https://doi.org/10.1007/978-1-4899-5352-0_2

Weissenberger J, Grossmann S (1998) Experimental formation of sea ice: importance of water circulation and wave action for incorporation of phytoplankton and bacteria. Polar Biol 20:178–188. https://doi.org/10.1007/s003000050294

Wells LE, Deming JW (2006a) Characterization of a cold-active bacteriophage on two psychrophilic marine hosts. Aquat Microb Ecol 45:15–29. https://doi.org/10.3354/ame045015

Wells LE, Deming JW (2006b) Modelled and measured dynamics of viruses in Arctic winter sea-ice brines. Environ Microbiol 8:1115–1121. https://doi.org/10.1111/j.1462-2920.2005.00984.x

Werner I, Auel H (2004) Environmental conditions and overwintering strategies of planktonic metazoans in and below coastal fast ice in the Gulf of Finland (Baltic Sea). Sarsia 89:102–116. https://doi.org/10.1080/00364820410003504

Worby AP, Bush GM, Allison I (2001) Seasonal development of the sea-ice thickness distribution in East Antarctica: measurements from upward-looking sonar. Ann Glaciol 33:177–180. https://doi.org/10.3189/172756401781818167

Yergeau E, Michel C, Tremblay J et al (2017) Metagenomic survey of the taxonomic and functional microbial communities of seawater and sea ice from the Canadian Arctic. Sci Rep 7:42242. https://doi.org/10.1038/srep42242

Zhang Q, Gradinger R, Zhou QS (2003) Competition within the marine microalgae over the polar dark period in the Greenland Sea of high Arctic. Acta Oceanol Sin 22:233–242

Terrestrial Inputs Shape Coastal Microbial Communities in a High Arctic Fjord (Isfjorden, Svalbard)

Lisa-Marie Delpech[1,2*], Tobias R. Vonnahme[2*], Maeve McGovern[2,4], Rolf Gradinger[2], Kim Præbel[3], Amanda Poste[4]

[1]École Normale Supérieure de Lyon, Université Claude Bernard Lyon I, Université de Lyon, 69342 Lyon Cedex 07, France

[2]Department of Arctic Marine Biology, UiT The Arctic University of Norway, Tromsø, Norway

[3]Norwegian College of Fishery Science, UiT The Arctic University of Norway, Tromsø, Norway

[4]Norwegian Institute for Water Research (NIVA), Tromsø, Norway

*** Correspondence:**
Lisa-Marie Delpech (lisa-marie.delpech@ens-lyon.fr), Tobias R. Vonnahme (tobias.vonnahme@uit.no)

Keywords: Arctic, climate change, land-ocean interactions, microbial communities, freshwater runoff, melt season, DOM, biogeochemical cycle.

Running Title: Terrestrial Inputs Shape Microbial Communities

Wordcount: 9452 words

Number of figures: 8

Number of tables: 1

Abstract

Warming faster than the rest of the world, the Arctic is experiencing dramatic changes including increases in precipitation, glacial melt, and permafrost thaw, resulting in increasing summer freshwater runoff. During the melt season, terrestrial runoff delivers carbon and nutrient rich freshwater to Arctic coastal waters, with unknown consequences for the microbial communities that play a key role in determining the cycling and fate of terrestrial matter at the land-ocean interface. To determine the impacts of runoff on coastal microbial communities in Isfjorden, Svalbard, we investigated changes in pelagic microbial community structure between the early and late melt season as well as changes in both pelagic and benthic microbial community structure along a gradient from rivers and glaciers to the outer fjord. Amplicon sequences of the 16S rRNA gene were generated for water column, river and sediment samples collected in Isfjorden along a gradient from shallow nearshore stations to the outer fjord during the summer melt season in 2018 (June and August). This study identified strong seasonal and spatial reorganizations in the structure and composition of microbial communities during the summer months, in relation to environmental conditions. The microbial diversity patterns highlighted a reorganization from rich communities in June towards more even and less rich communities in August. The organic matter source, DOC concentration and water temperature strongly contributed to shaping seasonal changes in microbial community structure. In June, waters enriched in dissolved

organic carbon (DOC) provided a niche for copiotrophic taxa such as *Sulfitobacter* and *Octadecabacter*. The reduction in DOC concentrations and the higher nutrient inputs from the rivers in August favored a shift towards more cosmopolitan taxa usually associated with summer stratified periods such as the SAR11 *Clade Ia*, and prevalent oligotrophic marine clades (OM60, SAR92). A stratification of the communities was observed in August in relation to the physical and biogeochemical stratification of the water column. Sentinel taxa of this late summer fjord environment included taxa from the Verrucomicrobiae (*Roseibacillus*, *Luteolibacter*) and Bacteroidetes classes. In June, we also found indications of allochthonous inputs of river taxa, which, while unlikely to thrive in fjord waters, amplified the species richness in the water column. This study demonstrates an ecological impact of terrestrial runoff on Arctic coastal microbial communities driven by changes in biogeochemical conditions and highlights the need to understand land-ocean connectivity when studying climate change impacts on coastal ecosystems.

1 Introduction

Arctic regions are warming two times faster than lower latitudes (Serreze and Barry, 2011; Osborne et al., 2018). Subsequent increases in the quantity (Bintanja and Selten, 2014) and variability (Bintanja et al., 2020) of precipitation, melting glaciers, and thawing permafrost are expected to lead to increased terrestrial runoff (Shiklomanov and Shiklomanov, 2003; Milner et al., 2017) alongside changes in geochemistry of runoff (Holmes et al., 2012). Coastal environments are prominent habitats on a pan Arctic scale where there is a high degree of connectivity between land and see (McClelland et al., 2012). These ecosystems can act as hotspots for carbon burial (Bianchi et al., 2018) and organic matter (OM) cycling (Bianchi et al., 2020), but are also likely very sensitive to ongoing climate change (Jeffries et al., 2013; Bhatt et al., 2014; Fritz et al., 2017).

Microorganisms play a key role in climate change biology, as they will likely affect and be affected by climate change (Vincent, 2010; Cavicchioli et al., 2019). Especially in polar environments, aquatic microorganisms play an essential role (Kirchman et al., 2009) in driving cycles of carbon, nitrogen, and of other elements (Arrigo, 2005; Garcia-Descalzo et al., 2013), including the recycling of organic matter and inorganic nutrients into food webs (Falkowski et al., 2008; Ferrera et al., 2015; Worden et al., 2015). The realization of these functions strongly depends on environmental conditions (Gilbert et al., 2012), and their influence on microbial community structure and function (Allison and Martiny, 2008; Shade et al., 2012; Louca et al., 2016). In coastal ecosystems, seasonal processes — *e.g.* light and nutrient availability, temperature, salinity — shape microbial communities (Gilbert et al., 2012; Cram et al., 2015). However, in the Arctic, climate change is amplifying seasonal changes in temperature (Serreze and Barry, 2011) and terrestrial runoff (Holmes et al., 2012). Hence, understanding how coastal microbial communities respond to environmental variables influenced by terrestrial runoff throughout the melt season is key to predicting how future climate-influenced changes might affect microbial communities in Arctic coastal waters.

Despite the importance of microbial communities in coastal environments, their vulnerability to the warming Arctic and their response to increased terrestrial runoff is poorly studied, especially in nearshore coastal waters. Previous studies have demonstrated a direct effect of river runoff on coastal microbial community composition and diversity (Fortunato et al., 2013; Hauptmann et al., 2016), as well as indirect effects of the physico-chemical variables (Sipler et al., 2017; Müller et al., 2018; Underwood et al., 2019; Thomas et al., 2020) on seasonal (Marquardt et al., 2016; Kellogg et al., 2019) and spatial variation (Bourgeois et al., 2016) in microbial community composition in Arctic regions. However, very few studies include nearshore coastal waters which are often heavily terrestrially-influences. The few available studies from Svalbard have focused on local microbial community

structure. For instance, they revealed spatial effects of glacial runoff on coastal marine sediment communities (Park et al. 2011, Bourgeois et al. 2016), compositional differences between seawater and sediment communities (Teske et al. 2011), or potential direct effects of glacier microbial communities on coastal communities (Garcia-Lopez et al. 2019), but remain limited to one environmental compartment and one fjord, and rarely take environmental variables into account (Thomas et al., 2020). In Isfjorden, Marquardt et al. (2016) highlighted a link between community composition and seasonally influenced variables, but with a focus on outer-fjord stations, thus reducing the potential to determine the influence of runoff-affected variables. Hence, little is known on how terrestrial runoff and underlying environmental gradients affect microbial communities in Arctic nearshore waters. This knowledge gap impedes our ability to predict the impact of climate change on coastal Arctic microbial communities, and subsequent impacts on coastal food webs and biogeochemical cycles.

The Svalbard archipelago is of particular interest to study effects of climate change on coastal waters, as it is already characterized by higher temperatures than other Arctic systems at the same latitude due to advection of warmer ocean currents (Skogseth et al., 2020). Nevertheless, climate change effects are felt in Svalbard, where, due to increased precipitation and glacial melt, runoff is predicted to increase by 2100, especially in autumn (Adakudlu et al., 2019). In Isfjorden, runoff undergoes seasonal changes that highly affect physico-chemical conditions in the fjord, with spring freshet in June delivering high concentrations of DOC, and late season runoff in August characterized by high concentrations of nutrients and terrestrial particles (McGovern et al., 2020).

Our microbial study focused on the Isfjorden system on the west coast of Svalbard, building on a recent study that demonstrated extensive impacts of riverine inputs on temperature, light availability, inorganic nutrients and terrestrial organic matter (McGovern et al., 2020). We hypothesized that seasonal changes in runoff will cause seasonal and spatial variability in microbial community composition and function between the early and late summer snow and glacial melt season. Two main research objectives were addressed: (1) to determine how runoff affects microbial community structure at the land-ocean interface and (2) to identify possible changes in microbial community composition and function in terrestrially influenced Arctic waters, using 16S rRNA gene sequencing from samples collected along the freshwater-marine continuum in a high Arctic fjord (Isfjorden, Svalbard). In order to target two phases in the summer melt season – the spring freshet and late-runoff – samples were collected in June and August. We hypothesized that terrestrial runoff would lead to spatial changes along the sampled environmental gradient, *i.e.* from the estuaries to the outer fjord, either directly (*via* communities transported from the rivers), or indirectly (shaped by physico-chemical variables affected by the runoff).

2 Material and Methods

2.1 Sample Collection, Microbial Sample Processing, and Physico-chemical Variable Determination

In 2018, samples were collected during two field campaigns in June and August, from a total of 34 stations in Isfjorden along gradients from rivers and glacier fronts to the outer fjord (**Figure 1**). Water samples were collected from two water depths (surface and 15 m) using a Niskin bottle, and targeted surface waters (SW) and Atlantic advected waters (AdW). Surface sediment samples (0-1 cm) were collected with a van-Veen grab in August. Subsamples for DNA analysis were filtered onto 0.2 µm polycarbonate filters (water) or placed in 2 mL cryo vials (sediments), and frozen at -20°C until further processing.

Physical conditions and water chemistry were characterized in a parallel study (McGovern et al., 2020), and included in our data analysis. Measured variables included temperature, salinity, turbidity, concentrations of dissolved and particulate organic carbon (DOC, POC), stable isotope values for POC (POC $\delta^{13}C$) and particulate nitrogen (PN $\delta^{15}N$), concentrations of chlorophyll *a*, phaeophytin, dissolved nutrients (ammonium NH_4^+, phosphate PO_4^{3-}, nitrite and nitrate NO_2^-+NO_3^-, and silicate SiO_2), and suspended particulate matter (SPM). Specific UV absorbance at 254 nm ($SUVA_{254}$) was also measured as an indicator of aromaticity (humic content) of dissolved organic matter (DOM) (Weishaar et al., 2003).

2.2 DNA Extraction, Polymerase Chain Reaction, Library Preparation and MiSeq Sequencing

Microbial genomic DNA was isolated using the DNeasy® PowerSoil® Kit following the kit instructions with modifications after Hassett et al. (2019). Solution C1 was replaced with 600 µL Phenol:Chloroform:Isoamyl and washing with C2 and C3 was replaced with two washing steps using 850 µL chloroform. Before the last centrifugation step the column was incubated at 55°C for 5 min.

For microbial community composition analysis, we amplified the V4 region of a ca. 292 bp fragment of the 16S rRNA gene using the primers (515F, GTGCCAGCMGCCGCGGTAA and 806R, GGACTACHVGGGTWTCTAAT) (Caporaso et al., 2012; evaluated by Wear et al., 2018). The library preparation protocol is described in Wangensteen et al. (2018).

2.3 Sequence Analysis

Sequences were processed using a pipeline modified after Hassenrück (2019). Demultiplexing and primer clipping were done using cutadapt (Martin, 2011) (v2.8). The reads were quality trimmed with a sliding window of 4 and a quality threshold of 15 using trimmomatic (Bolger et al., 2014) (v0.39) and reads shorter than 100 bp were discarded. Remaining reads were merged using Pear (Zhang et al., 2014) (v0.9.6), with a minimum overlap of 10 bp, a minimum length of the merged reads of 200 bp (expected 292 bp), and a maximum of 500 bp. Successfully paired reads were quality controlled with FastQC (Babraham Bioinformatics) (v0.11.9), dereplicated using Swarm's dereplication code (Mahé et al., 2015), and clustered using Swarm v2 (Mahé et al., 2015) (v3.0.0) with the fastidious option. An Operational Taxonomic Unit (OTU) contingency table was created and taxonomy of the representative amplicons assigned using SINA (Pruesse et al., 2012) v1.6.0 against the SILVA SSU non redundant (v138) reference database (Quast et al., 2013). Further analyses were performed in R v.3.6.3 (R Core Team, 2020). Sequences related to chloroplasts or mitochondria were removed, and only OTUs with more than one sequence in more than two samples were kept, removing 9% of the sequences. A negative control was included in the sequencing, and sequences identified in this sample were removed from all samples. After these quality control steps, the average number of sequences per sample was 143,543.

To investigate taxonomic composition, remaining OTUs were pooled by taxonomic level using taxapooler v.1.4 (Gobet and Ramette, 2011), with the curated SILVA SSU database (v138) available from Hassenrück (2020). The abundance was calculated relatively to the sample composition to which the taxa belongs.

Functional analysis was performed using Tax4Fun (Aßhauer et al., 2015), with both KEGG Ortholog (KO) and KEGG Pathways reference profiles. KEGG pathway matrix was curated and functions irrelevant to bacteria were removed, the matrix was further used as community data with the same methods as described in the statistical analyses. To investigate targeted functions, KOs were used and the matrix subset to these functions, using the KEGG database. Metabolic functions were

165 determined with KEGG Orthologs genes or enzymes related to the KEGG reaction or pathway (**Table**
166 **1**).

167 **Table 1**. Table detailing KOs used for the analysis of targeted metabolic functions.

Function	KEGG Pathway	KEGG Enzyme	KEGG Genes	KEGG Orthologs (KO)
Carbon fixation by prokaryotic organisms	map00720	-	-	-
Carbon fixation by photosynthetic organisms	map00710	-	-	-
Photosynthesis	map00195	-	-	-
Denitrification	-	EC :1.7.99.4	*narGHI*	K0370-74
		EC :1.9.6.1	*napAB*	K02567-68
		EC :1.7.2.1	*nirKS*	K15864/K00368
		EC :1.7.2.5	*norBC*	K04561/K02305
		EC :1.7.2.4	*nosZ*	K00376
Nitrification	-	EC :1.4.99.39	*amoCAB*	K10944-46
		EC :1.7.3.4	*hao*	K10535
Nitrogen fixation	-	EC :1.18.6.1	*nifDKH*	K00531
				K02586
			anfG	K02588
				K02591
Phosphate utilization (oganic)	-	EC:3.6.1.11	*ppx*	K01524
Sulfate reduction (dissimilatory and assimilatory)	-	EC:2.7.7.4	*sat*	K00958
		EC:2.7.7.4	*cysND*	K00956-57
		EC:2.7.1.25	*PAPSS*	
		EC:2.7.1.25	*cysC*	K00860
		EC:1.8.4.8	*cysH*	K00390
		EC :1.8.1.2	*cysπ*	K00380-81
		EC :1.8.7.1	*sir*	K00392
		EC :1.8.99.2	*aprAB*	K00394-95
		EC :1.8.99.3	*dsrAB*	K11180-81
Methanogenesis	-	EC :1.5.99.9	*fwdABCDEFGH*	K00200-05
			ftr	K00672
			mtd	K00319
			hmd	
		EC :2.1.1.86	*mtrABCDEFGH*	K00577-84
		EC :2.8.4.1	*mcrABG*	K00399/K00401-02
		EC :1.8.98.1	*hdrA2B2C2*	K03388-90
		EC :1.8.98.1	*hdrD*	K08264
Methane oxidation	-	EC :1.1.2.7	-	K14028-29
		EC :1.14.13.25		K16157-61
				K16254-60
Iron chelation	-	-	-	K02016
Binding of iron ion	-	EC:1.16.3.1	-	K02217
Mercury methylation	-	EC:4.99.1.2	-	K00221
Laminarin degradation	-	EC:3.2.1.6	-	K01180
		EC:3.2.1.39		K01199

168

2.4 Statistical Analysis

Samples were analyzed using two categories: season and water type. Water type was determined based on location within the fjord and water mass determination based on Temperature-Salinity diagrams and water masses for Isfjorden (Nilsen et al., 2008). One grouping separates surface waters (SW; salinity < 34.7) from advected waters (AdW; salinity ≥ 34. 7), and SW were then further classified based on location within the fjord, leading to four groups of samples: estuarine SW (Estuary SW), glacier-front SW (Glacier SW), other fjord SW (Fjord SW), and AdW. The second grouping focused on the effect of seasonality and habitat; in order to distinguish between fjord water column, rivers and sediments, four groups were used: June (water column), August (water column), River, and Sediment.

Eight samples with few sequences were removed, and OTU tables randomly rarefied to 42,990 sequences for further analyses. Alpha diversity estimators were calculated after repeated (n = 100) random subsampling of the sequences, as the number of OTUs, Chao1 (Chao, 1984) and Abundance-based Coverage Estimator (ACE) (Chao and Lee, 1992) indices taking singletons and doubletons into account (Kim et al., 2017), evenness as Pielou's index, diversity indices Shannon and inverse Simpson's, and relative singletons (SSO) and doubletons (DSO). To test for differences in diversity among sample groupings, Shapiro-Wilk's test was used to test for normality, Bartlett's test for homoscedasticity, and ANOVA to test for differences. PostHoc Dunn's test was performed on Kruskal-Wallis tests to account for non-gaussian repartitions within some groups, and to test for pairwise differences (false discovery rate (FDR)-corrected *p*-values). To test for differences in metabolic functions, a Kruskal-Wallis test and the postHoc Dunn's test were performed to account for nonparametric data with heterogeneous variances. *p*-values were adjusted using the Benjamini-Hochberg (BH) correction (Benjamini and Hochberg, 1995).

Ordinations were performed in the Vegan package in R (v2.5-6) (Oksanen et al., 2019), using relative abundances of the OTUs and rarefied data. For beta diversity, the OTU turnover between or within sites was calculated using the Jaccard index. Microbial community structure was assessed using nonmetric multidimensional scaling (NMDS), based on Bray-Curtis dissimilarities. To test for differences among *a priori* sample groupings, permutational analysis of variance (PERMANOVA) (Anderson, 2017) and Analysis of Similarity (ANOSIM) (Clarke, 1993) were calculated using adonis and a postHoc modified version (Hassenrück, 2019) of the anosim function in Vegan (false discovery rate (FDR)-corrected *p*-values). PERMANOVA provides a pseudo F-ratio and *p*-value for group-wise tests, and tests for dispersion within groups. ANOSIM tests for similarity between and among groups. ANOSIM and its postHoc test provide an *R* value ranging from 0 to 1 with higher values indicating stronger differences between or among groups, and a FDR-corrected *p*-value for the ANOSIM *R* value, based on 999 permutations.

To investigate the relevance of environmental variables in explaining variation in microbial community structure, principal component analysis (PCA) was performed on the log-transformed environmental and Hellinger-transformed (Legendre and Gallagher, 2001) community matrices. Procrustes analysis was performed to compare ordinations, yielding a significance value. PCA and NMDS were used to explore the relationships between community data and environmental drivers by fitting variables onto unconstrained ordinations. Finally, redundancy analysis (RDA) was used to test hypotheses and to quantify the proportion of variation explained by the physico-chemical data. Constraining variables were selected using forward and reverse model selection with the double-stopping criterion described in Blanchet et al. (2008) implemented in the ordistep function in Vegan. Significance of each vector was tested using ANOVA. Correlations within physico-chemical variables

were tested prior to ordination using pairs (base), and multicollinearity of variables was verified using vif.cca (Vegan) after ordination. Other ordinations using unrarefied data, differentially abundant OTUs (ALDEx2) (Fernandes et al., 2013), Jaccard index (presence-absence) instead of Bray-Curtis, canonical correspondence analysis, and ordinations after Hellinger or central log-ratio transformation showed similar patterns.

Indicator species analysis (Dufrene and Legendre, 1997) was used to determine taxa that significantly contributed to seasonal differences in fjord waters. The multipatt function in the indicspecies package (v1.7.9) (Cáceres and Legendre, 2009) was used to calculate Dufrêne-Legendre Indicator Value (IV), with the control set to 9999 permutations designed by the function how in the permute R package. OTUs with an IV ≥ 0.7 and a p-value ≤ 0.001 were considered significant indicators. Highly abundant indicators were filtered based on a 0.5% relative abundance threshold within their group. Taxonomic affiliation of high-abundant indicator taxa was further analyzed. The correlation between top seasonal indicators (chosen among indicators with relative abundance over 1%) and environmental variables was calculated using Spearman correlations to account for non-homoscedastic repartitions. Correlations and p-values were calculated using the rcorr function in the Hmisc package (v4.4-0) (Harrell Jr and others, 2020). p-values were adjusted using the Benjamini-Hochberg correction with the p.adjust function in the R stats base package. All plots were generated using the ggplot2 package in R (v. 3.3.0) (Wickham, 2016).

3 Results

3.1 Alpha Diversity Differs Seasonally and Spatially in Isfjorden

We identified a total of 35,276 Operational Taxonomic Units (OTUs) across all samples. Sediment and river samples had a significantly higher OTU richness than fjord sites ($p < 0.001$) (**Figure 2A** and **Supplementary Figure S1A**). The same difference was observed for abundance-based richness indices Chao1 and ACE ($p < 0.001$ between sediment and fjord water column samples, $p < 0.05$ between rivers and water column) (**Figure 2B** and **Supplementary Figure 1A**). Pielou's evenness, and Shannon's and inverse Simpson's diversity indices were also greater in sediment and river samples compared to water column samples ($p < 0.0001$) (**Figure 2C,D,E** and **Supplementary Figure S1A**). Among fjord water column samples, diversity was not significantly different between water types (**Figure 2D,E** and **Supplementary Figure S1B**), although a decreasing richness gradient existed from estuary SW to outer fjord SW and AdW ($p < 0.05$ for OTUs richness, $p < 0.01$ for Chao1 and ACE) (**Figure 2AB and Supplementary Figure S1B**). Among fjord water column samples, richness was highest in June ($p < 0.005$), whereas evenness was highest in August ($p < 0.001$) (**Figure 2BC and Supplementary Figure S1A**). The rare biosphere, however, was higher in June compared to August ($p < 0.005$), but similar between water types (**Figure 2F and Supplementary Figure S1**). Overall, we observed variations in the diversity pattern according to the sample compartment, a shift between the early and late melt season and a spatial gradient in water column microbial diversity pattern.

3.2 Beta Diversity Reveals a Seasonal and Spatial Clustering of Microbial Communities

Beta diversity was evaluated to examine changes in microbial community structure between groups. We found that microbial communities differed seasonally and based on their water mass (**Figure 3A**). 45% of the variance in microbial community structure was explained by season and sample type – June and August fjord water column, rivers, and sediments ($p = 0.001$, PERMANOVA). Pairwise seasonal differences were significant between all seasonal groups (ANOSIM $p < 0.005$), and showed clear separation between sediment, river, June and August fjord microbial communities. The turnover between seasonal groups showed that June and August fjord samples shared the highest amount of OTUs (46%). June fjord waters shared the greatest amount of OTUs with river communities (44%, vs. 29% for August and 28% for sediments).

Although not all fjord microbial communities differed significantly according to their water type, in August, AdW significantly differed from all SW ($p \leq 0.01$). In August, ANOSIM R values indicated a gradient from estuaries to outer fjord SW and AdW, estuary communities being more related to rivers than any other fjord water ($R = 0.87$ vs. 1), glaciers more related to estuaries than to fjord SW, and fjord SW more related to estuaries than AdW ($R = 0.01$ glacier, 0.13 fjord SW, 0.41 AdW compared to estuaries). This spatial gradient only existed within August communities, whereas June communities were similar throughout the fjord (based on ANOSIM R values). In August, 26% of the variance in microbial community structure was explained by water type groups ($p = 0.001$, PERMANOVA), whereas these groups could not explain differences within June fjord communities ($p = 0.1$).

Sediments had a unique microbial community structure, influenced by rivers and fjord sites, with higher contribution from the rivers ($R = 0.83$ between rivers and sediments, 0.92 between fjord and sediments). Sediments shared more OTUs with June than with August or river communities, although they were collected in August (38% vs. 27% and 28% resp.). They were also more related to estuary SW than to any other water group (ANOSIM $R = 0.81$).

Functional diversity, as assessed with metabolic pathways, highlighted the same seasonal pattern as communities (**Figure 3B**). 63% of the variance was explained by seasonal groups (PERMANOVA $p = 0.001$), and 64% by water type groupings (PERMANOVA $p = 0.001$). In August, the same spatial gradient as for community structure existed. ANOSIM R values indicated the same clustering as community structure, with a less strong but significant difference between June and August functions ($R = 0.18$). The functional turnover showed a strong functional redundancy in fjord communities (96% shared functions between June and August). The sediments shared more functions with rivers and August samples than with June (81%, 71% and 68% resp.).

Among sediment samples, the same spatial clustering was observed along the fjord transect (**Figure 3C**). 46% of the variance was explained by the grouping related to location in the fjord (PERMANOVA $p \leq 0.001$). Sediment microbial communities located at the estuaries were more related to glacier sediment microbial communities (ANOSIM $R = 0.61$, $p > 0.05$) than to fjord transect sediment microbial communities (ANOSIM $R = 0.83$, $p < 0.05$). Hence, within environmental compartments, microbial communities showed similarities in their distribution depending on the water type and the location within the fjord.

3.3 Taxonomic Composition and Indicator OTUs of Seasonality

All communities were dominated by the phyla Proteobacteria – including the classes Alphaproteobacteria, Gammaproteobacteria – and Bacteroidetes – including the class Bacteroidia –, but they all showed specific patterns in their occurrence (**Figure 4A**). Fjord microbial communities in June and August were dominated by Gammaproteobacteria (36.0% and 24.2% respectively), Alphaproteobacteria (33.5% and 26.1%), and Bacteroidia (22.7% and 29.8%), although they differed in their dominance pattern, and clear seasonal differences existed (**Figure 4B)**.

In June, Gammaproteobacteria were dominated by the order Oceanospirillales (17.7% of community average composition) with the family Nitrincolaceae (14.5%) and Alteromonadales (*Pseudoalteromonas* sp.). Alphaproteobacteria were dominated by the order Rhodobacterales (27.2%), highly represented by sulfur-oxidizing bacteria of the *Sulfitobacter* sp. (20.1% of community average) and by the genus *Octadecabacter* (4.1%). Bacteroidia were predominantly represented by genera of the Flavobacteriales order, including *Polaribacter* (6.1%), *Formosa* (3.7%) and the NS5 marine group (2.8%), and by other Flavobacteriaceae (4.4%).

In August, community composition differed from June in the abundant members of these classes. Bacteroidia included the same taxa, but also the genus *Ulvibacter* (3.0%), which was rare in June (0.3%). Alphaproteobacteria were also dominated by the genus *Sulfitobacter*, but were represented by a more even community, including the SAR11 *Clade Ia* (5.8%), and the genera *Planktomarina* (3.2%) and *Ascidiaceihabitans* (2.4%), which was rare in June (0.1%). Gammaproteobacteria included members of the Cellvibrionales oligotrophic marine clades (OM60, SAR92), while Oceanospirillales and Altermonadales were less abundant (34% of the Gammaproteobacteria vs. 61% in June). August communities also differed from June communities because of highly abundant clades of the class Verrucomicrobiae, including the genera *Roseibacillus* (7.4% of average community composition), and *Luteolibacter* (1.3%), and with their composition in Actinobacteria (6.3% in August, 4.1% in June), of which the genera *Candidatus Aquiluna* (3.8%), *Sva0996* (1.4%) and *Illumatobacter* (1.4%) were abundant.

River communities were dominated by Burkholderiales (33%), mostly represented by the genera *Rhodoferax* (7.9%), *Polaromonas* (5.9%), *Thiobacillus* (4.9%), *Massilia* (2.8%), and *Gallionella* (2.3%)

but these taxa were equally abundant in June and August water column communities. Reciprocally, taxa that differentiated June from August water column communities were not abundant in the rivers (**Figure 4B**).

Sediments had a unique microbial community composition, and taxonomic overlap with both fjord (Flavobacteriales 19.1%, Cellvibrionales 7.4%, Rhodobacterales, Verrucomicrobiales, Oceanospirillales), and rivers (Burkholderiales, 6.8%). However, they showed different patterns in the members of these groups (**Figure 4B**).

Indicator taxa analyses supported these results, and also pointed out several taxa of lower abundance (**Supplementary Table 3**). In the water column, we identified 16 indicators in June and 28 in August. We identified 35 indicators in the rivers, and 38 in the sediments.

3.4 Metabolic Functions Inferred from Taxonomy

Based on the taxonomy, we identified several functions of which the potentials differed between seasonal groups (**Figure 5**). Overall, June water column communities showed higher potential for carbon and nitrogen fixation ($p < 0.01$), phosphorus utilization ($p < 0.005$), and for methane oxidation ($p < 0.005$) compared to August water column communities. The latter were associated with a higher potential for sulfate reduction ($p < 0.05$) and mercury methylation ($p < 0.001$) compared to June water column communities. In August, there was also a separation of the functions between SW and AdW, highlighting the spatial gradient already observed for community composition. For instance, carbon fixation by prokaryotic organisms and methane oxidation had higher potentials in fjord transect SW than in AdW ($p < 0.005$), potential for sulfate reduction was higher in AdW compared to fjord SW ($p < 0.005$) and estuary SW ($p < 0.05$). Finally, potential for laminarin degradation was also higher in AdW compared to estuary SW ($p < 0.05$), glacier SW ($p < 0.05$), and fjord SW ($p < 0.01$).

Rivers had a high potential for photosynthesis compared to the water column ($p < 0.001$). However, river samples were segregated from water column samples because of their low potential for other specific functions — nitrification ($p < 0.05$), denitrification ($p < 0.001$), methane oxidation ($p < 0.005$) and iron chelation ($p < 0.001$). Finally, rivers could be a source for Sulfate Reducing Bacteria (SRB) as they showed high sulfate reduction potential ($p < 0.001$ compared to water column).

Sediments were segregated from the other compartments with a specific functional footprint, as they showed very low carbon and nitrogen fixation, phosphorus utilization and methane oxidation potential, but the highest potentials for nitrification, methanogenesis and mercury methylation.

3.5 Environmental Drivers of Isfjorden Microbial Community Structure Within the Water Column

Microbial community structure was significantly correlated with coastal environmental conditions in Isfjorden (Procrustes, $p = 0.001$). Ordination analyses separated August from June communities, as well as inner fjord SWs from outer fjord AdWs.

Results of redundancy analysis highlighted a strong seasonal difference between June and August communities (**Figure 6A**). The first RDA axis, which accounted for 51% of the community variation between June and August, was positively correlated with temperature, Secchi depth, $\delta^{13}C$ of POC, and $SUVA_{254}$ (ANOVA $p < 0.005$), and negatively correlated with DOC ($p \leq 0.001$) and chlorophyll *a* ($p \leq 0.01$). While June communities correlated with higher DOC and chlorophyll *a* concentrations, August communities were related to higher temperature, higher $\delta^{13}C$ value of POC and an aromatic

signal of DOM. Separation of June from August communities was thus driven by temperature, terrestrial inputs, and productivity. These variables alone explained 72% of the total variation, of which 51% accounted for seasonal changes.

Results of redundancy analysis on functional data also highlighted this seasonal shift (**Supplementary Figure S4A**. June samples were characterized by a higher DOC concentration, while August samples correlated with higher δ^{13}C POC, suggesting that the seasonality was mostly explained by changes in terrestrial inputs and carbon availability. Interestingly, temperature did not explain this separation.

A secondary, spatial gradient existed within these communities, explained by the second RDA axis (**Figure 6A**). We built a second model to explore within-month drivers of microbial community structure. Redundancy analysis on August communities highlighted the physical and chemical effects of riverine inputs on spatial variations along the fjord SWs and AdWs, and highlighted different explanatory variables than the ones explaining the seasonal shift (**Figure 6B**). Both RDA axes explained this spatial gradient in August (ANOVA $p \leq 0.001$), with salinity ($p \leq 0.001$) on the one hand, and NO_2^-+NO_3^- ($p \leq 0.001$), particulate P ($p < 0.01$), particulate N ($p \leq 0.001$), and POC ($p < 0.05$) on the other, highlighting that this gradient in microbial community structure coincided with gradients in salinity and nutrients. 63% of the variability within August communities was explained by these variables. However, this gradient was almost non-existent in June, although salinity and NO_2^- +NO_3^- concentration significantly explained the variability within June samples (data not shown).

The inclusion of river samples in the analysis (**Supplementary Figure S4B**) showed that the variability between river, August, and June communities, was explained by salinity ($p \leq 0.001$), SPM, turbidity ($p < 0.05$), DOC ($p \leq 0.001$), and SiO_2 ($p < 0.05$), linking seasonal and spatial gradients. These variables explained 85% of the variability within the river-fjord system communities, of which 66% explained the river-fjord transition. Hence, the observed changes in microbial community structure coincided with environmental variables influenced by terrestrial inputs, both for the seasonal and spatial gradient.

Correlations between highly abundant indicators and physico-chemical variables corroborated these results (**Figure 7**). June indicator taxa correlated with conditions representing marine and terrestrial sources of carbon (positive correlations with DOC concentration, negative correlations with δ^{13}C of POC and $SUVA_{254}$). This was especially verified for highly abundant and very specific indicators (*e.g. Sulfitobacter*, *Octadecabacter*; **Figure 7**). They also correlated negatively with temperature. August indicator taxa correlated with conditions representing late melt season (positive correlation with temperature), and were negatively correlated to carbon indicators (DOC, POC). They also correlated with a marine source of carbon (positive correlations with δ^{13}C of POC). Finally, numerous August indicators positively correlated with silicate and ammonia concentrations, nutrients which were associated with riverine inputs.

4 Discussion

4.1 Environmental Compartments Shape Microbial Community Structure

We observed variations in microbial community structure in Isfjorden both between and among environmental compartments. Rivers, sediments and fjord water communities showed clear differences in their diversity pattern and microbial community structure. Furthermore, we observed seasonal and spatial variations in microbial community structure within fjord waters, where June and August communities differed, in relation to freshwater influence (**Figure 8**).

The lower OTU richness and higher OTU evenness observed in August compared to June have been documented in other Arctic coastal environments (Kellogg et al., 2019) and can be explained by several potential drivers. The high load of freshwater that enters the fjord in June with the spring freshet (McGovern et al., 2020) might temporally boost the richness in June, as allochthonous taxa from the rivers enter the fjord as part of the rare biosphere, but do not survive until summer. This is supported by June waters sharing a greater amount of OTUs with the rivers than August waters, and more generally, with the demonstrated influence of river taxa in estuaries (Fortunato et al., 2013; Hauptmann et al., 2016). However, given that this effect should be amplified nearshore in the estuaries, which was not the case in June, we suggest that additional environmental variables explain this pattern. We observed differences in functional diversity between the early and late melt season, although a strong redundancy existed between June and August communities, ensuring functional redundancy and resilience of the ecosystem (Walker, 1992). We suggest that other differences account for seasonal variations. Some functions are phylogenetically widespread (*e.g.* heterotrophic metabolism) and persist despite variation in microbial community composition (Langenheder et al., 2006). This explains the low variation in our functional analysis in comparison to greater variations observed in community composition. However, specific functions can show high variations with small differences in microbial community composition (Balser and Firestone, 2005; Bell et al., 2005; Balmonte et al., 2019), suggesting that these differences could lead to differential realization of element cycling in June and August, such as different efficiencies in the realization of the carbon, nitrogen, sulfur and phosphorus cycles.

Sediment microbial communities differed from all other communities in terms of diversity and function. However, they shared similarities with the rivers in terms of diversity and composition, which could be attributed to the particle-attached bacteria that enter the fjord *via* runoff and settle out. However, sediment communities also shared taxa with fjord waters, especially June waters, although they were collected in August. This can be explained by high sedimentation rates observed in June, subsequent to high loads of freshwater that enter the fjord (McGovern et al., 2020). However, the functional pattern in the sediments was more related to rivers and August fjord communities. This suggests that sinking particles are colonized by unique microbial assemblages with overlap from both rivers and fjord communities, that later constitute sediment communities. Particles indeed act as a direct substrate for bacterial utilization and select particle-attached microbial communities with specific structure and function (Jain et al., 2019), and can cause significant differences between free-living and particle-attached bacteria as has been observed in Kongsfjorden (Jain and Krishnan, 2017).

While we observed strong microbial community reorganization between the early and late melt season in relation to physical and biogeochemical drivers, other potentially relevant explanatory variables, *i.e.* protistan or metazoan grazing, virus lysis, or bacteria-bacteria relationships, were not measured in this study. Hence, environmental compartments play a key role in shaping microbial

communities, but other environmental and biological variables might explain within-compartment variations in community structure and functional characteristics.

4.2 River Runoff Drives Seasonal Changes in Water Column Community Structure

Our study revealed seasonal and spatial shifts in microbial community structure in Isfjorden in relation to physical and geochemical gradients related to freshwater influence.

Stratification and temperature of the water column were the two main physical drivers. The observed spatial gradient in August was related to sampling depth, with a stratification of the microbial communities between SW and AdW. The stratification of freshwater-influenced SW and warm, saline AdW might create separate niches for August communities. Galand et al. (2009) suggest that rare and abundant phylotypes follow different patterns of dispersion, with a more limited dispersal potential for the rare biosphere. Physical boundaries like water masses might thus lead to changes in the repartition of the rare biosphere. A reduction in the rare biosphere in August compared to June could thus be explained by a retention of the rare biosphere in the SW. As shown by McGovern et al. (2020), there was a stronger freshwater retention in the SW and a deeper influx of AdW from the shelf in August, enhancing stratification throughout the fjord. This likely creates separate habitats distinguished by physical boundaries in August, potentially limiting the dispersion of the rare biosphere in the water column, and also explaining the higher evenness and stratification of the communities. Hence, the different patterns observed in June and August could result from differences in the water column structure.

Seasonal changes in community structure were also related to water column temperature. Increased surface water temperature from June to August can partly be explained by expected seasonal increases in temperature, but also by the terrestrial inputs. River water temperatures were higher in August, and the associated high particle load (reduced Secchi depth nearshore) absorbs solar radiation creating a warmer environment locally in rivers and freshwater impacted parts of the fjord (McGovern et al., 2020). Although temperature was a strong driver differentiating microbial community structure between early and late melt season, we suggest it was not the main driver here. Firstly, removing temperature from the constraining variables did not suppress the observed seasonality. Moreover, seasonal variation in functional composition was unrelated to changes in temperature, suggesting that even though microbial metabolic changes can occur with temperature (Kirchman et al., 2005), other environmental variables explained differences between June and August communities and functional diversity.

Indeed, this study also suggests a geochemically driven seasonal shift, separating June from August microbial communities. We identified $\delta^{13}C$ of POC, DOC, chlorophyll *a* and $SUVA_{254}$ as main geochemical drivers for the seasonal shift from June to August. Low $\delta^{13}C$ of POC in June indicates a higher contribution of terrestrial carbon compared to August, but chlorophyll *a*, which mostly represents biomass coming from the water column, was also higher, suggesting that June communities respond to both autochthonous and allochthonous sources of carbon. The degradation of marine and terrestrial sources of carbon during the summer months could explain why DOM was more humic and refractory in August (higher $SUVA_{254}$), and of lower molecular weight (McGovern et al., 2020). Although previously considered refractory to microbial processes, recent studies demonstrated that microbial communities can degrade humic DOM to a greater degree than previously expected (Paulsen et al., 2019). The fact that DOC, $\delta^{13}C$ of POC and $SUVA_{254}$ explained the seasonal gradient suggests that June and August microbial communities partly differed depending on the source of carbon, corroborating previous findings that terrestrial DOM (tDOM) amendments induce changes in microbial

community composition (Mccarren et al., 2010; Sipler et al., 2017; Müller et al., 2018; Balmonte et al., 2019; Cerro-Gálvez et al., 2019).

The spatial gradient in microbial community structure identified in the water column in August, resulting in community stratification and separating inner from outer fjord samples was explained by NO_2^-+NO_3^-, particulate P, particulate N, and POC concentrations, which are strongly influenced by river runoff in this system (McGovern et al., 2020). Together with the fact that runoff influenced variables (temperature, carbon source, nutrients) explain both seasonal and spatial gradients, this suggests that the spatial gradient is also related to the seasonality in terrestrial runoff.

Thus, microbial community structure in the water column was related to physical and biogeochemical gradients. These main underlying gradients are tightly related to terrestrial inputs, which explained both seasonal and spatial gradients in microbial community structure. Hence, we suggest that between early and late melt season, communities undergo changes resulting from the intertwining of the strictly seasonal shift and the stratification of the microbial communities. In the open ocean, seasonal successions in microbial communities are explained by changes in temperature, stratification of the water column, and depletion in macronutrients (phosphorus, combined nitrogen) (Treusch et al., 2009). Here, these gradients are driven by the physical and chemical effects of terrestrial runoff, suggesting their overwhelming effect in shaping coastal microbial communities compared to seasonal succession.

The spatial effects of the terrestrial runoff were also observed in the sediments. Within this compartment, microbial communities showed differences in structure according to their location in the fjord. This suggests that either the bottom water physico-chemical variables induce a selection in the communities that colonize the sediments; or that the communities that colonize the sediments already reflect a spatial gradient before marine and terrestrial particle-attached communities settle out. The two hypotheses are not mutually exclusive, but both are related to the spatial gradient created by environmental variables influenced by the runoff. Although no study of a potential seasonality in the sediment microbial communities could be carried out, the coincidence of the spatial groupings between the water column and the sediments supports the hypothesis that Isfjorden microbial communities are responsive to the environmental gradients related to terrestrial runoff. Previous studies have already correlated changes in the geochemistry and benthic microbial community changes (Bertics and Ziebis, 2009; Abell et al., 2013), but measurements of environmental variables at a scale that allows microniche resolution would be needed to investigate the correlations between specific environmental variables and benthic microbial community structures along the gradient.

4.3 Seasonality and Water Column Stratification Influence Bacterial Functional Repartition

While functional inferences from taxonomy could be misleading and cannot replace whole metagenome profiling (Aßhauer et al., 2015), they can be useful to study potential impacts of the taxonomic differences on the functions, for further in-depth studies (*e.g.* Laroche et al., 2018). The results can aid metagenomics, metabolomics and in situ activity measurements for future studies. We hypothesize that the shift in microbial communities is reflected in their potential functions, similarly affected by seasonal environmental changes.

We observed lower relative abundances of taxa capable of chemotrophic or phototrophic inorganic carbon fixation in August, suggesting that the community is shifting to fewer phototrophic taxa. In both months, taxa with the potential for N_2 fixation, nitrification, and denitrification were found, but taxa with the potential for N_2 fixation were more abundant in June, suggesting that N_2 fixation may be a useful strategy under nitrogen limitation in coastal systems, but may also be related

to the import of cyanobacteria, which are often abundant in Arctic terrestrial systems (Kim et al., 2008; Komárek et al., 2012). In fact, the higher prevalence of potential N_2 fixers and phototrophs points to a higher fraction of cyanobacteria, potentially related to a higher surface runoff with snow melt incorporating cyanobacterial communities, such as soil crusts and cyanobacterial mats (Vonnahme et al., 2016). Both potential sulfur-oxidizers (SOB) and potential anaerobic sulfate-reducers (SRB) have been found in all systems. SRB (*e.g. Thiobacillus sp.*) were most abundant in rivers, but surprisingly also relatively abundant in August fjord water column, potentially related to increased river inputs, considering that sulfate reduction is an anaerobic process. This difference was also mostly driven by AdW, which harbored more of these taxa. Hence, this higher input of taxa most likely associated with terrestrial anoxic habitats, shows that inputs of river taxa seem to increase in August leading to the increased stratification. Besides, potentially anaerobic bacteria may hint to a change in hydrology with groundwater and thawing of deeper soil layers as source, in contrast to snow melt as the main source in June. SRB have been associated with mercury methylation, a process creating methylmercury, a highly toxic compound for higher trophic levels (Ekstrom et al., 2003; Merritt and Amirbahman, 2009; Podar et al., 2015). However, the degree to which the functions linked to anoxic conditions are realized in the studied communities are unclear, given the oxic conditions in the water column and sediments for these shallow coastal waters. The requirement for anoxic environments makes reduces the potential for mercury methylation in the water column, but previously produced methylmercury originating from terrestrial systems may be imported to the fjord together with the SRB. This makes SRB candidates for biomarkers associated with methylmercury. It also suggests that many of the taxa found in the fjord are likely not active, but passively imported via rivers. Similarly to SRB, bacteria potentially capable of other functions related to anoxic environments, such as methane oxidation are more abundant in the brackish surface layer in August.

In summary, August communities are characterized by taxa capable of functions that are either more related to terrestrial systems (N_2 fixation, sulfate reduction, methane oxidation), or simply not likely in oxygenated fjord water (sulfate reduction), showing that bacteria are transported into the fjord together with the freshwater leading to the observed stratification. As these bacteria were not dominant in their abundance, we suggest they can provide insight into the future of this rare biosphere. Besides, these bacteria are not necessarily active, but may be useful as biomarkers for terrestrial inputs, or contaminants (*e.g.* methymercury). Direct activity measurements or metatranscriptomics are necessary to study the actual functions important in the fjord. Besides, these results, although unable to predict exact changes in biogeochemical cycling, support our hypothesis that amplification of seasonal processes and a long lasting melt season due to increasing runoff, while leading to freshening of the SW, stratification of coastal waters, and a higher load of nutrients and particulate matter, could disrupt biogeochemical cycling driven by microorganisms in Arctic coastal waters.

4.4 Microbial Community Composition Responds to Seasonal Changes in Carbon Availability

Given the high load of terrestrial DOC delivered to the fjord during spring freshet, we hypothesized that June waters provide a niche for copiotrophic bacteria that rapidly thrive and deplete water in DOC. The resulting waters, with lower DOC concentrations, and lower light availability due to higher sediment loads, along with nutrient additions from the rivers, could then allow heterotrophs (high nutrient concentrations: particulate matter, combined nitrogen, phosphate, silicate) and oligotrophic marine clades (less available DOC) to outcompete autotrophs.

We identified potential sentinels for the observed changes in DOM source and higher nutrient concentrations. For example, Alphaproteobacteria were abundant in June and August communities, but diverged in their abundant members. In June they were dominated by *Sulfitobacter* sp., a

chemoorganotrophic aerobic and sulfur oxidizing clade (Sorokin, 1995), that has been reported in highly productive environments, mostly following phytoplankton blooms (Lee et al., 2019), and *Octadecabacter* sp., a typical polar marine species (Gosink et al., 1997). *Octadecabacter* sp. is psychrophilic and heterotrophic (Gosink et al., 1997), but lacks the machinery needed to degrade aromatics (Newton et al., 2010), which is likely why it was less abundant in August, when the DOM shifted to a higher aromaticity. In August, Alphaproteobacteria were dominated by the heterotrophic SAR11 Clade Ia. SAR 11 is an abundant clade in oligotrophic ocean systems (Rappé and Giovannoni, 2003; Malmstrom et al., 2007; Straza et al., 2010), and has also been described as abundant in stratified water columns (Field et al., 1997; Morris et al., 2002; Lee et al., 2019), typically in the end of a spring bloom associated bacterial succession (Treusch et al., 2009). In contrast to open ocean systems, where the presence of SAR11 is related to nutrient poor waters in summer stratified periods (Treusch et al., 2009; Bakenhus et al., 2018), fjords receive constant inputs of freshwater, DOM, and nutrients from the nearby terrestrial environment. Nevertheless, we found SAR11 Clade Ia to correlate positively with silicate, temperature and marine organic matter. The highest abundances were also observed later in the season, indicating that SAR11 may benefit from stratified oligotrophic waters, or from the river inputs. Overall, these results could suggest that, in August, a more diverse environment in Arctic coastal waters allows for more diverse and widely spread taxa, either because of stratified, warming waters or DOC-poor but nutrient-enriched waters. However, SAR11 consists of several subgroups that cannot be all related to specific environmental variables.

In August, alongside the reduction in DOC, a population of Cellvibrionales outnumbered the population of Oceanospirillales and Alteromonadales that was abundant in June, mostly with oligotrophic marine clades (OM60, SAR92). SAR92 is common in coastal waters at high (Ghiglione et al., 2012) and low (Teeling et al., 2012) latitudes. This supports the hypothesis that fresher stratified, terrestrial DOM influenced and warmer waters in Arctic coastlines could be a niche for pervasive marine clades that would outcompete Arctic specific marine clades in oligotrophic waters.

Finally, the genus *Polaribacter* was abundant in June and August coastal waters, and was slightly more abundant in June. This is not surprising given that these waters were enriched in DOC, and because *Polaribacter* sp. is known as a copiotrophic species thriving in environments with high concentrations of terrestrial DOM and phytoplankton degradation products (Sipler et al., 2017; Underwood et al., 2019). Its high abundance in both months supports the hypothesis that this genus may be resilient to the ongoing changes and increasing terrestrial inputs, with the ability to utilize a spectrum of terrestrial DOM quality (Sipler et al., 2017). Hence, the changes in microbial community composition observed in between early and late melt season follow the changing environmental conditions related to river runoff.

We suggest that the observed changes in microbial community composition of this abundant biosphere were independent from the transport of allochthonous freshwater-taxa from the rivers. Indeed, we identified taxa of the Verrucomicrobiae class as potential sentinels for August waters, notably of the *Roseibacillus* and *Luteolibacter* spp. Although known to be abundant in soils, they can be found in marine environments. Previous studies found that transport from terrestrial runoff is not the main cause for their abundance in marine coastal environments (Freitas et al., 2012), supporting our hypothesis that the composition shift in August is rather due to the load of nutrients from the rivers and subsequent environmental changes than to the transport of freshwater-taxa. *Roseibacillus* and *Luteolibacter* were observed in another Svalbard fjord (Cardman et al., 2014) in the water column, and reported to colonize, along with taxa from the Bacteroidetes phylum, particulate OM, because of their ability to degrade complex carbohydrates (Jain et al., 2019). Our observation supports the hypothesis that the dominance of these bacterial groups indicates availability of complex organic substrates (Jain

et al., 2019). Other August indicator taxa were not abundant in the rivers, suggesting that their presence was unrelated to a transport of freshwater-taxa. In this study, rivers were not a source of abundant taxa, but this observation does not exclude the possibility that terrestrial inputs might directly affect the rare biosphere, which is known to play an important role in biogeochemical cycles (Galand et al., 2009; Balmonte et al., 2019) and to respond to seasonal changes (Alonso-Sáez et al., 2015).

While assigning specific taxa to environmental characteristics could be misleading, our study suggests a reorganization of microbial communities in response to river runoff, in addition to expected microbial seasonal successions occurring during summer stratified periods — characterized by the prevalence of phototrophs such as the SAR11 clades Ia and Ib, and the SAR86 and SAR116 clades (Carlson et al., 2009; Treusch et al., 2009). Correlations between seasonal indicators and environmental variables of the Isfjorden system corroborated these hypotheses, as some of June water column indicators were related to higher DOC concentrations, a terrestrial signal of the POC and a low aromaticity of the DOM, whereas many August indicators correlated with low DOC concentrations, and a marine signal of the POC. Higher temperature in August coastal waters often correlated with Arctic non-specific taxa, which suggests that warming coastal waters could leave a niche for pervasive marine clades. Some indicators also correlated with concentrations in silicates and ammonia, again suggesting an indirect effect of the terrestrial runoff on shaping microbial communities in the late melt season.

4.5 Outlook and Perspectives

Whereas the relative importance of top-down and bottom-up effects on bacterial communities is still discussed, studies have demonstrated that bottom-up effects might be prevalent in post-bloom conditions in the Arctic, when bacterioplankton communities are stimulated by resource supply (Vaqué et al., 2008). The overwhelming role of seasonality in environmental conditions in the Arctic may also favor bottom-up regulation of microbial communities (Gilbert et al., 2012). In this study, we find an important role of the environmental compartment and the environmental conditions in shaping microbial communities during the melt season. Hence, our study is another illustration of the concept "everything is everywhere – the environment selects" – the 'Baas-Becking' hypothesis (Baas-Becking, 1934). Nevertheless, it also shows that the source of the bacteria and the environmental conditions are not mutually exclusive, as suggested by Langenheder et al. (2006). Consistent with previous findings (*e.g.* Crump et al., 2004), we find an overwhelming role of the environment in shaping microbial community structure. In the Isfjorden system, bacteria may come from the open ocean, the fjord, the rivers, the land, or the glaciers. While the environmental compartment determines the type of assemblage within each compartment, the physical and chemical conditions selected for or against some taxa, ensuring seasonal transition in response to a changing environment. The role of both the source of bacteria and environmental conditions have to be taken into consideration when it comes to determining the drivers of microbial community structures, as discussed in Bertics and Ziebis (2009). Our study thus suggests the presence of both autochthonous and allochthonous taxa within the water column, but a selection against or for them through the environment.

In the Arctic, and in particular in coastal environments, environmental conditions are highly variable both seasonally and over short time scales. However, our data suggest that the amplitude and time-scale of these changes were sufficient to engender detectable changes in the communities. Here within one compartment, with similar sources of bacteria, the environment plays a key role in shaping different microbial communities, and even though very small variability in potential functionality was revealed, these seasonal variations could be enhanced in response to projected changes in Arctic terrestrial and marine systems. We thus suggest that in response to climate change and amplified

seasonal processes, early summer, post-bloom microbial communities might be reorganized towards more copiotrophic taxa that will rapidly deprive coastal waters in organic and bioavailable carbon. Meanwhile, late melt season microbial communities may arise after those very specific taxa. Hence, microbial communities are likely to play a role in the amplification of seasonal processes, and with expected increases in terrestrial runoff in response to climate change, this study provides insight into the potential changes in microbial communities that could occur subsequently to these environmental changes.

As one of the first studies of this scale in an Arctic fjord system, it is a first step in understanding possible future effects of increased terrestrial inputs on microbial communities along Arctic coastlines. Amplicon sequencing provided an in-depth overview of the variants in our system and identified potential sentinels for the observed changes in the water column biogeochemistry between the early and late melt season. However, it is not deprived of biases, from the extraction protocol, the PCR biases engendered by the primers for certain taxa (Wear et al., 2018), the gene copy number, and informatic processing. The abundances provide relative knowledge but absolute quantification with *e.g.* CARD-FISH (Kubota, 2013) would be needed to compare among other studies. Although amplicon sequencing is unreliable for powerful functional analyses, which require targeting key genes using metagenomics or quantitative PCR, it could aid in developing further hypotheses on expected changes in element cycling. To test for taxonomic and functional differences, an integrated "-omics" study would be needed, as well as activity measurements. Here, amplicon sequencing is useful to predict possible seasonal changes, but does not identify sentinels of seasonal changes and terrestrial inputs, or exact perturbations of the biogeochemical cycles. Bioassay experimentations using an integrated approach with amplicon sequencing and DOM characterization with FT-ICR MS (Sipler et al., 2017) would facilitate characterization of specific changes in response to DOM availability. Finally, the "snap-shot" nature of our study design can engender bias because of short-term variability in the oceanographic conditions in stratified Arctic fjords, especially during the summer months (Skarðhamar and Svendsen, 2010). Future studies should include high spatial, seasonal and interannual resolution to provide a strong background for predicting future changes, as well as benthic community analyses and eukaryotic microbial community analyses, to provide an in-depth overview of the system.

5 Data Availability Statement

The sequence data generated for this study can be found in the ENA European Nucleotide Archive # PRJEB40446 (ERR4653578-ERR3672). The environmental data are published by McGovern et al. (2020). The scripts generated and used for this study are available on demand from the corresponding authors.

6 Conflict of Interest

The authors declare that the research was conducted in the absence of any commercial or financial relationships that could be construed as a potential conflict of interest.

7 Author Contributions

AP and MM took the samples in the field and developed the sampling design. LMD, TRV, AP, and KP initiated and designed the 16S barcoding study. LMD did the lab work and the bioinformatic analyses with support from TRV and KP. LMD did the statistical analyses with support from MM and TRV. LMD wrote the manuscript with contributions from all co-authors.

8 Funding

This study was funded in part by ArcticSIZE – a research group on the productive Marginal Ice Zone at UiT (project number 01vm/h15), by the Norwegian research council (TerrACE; project number: 268458), the Fram Center Flagship "Fjord and Coast" grant (FreshFate; project number 132019), and the Svalbard Science Forum's Arctic Field Grant (RIS number: 10914), and in part by a funding to KP from UiT.

9 Acknowledgments

The authors thank Emelie Skogsberg, Hannah Miller, Charlotte Pedersen Ugelstad and Anne Deininger for their help with field sampling. We also thank Julie Bitz-Thorsen and Owen Wangensteen for the help with the library preparation and sequencing. Finally, we thank Christiane Hassenrück for the help with bioinformatics and Jørn Dietze for the help with the Stallo HPC.

10 References

Abell, G. C. J., Ross, D. J., Keane, J. P., Oakes, J. M., Eyre, B. D., Robert, S. S., et al. (2013). Nitrifying and denitrifying microbial communities and their relationship to nutrient fluxes and sediment geochemistry in the Derwent Estuary, Tasmania. *Aquatic Microbial Ecology* 70, 63–75. doi:10.3354/ame01642.

Adakudlu, M., Andresen, J., Bakke, J., Beldring, S., Benestad, R., Bilt, W. van der, et al. (2019). Climate in Svalbard 2100. Available at: https://bora.uib.no/handle/1956/19136 [Accessed June 8, 2020].

Allison, S. D., and Martiny, J. B. H. (2008). Resistance, resilience, and redundancy in microbial communities. *PNAS* 105, 11512–11519. doi:10.1073/pnas.0801925105.

Alonso-Sáez, L., Díaz-Pérez, L., and Morán, X. A. G. (2015). The hidden seasonality of the rare biosphere in coastal marine bacterioplankton. *Environmental Microbiology* 17, 3766–3780. doi:10.1111/1462-2920.12801.

Anderson, M. J. (2017). "Permutational Multivariate Analysis of Variance (PERMANOVA)," in *Wiley StatsRef: Statistics Reference Online* (American Cancer Society), 1–15. doi:10.1002/9781118445112.stat07841.

Arrigo, K. R. (2005). Marine microorganisms and global nutrient cycles. *Nature* 437, 349–355. doi:10.1038/nature04159.

Aßhauer, K. P., Wemheuer, B., Daniel, R., and Meinicke, P. (2015). Tax4Fun: predicting functional profiles from metagenomic 16S rRNA data. *Bioinformatics* 31, 2882–2884. doi:10.1093/bioinformatics/btv287.

Baas-Becking, L. G. M. (1934). *Geobiologie; of inleiding tot de milieukunde*. WP Van Stockum & Zoon NV.

Babraham Bioinformatics FastQC A Quality Control tool for High Throughput Sequence Data. Available at: http://www.bioinformatics.babraham.ac.uk/projects/fastqc/ [Accessed June 14, 2020].

738 Bakenhus, I., Dlugosch, L., Giebel, H.-A., Beardsley, C., Simon, M., and Wietz, M. (2018). Distinct
739 biogeographic patterns of bacterioplankton composition and single-cell activity between the subtropics
740 and Antarctica. *Environmental Microbiology* 20, 3100–3108. doi:10.1111/1462-2920.14383.

741 Balmonte, J. P., Buckley, A., Hoarfrost, A., Ghobrial, S., Ziervogel, K., Teske, A., et al. (2019).
742 Community structural differences shape microbial responses to high molecular weight organic matter.
743 *Environmental Microbiology* 21, 557–571. doi:10.1111/1462-2920.14485.

744 Balser, T. C., and Firestone, M. K. (2005). Linking microbial community composition and soil
745 processes in a California annual grassland and mixed-conifer forest. *Biogeochemistry* 73, 395–415.
746 doi:10.1007/s10533-004-0372-y.

747 Bell, T., Newman, J. A., Silverman, B. W., Turner, S. L., and Lilley, A. K. (2005). The contribution of
748 species richness and composition to bacterial services. *Nature* 436, 1157–1160.
749 doi:10.1038/nature03891.

750 Benjamini, Y., and Hochberg, Y. (1995). Controlling the False Discovery Rate: A Practical and
751 Powerful Approach to Multiple Testing. *Journal of the Royal Statistical Society: Series B*
752 *(Methodological)* 57, 289–300. doi:10.1111/j.2517-6161.1995.tb02031.x.

753 Bertics, V. J., and Ziebis, W. (2009). Biodiversity of benthic microbial communities in bioturbated
754 coastal sediments is controlled by geochemical microniches. *The ISME Journal* 3, 1269–1285.
755 doi:10.1038/ismej.2009.62.

756 Bhatt, U. S., Walker, D. A., Walsh, J. E., Carmack, E. C., Frey, K. E., Meier, W. N., et al. (2014).
757 Implications of Arctic Sea Ice Decline for the Earth System. *Annu. Rev. Environ. Resour.* 39, 57–89.
758 doi:10.1146/annurev-environ-122012-094357.

759 Bianchi, T. S., Arndt, S., Austin, W. E. N., Benn, D. I., Bertrand, S., Cui, X., et al. (2020). Fjords as
760 Aquatic Critical Zones (ACZs). *Earth-Science Reviews* 203, 103145.
761 doi:10.1016/j.earscirev.2020.103145.

762 Bianchi, T. S., Cui, X., Blair, N. E., Burdige, D. J., Eglinton, T. I., and Galy, V. (2018). Centers of
763 organic carbon burial and oxidation at the land-ocean interface. *Organic Geochemistry* 115, 138–155.
764 doi:10.1016/j.orggeochem.2017.09.008.

765 Bintanja, R., and Selten, F. M. (2014). Future increases in Arctic precipitation linked to local
766 evaporation and sea-ice retreat. *Nature* 509, 479–482. doi:10.1038/nature13259.

767 Bintanja, R., van der Wiel, K., van der Linden, E. C., Reusen, J., Bogerd, L., Krikken, F., et al. (2020).
768 Strong future increases in Arctic precipitation variability linked to poleward moisture transport. *Sci*
769 *Adv* 6, eaax6869. doi:10.1126/sciadv.aax6869.

770 Blanchet, F. G., Legendre, P., and Borcard, D. (2008). Forward Selection of Explanatory Variables.
771 *Ecology* 89, 2623–2632. doi:10.1890/07-0986.1.

772 Bolger, A. M., Lohse, M., and Usadel, B. (2014). Trimmomatic: a flexible trimmer for Illumina
773 sequence data. *Bioinformatics* 30, 2114–2120. doi:10.1093/bioinformatics/btu170.

774 Bourgeois, S., Kerhervé, P., Calleja, M. Ll., Many, G., and Morata, N. (2016). Glacier inputs influence

775 organic matter composition and prokaryotic distribution in a high Arctic fjord (Kongsfjorden,
776 Svalbard). *Journal of Marine Systems* 164, 112–127. doi:10.1016/j.jmarsys.2016.08.009.

777 Cáceres, M. D., and Legendre, P. (2009). Associations between species and groups of sites: indices
778 and statistical inference. *Ecology* 90, 3566–3574. doi:10.1890/08-1823.1.

779 Caporaso, J. G., Lauber, C. L., Walters, W. A., Berg-Lyons, D., Huntley, J., Fierer, N., et al. (2012).
780 Ultra-high-throughput microbial community analysis on the Illumina HiSeq and MiSeq platforms.
781 *ISME J* 6, 1621–1624. doi:10.1038/ismej.2012.8.

782 Cardman, Z., Arnosti, C., Durbin, A., Ziervogel, K., Cox, C., Steen, A. D., et al. (2014).
783 Verrucomicrobia Are Candidates for Polysaccharide-Degrading Bacterioplankton in an Arctic Fjord
784 of Svalbard. *Appl Environ Microbiol* 80, 3749–3756. doi:10.1128/AEM.00899-14.

785 Carlson, C. A., Morris, R., Parsons, R., Treusch, A. H., Giovannoni, S. J., and Vergin, K. (2009).
786 Seasonal dynamics of SAR11 populations in the euphotic and mesopelagic zones of the northwestern
787 Sargasso Sea. *ISME J* 3, 283–295. doi:10.1038/ismej.2008.117.

788 Cavicchioli, R., Ripple, W. J., Timmis, K. N., Azam, F., Bakken, L. R., Baylis, M., et al. (2019).
789 Scientists' warning to humanity: microorganisms and climate change. *Nat Rev Microbiol* 17, 569–586.
790 doi:10.1038/s41579-019-0222-5.

791 Cerro-Gálvez, E., Casal, P., Lundin, D., Piña, B., Pinhassi, J., Dachs, J., et al. (2019). Microbial
792 responses to anthropogenic dissolved organic carbon in the Arctic and Antarctic coastal seawaters.
793 *Environ. Microbiol.* 21, 1466–1481. doi:10.1111/1462-2920.14580.

794 Chao, A. (1984). Non-parametric estimation of the classes in a population. *Scandinavian Journal of*
795 *Statistics* 11, 265–270. doi:10.2307/4615964.

796 Chao, A., and Lee, S.-M. (1992). Estimating the Number of Classes via Sample Coverage. *Journal of*
797 *the American Statistical Association* 87, 210–217. doi:10.1080/01621459.1992.10475194.

798 Clarke, K. R. (1993). Non-parametric multivariate analyses of changes in community structure.
799 *Australian Journal of Ecology* 18, 117–143. doi:10.1111/j.1442-9993.1993.tb00438.x.

800 Cram, J. A., Chow, C.-E. T., Sachdeva, R., Needham, D. M., Parada, A. E., Steele, J. A., et al. (2015).
801 Seasonal and interannual variability of the marine bacterioplankton community throughout the water
802 column over ten years. *ISME J* 9, 563–580. doi:10.1038/ismej.2014.153.

803 Crump, B. C., Hopkinson, C. S., Sogin, M. L., and Hobbie, J. E. (2004). Microbial Biogeography along
804 an Estuarine Salinity Gradient: Combined Influences of Bacterial Growth and Residence Time. *Appl.*
805 *Environ. Microbiol.* 70, 1494–1505. doi:10.1128/AEM.70.3.1494-1505.2004.

806 Dufrene, M., and Legendre, P. (1997). Species Assemblages and Indicator Species: The Need for a
807 Flexible Asymmetrical Approach. *Ecological monographs* 67, 345–366. doi:10.2307/2963459.

808 Ekstrom, E. B., Morel, F. M. M., and Benoit, J. M. (2003). Mercury Methylation Independent of the
809 Acetyl-Coenzyme A Pathway in Sulfate-Reducing Bacteria. *Appl. Environ. Microbiol.* 69, 5414–5422.
810 doi:10.1128/AEM.69.9.5414-5422.2003.

811 Falkowski, P. G., Fenchel, T., and Delong, E. F. (2008). The Microbial Engines That Drive Earth's
812 Biogeochemical Cycles. *Science* 320, 1034–1039. doi:10.1126/science.1153213.

813 Fernandes, A. D., Macklaim, J. M., Linn, T. G., Reid, G., and Gloor, G. B. (2013). ANOVA-Like
814 Differential Expression (ALDEx) Analysis for Mixed Population RNA-Seq. *PLoS One* 8.
815 doi:10.1371/journal.pone.0067019.

816 Ferrera, I., Sebastian, M., Acinas, S. G., and Gasol, J. M. (2015). Prokaryotic functional gene diversity
817 in the sunlit ocean: Stumbling in the dark. *Current Opinion in Microbiology* 25, 33–39.
818 doi:10.1016/j.mib.2015.03.007.

819 Field, K. G., Gordon, D., Wright, T., Rappé, M., Urback, E., Vergin, K., et al. (1997). Diversity and
820 depth-specific distribution of SAR11 cluster rRNA genes from marine planktonic bacteria. *Appl.*
821 *Environ. Microbiol.* 63, 63–70.

822 Fortunato, C. S., Eiler, A., Herfort, L., Needoba, J. A., Peterson, T. D., and Crump, B. C. (2013).
823 Determining indicator taxa across spatial and seasonal gradients in the Columbia River coastal margin.
824 *The ISME journal* 7, 1899–1911. doi:10.1038/ismej.2013.79.

825 Freitas, S., Hatosy, S., Fuhrman, J. A., Huse, S. M., Mark Welch, D. B., Sogin, M. L., et al. (2012).
826 Global distribution and diversity of marine Verrucomicrobia. *ISME J* 6, 1499–1505.
827 doi:10.1038/ismej.2012.3.

828 Fritz, M., Vonk, J., and Lantuit, H. (2017). Collapsing Arctic coastlines. *Nature Climate Change* 7, 6–
829 7. doi:10.1038/nclimate3188.

830 Galand, P. E., Casamayor, E. O., Kirchman, D. L., and Lovejoy, C. (2009). Ecology of the rare
831 microbial biosphere of the Arctic Ocean. *Proc. Natl. Acad. Sci. U.S.A.* 106, 22427–22432.
832 doi:10.1073/pnas.0908284106.

833 Garcia-Descalzo, L., Garcia-Lopez, E., Postigo, M., Baquero, F., Alcazar, A., and Cid, C. (2013).
834 Eukaryotic microorganisms in cold environments: examples from Pyrenean glaciers. *Front. Microbiol.*
835 4. doi:10.3389/fmicb.2013.00055.

836 Ghiglione, J.-F., Galand, P. E., Pommier, T., Pedrós-Alió, C., Maas, E. W., Bakker, K., et al. (2012).
837 Pole-to-pole biogeography of surface and deep marine bacterial communities. *PNAS* 109, 17633–
838 17638. doi:10.1073/pnas.1208160109.

839 Gilbert, J. A., Steele, J. A., Caporaso, J. G., Steinbrück, L., Reeder, J., Temperton, B., et al. (2012).
840 Defining seasonal marine microbial community dynamics. *ISME J* 6, 298–308.
841 doi:10.1038/ismej.2011.107.

842 Gobet, A., and Ramette, A. (2011). Taxapooler v1.4. *GitLab*. Available at: https://gitlab.leibniz-
843 zmt.de/chh/bioinf/blob/788dc1a3e2a03ba0e60c120e12663e99599ab3e1/taxa.pooler.1.4.r [Accessed
844 June 8, 2020].

845 Gosink, J. J., Herwig, R. P., and Staley, J. T. (1997). Octadecabacter arcticus gen. nov., sp. nov., and
846 O. antarcticus, sp. nov., Nonpigmented, Psychrophilic Gas Vacuolate Bacteria from Polar Sea Ice and
847 Water. *Systematic and Applied Microbiology* 20, 356–365. doi:10.1016/S0723-2020(97)80003-3.

Harrell Jr, F. E., and others, with contributions from C. D. and many others (2020). *Hmisc: Harrell Miscellaneous*. Available at: https://CRAN.R-project.org/package=Hmisc [Accessed August 8, 2020].

Hassenrück, C. (2019). R and bash scripts for sequence processing of amplicon and shotgun sequencing data. Available at: https://github.com/chassenr/NGS/tree/master/AMPLICON.

Hassenrück, C. (2020). Scripts for the bioinformatic analysis of sequencing data. Available at: https://gitlab.leibniz-zmt.de/chh/bioinf.

Hassett, B. T., Borrego, E. J., Vonnahme, T. R., Rämä, T., Kolomiets, M. V., and Gradinger, R. (2019). Arctic marine fungi: biomass, functional genes, and putative ecological roles. *ISME J* 13, 1484–1496. doi:10.1038/s41396-019-0368-1.

Hauptmann, A. L., Markussen, T. N., Stibal, M., Olsen, N. S., Elberling, B., Bælum, J., et al. (2016). Upstream Freshwater and Terrestrial Sources Are Differentially Reflected in the Bacterial Community Structure along a Small Arctic River and Its Estuary. *Front. Microbiol.* 7. doi:10.3389/fmicb.2016.01474.

Holmes, R. M., Coe, M. T., Fiske, G. J., Gurtovaya, T., McClelland, J. W., Shiklomanov, A. I., et al. (2012). "Climate Change Impacts on the Hydrology and Biogeochemistry of Arctic Rivers," in *Climatic Change and Global Warming of Inland Waters* (John Wiley & Sons, Ltd), 1–26. doi:10.1002/9781118470596.ch1.

Jain, A., and Krishnan, K. P. (2017). Differences in free-living and particle-associated bacterial communities and their spatial variation in Kongsfjorden, Arctic. *J. Basic Microbiol.* 57, 827–838. doi:10.1002/jobm.201700216.

Jain, A., Krishnan, K. P., Singh, A., Thomas, F. A., Begum, N., Tiwari, M., et al. (2019). Biochemical composition of particles shape particle-attached bacterial community structure in a high Arctic fjord. *Ecological Indicators* 102, 581–592. doi:10.1016/j.ecolind.2019.03.015.

Jeffries, M. O., Overland, J. E., and Perovich, D. K. (2013). The Arctic shifts to a new normal. *Physics Today* 66, 35–40. doi:10.1063/PT.3.2147.

Kellogg, C. T. E., McClelland, J. W., Dunton, K. H., and Crump, B. C. (2019). Strong Seasonality in Arctic Estuarine Microbial Food Webs. *Front Microbiol* 10, 2628. doi:10.3389/fmicb.2019.02628.

Kim, B.-R., Shin, J., Guevarra, R., Lee, J. H., Kim, D. W., Seol, K.-H., et al. (2017). Deciphering Diversity Indices for a Better Understanding of Microbial Communities. *J. Microbiol. Biotechnol.* 27, 2089–2093. doi:10.4014/jmb.1709.09027.

Kim, G. H., Klochkova, T. A., and Kang, S. H. (2008). Notes on freshwater and terrestrial algae from Ny-\AAlesund, Svalbard (high Arctic sea area). *Journal of Environmental Biology* 29, 485–491.

Kirchman, D. L., Malmstrom, R. R., and Cottrell, M. T. (2005). Control of bacterial growth by temperature and organic matter in the Western Arctic. *Deep Sea Research Part II: Topical Studies in Oceanography* 52, 3386–3395. doi:10.1016/j.dsr2.2005.09.005.

Kirchman, D. L., Morán, X. A. G., and Ducklow, H. (2009). Microbial growth in the polar oceans — role of temperature and potential impact of climate change. *Nat Rev Microbiol* 7, 451–459.

885 doi:10.1038/nrmicro2115.

886 Komárek, J., Kováčik, L., Elster, J., and Komárek, O. (2012). Cyanobacterial diversity of Petuniabukta,
887 Billefjorden, central Spitsbergen. *Polish Polar Research* 33, 347–368. doi:10.2478/v10183-012-0024-
888 1.

889 Kubota, K. (2013). CARD-FISH for Environmental Microorganisms: Technical Advancement and
890 Future Applications. *Microbes Environ* 28, 3–12. doi:10.1264/jsme2.ME12107.

891 Langenheder, S., Lindström, E. S., and Tranvik, L. J. (2006). Structure and function of bacterial
892 communities emerging from different sources under identical conditions. *Appl. Environ. Microbiol.*
893 72, 212–220. doi:10.1128/AEM.72.1.212-220.2006.

894 Laroche, O., Pochon, X., Tremblay, L. A., Ellis, J. I., Lear, G., and Wood, S. A. (2018). Incorporating
895 molecular-based functional and co-occurrence network properties into benthic marine impact
896 assessments. *FEMS Microbiol Ecol* 94. doi:10.1093/femsec/fiy167.

897 Lee, J., Kang, S.-H., Yang, E. J., Macdonald, A. M., Joo, H. M., Park, J., et al. (2019). Latitudinal
898 Distributions and Controls of Bacterial Community Composition during the Summer of 2017 in
899 Western Arctic Surface Waters (from the Bering Strait to the Chukchi Borderland). *Sci Rep* 9.
900 doi:10.1038/s41598-019-53427-4.

901 Legendre, P., and Gallagher, E. D. (2001). Ecologically meaningful transformations for ordination of
902 species data. *Oecologia* 129, 271–280. doi:10.1007/s004420100716.

903 Louca, S., Parfrey, L. W., and Doebeli, M. (2016). Decoupling function and taxonomy in the global
904 ocean microbiome. *Science* 353, 1272–1277. doi:10.1126/science.aaf4507.

905 Mahé, F., Rognes, T., Quince, C., de Vargas, C., and Dunthorn, M. (2015). Swarmv2: Highly-scalable
906 and high-resolution amplicon clustering. *PeerJ* 3, e1420. doi:10.7717/peerj.1420.

907 Malmstrom, R. R., Straza, T. R. A., Cottrell, M. T., and Kirchman, D. L. (2007). Diversity, abundance,
908 and biomass production of bacterial groups in the western Arctic Ocean. *Aquatic Microbial Ecology*
909 47, 45–55. doi:10.3354/ame047045.

910 Marquardt, M., Vader, A., Stübner, E. I., Reigstad, M., and Gabrielsen, T. M. (2016). Strong
911 Seasonality of Marine Microbial Eukaryotes in a High-Arctic Fjord (Isfjorden, in West Spitsbergen,
912 Norway). *Appl. Environ. Microbiol.* 82, 1868–1880. doi:10.1128/AEM.03208-15.

913 Martin, M. (2011). Cutadapt removes adapter sequences from high-throughput sequencing reads.
914 *EMBnet.journal* 17, 10–12. doi:10.14806/ej.17.1.200.

915 Mccarren, J., Becker, J., Repeta, D., Shi, Y., Young, C., Malmstrom, R., et al. (2010). Microbial
916 community transcriptomes reveal microbes and metabolic pathways associated with dissolved organic
917 matter turnover in the sea. *Proceedings of the National Academy of Sciences of the United States of*
918 *America* 107, 16420–7. doi:10.1073/pnas.1010732107.

919 McClelland, J. W., Holmes, R. M., Dunton, K. H., and Macdonald, R. W. (2012). The Arctic Ocean
920 Estuary. *Estuaries and Coasts* 35, 353–368. doi:10.1007/s12237-010-9357-3.

McGovern, M., Pavlov, A. K., Deininger, A., Granskog, M. A., Leu, E., Søreide, J. E., et al. (2020). Terrestrial Inputs Drive Seasonality in Organic Matter and Nutrient Biogeochemistry in a High Arctic Fjord System (Isfjorden, Svalbard). *Front. Mar. Sci.* 7. doi:10.3389/fmars.2020.542563.

Merritt, K. A., and Amirbahman, A. (2009). Mercury methylation dynamics in estuarine and coastal marine environments — A critical review. *Earth-Science Reviews* 96, 54–66. doi:10.1016/j.earscirev.2009.06.002.

Milner, A. M., Khamis, K., Battin, T. J., Brittain, J. E., Barrand, N. E., Füreder, L., et al. (2017). Glacier shrinkage driving global changes in downstream systems. *Proc. Natl. Acad. Sci. U.S.A.* 114, 9770–9778. doi:10.1073/pnas.1619807114.

Morris, R. M., Rappé, M. S., Connon, S. A., Vergin, K. L., Siebold, W. A., Carlson, C. A., et al. (2002). SAR11 clade dominates ocean surface bacterioplankton communities. *Nature* 420, 806–810. doi:10.1038/nature01240.

Müller, O., Seuthe, L., Bratbak, G., and Paulsen, M. L. (2018). Bacterial Response to Permafrost Derived Organic Matter Input in an Arctic Fjord. doi:10.3389/fmars.2018.00263.

Newton, R. J., Griffin, L. E., Bowles, K. M., Meile, C., Gifford, S., Givens, C. E., et al. (2010). Genome characteristics of a generalist marine bacterial lineage. *ISME J* 4, 784–798. doi:10.1038/ismej.2009.150.

Nilsen, F., Cottier, F., Skogseth, R., and Mattsson, S. (2008). Fjord–shelf exchanges controlled by ice and brine production: The interannual variation of Atlantic Water in Isfjorden, Svalbard. *Continental Shelf Research* 28, 1838–1853. doi:10.1016/j.csr.2008.04.015.

Oksanen, J., Blanchet, F. G., Friendly, M., Kindt, R., Legendre, P., McGlinn, D., et al. (2019). *vegan: Community Ecology Package. R package version 2.5-6.* Available at: https://CRAN.R-project.org/package=vegan.

Osborne, E., Richter-Menge, J., and Jeffries, M. (2018). Arctic Report Card 2018.

Paulsen, M. L., Müller, O., Larsen, A., Møller, E. F., Middelboe, M., Sejr, M. K., et al. (2019). Biological transformation of Arctic dissolved organic matter in a NE Greenland fjord. *Limnology and Oceanography* 64, 1014–1033. doi:10.1002/lno.11091.

Podar, M., Gilmour, C. C., Brandt, C. C., Soren, A., Brown, S. D., Crable, B. R., et al. (2015). Global prevalence and distribution of genes and microorganisms involved in mercury methylation. *Sci Adv* 1, e1500675. doi:10.1126/sciadv.1500675.

Pruesse, E., Peplies, J., and Glöckner, F. O. (2012). SINA: accurate high-throughput multiple sequence alignment of ribosomal RNA genes. *Bioinformatics* 28, 1823–1829. doi:10.1093/bioinformatics/bts252.

Quast, C., Pruesse, E., Yilmaz, P., Gerken, J., Schweer, T., Yarza, P., et al. (2013). The SILVA ribosomal RNA gene database project: improved data processing and web-based tools. *Nucleic Acids Res.* 41, D590-596. doi:10.1093/nar/gks1219.

R Core Team (2020). *R: A language and environment for statistical computing*. R Foundation for

Statistical Computing, Vienna, Austria Available at: https://www.R-project.org/.

Rappé, M. S., and Giovannoni, S. J. (2003). The uncultured microbial majority. *Annu. Rev. Microbiol.* 57, 369–394. doi:10.1146/annurev.micro.57.030502.090759.

Serreze, M. C., and Barry, R. G. (2011). Processes and impacts of Arctic amplification: A research synthesis. *Global and Planetary Change* 77, 85–96. doi:10.1016/j.gloplacha.2011.03.004.

Shade, A., Peter, H., Allison, S. D., Baho, D., Berga, M., Buergmann, H., et al. (2012). Fundamentals of Microbial Community Resistance and Resilience. *Front. Microbiol.* 3. doi:10.3389/fmicb.2012.00417.

Shiklomanov, I. A., and Shiklomanov, A. I. (2003). Climatic Change and the Dynamics of River Runoff into the Arctic Ocean. *Water Resources* 30, 593–601. doi:10.1023/B:WARE.0000007584.73692.ca.

Sipler, R. E., Kellogg, C. T. E., Connelly, T. L., Roberts, Q. N., Yager, P. L., and Bronk, D. A. (2017). Microbial Community Response to Terrestrially Derived Dissolved Organic Matter in the Coastal Arctic. *Front Microbiol* 8, 1018. doi:10.3389/fmicb.2017.01018.

Skarðhamar, J., and Svendsen, H. (2010). Short-term hydrographic variability in a stratified Arctic fjord. *Geological Society, London, Special Publications* 344, 51–60. doi:10.1144/SP344.5.

Skogseth, R., Olivier, L. L. A., Nilsen, F., Falck, E., Fraser, N., Tverberg, V., et al. (2020). Variability and decadal trends in the Isfjorden (Svalbard) ocean climate and circulation – An indicator for climate change in the European Arctic. *Progress in Oceanography* 187, 102394. doi:10.1016/j.pocean.2020.102394.

Sorokin, D. (1995). Sulfitobacter pontiacus gen. nov., sp. nov. - A new heterotrophic bacterium from the Black Sea, specialized on sulfite oxidation. *Microbiology* 64, 295–305.

Straza, T. R. A., Ducklow, H. W., Murray, A. E., and Kirchman, D. L. (2010). Abundance and single-cell activity of bacterial groups in Antarctic coastal waters. *Limnology and Oceanography* 55, 2526–2536. doi:10.4319/lo.2010.55.6.2526.

Teeling, H., Fuchs, B. M., Becher, D., Klockow, C., Gardebrecht, A., Bennke, C. M., et al. (2012). Substrate-Controlled Succession of Marine Bacterioplankton Populations Induced by a Phytoplankton Bloom. *Science* 336, 608–611. doi:10.1126/science.1218344.

Thomas, F. A., Sinha, R. K., and Krishnan, K. P. (2020). Bacterial community structure of a glacio-marine system in the Arctic (Ny-Ålesund, Svalbard). *Science of The Total Environment* 718, 135264. doi:10.1016/j.scitotenv.2019.135264.

Treusch, A. H., Vergin, K. L., Finlay, L. A., Donatz, M. G., Burton, R. M., Carlson, C. A., et al. (2009). Seasonality and vertical structure of microbial communities in an ocean gyre. *ISME J* 3, 1148–1163. doi:10.1038/ismej.2009.60.

Underwood, G. J. C., Michel, C., Meisterhans, G., Niemi, A., Belzile, C., Witt, M., et al. (2019). Organic matter from Arctic sea-ice loss alters bacterial community structure and function. *Nature Clim Change* 9, 170–176. doi:10.1038/s41558-018-0391-7.

995 Vaqué, D., Guadayol, Ò., Peters, F., Felipe, J., Angel-Ripoll, L., Terrado, R., et al. (2008). Seasonal
996 changes in planktonic bacterivory rates under the ice-covered coastal Arctic Ocean. *Limnol. Oceanogr.*
997 53, 2427–2438. doi:10.4319/lo.2008.53.6.2427.

998 Vihtakari, M. (2019). PlotSvalbard: PlotSvalbard - Plot research data from Svalbard on maps.
999 Available at: https://github.com/MikkoVihtakari/PlotSvalbard.

1000 Vincent, W. F. (2010). Microbial ecosystem responses to rapid climate change in the Arctic. *ISME J*
1001 4, 1087–1090. doi:10.1038/ismej.2010.108.

1002 Vonnahme, T. R., Devetter, M., Žárský, J. D., Šabacká, M., and Elster, J. (2016). Controls on
1003 microalgal community structures in cryoconite holes upon high-Arctic glaciers, Svalbard.
1004 *Biogeosciences* 13, 659–674. doi:10.5194/bg-13-659-2016.

1005 Walker, B. H. (1992). Biodiversity and Ecological Redundancy. *Conservation Biology* 6, 18–23.
1006 doi:10.1046/j.1523-1739.1992.610018.x.

1007 Wangensteen, O. S., Palacín, C., Guardiola, M., and Turon, X. (2018). DNA metabarcoding of littoral
1008 hard-bottom communities: high diversity and database gaps revealed by two molecular markers. *PeerJ*
1009 6, e4705. doi:10.7717/peerj.4705.

1010 Wear, E. K., Wilbanks, E. G., Nelson, C. E., and Carlson, C. A. (2018). Primer selection impacts
1011 specific population abundances but not community dynamics in a monthly time-series 16S rRNA gene
1012 amplicon analysis of coastal marine bacterioplankton. *Environmental Microbiology* 20, 2709–2726.
1013 doi:10.1111/1462-2920.14091.

1014 Weishaar, J. L., Aiken, G. R., Bergamaschi, B. A., Fram, M. S., Fujii, R., and Mopper, K. (2003).
1015 Evaluation of Specific Ultraviolet Absorbance as an Indicator of the Chemical Composition and
1016 Reactivity of Dissolved Organic Carbon. *Environ. Sci. Technol.* 37, 4702–4708.
1017 doi:10.1021/es030360x.

1018 Wickham, H. (2016). *ggplot2: Elegant Graphics for Data Analysis*. Springer-Verlag New York
1019 Available at: https://ggplot2.tidyverse.org.

1020 Worden, A. Z., Follows, M. J., Giovannoni, S. J., Wilken, S., Zimmerman, A. E., and Keeling, P. J.
1021 (2015). Rethinking the marine carbon cycle: Factoring in the multifarious lifestyles of microbes.
1022 *Science* 347. doi:10.1126/science.1257594.

1023 Zhang, J., Kobert, K., Flouri, T., and Stamatakis, A. (2014). PEAR: a fast and accurate Illumina Paired-
1024 End reAd mergeR. *Bioinformatics* 30, 614–620. doi:10.1093/bioinformatics/btt593.

1025

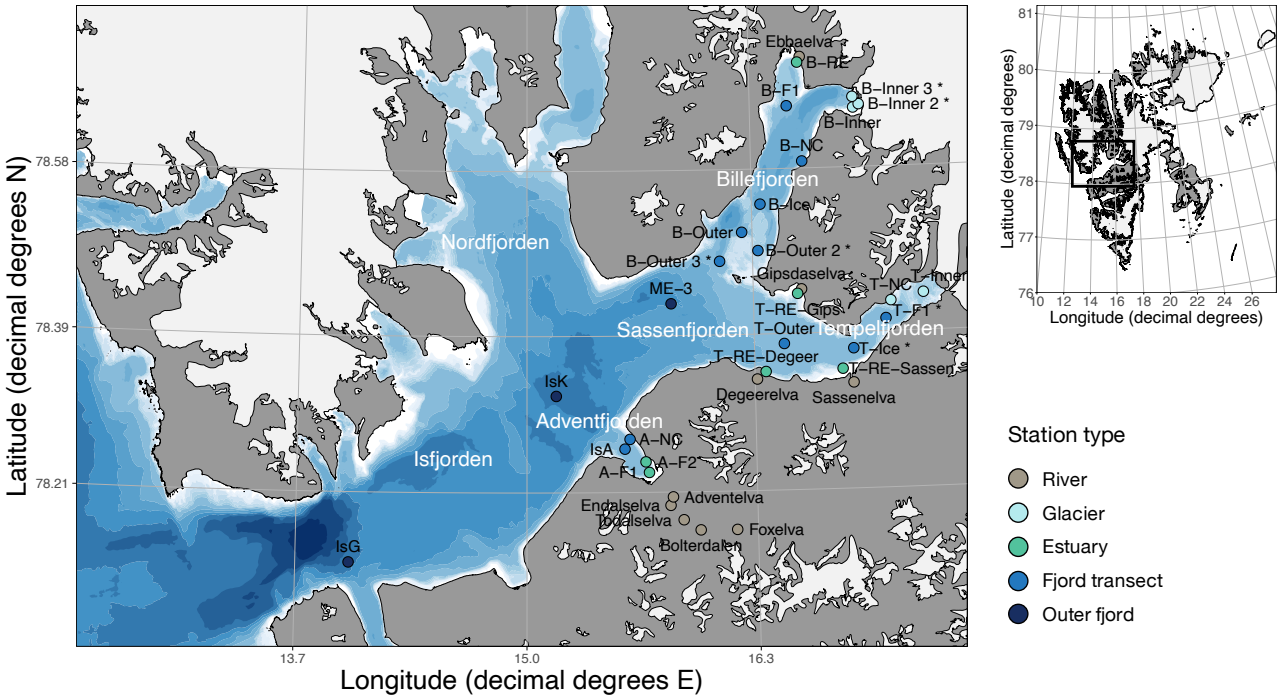

1026

1027 **Figure 1.** Station map of Isfjorden. Samples were collected from two depths in June and August 2018.
1028 Color of the symbols indicates the location in the fjord. An asterisk indicates sites where only sediments
1029 were collected. Other stations include both water column samples and sediment samples. Glaciers are
1030 represented in white. The insert indicates where the fjord is located in Svalbard. Details of the sample
1031 names, coordinates, location and type are available in **Supplementary Table S1**. The map was made
1032 using PlotSvalbard (v0.8.11) in R (Vihtakari, 2019). The Svalbard map originates from the Norwegian
1033 Polar Institute and the bathymetry shapefile from the Norwegian Mapping Authority.

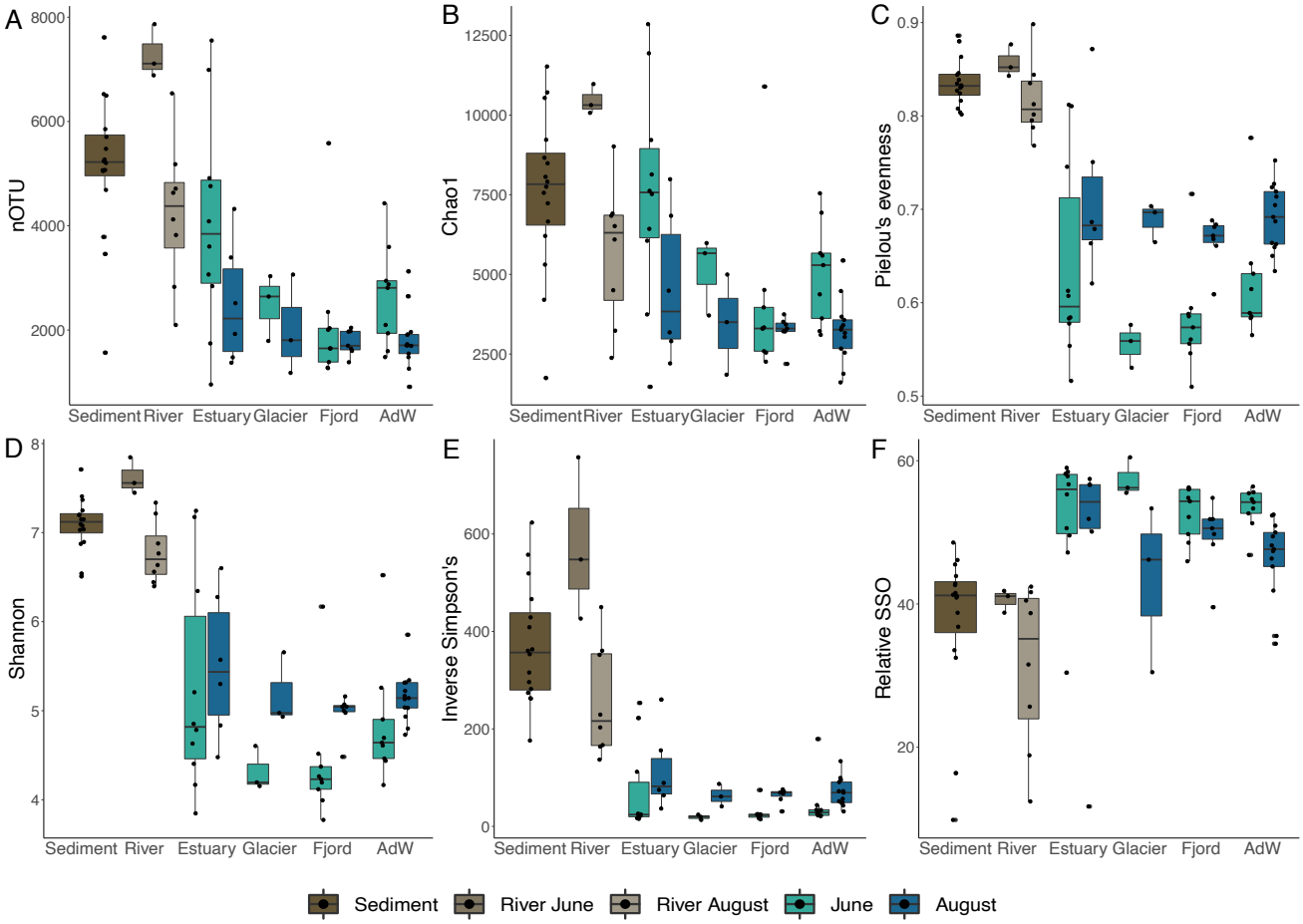

Figure 2. Boxplots showing mean alpha diversity indices according to water type and seasonal groupings. Alpha diversity indices (indicated on the left axis) were calculated as number of OTUs (**A**), Chao1 (**B**) an ACE abundance-based richness, Pielou's index for evenness (**C**), Shannon (**D**) and inverse Simpson (**E**) diversity indices, and rare biosphere as singletons (SSO) (**F**) calculated relative to all groups. ACE (not shown) followed the same trend as Chao1. The bottom axis indicates the habitat (sediment, river) or the water type (water column). Estuary, glacier and fjord refer to the SW sub-groupings. A postHoc Dunn's test was performed on a Kruskal-Wallis test to test for differences between seasonal groups and water type groups (**Supplementary Figure S1 and Supplementary Table S2**)

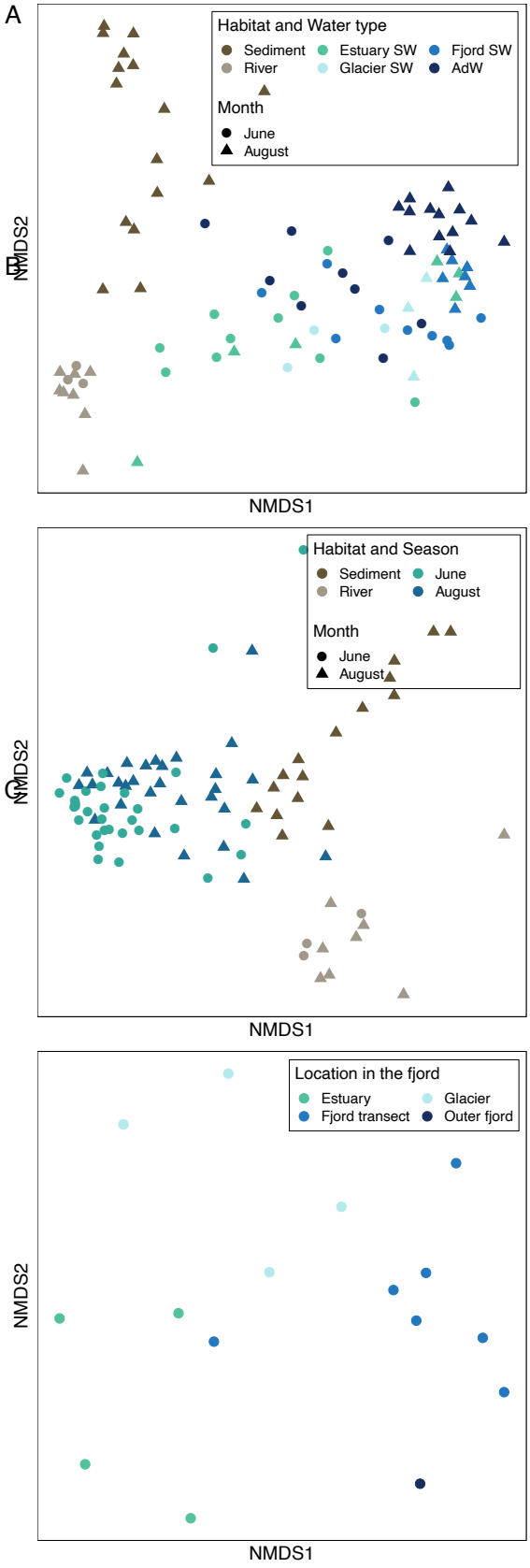

Figure 3. Non-metric multidimensional scaling (NMDS) plots showing bacterial beta diversity based on Bray-Curtis distances of (**A**) microbial community structure in the fjord (stress value = 0.15) (**B**) functional composition based on KEGG metabolic pathways (stress value = 0.06) and (**C**) sediment microbial community structure (stress value = 0.07).

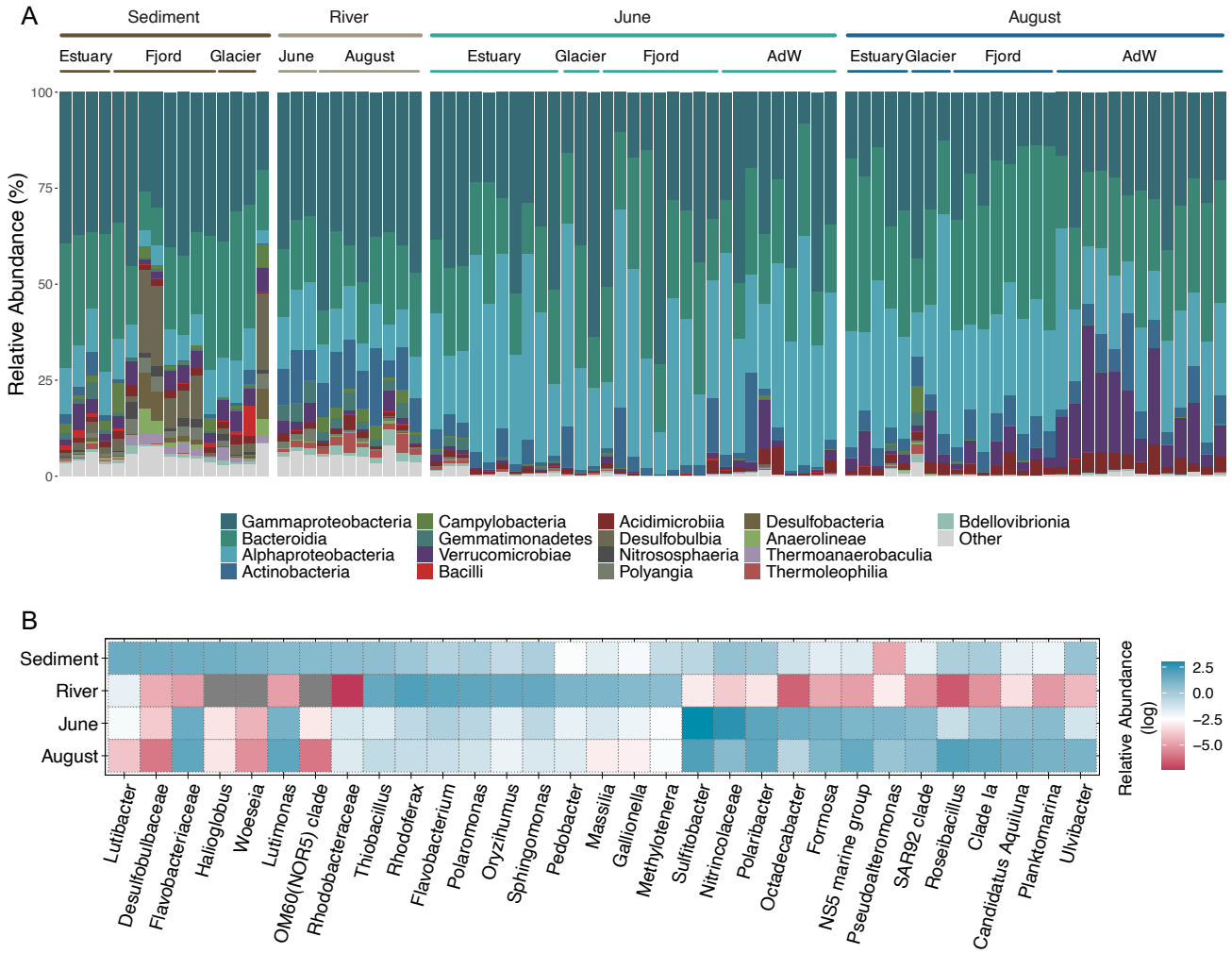

Figure 4. Taxonomic affiliation of the abundant biosphere. (**A**) Bacterial relative abundance of the most abundant classes. Assignment of a sample to a seasonal group is indicated above the plot, and samples are further classified according to their water type for the water column, to their location for the sediments, and to their month for the rivers, indicated above the plot. Estuary, glacier and fjord refer to the SW sub-groupings. Details of the samples corresponding to each bar is available in **Supplementary Figure S2**. (**B**) Heatmap of the mean relative abundances for the most abundant genera for habitat and seasonal groupings. Relative abundances are shown on a log-scale for higher resolution. A high relative abundance is indicated by a blue color, a lower abundance is indicated by a red color, and a grey color indicates the absence of the taxon. Taxa were pooled by seasonal group prior to analysis.

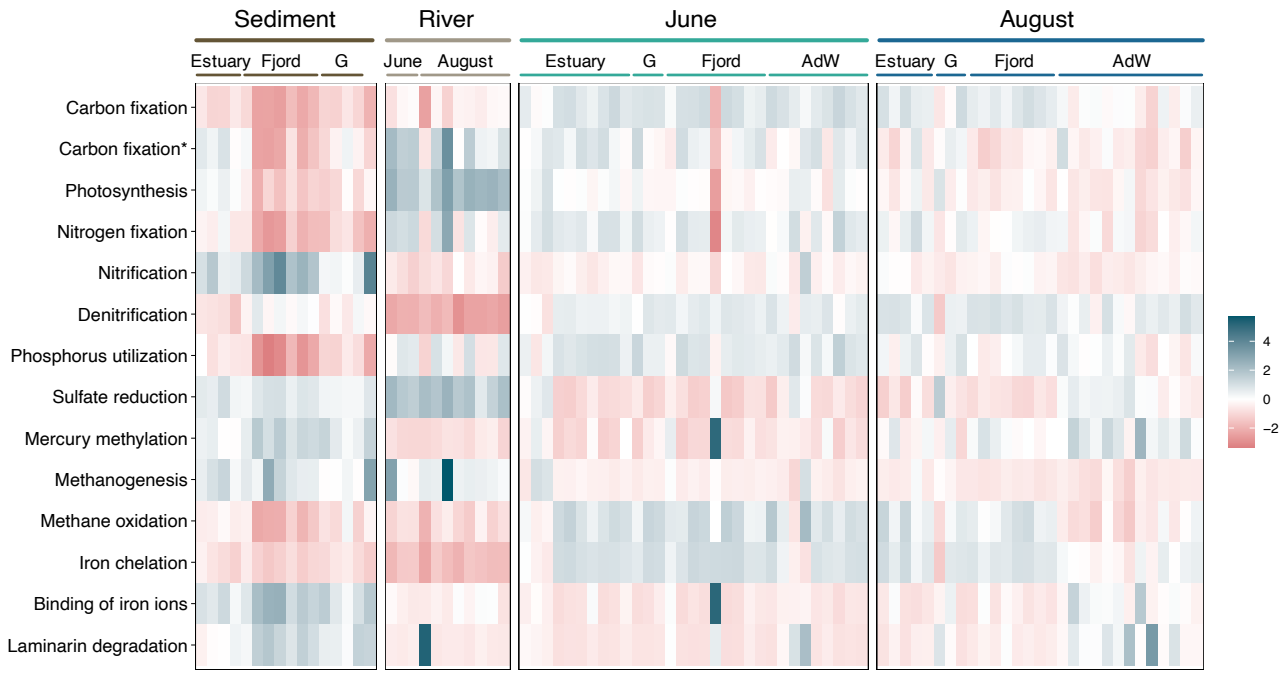

Figure 5. Heatmap of the principal functions in element cycling. Relative abundances were z scaled to be comparable and samples ordered by habitat and seasonal groups. Assignment of a sample to a habitat or seasonal group is indicated above the plot. Water column samples are further classified according to their water type, sediments according to their location in the fjord, and rivers according to sampling month. For the water column, estuary, glacier (G) and fjord refer to the SW sub-groupings. Blue indicates a high abundance, and red a low abundance. Metabolic functions were determined with KEGG Orthologs genes or enzymes related to the KEGG reaction or pathway (**Table 1**). * Carbon fixation in photosynthetic organisms. Details of each sample station and depth are available in **Supplementary Figure S3**.

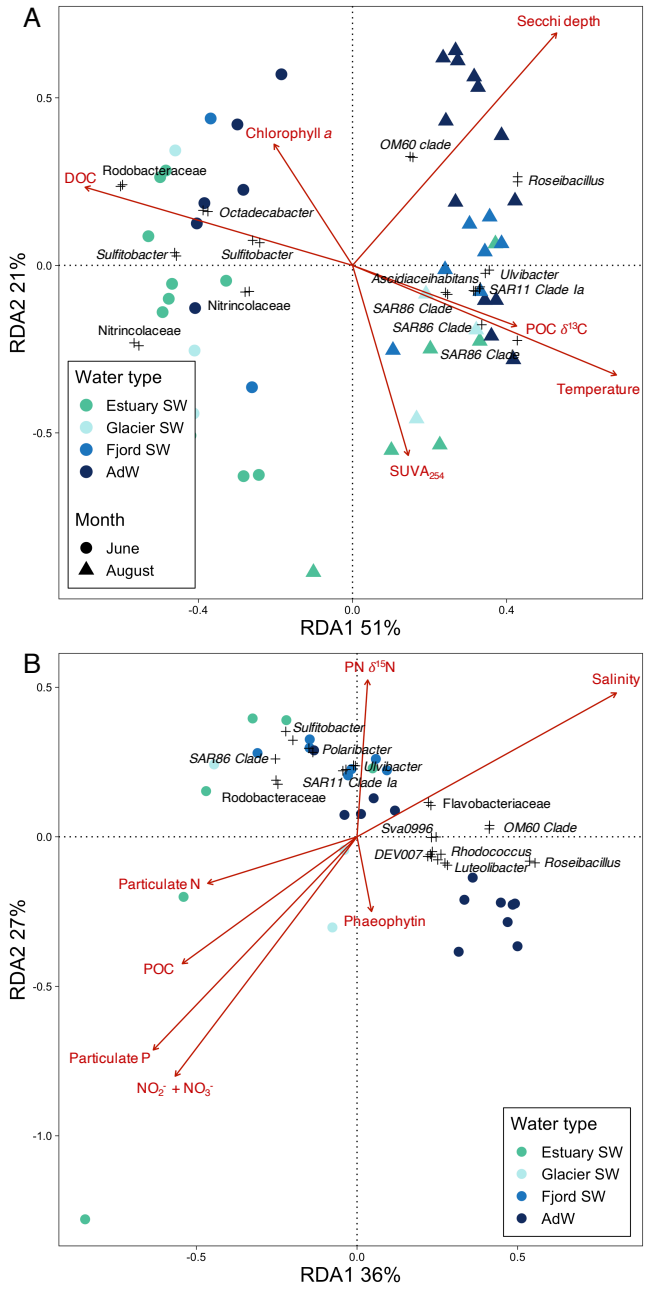

Figure 6. Redundancy analysis (RDA) with environmental drivers of community structure for different sampling groups: (**A**) highlighting seasonal gradients in the fjord, and (**B**) the spatial gradient in the fjord in August. Constraining variables are indicated in red. Only species with an RDA score > 0.08 are represented on (**A**) and with an RDA score > 0.07 on (**B**), and are scaled by 3. Percentages indicate the amount of variation explained by each axis.

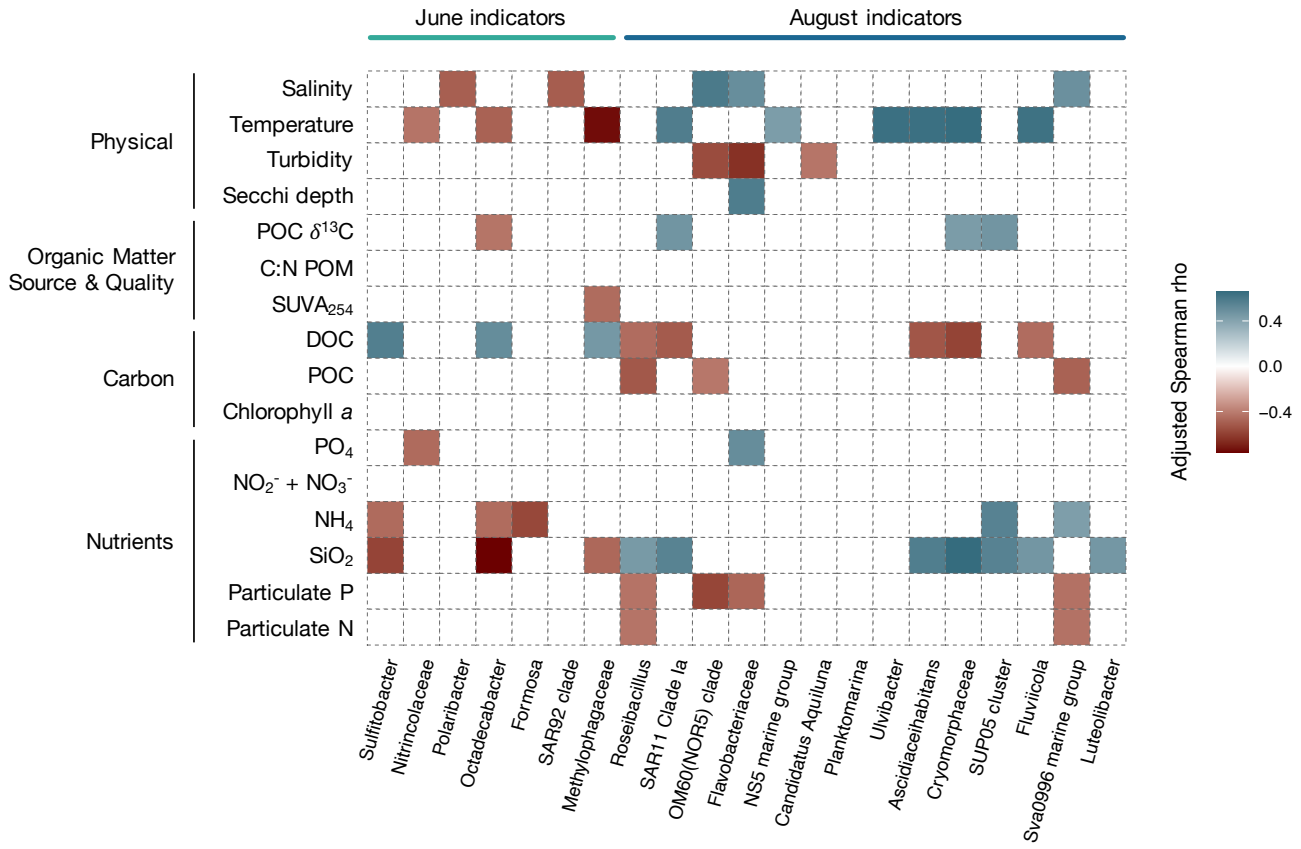

Figure 7. Heatmap of significant Spearman correlations between seasonal indicator taxa and Isfjorden physico-chemical variables. The seasonal group is indicated above the plot and the taxonomic affiliations are indicated beneath the plot. Indicators are ordered by decreasing abundance for each month. Relevant indicators were chosen among highly abundant indicators. For a full overview of indicator species, see **Supplementary Table S3**. Only significant correlations are shown. A blue color indicates a positive correlation and a red color indicates a negative correlation. *p*-values were FDR-corrected with the BH correction.

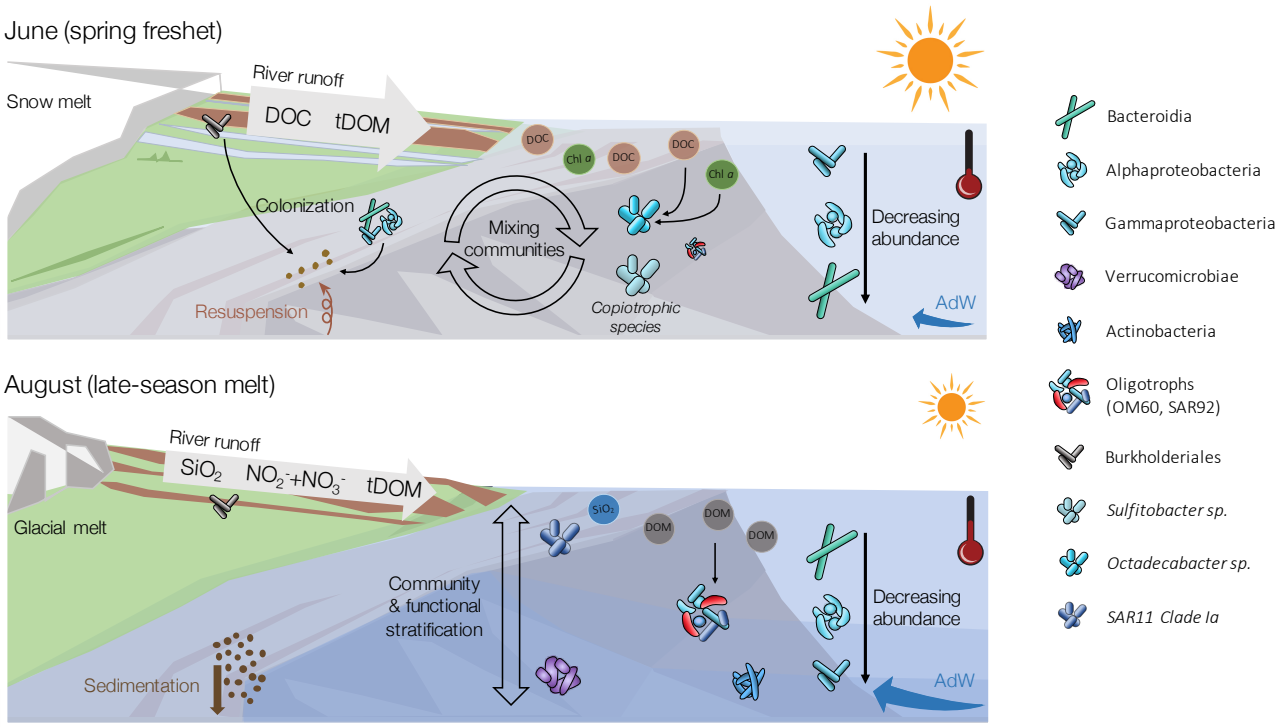

Figure 8. Conceptual figure depicting major seasonal changes in the microbial communities in relation to changing physico-chemical variables between the early and late melt season, in response to terrestrial runoff. This figures includes components of conceptual figures presented by McGovern et al. (2020) and Kellogg et al. (2019), and some symbols are courtesy of the Integration and Application Network (ian.umces.edu/symbols/). For detailed information on biogeochemistry of the system, see McGovern et al. (2020).

Modelling Silicate – Nitrate - Ammonium co-limitation of algal growth and the importance of bacterial remineralisation based on an experimental Arctic coastal spring bloom culture study

Tobias R. Vonnahme[1], Martial Leroy[2], Silke Thoms[3], Dick van Oevelen[4], H. Rodger Harvey[5], Svein Kristiansen[1], Rolf Gradinger[1], Ulrike Dietrich[1], Christoph Voelker[3]

[1] Department of Arctic and Marine Biology, UiT – The Arctic University of Norway, Tromsø, Norway
[2] Université Grenoble Alpes, Grenoble, France
[3] Alfred-Wegener Institute for Polar and Marine Research, Bremerhaven, Germany
[4] Department of Estuarine and Delta Systems, NIOZ Royal Netherlands Institute for Sea Research, and Utrecht University, Texel, Yerseke, Netherlands
[5] Department of Ocean and Earth Sciences, Old Dominion University, Norfolk, USA

Correspondence to: Tobias R. Vonnahme (Tobias.Vonnahme@uit.no) and Christoph Voelker (christoph.voelker@awi.de)

Abstract. Arctic coastal ecosystems are rapidly changing due to climate warming, which makes modelling their productivity crucially important to better understand future changes. System primary production in these systems is highest during the pronounced spring bloom, typically dominated by diatoms. Eventually the spring blooms terminate due to silicon or nitrogen limitation. Bacteria can play an important role for extending bloom duration and total CO_2 fixation through ammonium regeneration. Current ecosystem models often simplify the effects of nutrient co-limitations on algal physiology and cellular ratios and simplify nutrient regeneration, leading to an underestimation of primary production. Detailed biochemistry- and cell-based models can represent these dynamics but are difficult to tune in the environment. We performed a cultivation experiment that showed typical spring bloom dynamics, such as EXT algal growth via bacterial ammonium remineralisation, reduced algal growth and inhibited chlorophyll synthesis under silicate limitation, and gradually reduced nitrogen assimilation and chlorophyll synthesis under nitrogen limitation. We developed a simplified dynamic model to represent these processes. Overall, model complexity (number of parameters) is comparable to the phytoplankton growth and nutrient biogeochemistry formulations in common ecosystem models used in the Arctic while improving the representation of nutrient co-limitation related processes. Such model enhancements that now incorporate increased nutrient inputs and higher mineralization rates in a warmer climate will improve future predictions in this vulnerable system.

1 Introduction

Marine phytoplankton are responsible for half of the CO_2 fixation on Earth (Field et al., 1998; Westberry et al., 2008). In high latitude oceans, diatoms are an important group contributing 20-40% of the global CO_2 fixation (Nelson et al., 1995; Uitz et al., 2010). Marine primary production can be bottom-up limited by light and/or nutrients like nitrogen (N), phosphorous (P), silicon (Si), and iron (Fe) with pronounced geographical and seasonal variations in their availability (Eilertsen et al., 1989; Loebl et al., 2009; Iversen and Seuthe, 2011; Moore et al., 2013). Arctic coasts are one of the fastest changing systems due to climate change and modelling their dynamics is difficult but crucial for predictions of primary production with climate change (e.g. Slagstad et al., 2015; Fritz et al., 2017; Lannuzel et al., 2020). In Arctic coastal ecosystems primary production is typically highest in spring, after winter mixing supplied fresh nutrients, sea ice has melted, and combined with increasing temperatures, caused the formation of a stratified surface layer with sufficient light (Sverdrup, 1953; Eilertsen et al., 1989; Eilertsen and Frantzen, 2007; Iversen and Seuthe, 2011). With increasing temperatures and runoff, stratification in coastal Arctic systems is expected to increase, leading to decreased mixing and nutrient upwelling in autumn and winter and an earlier stratified surface layer in spring (Tremblay and Gagnon, 2009). The spring bloom typically consists of chain-forming diatoms and is terminated by Si or N limitation (Eilertsen et al., 1989; Iversen and Seuthe, 2011). Zooplankton grazing is typically of low importance for terminating blooms (e.g. Saiz et al., 2013), while inorganic nutrients are considered driving bloom termination (Krause et al. 2019, Mills et al. 2018). Heterotrophic bacteria remineralisation of organic matter may supply additional N and Si (Legendre and Rassoulzadegan, 1995; Bidle and Azam, 1999; Johnson et al., 2007). N regeneration has been described as a mostly bacteria-related process (Legendre and Rassoulzadegan, 1995), while Si dissolution is mainly controlled by abiotic dissolution of silica (Bidle and Azam, 1999). Zooplankton may also release some ammonium after feeding on phytoplankton, but we suggest that this process is likely far less important than bacterial regeneration (e.g. Saiz et al., 2013). Previously measured ammonium exrection of Arctic mesozooplankton is typically low compared to bacterial remineralization (Conover and Gustavson, 1999), with the exception for one study in summer in a more open ocean setting (Alcaraz et al., 2010). A warmer climate will increase both bacteria-related remineralisation rates (Legendre and Rassoulzadegan, 1995; Lannuzel et al., 2020) and abiotic silica dissolution (Bidle and Azam, 1999), but the magnitude is not well understood.

Phytoplankton blooms may be dominated by a single or a few algal species, often with a similar physiology during certain phases of the bloom (e.g. Eilertsen et al., 1989; Degerlund and Eilertsen, 2010; Iversen and Seuthe, 2011). Chain-forming centric diatoms, sharing physiological needs and responses to nutrient limitations (e.g. Eilertsen et al., 1989; von Quillfeldt, 2005), typically dominate these blooms. In some Arctic and sub-Arctic areas the Arctic phytoplankton species chosen for this model, *Chaetoceros socialis*, can be dominant during spring blooms (Rey and Skjoldal, 1987; Eilertsen et al., 1989; Booth et al., 2002; Ratkova and Wassmann, 2002; von Quillfeldt, 2005; Degerlund and Eilertsen, 2010). Such spring phytoplankton blooms are accompanied by heterotrophic bacterioplankton blooms also showing typical succession patterns and distinct re-occurring taxa that dominate the community (Teeling et al., 2012; Teeling et al., 2016). The importance of bacterial nutrient recycling for regenerated production has been recognized in several ecosystem models (e.g. van der Meersche et al., 2004; Vichi et al., 2007; Weitz et al., 2015) and algae bioreactor models focussing on nutrient conversions (e.g. Zambrano et al., 2016),

but is typically highly simplified or omitted in more sophisticated dynamic multi-nutrient, quota based models (e.g. Flynn and Fasham, 1997b.; Wassmann et al., 2006; Ross and Geider, 2009). These latter models have been often developed and tuned based on cultivation experiments in which microbial remineralization reactions were assumed to be absent (e.g. Geider et al., 1998; Flynn, 2001) despite the fact that most algae cultures, likely including Geider et al., (1998) and Flynn (2001) are not axenic. Parameters estimated by fitting axenic models on non-axenic experiment may be misleading, mostly by an inflated efficiency of DIN uptake. Additional positive effects of bacteria include vitamin synthesis (Amin et al., 2012), trace metal chelation (Amin et al., 2012), the scavenging of oxidative stressors (Hünken et al., 2008), and exchange of growth factors (Amin et al., 2015). However, especially in the stationary algal growth phase, Christie-Oleza et al. (2017) found that marine phototrophic cyanobacteria cultures are dependent on heterotrophic bacteria contaminants mainly due to their importance in degrading potentially toxic DOM exudates and regenerating ammonium. The current study aimed to bridge the gap between detailed representations of algae physiology and the role of microbial activity in an accurate way while keeping model complexity low.

Most ecosystem models consider only a single limiting nutrient to control primary production after Liebig's Law of the minimum (Wassmann et al., 2006; Vichi et al., 2007). Yet we know that nutrient co-limitation is more complex; for example ammonium and glutamate can inhibit nitrate uptake (Morris, 1974; Dortch, 1990; Flynn et al., 1997), C and N uptake is reduced under Fe limitation, while Si uptake continues, leading to increasing Si:C/N ratios (Werner, 1977; Firme et al., 2003), and the effects on photosynthesis differs for nitrogen and silicon limitations also for different algal groups (Werner, 1977; Flynn, 2003; Hohn et al., 2009). Complex interaction models considering intracellular biochemistry (NH_4-NO_3 co-limitation, Flynn et al., 1997) and cell cycles (Si limitation, Flynn, 2001) can accurately describe these dynamics (Flynn, 2003), but are ultimately too computationally expensive to be integrated and parameterized in large scale ecosystem models. Some models (Hohn et al., 2009, Le Quéré et al., 2016) implemented multinutrient (Hohn et al., 2009) and heterotrophic bacterial dynamics (Le Quéré et al., 2016) in Southern Ocean ecosystem models, but have their limitations in representing bacterial remineralisation (Hohn et al., 2009), or ammonium and silicate co-limitations (Le Quéré et al., 2016). In contrast to Antarctica, DIN is the primary limiting nutrient for phytoplankton growth while iron is not limiting in most Arctic systems (Tremblay and Gagnon, 2009; Moore et al., 2013).

While simple lab experiments cannot represent all nutrient dynamics found in the environment (e.g. N excretion by zooplankton), they can focus on the quantitatively most important dynamics, to facilitate the development of simple, but accurate multinutrient models scalable to larger ecosystem models. The current study investigated the relevance of silicate, ammonium - nitrate co-limitation, bacterial nutrient regeneration and changes in photosynthesis, nitrogen assimilation, and cellular quotas in response to the changing nutrient limitations based on data from a culture based Arctic spring bloom system. The culture consisted of an axenic isolate of *Chaetoceros socialis*, dominating a phytoplankton net haul of a Svalbard fjord, used experimentally either under axenic conditions or after inoculation with bacteria cultures, isolated beforehand from the non-axenic culture. Parametrization and insights from these incubations were then used to develop and parameterize a simple Carbon quota based dynamic model (based on Geider et al., 1998), aiming to keep the number of parameters, and computational costs low to allow its use in larger ecosystem models.

The aims of the study was I) to study the bloom dynamics of simplified Arctic coastal pelagic system in a culture experiment consisting of one Arctic diatom species and co-cultured bacteria, II) to develop a simple dynamic model representing the observed interactions, and III) to discuss the importance of more complex bloom dynamics and their importance for an accurate ecosystem model.

We hypothesize that: I) Bacterial regeneration extends a phytoplankton growth period and gross carbon fixation; II) Diatoms continue photosynthesis under silicate limitation at a reduced rate if DIN is available; III) Cultivation experiments are powerful for understanding the major spring bloom dynamics.

2 Methods

2.1 Cultivation experiment

The most abundant phytoplankton species from a net haul (20µm mesh size) in April 2017 in van Mijenfjorden (Svalbard) *Chaetoceros socialis* was isolated via the dilution isolation method (Andersen et al., 2005) on F/2 medium (Guillard, 1975). Bacteria were isolated on LB-medium (evaluated by Bertani, 2004) Agar plates using the algae culture as inoculum and sequenced at GENEWIZ LLC using the Sanger method and standard 16S rRNA primers targeting the V1-V9 region (Forwards 5'-AGAGTTTGATCCTGGCTCAG -3', Reverse 5'- ACGGCTACCTTGTTACGACTT -3') provided by GENEWIZ LLC for identification via blastn (Altschul et al., 1990). Two strains of *Pseudoalteromonas elyakovii*, a taxon previously isolated from the Arctic (Khudary et al., 2008) and known to degrade algae polysaccharides (Ma et al., 2008) and to excrete polymeric substances (Kim et al., 2016), were successfully isolated and used for the experiments. Before the start of the experiment, all bacteria in the algae culture were killed using a mixture of the antibiotics penicillin and streptomycin. The success was confirmed via incubation of the cultures on LB-Agar plates and bacterial counts after DAPI staining (Porter et al., 1980). The axenic cultures were diluted in fresh F/2 medium lacking nitrate addition (Guillard, 1975) using sterile filtered seawater of Tromsø sound (Norway) as basis. The algae cultures were transferred into 96 200ml sterile cultivation bottles with three replicates for each treatment. Half of the incubations were inoculated with bacteria cultures (BAC+), while the other half was kept axenic (BAC-). The cultures were incubated at 4°C and 100 µE m^{-2} s^{-1} continuous light and mixed 2-3 times a day to keep the algae and bacteria in suspension. We ensured sterile conditions during the experiment by keeping the cultivation bottles closed until sampling. However, endospores may survive the antibiotic treatment in low numbers and start growing especially towards the end of the experiment. Over 16 days three axenic and three BAC+ bottles were sacrificed daily for measurements of chlorophyll a (Chl), particulate organic carbon (POC) and nitrogen (PON), bacterial and algal abundances, nutrients (nitrate, nitrite, ammonium, phosphate, silicate), dissolved organic carbon (DOC), and the maximum quantum yield (QY) of PSII (Fv/Fm) as a measure of healthy photosystems.

Chlorophyll a was extracted from a GF/F (50ml filtered at 200mbar) filter at 4C° for 12-24h in 98% methanol in the dark before measurement in a Turner Trilogy™ Fluorometer (evaluated by Jacobsen and Rai, 1990). POC and PON were measured after filtration onto precombusted (4h at 450°C) GF/F (Whatman) filters (50ml filtered at 200mbar), using a Flash 2000 elemental analyser (Thermo Fisher Scientific, Waltham, MA, USA) and Euro elemental analyser (Hekatech) following the protocol by Pella

and Colombo (1973) after removing inorganic carbon by fuming with saturated HCl in a desiccator. Bacteria were counted after fixation of a water sample for 3-4h with 2% Formaldehyde (final concentration), filtration of 25ml on 0.2µm pore size Polycarbonate filter, washing with filtered Seawater and Ethanol, DAPI staining for 7 minutes after Porter et al. (1980), and embedding in Citifluor-Vectashield (3:1). Bacteria were counted in at least 20 grids under an epifluorescence microscope (Leica DM LB2, Leica Microsystems, Germany) at 10x100 magnification. In the same sample the average diameter of diatom cells at the start and end of the experiment was measured. Algae were counted in 2ml wells under an inverted microscope (Zeiss Primovert, Carl Zeiss AG, Germany) at 20x10 magnification after gentle mixing of the cultivation bottle. Algae cells incorporated in biofilms after day 9 in the BAC+ cultures were counted after sonication in a sonication bath until all cells were in suspension. Nutrient and DOC samples were sterile filtered (0.2µm) and stored at -20°C before measurements. Nutrients were measured in triplicates after using standard colorimetric on a nutrient analyser (QuAAtro 39, SEAL Analytical, Germany) using the protocols No. Q-068-05 Rev. 12 for nitrate (detection limit = 0.02 µmol L^{-1}), No. Q-068-05 Rev. 12 for nitrite (detection limit = 0.02 µmol L^{-1}), No. Q-066-05 Rev. 5 for silicate (detection limit = 0.07 µmol L^{-1}), and No. Q-064-05 Rev. 8 for phosphate (detection limit = 0.01 µmol L^{-1}). The data were analysed using the software AACE. The nutrient analyzer was calibrated with reference seawater (Ocean Scientific International Ltd., United Kingdom). Ammonium was measured manually using the colorimetric method after McCarthy et al., (1977) on a spectrophotometer (Shimadzu UV-1201, detection limit = 0.01 µmol L^{-1}). DOC was measured by high temperature catalytic oxidation (HTCO) using a Shimadzu TOC-5000 total C analyser following methods for seawater samples (Burdige and Homstead, 1994). The photosynthetic quantum yield was determined using an Aquapen PA-C 100 (Photon Systems Instruments, Czech Republic).

Certain factors, such as grazing, settling out of the euphotic zone, and bacterial and algae succession were not included into the experimental set-up to reduce complexity, and focus on nutrient dynamics. Trace metals, phosphate, and Vitamin B12 in coastal systems are assumed to be not limiting in Arctic coastal systems and were supplied in excess to the culture medium. Realistic pre-bloom DOC concentrations were present in the medium as it was prepared with sterilized seawater from the Fjord outside Tromsø before the onset of the spring bloom (March 2018).

All plots were done in R. The f-ratio as indication for the importance of regenerated production (Eppley, 1981) was calculated based on the average PON fixation in the last three days of the experiment (Eq C1). Here, nitrogen assimilation in the BAC- culture was assumed to be based on new (nitrate based) production, while fixation in the BAC+ experiment was assumed to also be based on regenerated (ammonium based) production.

2.2 Model structure

This section outlines the overall model structure followed by a description of the chosen parametrization approach for each relevant process. Details regarding model equations are provided in the Appendix (Table A1) and a schematic representation of the models is given in Figure 1. We used a dynamic cell quota model by Geider et al. (1998) to describe the BAC- experiment (G98). We then extended the G98 model to represent the role of silicate limitation, bacterial regeneration of ammonium, and different

kinetics for ammonium and nitrate uptake (EXT) and fitted it to the BAC+ experiment while retaining the parameter values estimated for G98.

The Geider et al. (1998) model (G98) describes the response of phytoplankton to different nitrogen and light conditions and is based on both intracellular quotas and extracellular dissolved inorganic nitrogen (DIN) concentrations, allowing decoupled C and N growth (Fig. 1). Within this model, light is a control of photosynthesis and chlorophyll synthesis. C:N ratios and DIN concentrations control nitrogen assimilation, which is coupled to chlorophyll synthesis and photosynthesis. Chl:N ratios are controlling photosynthesis and chlorophyll synthesis. G98 has been used in a variety of large scale ecosystem models with some extensions representing the actual conditions in the environment or mesocosms (e.g. Moore et al., 2004; Schartau et al., 2007; Hauck et al., 2013). Photoacclimation dynamics in Geider type models have been evaluated as quick and robust (Flynn et al., 2001), while the N-assimilation component has some shortcomings in regard to ammonium-nitrate interactions. The original model of Geider et al. (1998) for C and N was corrected for minor typographical errors (see Ross and Geider, (2009); Appendix Tables A6 A7).

One aim of the study was to develop a model (EXT) with simplified dynamics of nutrient co-limitation, which is suitable for future implementation in coupled biogeochemistry-circulation models. The EXT model keeps all formulations of the G98 and adds dynamics and interactions of silicate, nitrate and ammonium uptake, carbon and nitrogen excretion and bacterial remineralisation (Fig. 1). The aim of the model was to describe the response in photosynthesis, chlorophyll synthesis and nitrogen assimilation with a minimal number of parameters. Hence, dynamics in silicate cycling and bacterial physiology were highly simplified. The limitations of these simplifications and the potential need for more complex models are discussed later.

Silicate uptake was modelled using Monod kinetics after Spilling et al. (2010). The response of silicate limitation on photosynthesis and chlorophyll synthesis was implemented after findings by Werner (1978), Martin-Jézéquel et al. (2000), and Claquin et al. (2002). Werner (1978) found that silicate limitation can lead to a 80% reduction in photosynthesis and a stop of chlorophyll synthesis in diatoms within a few hours. Hence, we added a parameter for the reduction of photosynthesis under silicate limitation (Si_{PS}) and formulated a stop of chlorophyll synthesis under silicate limitations.

N and Si metabolism have different controls and intracellular dynamics, with N uptake fuelled by photosynthesis (as P_C^{ref} in G98) and Si mainly fuelled by heterotrophic respiration (Martin-Jezequel et al., 2000). In general, we assume that nitrogen metabolism is not directly affected by silicate limitation (Hildebrand 2002, Claquin et al., 2002), but we expect cellular ratios to be affected by reduced photosynthesis and chlorophyll synthesis under Si limitation (Hildebrand, 2002; Gilpin, 2004).

The algal respiration term included both respiration and excretion of dissolved organic nitrogen and carbon as a fraction of the carbon and nitrogen assimilated. For testing the importance of DON excretion we also ran the EXT model without DON excretion (EXT_{-excr}). Dissolved organic nitrogen (DON) was recycled into ammonium via bacterial remineralisation. It was assumed that this process is faster for freshly excreted DON compared to DON already present in the medium. Thus, we implemented a labile (DON_l) and refractory (DON_r) DON pool with different remineralization rates (rem, rem_d). We also assumed that excreted DON and DOC do not coagulate as extracellular polymeric substances (EPS) during the course of the experiment. After Tezuka (1989), net bacterial regeneration of ammonium occurs at DOM C/N mass ratio below 10 and is proportional to bacterial abundances. Higher thresholds up to 29

have been found (e.g. Kirchmann, 2000), but we selected a lower number to stay conservative. DOM C/N ratios are assumed to be proportional to algae C/N ratios (van der Meersche et al., 2004), with algal C/N ratios below 10 representing substrate (DOM) C/N ratios below 10.5. Hence, we assume net bacterial ammonium regeneration to occur at POC/PON ratios below 10, while higher ratios lead to bacteria retaining more N for growth than they release. Bacteria abundance change was estimated using a simple logistic growth curve as a function of DOM since the number of parameters is low (2) and the fit sufficient for the purpose of modelling algae physiology. Michaelis-Menton kinetics based on bacteria growth on DOM with different labilities kinetics could give a more accurate representation of bacterial growth, but would not change the fit of the other model parameters aiming for the best fit of the model output to algal PON, POC, Chl, and DIN. Algal nitrate uptake was modelled after the original model by Geider et al. (1998) and ammonium assimilation was based on the simplified SHANIM model by Flynn and Fasham (1997b), excluding the internal nutrient and glutamine concentrations. Ammonium uptake is preferred over nitrate (lower half saturation constant) and reduces nitrate assimilation if available above a certain threshold concentration of ammonium (Dortch, 1990; Flynn, 1999). Ammonium is the primary product of bacterial regeneration N-compound after remineralization of DON. Nitrification was assumed to be absent, since the bacteria in our experiment are not known to be capable of nitrification.

2.3 Model fitting

The model was written as a function of differential equations in R. All model equations are provided in the Appendix (Table A6) and the R code is available in the supplement. The differential equations were solved using the ode function of the deSolve package (Soetart et al., 2010) with the 2nd-3rd order Runge-Kutta method with automated stepsize control. deSolve is one of the most widely used packages for solving differential equations in R.

Parameter of the G98 model were fitted to the BAC- experiment data and the EXT model was fitted to the BAC+ experiment data. The G98 parameter values were fitted first and retained without changes for the EXT model fitting. The maximum Chl:N ratio (θ^{N}_{max}), minimum and maximum N:C ratios (Q_{min}, Q_{max}), and irradiance (I) are given by the experimental data and needed no further fitting (Table A2). The start values and constraints for the remaining six variables (ζ, R_C, α_{Chl}, n, K_{no3}, P^{C}_{ref}, Table A3) were based on model fits of G98 to other diatom cultures in previous studies (Geider 1998, Ross and Geider 2009). The parameters were first fitted manually via graphical comparisons with the experimental data (POC, PON, Chl, DIN, Fig. 5 and 5), and via minimizing the model cost calculated as the root of the sum of squares normalized by dividing the squares with the variance (RMSE Eq. C2, Stow et al., 2009). The initial manual tuning approach allowed control of the model dynamics, considering potential problems with known limitations of the G98 model (e.g lag phase not modelled; Pahlow, 2005). The manual tuning also allowed obtaining good start parameters for the automated tuning approach and sensitivity/ collinearity analyses, which are sensitive to the start parameters.

After the manual tuning, an automated tuning approach was used to optimize the fits. The automated tuning was done using the FME package (Soetart et al., 2010b), a package commonly used for fitting dynamic and inverse models based on differential equations (i.e. deSolve) to measured data. The automated analyses were based on minimizing the model cost calculated as the sum of squares of the residuals (SSR, Fitted vs measured data). The experimental data were normalized so that all normalized

data were in a similar absolute range of values. This involved increasing Chl and PON values by an order of magnitude while decreasing DIN (NH_4 + NO_3) data by one order of magnitude The data were not weighted, assuming equal data quality and importance. Prior to the automated fitting, parameters were tested for local sensitivity (SensFun) and collinearity, or parameter identifiability (collin; e.g. Wu et al., 2014). sensFun tests for changes in output variables at each time point based on local perturbations of the model parameter. The sensitivity is calculated as L1 and L2 norms (Soetart et al. 2009; Soetart et al., 2010b). The sensFun output is further used as input for the collinearity, or parameter identifiability analyses. Parameters were considered collinear and not identifiable in combination with a collinearity index higher than 20 (Brun et al., 2001). In this case, only the more sensitive parameter was used for further tuning. Eventually, RC, K_{no3}, n, and α_{Chl} were subject to the automated tuning approach using the modfit function, based on minimizing the SSR within the given constraints. Parameters were first fitted using a Pseudorandom search algorithm (Price, 1977) to ensure a global optimum. The resulting parameters were then fine-tuned using the Nelder-Mead algorithm (Soetart et al., 2010b) for finding a local optimum. A model run with the new parameters was then compared to the initial model via graphical comparisons of the model fit to the experimental data, and via the RMSE value.

The parameter values obtained for the G98 fit to the BAC- experiment were retained without changes or further fitting in the EXT model. The additional parameters of the EXT model were then fitted to the BAC+ experimental data (POC, Chl, PON, DIN). The model was only fitted to total DIN, due to the potential uncertainties related to ammonium measurements on frozen samples. In fact, a test run, fitting the EXT model to NO_3 and NH_4 separately lead to a substantially worse overall fit (RMSE=8.79). Otherwise, the data were not weighted. Since the aim of the study was to model the effects of silicate and bacteria on algae growth and not to develop an accurate model for bacteria biomass and silicate concentrations, the parameters μ_{bact}, $bact_{max}$, K_{si}, and V_{max} were only fitted to the corresponding data (Bacteria, Silicate) prior to fitting the other parameters of the Ext model. Bacterial growth parameters (μ_{bact}, $bact_{max}$) were fitted to the bacterial growth curve. Silicate related parameters (K_{si}, V_{max}) were constrained by the study of Werner (1978) and fitted to the measured silicate concentrations. The remaining parameters were subject to the tuning approach described for G98. Ammonium related parameters (K_{nh4}, $nh4_{thres}$) were constrained by measured ammonium concentrations, and constants available for other diatom taxa described by Eppley et al. (1969). Remineralization parameters for excreted (rem) and background (rem_d) DOM were constrained by the data with the limitation of rem > rem_d, assuming that the excreted DOM is more labile. The parameters related to the effect of silicate limitation on photosynthesis and chlorophyll production (s_{min}, Si_{PS}) were constrained by the study of Werner (1978) and fitted as described for G98. None of the added parameters were collinear/ unidentifiable or given by the measured data and thus retained for the automated tuning approach. Eventually, the 15 parameters (Table A3) were fitted against 160 data points (Table A1).

3 Results

3.1 Cultivation experiment

The concentrations of nitrate and silicate declined rapidly over the course of the experiment (Fig. 2). After eight days, silicate decreased to concentrations below 2 µmol L^{-1} a threshold known to limit diatom dominance in phytoplankton (Egge and Aksnes, 1992), while inorganic nitrogen (nitrate, nitrite, and ammonium) became limiting (<0.5 µmol L^{-1} , POC:PON >8-9 DIN:DIP<16) only in the BAC- culture. DIN:DIP ratios far below 16, or DIN concentrations below 2 µmol L^{-1} have been described as indication for DIN limitation (Pedersen and Borum, 1996), as well as POC:PON ratios >9 (Geider and La Roche, 2002). Phosphate was not potentially growth limiting with molar DIN to PO_4 ratios consistently far below 16 (Redfield, 1934) and concentrations around 15 µmol L^{-1}. Typically phosphate concentrations below 0.3 µmol L^{-1} are typically considered limiting (e.g. Haecky and Andersson, 1999). Regeneration of ammonium and phosphate were important after eight days as seen by increasing concentrations of both nutrients and showed higher concentrations in the BAC+ experiments compared to the BAC- cultures (Fig. 2a,b). Ammonium concentrations were consistently higher, and nitrate was removed more slowly in the presence of bacteria, especially during the exponential phase. With the onset of the stationary phase in the BAC+ experiment, PO_4 and NH_4 concentrations doubled within 2 to 4 days and stayed high with variations in phosphate concentrations, while they stayed low in BAC-. With depletion of NO_3 in BAC+, NH_4 concentrations remained high, while PO_4 concentrations dropped.

DOC values were very high from the start (approx. 2-4 mmol L^{-1}) and remained largely constant throughout the experiment (Table A8).

The diatom *Chaetoceros socialis* grew exponentially in both treatments until day 8 before reaching a stationary phase with declining cell numbers (Fig. 3). The growth rate of the BAC- culture (0.36 d^{-1}) was slightly lower than in the treatment with bacteria present (0.42 d^{-1}) during the exponential phase. Algal cellular abundance was higher in the BAC+ cultures. Towards the end of the exponential phase, the diatom started to form noticeable aggregates in cultures with bacteria present, but only to a limited extent in the BAC- cultures. Such aggregate formation with associated EPS production is typical for *C. socialis*. With the onset of the stationary phase in the BAC+ cultures about 30% of the cells formed biofilms on the walls of the cultivation bottles (estimated after sonication treatment). Bacteria (Fig. 3) continued to grow throughout the entire experiment, but growth rates slowed down from 0.9 to 0.6 after day 8. In the BAC- cultures, bacterial numbers increased after 8 days, but abundances remained two order of magnitude below the BAC+ cultures and effectively BAC- over the experimental incubation period. The maximum photosynthetic quantum yield (Fv/Fm) is commonly used as a proxy of photosynthetic fitness (high QY), indicating the efficiency of energy transfer after adsorption in photosystem II. Low values are typically related to stress, including for example nitrogen limitation (Cleveland and Perry, 1987). We found an increase in QY from approx. 0.62 to 0.67 d^{-1} in the exponential phase and a decrease to approx. 0.62 in the BAC+ treatment after 8 days and to approx. 0.58 in the BAC- treatment (Table A8).

During algal exponential growth, POC and PON concentrations followed changes in algal abundances increasing four, seven, and 19-fold respectively, within 8 days (Fig. 3a, 4). Interestingly, with the beginning of the stationary phase, POC and PON continued to increase in the BAC+ cultures, while their concentrations stayed constant (POC), or decreased due to maintenance respiration (PON) in BAC-

cultures. POC and PON concentrations were consistently higher (1.2 times POC, 1.4 times PON) in BAC+ cultures during the exponential phase. gC : gN ratios decreased in both cultures, but increased again after 11 days in the BAC- culture. Chlorophyll *a* concentrations also increased exponentially over the first eight days in both treatments, and thereafter decreased within the stationary phase in the BAC- cultures. In contrast, cell numbers remained nearly constant in the BAC+ cultures, before declining at the last sampling day.

Overall, both experimental cultures showed similar growth dynamics until day 8, with silicate becoming limiting for both treatments and nitrogen only limiting in BAC- cultures. Algal growth with bacteria present was slightly, but consistently higher during this phase. After eight days, algae growth stopped in both treatments, but nitrogen and carbon were continuously assimilated in BAC+ cultures. BAC- cultures started to degrade chlorophyll, while it stayed the same in BAC+ cultures. Algal abundances in the BAC+ treatment at the end of the experiment were ca 30% higher due to biofilm formation, and considerably more carbon (2x total POC, or 10-20% per cell) and nitrogen (3x total PON) per cell had been assimilated, and considerably more chlorophyll (2-3x total chlorophyll) produced at day 16. Cell size differences were not detectable (ca 4µm diameter, Table A8). POC to PON ratios increased after 11 days in BAC- cultures to maximum values of 7.2 and 1.3 mmol L^{-1}, respectively, but showed no change in BAC+ cultures. POC to Chl ratios were comparable in both treatments (Fig. 5). Assuming BAC- N fixation was mostly based on new production (nitrate as N source), while the algal N fixation in bacterial enriched treatments was based on new and regenerated (ammonium as N source) production, two-thirds of the production was based on regenerated production (f-ratio = 0.31).

3.2 Modelling

A comparison of the traditional G98 model with the EXT model allowed an estimate of importance of bacterial DIN regeneration and Si co-limitations for describing the experimental growth dynamics. The EXT model led to a slightly improved fit to the BAC- experiment ($RMSE_{G98}$ = 3.64 $RMSE_{EXT}$ = 3.17, Fig. 5 & 6). The real strength of the EXT model was in representing growth dynamics with bacteria present (Fig. 5 & 6). Here, the fitted lines mostly overlapped with the range of measured data and the RMSE was reduced by 55% from $RMSE_{G98}$ = 4.57 down to $RMSE_{EXT}$ = 2.04.

Both, the G98 and EXT model fits of the BAC- experiment were equally good for POC and PON with a slightly lower modelled growth rate. However, both models had limitations in modelling chlorophyll production, which was underestimated by about 20% at the onset of the stationary phase (Fig. 5c). The degradation of chlorophyll *a* in the stationary phase was not modelled either (Fig. 5c). PON in the BAC+ experiment was poorly modelled without consideration of silicate limitation or regenerated production specifically towards the end of the exponential phase and during the stationary phase. Maximum PON values were about 3 times lower using the G98 model (Fig. B3). In addition, the start of the stationary phase in the BAC+ experiment was estimated 3 days too late via G98, even though modelled DIN was depleted 2 days too soon (Fig. B3). Under BAC- conditions, where silicate limitation does not play a major role the G98 model appears sufficient.

The EXT model allowed representing detailed dynamics in a bacteria influenced system such as the responses to silicate limitation with a decrease in POC production, continued PON production, and the stagnation of Chl synthesis (Fig. 5). Apart from the lag phase, the mass ratios of C:N and C:Chl were

represented accurately (Fig. 5). The model fits without the separate carbon excretion term (x_f) were overall similar to the model with excretion, indicating the importance of the high background dissolved organic matter (DOM) concentrations, rather than excreted DOM for the regenerated ammonium, and the lack of significant aggregation of excreted DOM ($RMSE_{EXT\text{-}exr}$ of 2.32).

Fine scale DIN dynamics caused by ammonium – nitrate interactions were represented well (Fig. 6a). However, at the onset of the stationary phase, ammonium concentrations of the model were one order of magnitude lower than in the experiment, showing a major weakness (Fig. 6c). Increased weighting of ammonium during the model fitting led to a slightly better fit to ammonium, but a substantially worse fit of the model to POC, PON, and Chl ($RMSE_{EXT}$=8.79), indicating that the problem lies with the ammonium data, which were done on filtered and frozen samples. The silicate uptake estimation was highly simplified using simple Monod kinetics, leading to too high modelled values in the stationary phase and a too quick depletion in the start (Fig. 6d). Carbon excretion (x_f) did not have any effect on the model fit to nutrients.

The sensitivity analysis (Fig. B1, Table A1) revealed that the sensitivity of the added parameters in EXT is overall comparable to the sensitivity of the original parameters in G98. The model outputs were most sensitive to P_C^{Ref} (L1=0.8, L2=1.5), which is a parameter in both G98 and EXT. The most sensitive added parameters in EXT were the remineralisation rate of refractory DON (rem_d, L1=0.24), the half saturation constant for ammonium (K_{nh4}, L1=0.1) and the inhibition of photosynthesis under Si limitation (Si_{PS}, L1=0.07), which was comparable to other sensitive parameters of the G98 model (Q_{max}, R_C, α_{Chl}, ζ, n, I, Θ_N^{max}, Table A1). Small perturbations of the parameters only indirectly related to the fitted output variables did not lead to changes in POC, PON, Chl, or DIN.

4 Discussion

The experimental incubations represented typical spring bloom dynamics for coastal Arctic systems, including an initial exponential growth phase terminated by N and Si limitation and the potential for an extended growth period via regenerated production. Our model incorporating these results was able to reflect these dynamics by adding NH_4-NO_3-$Si(OH)_4$ co-limitations and bacterial NH_4 regeneration to the widely used G98 model. In addition, bacteria-algae interactions and DOC and biofilm dynamics were important in the experiment, but those were not crucial for quantitatively modelling algal C:N:Chl quotas. While *C. socialis* may not be the dominant species in all coastal Arctic phytoplankton blooms, we argue that it is representative for chain-forming diatoms typically dominating these systems due to their shared needs and responses to nutrient limitations (e.g. Eilertsen et al., 1989; von Quillfeldt, 2005).

4.1 Silicon-nitrogen regeneration

Spring phytoplankton dynamics in Arctic and sub-Arctic coastal areas is typically characterised by an initial exponential growth of diatoms, followed by peaks of other taxa (like *Phaeocystis pouchetii*) soon after the onset of silicate limitation (Eilertsen et al. 1989). Thus, a shift in species composition for the secondary bloom is linked to silicate limitation prior to final bloom termination caused by inorganic nitrogen limitation. Photosynthesis was reduced by approx. 70% after silicate became limiting, which is comparable to earlier experimental studies (Tezuka, 1989). However, the secondary bloom was extended

in time by bacterial regeneration of ammonium, allowing regenerated production to contribute about 69% of the total production (f-ratio=0.31) even during the diatom dominated scenario in our experimental incubation. With the start of the stationary phase, NH_4 and PO_4 concentrations doubled, presumably due to decreased assimilation by the silicate starved diatoms and increased regeneration by bacteria, supplied with increasing labile DOM (doubled remineralisation rate in EXT) excreted by the stressed algae. After NO_3 depletion at day 15, also PO_4 concentrations drop, indicating a coupling of N:P metabolism and issues with the absolute measured NH_4 values. Excretion of organic phosphate by diatoms is also common in cultures with surplus orthophosphate (Admiraal and Werner, 1983), which can be another explanation of the phosphate peak after silicate becomes limiting. The presence of bacteria and thus regenerated production allowed diatom growth to continue 8 days after silicate became limiting (Figs. 2, 3 & 4), nearly doubling the growth period similar to observations in the field (e.g. Legendre and Rassoulzadegan, 1995; Johnson et al., 2007).

The G98 model has its most severe limitation, the modelling of PON, simply due to the lack of the ammonium pool, supplied via bacterial regeneration. The substantially better fit of PON in the EXT model shows therefore clearly that bacterial remineralisation is crucial to successfully model spring bloom dynamics, especially near bloom termination. Many biogeochemical models used in the Arctic include remineralisation, but rely on fixed or temperature dependent rates and do not consider them bacteria-dependent (MEDUSA, LANL, NEMURONPZD, see Table 1). While this simplification allows modelling regenerated production, using bacteria-independent remineralisation rates does have limitations under spring bloom scenarios, where bacteria biomass can vary over orders of magnitudes (e.g. Sturluson et al., 2008) as also seen in our experimental study.

While we do not expect the f-ratio in our bottle experiment to be directly comparable to open ocean system, which does include a variety of algal taxa beyond *C. socialis*, a comparison can aid to identify limitations in our experiment and model. Regenerated production is significant in polar systems and our estimated experimental f-value of 0.31 is slightly below the average for polar systems (Harrison and Cota, 1990, mean f-ratio=0.54). Nitrification is a process supplying about 50% of the NO_3 used for primary production in the oceans, which may lead to a substantial underestimation of regenerated production (Yool et al., 2007), inflating the f-ratio interpreted as estimate for new production, potentially also in the study by Harrison and Cota (1990). The absence of vertical PON export in our experiment may be another explanation for the above average fraction of regenerated production. In the ocean environment, regenerated production is also affected by vertical export (sedimentation) and grazing which are not represented in the experimental incubations. Via sedimentation, a fraction of the bloom either in the form of direct algal sinking of fecal pellets is typically exported to deeper water layers, reducing the potential for N regeneration within the euphotic zone (e.g. Keck and Wassmann, 1996). Larger zooplankton grazing can lead to increased export of PON via fecal pellet aggregation, or diel vertical migration (Banse, 1995). In contrast, bacterial death by microflagellate grazing and viral lysis may supply additional nutrients, or DON available for N regeneration in the euphotic zone (e.g. Goldman and Caron, 1985), which potentially leads to an overestimation of regenerated production. Hence, ecosystem scale models will need to consider these dynamics regarding bacterial abundances, microbial networks and particle export in addition to bacterial remineralization in order to model realistic ammonium regeneration in the euphotic zone.

Bacteria-mediated silicate regeneration is absent from the modelling approach, as indicated by the identical silicate concentrations in both treatments (Fig. 2). In the environment silicate dissolution is, in fact, mostly described as an abiotic process with temperature as the main control, and a minor contribution by bacterial remineralisation (Bidle and Azam, 1999). Our experiment indicates that silicate dissolution for *Chaetoceros socialis* was negligible at cold temperatures and the time scale of the incubations and typical for bloom durations and residence times of algae cells in the euphotic zone (Eilertsen et al., 1989, Keck and Wassmann, 1996). We conclude that silicate dissolution in coastal Arctic systems happens most likely in the sediment or deeper water layers and is only supplied via mixing in winter. In Antarctica substantial silicate dissolution has been observed but not in the upper 100 m, which has been related to the low temperatures (Nelson and Gordon, 1981) in agreement with our conclusion. Hence, modelling silicate regeneration in the euphotic zone is not necessary in these systems.

4.2 Algal growth response to Si and N limitation

The response of diatoms to Si or N limitation is based on different dynamics and different roles of N and Si in diatom growth. N is needed for proteins and nucleic acids and its uptake is mainly fueled by phototrophic reactions (Martin-Jézéquel et al., 2000). Si is only needed for frustule formation, mostly during a specific time in the cell cycle (G2 and M phase, Hildebrand, 2002) and the assimilation mostly fueled by heterotrophic reactions (Martin-Jézéquel et al., 2000). Once N is limiting, growth rapidly stops (Geider et al. 1998). In the case of Si limitation, however, growth can continue with a slower rate if N is still available (Werner, 1978; Gilpin et al., 2004). Several studies found a reduced growth rate with weaker silicified cell walls (Hildebrand, 2002; Gilpin, 2004), but unaffected nitrogen assimilation under silicate limitation (Hildebrand 2002, Claquin et al., 2002) in accordance with our study. Claquin et al. (2002) found variable Si:C and Si:N ratios and highly silicified cells under nitrogen limitation, indicating uncoupled Si and N:C metabolism.

Nitrogen is a crucial element as part of amino acids and nucleic acids, which are necessary for cell activity and growth. If N becomes limiting major cellular processes are affected and growth or chlorophyll synthesis is not possible. Photosynthesis can continue for a while leading to carbon overconsumption (Schartau et al., 2007), which is well modelled by G98 for both BAC+ and BAC-. A part of the excess carbon can be stored as intracellular reserves, and a part is excreted as DOC, which may aggregate as EPS, contributing to the total POC pool. The excess carbon can potentially be toxic for the algae and excretion and extracellular degradation by bacteria may be crucial for algal survival (Christie-Oleza et al., 2017). Quantitatively, N limitation is well modelled by G98 under BAC- conditions, if only one nitrogen source plays a role. However, under longer nitrogen starvation times or higher light intensities, alternative models that include carbon excretion and aggregation (Schartau et al., 2007) or intracellular storage in reserve pools (Ross & Geider 2009) might be needed. Our growth experiment shows clearly, that C:N ratios are not fixed and variable quotas are needed. Vichi et al. (2007) estimated that Carbon based models may underestimate net primary production (NPP) by 50%, arguing for the importance of quota based models (Fransner et al., 2018). However, most ecosystem scale models are simplified by using fixed C:N ratios (Table 1).

The type of inorganic nitrogen available also affects nitrogen uptake. Due to the metabolic costs related to nitrate reduction to ammonium, ammonium uptake is preferred over nitrate, potentially leaving more

energy for other processes (Lachmann et al., 2019). Ammonium can even inhibit or reduce nitrate uptake over certain concentrations (Morris, 1974). The dynamics are mostly controlled by intracellular processes, such as glutamate feedbacks on nitrogen assimilation, cost for nitrate conversion to ammonium, or lower half saturation constants of ammonium transporters (Flynn et al., 1997). The most accurate representation of these dynamics are given in the ANIM model by Flynn et al. (1997), but the model is too complex for implementations in larger ecosystem models. The number of parameters is difficult to tune with the typically limited availability of measured data and its complexity makes it also computationally costly to scale the models up. Typically, modelling ammonium-nitrate interactions by different half-saturation constants and inhibition of nitrate uptake by ammonium appears sufficient (e.g. BFM, LANL, NEMURO, Table 1) and has been adapted in our model.

Studies on the coupling of silicate limitation on C, N, and Chl show inconclusive patterns, including a complete decoupling (Claquin et al., 2002), a relation of N to Si (Gilpin et al., 2004) and reduction of photosynthesis (Werner, 1978; Gilpin et al., 2004) while no new chlorophyll is produced (Werner, 1978; Gilpin et al., 2004). Cell size is limited by the frustules, but cells may become more nutritious (higher N:C ratio), or simply excrete more DOM, which may aggregate and contribute to the PON and POC pools. A detailed cell-cycle based model has been suggested by Flynn (2001), but the number of parameters (30) make the model too complex for ecosystem scale models. In ecosystem scale models Si limitation is modelled in various simplifications, such as thresholds triggering a stop (MEDUSA), or reduction (e.g. BFM, MEDUSA, SINMOD)of the Si dependent production (Table 1), or Si:N ratio scaled production (NEMURO, Table 1).

Our cultivation study shows i) that a threshold value, leading to a stop or solely Si dependent photosynthesis has its limitations, since DIN controlled photosynthesis continues at lower rates, and ii) that coupling of Si:N:C:Chl is present. We do not expect a direct Si:N coupling, due to different controls of Si and N metabolism (Martin-Jézéquel et al., 2000.), but suggest indirect coupling via reduced photosynthesis. Thus, we modelled the response of diatom growth to silicate limitation by reducing photosynthesis through a parameterized fraction (Si_{PS}) and a stop of chlorophyll synthesis below a certain threshold, based on experimental studies (Werner, 1978; Gilpin et al., 2004) and in accordance to other ecosystem scale approaches. Automated fitting showed the same 80 % reduction of photosynthesis as described by Werner (1978). We suggest that this extension is more accurate than the typical threshold based dynamics, with one limiting nutrient controlling the growth equally for POC and Chl production (e.g. SINMOD by Wassmann et al., 2006; BFM by Vichi et al., 2007), while still keeping the number of parameters low compared to very detailed cell-cycle based models (Flynn, 2001).

4.3 Importance of algae-bacteria interactions and DOC excretion

As described above, N or Si limitation can lead to excretion of DON and DOC, which can aggregate as EPS and be available for bacterial regeneration of ammonium. For including EPS dynamics in the model additional data would be needed. However, the importance of EPS formation is clear in the end of the BAC+ experiment. Firstly, a biofilm was clearly visible containing about 30% of the algae cells. While we would not expect biofilms in the open ocean, aggregation of algae cells, facilitated by EPS is common towards the end of spring blooms, increasing vertical export fluxes (e.g. Thornton, 2002). *Chaetoceros socialis* is in fact a colony forming diatom building EPS-rich aggregates in nature (Booth et al., 2002).

Secondly, POC and PON concentrations increased, while cell numbers and sizes stayed constant, showing that the additional POC and PON was most likely part of an extracellular pool. Silicate limitation could be one trigger for enhanced exudation. Interestingly, algae – bacteria interactions can be species specific with specific organic molecules excreted by the algae to attract specific beneficial bacteria (Mühlenbruch et al., 2018). Thereby bacteria are crucial for recycling ammonium, but also to degrade potentially toxic exudates (Christie-Oleza et al., 2017).

In the BAC- experiment, Carbon excretion after Carbon overconsumption could be expected after Schartau et al. (2007), but no indications, such as biofilm formation, or increased POC per cell were found. This indicates that carbon overconsumption has been of minor importance likely due to the low light levels. An alternative explanation is that bacteria and potentially chemotaxis are important controls on algal carbon excretion (Mühlenbruch et al., 2018). Overall, DOM excretion and EPS dynamics appear to play a minor role in quantitatively modelling C:N:Chl quotas in our experiment, with similar $RMSE_{EXT-excr}$=2.32, $RMSE_{EXT}$=2.04) for a model run with and without the excretion term x_f. However, in systems with less allochthonous DOM inputs, such as open oceans compared to coastal sites, these dynamics will most likely play a more important role.

4.4 Considerations in a changing climate

Due to a rapid changing climate, especially in Arctic coastal systems, the dynamics addressed in this study will change (Tremblay and Gagnon 2009). With warmer temperatures, heterotrophic activities, and thereby bacterial recycling will increase (Kirchman et al., 2009). Our study showed that regenerated production is crucial for an extended spring bloom. Hence, higher heterotrophic activities may lead to extended blooms (increased bacterial regeneration). At the same time, higher temperatures and increased precipitation will lead to stronger and earlier stratified water columns, which will lead to less nutrients reaching the surface by winter mixing, reducing new production (decreased bacterial regeneration)(Tremblay and Gagnon, 2009; Fu et al., 2016). Consequently, the phenology of Arctic coastal primary production in a warmer climate will likely be increasingly driven by bacterial remineralization, showing the necessity to include this process into biogeochemical models. An earlier temperature driven water column stratification will also lead to an earlier bloom however with potentially lower light intensities. In this case, less light is available earlier in the Arctic spring season and carbon overconsumption as described by Schartau et al. (2007) may become less important. An earlier phytoplankton bloom can lead to a mismatch with zooplankton grazers (Durant et al., 2007; Sommer et al., 2007), which could decrease the fecal pellet driven vertical export and thereby increase the residence time of POM in the euphotic zone and the potential for ammonium regeneration, making the incorporation of bacterial recycling into ecosystem models even more imporatant as also evident from our experimental data and model output. In fact, global climate change models agree that vertical carbon export is decreasing overall (Fu et al., 2016). Silicate regeneration is thought to be mostly controlled abiotically by temperature (Bidle and Azam, 1999). Thus, increasing temperature and a stronger stratification will allow recycling of silicate in the euphotic zone before sinking out and thus could cause a shift in the algal succession observed during spring with prolonged contributions of diatoms (Kamatani, 1982). Thus, a temperature dependent silica dissolution may need to be included for models in a substantially warmer climate in further model developments. Increased precipitation will also lead to increased runoff and

allochthonous DOM inputs, increasing the importance of terrestrial DOM degradation and decreasing the relative importance of algal exudate regeneration (Jansson et al., 2008). The high fraction of regenerated production mostly based on allochtonous DOM degradation, the limited role of excreted DOM degradation, low light levels, and the absence of grazing and export fluxes are simplifications of our study, which are, however, expected to be realistic scenarios under climate change. Hence, we suggest that our experiment and model are well suited as a baseline for predictive ecosystem models investigating the impacts of climate change on coastal Arctic spring blooms. However, climate change may lead to shifts in algae communities with non-silicifying algae dominating over diatoms (e.g. Falkowski and Oliver, 2007), reducing the importance of silicate limitation. Thus, conducting similar experiments and modelling exercises with a wider range of algal taxa and different temperature and nutrient regimes is suggested.

Acknowledgements

The project was supported by ArcticSIZE - A research group on the productive Marginal Ice Zone at UiT (project number 01vm/h15). We want to thank Paul Dubourg and Elzbieta Anna Petelenz-Kurdziel for the help with Nutrient and POC/PON analyses. DOC analyses was supported through a Fulbright Distinguished Scholar Award to HRH.

Authors contributions

TRV designed the experiment with contributions by RG and ML. TRV isolated and identified the cultures. ML performed the experiment with contributions of TRV and UD. RH measured DOC and SK measured the Nutrients. The other parameters where measured by ML and TRV. TRV programmed the model with contributions of CV, ST and DvO. TRV wrote the manuscript with contributions from all co-authors.

Data availability

The experimental data are archived at DataverseNO under the doi number doi.org/10.18710/VA4IU9. The Rscripts for the model are available at github under https://github.com/tvonnahm/Dynamic-Algae-Bacteria-model.

Competing interests

The authors declare that they have no conflict of interest.

References

Admiraal, W., and Werner, D.: Utilization of limiting concentrations of ortho-phosphate and production of extracellular organic phosphates in cultures of marine diatoms, Journal of plankton research, 5(4), 495-513, 1983.

Al Khudary, R., Stößer, N. I., Qoura, F., and Antranikian, G.: Pseudoalteromonas arctica sp. nov., an aerobic, psychrotolerant, marine bacterium isolated from Spitzbergen, Int. J. Syst. Evol. Microbiol., 58, 2018-2024, 2008.

Alcaraz, M., Almeda, R., Calbet, A., Saiz, E., Duarte, C. M., Lasternas, S., Agusti, S., Santiago, R., Movilla, J., and Alonso, A.: The role of arctic zooplankton in biogeochemical cycles: respiration and excretion of ammonia and phosphate during summer, Polar Biology, 33(12), 1719-1731, 2010.

Altschul, S. F., Gish, W., Miller, W., Myers, E. W. and Lipman, D. J.: Basic local alignment search tool, J. Mol. Biol., 215, 403-410, 1990.

Amin, S. A., Parker, M. S., and Armbrust, E. V.: Interactions between diatoms and bacteria, Microbiol. Mol. Biol. Rev., 76(3), 667-684, 2012.

Amin, S. A., Hmelo, L. R., Van Tol, H. M., Durham, B. P., Carlson, L. T., Heal, K. R., Morales, R. L., Berthiaume, C. T., Parker, M. S., Djunaedi, B., Ingalls, A. E., Parsek, M. R., Moran, M. A., and Armbrust, E.V.: Interaction and signalling between a cosmopolitan phytoplankton and associated bacteria, Nature, 522, 98-101, 2015.

Andersen, R. A., and Kawachi, M.: Microalgae isolation techniques, in: Algal culturing techniques, edited by: Andersen, R. A., Elsevier, 83, 2005.

Banse, K.: Zooplankton: pivotal role in the control of ocean production: I. Biomass and production, ICES J. Mar. Sci., 52, 265-277, 1995.

Bertani, G.: Lysogeny at mid-twentieth century: P1, P2, and other experimental systems, J. Bacteriol., 186, 595-600, 2004.

Bidle, K. D., and Azam, F.: Accelerated dissolution of diatom silica by marine bacterial assemblages, Nature, 397, 508-512, 1999.

Booth, B. C., Larouche, P., Bélanger, S., Klein, B., Amiel, D., and Mei, Z. P.: Dynamics of Chaetoceros socialis blooms in the North Water, Deep Sea Res. Part II Top. Stud. Oceanogr., 49, 5003-5025, 2002.

Brun, R., Reichert, P. and Kunsch, H. R.: Practical Identifiability Analysis of Large Environmental Simulation Models, Water Resour. Res. 37(4): 1015–1030, 2001.

Burdige, D.J., and Homstead, J.: Fluxes of dissolved organi carbon from Chesapeake Bay sediments. Geochim. Cosmochim. Acta, 58, 3407-3424, 1994.

Christie-Oleza, J. A., Sousoni, D., Lloyd, M., Armengaud, J., and Scanlan, D. J.: Nutrient recycling facilitates long-term stability of marine microbial phototroph–heterotroph interactions, Nat Microbiol, 2, 17100, 2017.

Claquin, P., Martin-Jézéquel, V., Kromkamp, J. C., Veldhuis, M. J. W., and Kraay, G. W.: Uncoupling of Silicon Compared With Carbon and Nitrogen Metabolisms and the Role of the Cell Cycle in Continuous Cultures of Thalassiosira Pseudonana (Bacillariophyceae) Under Light, Nitrogen, and Phosphorus Control, J. Phycol., 38(5), 922–930, 2002.

Cleveland, J. S., & Perry, M. J.: Quantum yield, relative specific absorption and fluorescence in nitrogen-limited Chaetoceros gracilis. Marine Biology, 94(4), 489-497, 1987.

Conover, R. J., and Gustavson, K. R.: Sources of urea in arctic seas: zooplankton metabolism, Marine Ecology Progress Series, 179, 41-54, 1999.
Degerlund, M., and Eilertsen, H. C.: Main species characteristics of phytoplankton spring blooms in NE Atlantic and Arctic waters (68–80 N), Estuaries Coast, 33, 242-269, 2010.
Dortch, Q.: The interaction between ammonium and nitrate uptake in phytoplankton. Mar. Ecol. Prog. Ser., Oldendorf, 61, 183-201, 1990.
Durant, J. M., Hjermann, D. Ø., Ottersen, G., and Stenseth, N. C.: Climate and the match or mismatch between predator requirements and resource availability, Climate research, 33, 271-283, 2007.
Egge, J. K., and Aksnes, D.L.: Silicate as regulating nutrient in phytoplankton competition, Mar. Ecol. Prog. ser., 83, 281-289, 1992.
Eilertsen, H. C., and Frantzen, S.: Phytoplankton from two sub-Arctic fjords in northern Norway 2002–2004: I. Seasonal variations in chlorophyll a and bloom dynamics, Mar. Biol. Res., 3, 319-332, 2007.
Eilertsen, H. C., Taasen, J. P., and WesIawski, J. M.: Phytoplankton studies in the fjords of West Spitzbergen: physical environment and production in spring and summer, J. Plankton Res., 11, 1245-1260, 1989.
Eppley, R. W., Rogers, J. N., and McCarthy, J. J.: Half-saturation constants for uptake of nitrate and ammonium by marine phytoplankton, Limnology and oceanography, 14(6), 912-920, 1969.
Eppley, R. W.: Autotrophic production of particulate matter, Analysis of marine ecosystems/AR Longhurst, 1981.
Falkowski, P. G., and Oliver, M. J.: Mix and match: how climate selects phytoplankton, Nat. Rev. Microbiol., 5, 813-819, 2007.
Field, C. B., Behrenfeld, M. J., Randerson, J. T., and Falkowski, P.: Primary production of the biosphere: integrating terrestrial and oceanic components, Science, 281, 237-240, 1998.
Firme, G. F., Rue, E. L., Weeks, D. A., Bruland, K. W., and Hutchins, D. A.: Spatial and temporal variability in phytoplankton iron limitation along the California coast and consequences for Si, N, and C biogeochemistry, Global Biogeochemical Cycles, 17(1), 2003.
Flynn, K. J.: A mechanistic model for describing dynamic multi-nutrient, light, temperature interactions in phytoplankton, J. Plankton Res., 23, 977-997, 2001.
Flynn, K. J.: Modelling multi-nutrient interactions in phytoplankton; balancing simplicity and realism, Prog. Oceanogr., 56, 249-279, 2003.
Flynn, K. J., and Fasham, M. J.: A short version of the ammonium-nitrate interaction model, J. Plankton Res., 19, 1881-1897, 1997.
Flynn, K. J., Fasham, M. J., and Hipkin, C. R.: Modelling the interactions between ammonium and nitrate uptake in marine phytoplankton. Philosophical Transactions of the Royal Society of London, Series B: Biological Sciences, 352, 1625-1645, 1997.
Flynn, K. J.: Nitrate transport and ammonium-nitrate interactions at high nitrate concentrations and low temperature, Mar. Ecol. Prog. Ser., 187, 283-287, 1999.
Flynn, K. J., Marshall, H., and Geider, R. J.: A comparison of two N-irradiance interaction models of phytoplankton growth, Limnol. Oceanogr., 46, 1794-1802, 2001.
Fransner, F., Gustafsson, E., Tedesco, L., Vichi, M., Hordoir, R., Roquet, F., Spilling, K., Kuznetsov, I., Eilola, K., Mörth, C., Humborg, C., and Nycander, J.; Non-Redfieldian Dynamics Explain Seasonal pCO2 Drawdown in the Gulf of Bothnia, J Geophys Res Oceans, 123, 166-188, 2017.

Fritz, M., Vonk, J. E., and Lantuit, H.: Collapsing arctic coastlines, Nat Clim Chang, 7, 6, 2017.
Fu, W., Randerson, J. T., and Moore, J. K.: Climate change impacts on net primary production (NPP) and export production (EP) regulated by increasing stratification and phytoplankton community structure in the CMIP5 models, Biogeosciences, 13, 5151-5170, 2016.
Geider, R., and La Roche, J.: Redfield revisited: variability of C: N: P in marine microalgae and its biochemical basis, European J. Phycol., 37(1), 1-17, 2002.
Geider, R. J., Maclntyre, H. L., and Kana, T. M.: A dynamic regulatory model of phytoplanktonic acclimation to light, nutrients, and temperature, Limnol. Oceanogr., 43, 679-694, 1998.
Gilpin, L.: The influence of changes in nitrogen: silicon ratios on diatom growth dynamics, J. Sea Res., 51, 21–35, 2004.
Goldman, J. C., and Caron, D. A.: Experimental studies on an omnivorous microflagellate: implications for grazing and nutrient regeneration in the marine microbial food chain, Deep Sea Res A, 32, 899-915, 1985.
Gruber, N., Frenzel, H., Doney, S. C., Marchesiello, P., McWilliams, J. C., Moisan, J. R., Oram, J. J., Plattner, G., and Stolzenbach, K. D.: Eddy-resolving simulation of plankton ecosystem dynamics in the California Current System, Deep Sea Research Part I: Oceanographic Research Papers, 53(9), 1483-1516, 2006.
Guillard, R.L.L.: Culture of phytoplankton for feeding marine invertebrates, in: Culture of Marine Invertebrates Animals, edited by: Smith, W.L., Chanley, M.H., Plenum Press, New York, 29–60, 1975.
Harrison, W. G., and Cota, G. F.: Primary production in polar waters: relation to nutrient availability, Polar Res, 10, 87-104, 1991
Haecky, P., & Andersson, A.: Primary and bacterial production in sea ice in the northern Baltic Sea, Aquat. Microb. Ecol., 20(2), 107-118, 1999.
Hauck, J., Völker, C., Wang, T., Hoppema, M., Losch, M., & Wolf-Gladrow, D. A.: Seasonally different carbon flux changes in the Southern Ocean in response to the southern annular mode, Global Biogeochem Cycles, 27, 1–10, 2013.
Hildebrand, M.: Lack of coupling between silicon and other elemental metabolisms in diatoms, J. Phycol., 38, 841–843, 2002.
Hohn, S.: A model of the carbon:nitrogen:silicon stoichiometry of diatoms based on metabolic processes, PhD thesis, Universit¨at Bremen, Bremen, 43-57, 2009.
Hünken, M., Harder, J., and Kirst, G. O.: Epiphytic bacteria on the Antarctic ice diatom Amphiprora kufferathii Manguin cleave hydrogen peroxide produced during algal photosynthesis, Plant Biology, 10, 519-526, 2008.
Iversen, K. R., and Seuthe, L.: Seasonal microbial processes in a high-latitude fjord (Kongsfjorden, Svalbard): I. Heterotrophic bacteria, picoplankton and nanoflagellates, Polar Biol., 34, 731-749, 2011.
Jacobsen, T. R., and Rai, H.: Comparison of spectrophotometric, fluorometric and high performance liquid chromatography methods for determination of chlorophyll a in aquatic samples: effects of solvent and extraction procedures, Internationale Revue der gesamten Hydrobiologie und Hydrographie, 75, 207-217, 1990.
Jansson, M., Hickler, T., Jonsson, A. and Karlsson, J.: Links between terrestrial primary production and bacterial production and respiration in lakes in a climate gradient in subarctic Sweden, Ecosystems, 11, 367–376, 2008.

Johnson, M., Sanders, R., Avgoustidi, V., Lucas, M., Brown, L., Hansell, D., Moore, M., Gibb, S., Liss, P., and Jickells, T.: Ammonium accumulation during a silicate-limited diatom bloom indicates the potential for ammonia emission events, Mar Chem, 106, 63-75, 2007.

Kamatani, A.: Dissolution rates of silica from diatoms decomposing at various temperatures, Mar. Biol., 68, 91– 96, 1982.

Keck, A., and Wassmann, P.: Temporal and spatial patterns of sedimentation in the subarctic fjord Malangen, northern Norway, Sarsia, 80, 259-276, 1996.

Kim, S. J., Kim, B. G., Park, H. J., and Yim, J. H.: Cryoprotective properties and preliminary characterization of exopolysaccharide (P-Arcpo 15) produced by the Arctic bacterium Pseudoalteromonas elyakovii Arcpo 15, Prep. Biochem. Biotechnol., 46, 261-266, 2016.

Kirchman, D. L.: Uptake and regeneration of inorganic nutrients by marine heterotrophic bacteria, Microbial ecology of the oceans, 2000.

Kirchman, D. L., Morán, X. A. G., and Ducklow, H.: Microbial growth in the polar oceans—role of temperature and potential impact of climate change, Nat. Rev. Microbiol., 7, 451-459, 2009.

Kishi, M. J., Kashiwai, M., Ware, D. M., Megrey, B. A., Eslinger, D. L., Werner, F. E., Noguchi-Aita, M., Azumaya, T., Fujii, M., Hashimoto, S., Huang, D., Iizumi, H., Ishida, Y., Kang, S., Kantakov, G. A., Kim, H., Komatsu, K., Navrotsky, V. V., Smith, S. L., Tadokoro, K., Tsuda, A., Yamamura, O., Yamanaka, Y., Yokouchi, K., Yoshie, N., Zhang, J., Zuenko, Y. I., and Zvalinsky, V. I.: NEMURO – a lower trophic level model for the North Pacific marine ecosystem, Ecol. Model., 202, 12–25, 2007.

Krause, J. W., Schulz, I. K., Rowe, K. A., Dobbins, W., Winding, M. H., Sejr, M. K., Duarte, C. M.,. and Agustí, S.: Silicic acid limitation drives bloom termination and potential carbon sequestration in an Arctic bloom, Sci Rep, 9(1), 1-11, 2019.

Lachmann, S. C., Mettler-Altmann, T., Wacker, A., & Spijkerman, E.: Nitrate or ammonium: Influences of nitrogen source on the physiology of a green alga, Ecology and evolution, 9(3), 1070-1082, 2019.

Lannuzel, D., Tedesco, L., Van Leeuwe, M., Campbell, K., Flores, H., Delille, B., Miller, L., Stefels, J., Assmy, P., Bowman, J., Brown, K., Castellani, G., Chierici, M., Crabeck, O., Damm, E., Else, B., Fransson, A., Fripiat, F., Geilfus, N, Jacques, C., Jones, E., Kaartokallio, H., Kotovitch, M., Meiners, K., Moreau, S., Nomura, D., Peeken, I., Rintala, J., Steiner, N., Tison, J., Vancoppenolle, M., van der Linden, F., Vichi, M., and Wongpan, P.: The future of Arctic sea-ice biogeochemistry and ice-associated ecosystems, Nature Climate Change, 1-10, 2020.

Le Quéré, C., Andrew, R. M., Canadell, J. G., Sitch, S., Korsbakken, J. I., Peters, G. P., Manning, A. C., Boden, T. A., Tans, P. P., Houghton, R. A., Keeling, R. F., Alin, S., Andrews, O. D., Anthoni, P., Barbero, L., Bopp, L., Chevallier, F., Chini, L. P., Ciais, P., Currie, K., Delire, C., Doney, S. C., Friedlingstein, P., Gkritzalis, T., Harris, I., Hauck, J., Haverd, V., Hoppema, M., Klein Goldewijk, K., Jain, A. K., Kato, E., Körtzinger, A., Landschützer, P., Lefèvre, N., Lenton, A., Lienert, S., Lombardozzi, D., Melton, J. R., Metzl, N., Millero, F., Monteiro, P. M. S., Munro, D. R., Nabel, J. E. M. S., Nakaoka, S.-I., O'Brien, K., Olsen, A., Omar, A. M., Ono, T., Pierrot, D., Poulter, B., Rödenbeck, C., Salisbury, J., Schuster, U., Schwinger, J., Séférian, R., Skjelvan, I., Stocker, B. D., Sutton, A. J., Takahashi, T., Tian, H., Tilbrook, B., van der Laan-Luijkx, I. T., van der Werf, G. R., Viovy, N., Walker, A. P., Wiltshire, A. J., and Zaehle, S.: Global carbon budget 2016, Earth Syst Sci Data, 8(2), 605-649, 2016.

Legendre, L., and Rassoulzadegan, F.: Plankton and nutrient dynamics in marine waters, Ophelia, 41, 153-172, 1995

~~Lima, I. D., Olson, D. B., and Doney, S. C.: Intrinsic dynamics and stability properties of size-structured pelagic ecosystem models, J. Plankton Res., 24, 533-556, 2002.~~

Loebl, M., Colijn, F., van Beusekom, J. E., Baretta-Bekker, J. G., Lancelot, C., Philippart, C. J., Rousseau, V., and Wiltshire, K. H.: Recent patterns in potential phytoplankton limitation along the Northwest European continental coast, J. Sea Res., 61, 34-43, 2009.

Ma, L. Y., Chi, Z. M., Li, J., and Wu, L. F.: Overexpression of alginate lyase of Pseudoalteromonas elyakovii in Escherichia coli, purification, and characterization of the recombinant alginate lyase, World J. Microbiol. Biotechnol., 24, 89-96, 2008.

Martin-Jézéquel, V., Hildebrand, M., and Brzezinski, M. A.: Silicon Metabolism in Diatoms : Implications for Growth, J. Phycol., 36, 821–840, 2000.

Mills, M. M., Brown, Z. W., Laney, S. R., Ortega-Retuerta, E., Lowry, K. E., Van Dijken, G. L., and Arrigo, K. R.: Nitrogen limitation of the summer phytoplankton and heterotrophic prokaryote communities in the Chukchi Sea, Frontiers in Marine Science, 5, 362, 2018.

Moore, J. K., Doney, S. C., and Lindsay, K.: Upper ocean ecosystem dynamics and iron cycling in a global three-dimensional model, Global Biogeochem Cycles, 18, 2004.

Moore, C. M., Mills, M. M., Arrigo, K. R., Berman-Frank, I., Bopp,L., Boyd, P. W., Galbraith, E. D., Geider, R. J., Guieu, C., Jac-card, S. L., Jickells, T. D., La Roche, J., Lenton, T. M., Ma-howald, N. M., Maranon, E., Marinov, I., Moore, J. K., Nakat-suka, T., Oschlies, A., Saito, M. A., Thingstad, T. F., Tsuda, A.,and Ulloa, O.: Processes and patterns of oceanic nutrient limitation, Nat Geosci, 6, 701-710, 2013.

Morris, I.: Nitrogen assimilation and protein synthesis, Algal physiology and biochemistry, 10, 1974.

Mühlenbruch, M., Grossart, H. P., Eigemann, F., and Voss, M.: Mini-review: Phytoplankton-derived polysaccharides in the marine environment and their interactions with heterotrophic bacteria, Environ. Microbiol., 20, 2671-2685, 2018.

Nelson, D. M., & Gordon, L. I.: Production and pelagic dissolution of biogenic silica in the Southern Ocean, Geochim. Cosmochim. Acta, 46(4), 491-501, 1982.

Nelson, D. M., Treguer, P., Brzezinski, M. A., Leynaert, A., and Queguiner, B.: Production and dissolution of biogenic silica in the ocean: revised global estimates, comparison with regional data and relationship to biogenic sedimentation, Glob. Biogeochem. Cycles, 9, 359–372, 1995.

Pahlow, M.: Linking chlorophyll-nutrient dynamics to the Redfield N: C ratio with a model of optimal phytoplankton growth, Marine Ecology Progress Series, 287, 33-43, 2005.

Pedersen, M. F., and Borum, J.: Nutrient control of algal growth in estuarine waters. Nutrient limitation and the importance of nitrogen requirements and nitrogen storage among phytoplankton and species of macroalgae, Mar. Ecol. Prog. Ser., 142, 261-272, 1996

Pella E, Colombo B. Study of carbon, hydrogen and nitrogen determination by combustion-gas chromatography, Microchim Acta. 61, 697–719, 1973.

Ratkova, T. N., Wassmann, P.: Seasonal variation and spatial distribution of phyto- and protozooplankton in the central Barents Sea, Journal of Marine Systems, 38, 47-75, 2002.

Redfield, A. C.: On the proportions of organic derivatives in sea water and their relation to the composition of plankton, James Johnstone memorial volume, 176-192, 1934.

Rey, F., Skjoldal, H. R.: Consumption of silicic acid below the euphotic zone by sedimenting diatom blooms in the Barents Sea. MEPS, 36, 307-312, 1987.

Ross, O. N., and Geider, R. J.: New cell-based model of photosynthesis and photo-acclimation: accumulation and mobilisation of energy reserves in phytoplankton, Mar. Ecol. Prog. Ser., 383, 53-71, 2009.

Saiz, E., Calbet, A., Isari, S., Anto, M., Velasco, E. M., Almeda, R., Movilla, J., and Alcaraz, M.: Zooplankton distribution and feeding in the Arctic Ocean during a Phaeocystis pouchetii bloom, Deep Sea Research Part I: Oceanographic Research Papers, 72, 17-33, 2013.

Schartau, M., Engel, A., Schröter, J., Thoms, S., Völker, C., and Wolf-Gladrow, D.: Modelling carbon overconsumption and the formation of extracellular particulate organic carbon, Biogeosciences, 4, 13-67, 2007.

Slagstad, D., Wassmann, P. F., and Ellingsen, I.: Physical constrains and productivity in the future Arctic Ocean, Front Mar Sci, 2, 85, 2015.

Soetaert, K. and Herman, P. M. J.: A Practical Guide to EcologicalModelling -- Using R as a Simulation Platform, Springer, 390 pp, 2009.

Soetaert, K., Petzoldt, T.: Inverse Modelling, Sensitivity and Monte Carlo Analysis in R Using Package FME, J Stat Softw, 33, 1–28, doi: 10.18637/jss.v033.i03, 2010.

Soetaert, K., Petzoldt, T., and Setzer, R. W.: Solving Differential Equations in R: Package deSolve, J Stat Softw, 33, 1548-7660, doi: 10.18637/jss.v033.i09, 2010.

Sommer, U., Aberle, N., Engel, A., Hansen, T., Lengfellner, K., Sandow, M., Wohlers, J., Zollner, E., and Riebesell, U.: An indoor mesocosm system to study the effect of climate change on the late winter and spring succession of Baltic Sea phyto-and zooplankton, Oecologia, 150, 655-667, 2007.

Spilling, K., Tamminen, T., Andersen, T., and Kremp, A.: Nutrient kinetics modeled from time series of substrate depletion and growth: dissolved silicate uptake of Baltic Sea spring diatoms, Marine biology, 157, 427-436, 2010

Stow, C. A., Jolliff, J., McGillicuddy Jr, D. J., Doney, S. C., Allen, J. I., Friedrichs, M. A., Kenneth, A. R., and Wallhead, P.: Skill assessment for coupled biological/physical models of marine systems, J Mar Syst, 76, 4-15, 2009.

Sturluson, M., Nielsen, T. G., and Wassmann, P.: Bacterial abundance, biomass and production during spring blooms in the northern Barents Sea, Deep Sea Res. Part II Top. Stud. Oceanogr., 55, 2186-2198, 2008.

Sverdrup.H.U.: On conditions for the vernal blooming of phytoplankton, Cons. Perm. Int. Expl. Mer, 18, 287-295, 1953.

Teeling, H., Fuchs, B. M., Becher, D., Klockow, C., Gardebrecht, A., Bennke, C. M., Kassabgy, M., Huang, S., Mann, A. J., Waldmann, J., Weber, M., Klindworth, A., Otto, A., Lange,J., Bernhardt, J., Reinsch, C., Hecker, M., Peplies, J., Bockel-mann, F. D., Callies, U., Gerdts, G., Wichels, A., Wiltshire, K.H., Glöckner, F. O., Schweder, T., and Amann, R.: Substrate-controlled succession of marine bacterioplankton populations induced by a phytoplankton bloom, Science, 336, 608-611, 2012.

Teeling, H., Fuchs, B. M., Bennke, C. M., Krueger, K., Chafee, M., Kappelmann, L., Reintjes, G., Waldmann, J., Quast, C., Glöckner, F. O., Lucas, J., Wichels, A., Gerdts, G., Wiltshire, K. H., Amann, R.: Recurring patterns in bacterioplankton dynamics during coastal spring algae blooms, Elife, 5, 2016.

Tezuka, Y.: The C: N: P ratio of phytoplankton determines the relative amounts of dissolved inorganic nitrogen and phosphorus released during aerobic decomposition, Hydrobiologia, 173, 55-62, 1989.

Thornton, D.: Diatom aggregation in the sea: mechanisms and ecological implications, European Journal of Phycology, 37(2), 149-161, 2002.

Tremblay, J. É., and Gagnon, J.: The effects of irradiance and nutrient supply on the productivity of Arctic waters: a perspective on climate change, in: Influence of climate change on the changing arctic and sub-arctic conditions, edited by: Nihoul, J. C., J., Kostianoy, A. G., Springer, Dordrecht, 73-93, 2009.

Uitz, J., Claustre, H., Gentili, B., and Stramski, D.: Phytoplankton class-specific primary production in the world's oceans: Seasonal and interannual variability from satellite observations, Global Biogeochem Cycles, 24, 2010.

Van den Meersche, K., Middelburg, J. J., Soetaert, K., Van Rijswijk, P., Boschker, H. T., and Heip, C. H.: Carbon-nitrogen coupling and algal-bacterial interactions during an experimental bloom: Modeling a 13C tracer experiment, Limnol. Oceanogr., 49, 862-878, 2004.

Vichi, M., Pinardi, N., and Masina, S.: A generalized model of pelagic biogeochemistry for the global ocean ecosystem. Part I: Theory, J Mar Syst, 64, 89-109, 2007.

von Quillfeldt, C. H.: Common Diatom Species in Arctic Spring Blooms: Their Distribution and Abundance, Botanica Marina, 43(6), 499-516, https://doi.org/10.1515/BOT.2000.050, 2005.

Wassmann, P., Slagstad, D., Riser, C. W., and Reigstad, M.: Modelling the ecosystem dynamics of the Barents Sea including the marginal ice zone: II. Carbon flux and interannual variability, J Mar Syst, 59, 1-24, 2006.

Weitz, J. S., Stock, C. A., Wilhelm, S. W., Bourouiba, L., Coleman, M. L., Buchan, A., Follows, M.J., Fuhrman, J. A., Jover, L., Lennon, J. T., Middelboe, M., Sonderegger, D. L., Suttle, C. A., Taylor, B. P.,Thingstad, T. F., Wilson, W., and Wommack, K. E.: A multitrophic model to quantify the effects of marine viruses on microbial food webs and ecosystem processes, ISME J, 9, 1352-1364, 2015.

Werner, D.: Silicate metabolism, in: The biology of diatoms, edited by: Werner, D., Blackwell Scientific Publications, California, 13, 111-149, 1977.

Werner, D.: Regulation of metabolism by silicate in diatoms, in: Biochemistry of silicon and related problems, edited by: Bendz, G., and Lindqvist, I., Springer, Boston, MA, 149-176, 1978.

Westberry, T. K., Behrenfeld, M. J., Siegel, D. A., Boss, E.: Carbon-based primary productivity modeling with vertically resolved photoacclimation, Global Biogeochem Cycles, 22,1–18, 2008.

Wu, Y., Liu, S., Huang, Z., and Yan, W.: Parameter optimization, sensitivity, and uncertainty analysis of an ecosystem model at a forest flux tower site in the United States, Journal of Advances in Modeling Earth Systems, 6(2), 405-419, 2014.

Yool, A., Martin, A. P., Fernández, C., and Clark, D. R.: The significance of nitrification for oceanic new production, Nature, 447(7147), 999-1002, 2007.

Yool, A., and Popova, E. E.: Medusa-1.0: a new intermediate complexity plankton ecosystem model for the global domain, Geosci Model Dev, 4, 381, 2011.

Zambrano, J., Krustok, I., Nehrenheim, E., and Carlsson, B.: A simple model for algae-bacteria interaction in photo-bioreactors, Algal Res, 19, 155-161, 2016.

910 **Figures**

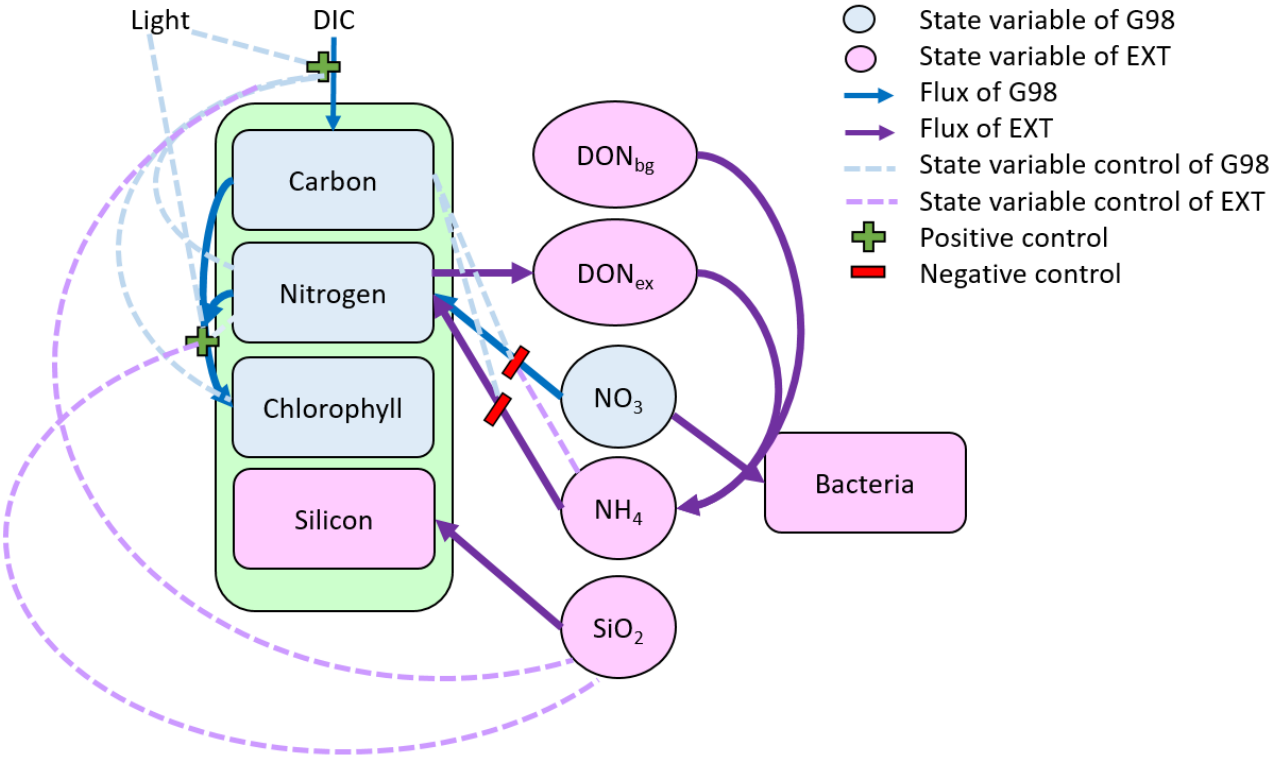

Figure 1. Schematic representation of the state variables and connections and controls in the G98 model (blue) and EXT model (purple). The EXT model has the same formulations as G98 with the additions shown in purple.

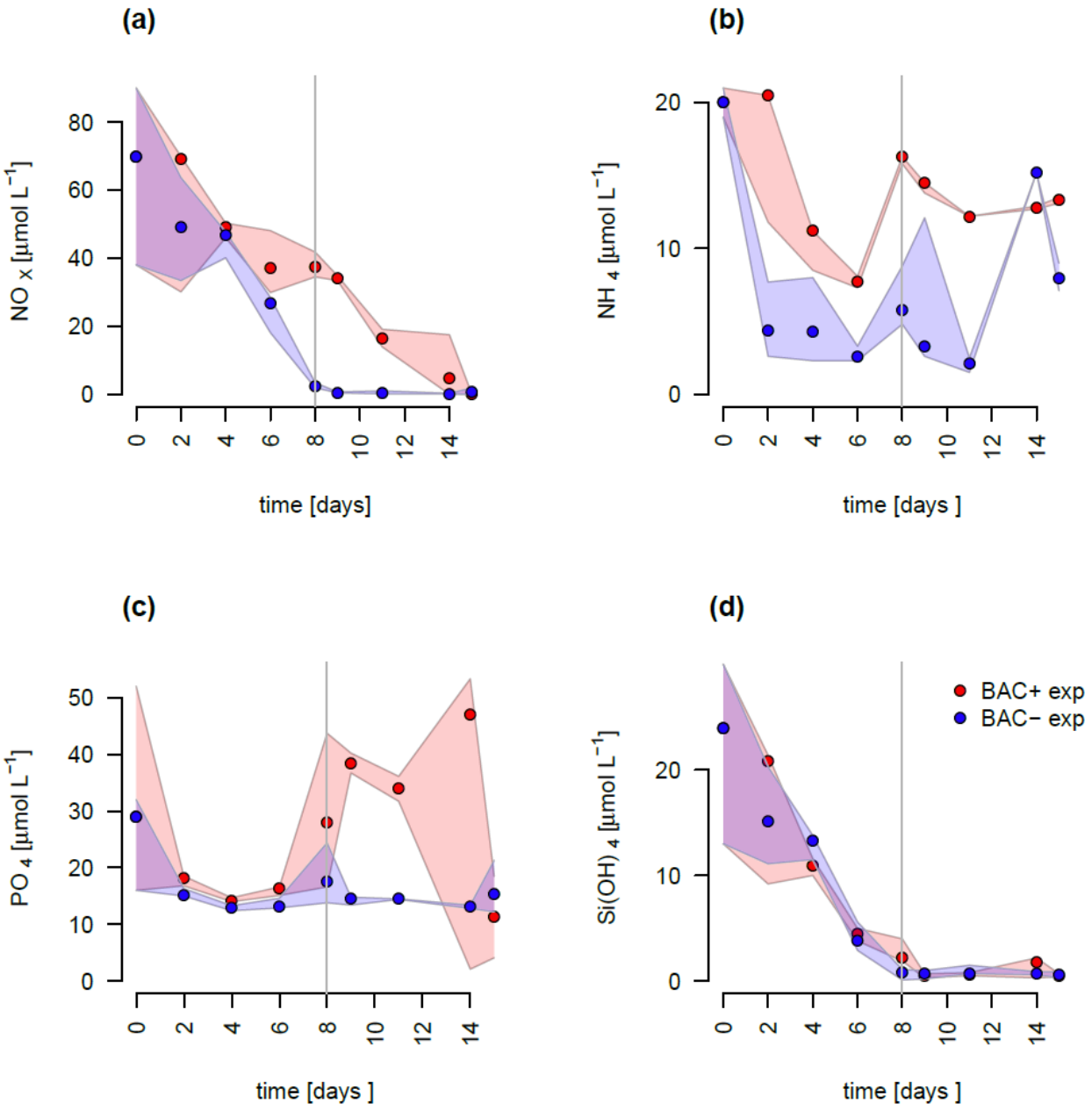

Figure 2. Nutrient measurements over the experimental incubations of a) NO_x, (NO_3^- + NO_2^-) b) NH_4^+, c) PO_4^{2-} with a potential outlier at day 14 leading to a negative peak, d) Silicate, red circles are BAC- cultures and green symbols are BAC+ cultures. Circles show median values (blue = BAC-, red = BAC+) and the colored polygons show maximum and minimum of measured data (n=3). The grey line shows the beginning of the stationary growth phase of *Chaetoceros socialis*.

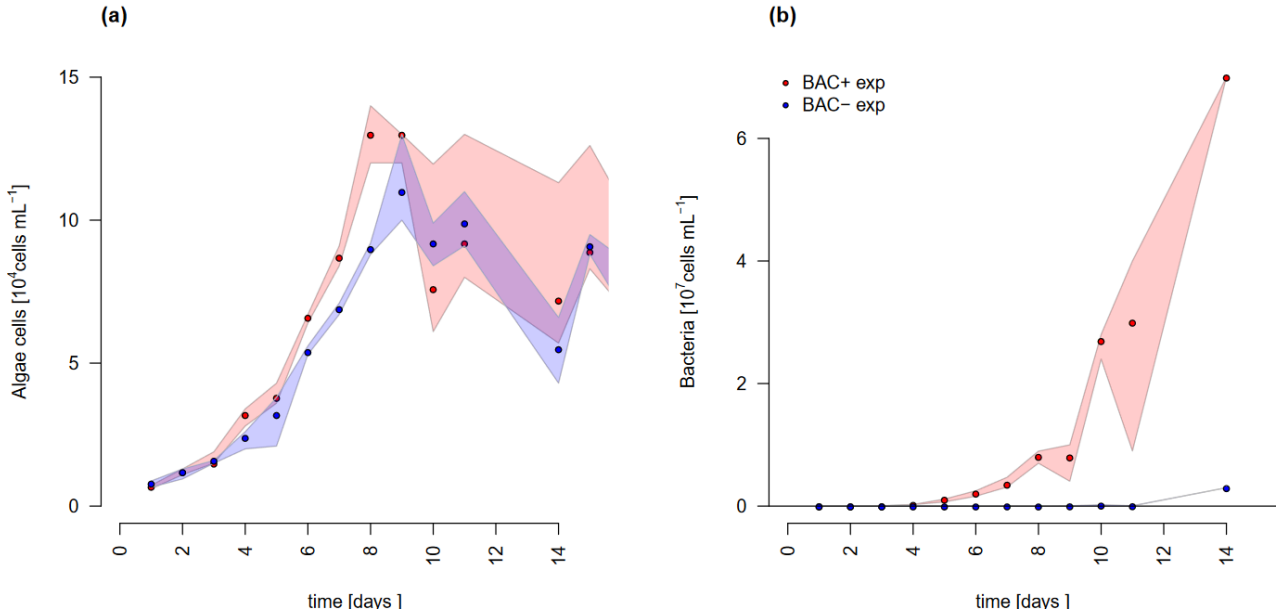

Figure 3. Abundances of a) *Chaetoceros socialis* and b) bacteria over the 14 day experimental period. Blue data are from BAC- cultures and red from BAC+ cultures. Circles represent median values (blue= BAC-, red = BAC+) and the colored polygons show maximum and minimum of measured data (n=3) (Not visible for bacteria counts in BAC- cultures due to very small range). The maximum values of the BAC+ experiment includes algae cells in the biofilm (after day 9).

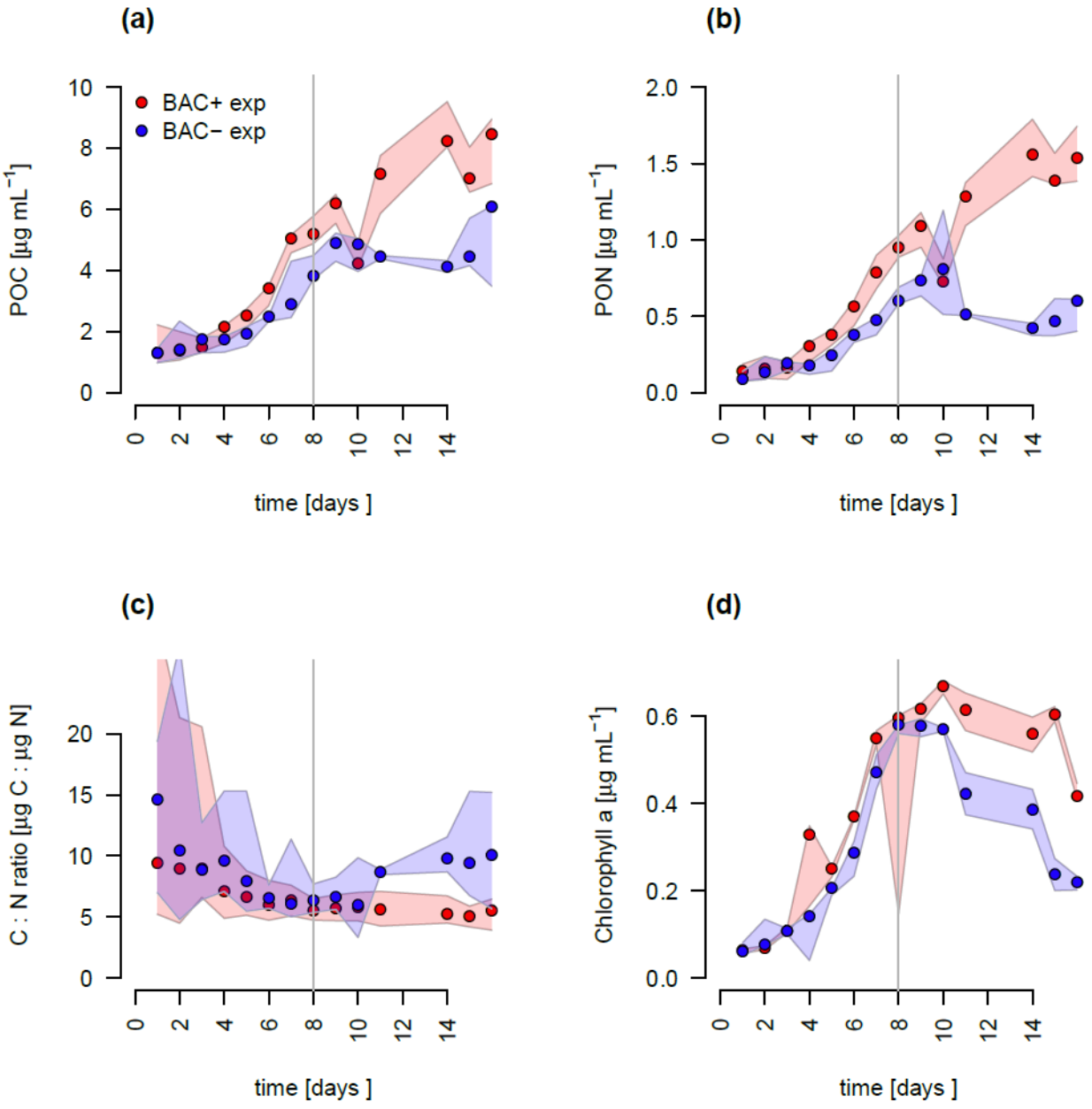

Figure 4. Total particulate organic a) Carbon (POC) b) Nitrogen (PON), c) C : N ratios, and d) Chlorophyll a concentration in experimental cultures with a potential outlier at day 8, presumably due to photodegradation, causing a negative spike. Blue symbols are BAC- cultures and red show BAC+ cultures. Circles show median values (blue = BAC-, red = BAC+) and the colored polygons show the maximum and minimum of measured data (n=3). The grey line indicates the start of the stationary phase.

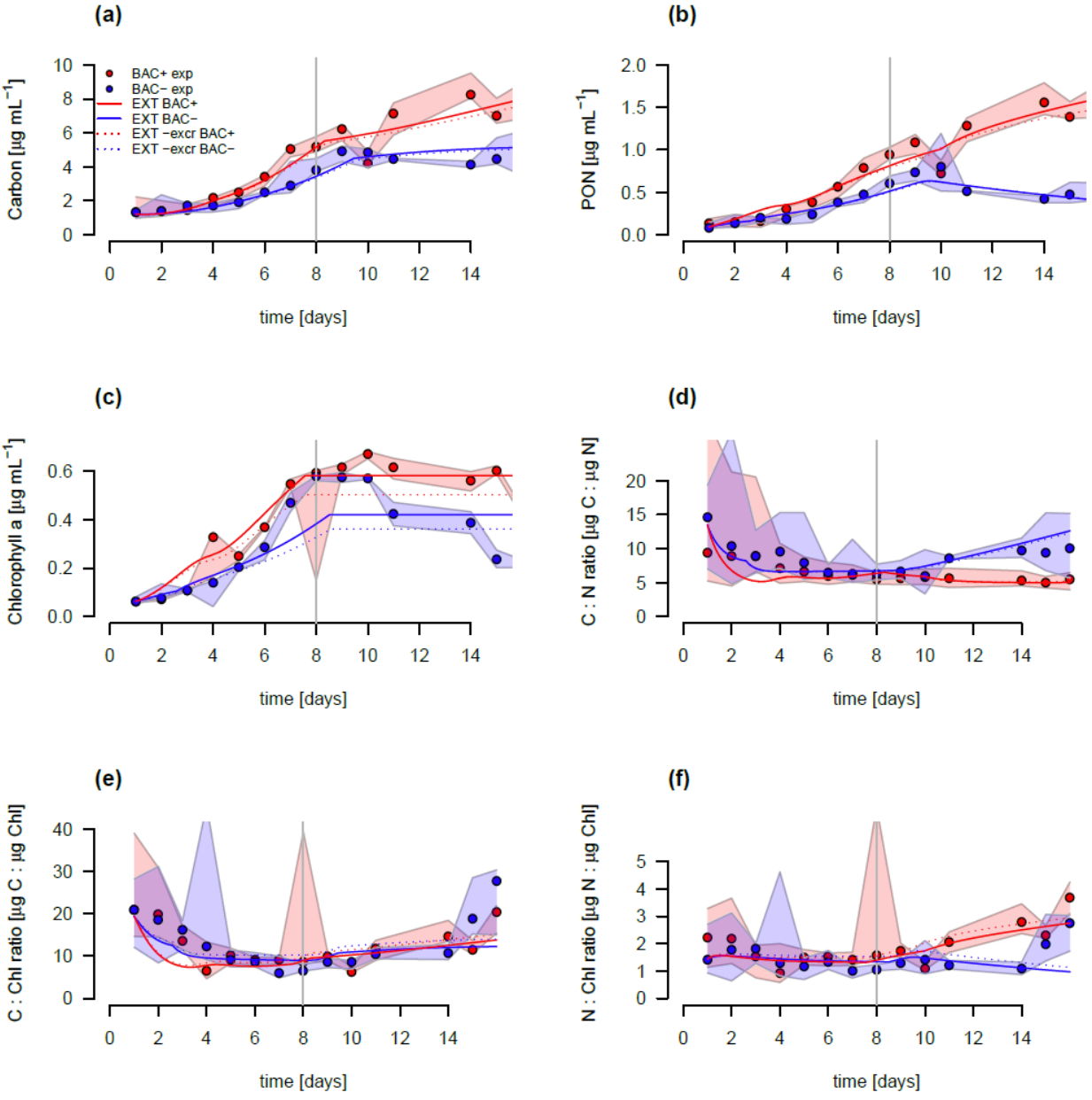

Figure 5. Model fit of the EXT model to the BAC- (blue) and BAC+ (red) experiment. Circles show median values and the colored polygons show the maximum and minimum of measured data (n=3). Solid lines show the model outputs of a) POC, b) PON, c) Chl (including an outlier at day 9 BAC+), d) C:N, e) C:Chl, and f) N:Chl. Dotted lines show the model fit without additional Carbon excretion term x_f. At day 8 the threshold for silicate limitation is reached leading to reduced photosynthesis (by the factor given by Si_{PS}) and inhibited Chl synthesis, which is visible as sharp transitions in POC and Chl.

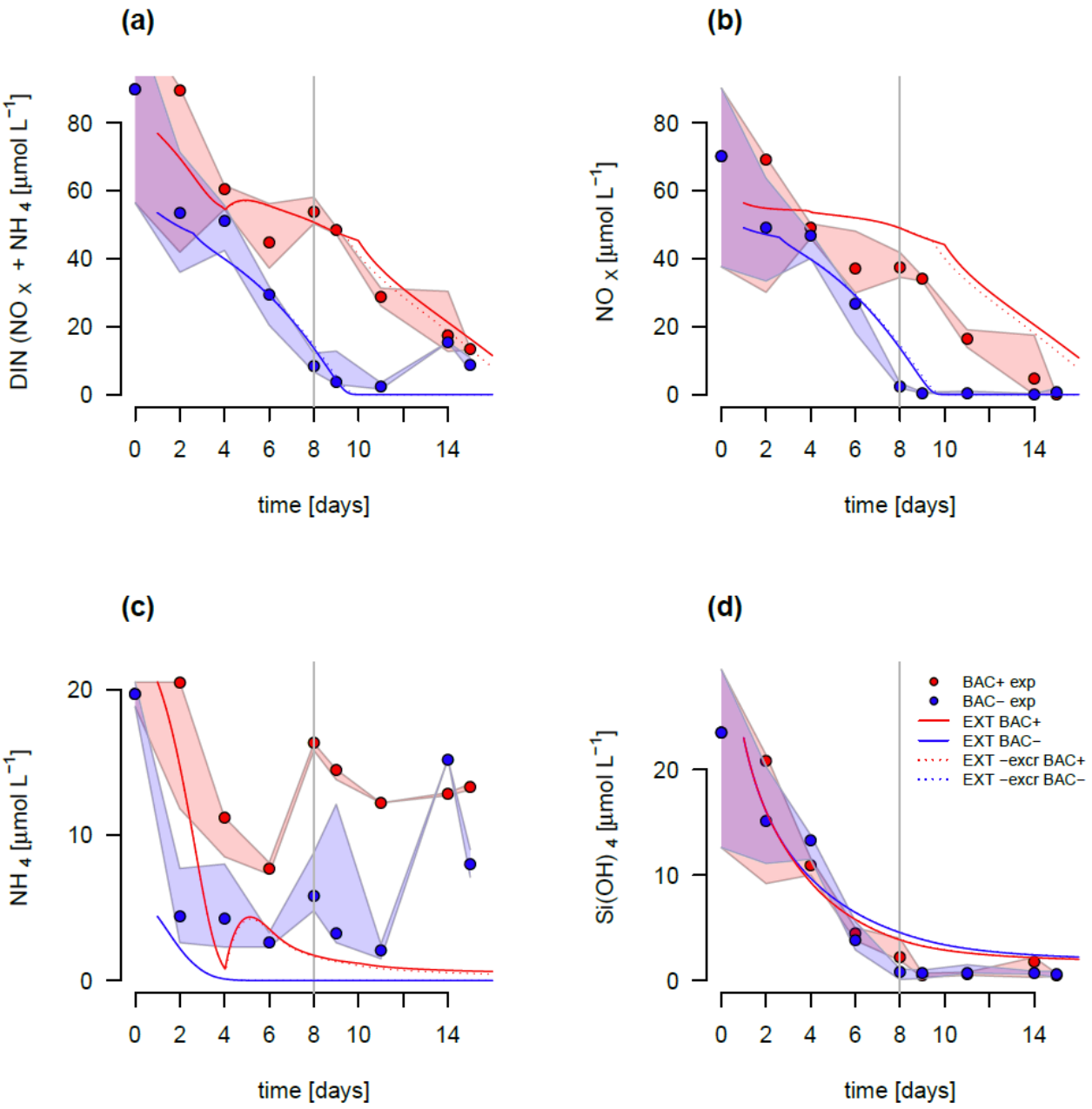

945 Figure 6. Model fit of the EXT model to the BAC- (blue) and BAC+ (red) experiment. Circles show median values and the colored polygons show the maximum and minimum of measured data (n=3). Solid lines show the model outputs of a) DIN (NOX and NH4), b) NO_X, c) NH_4, and d) $Si(OH)_4$ (All model fits overlap).

950

Table

Table 1. A comparison of major components contributing to the complexity of different models discussed. #param is the number of parameters. In case of ecosystem models (SINMOD, BFM, MEDUSA, LANL, NEMURO, NPZD only the model formulations representing the components of the current model (phytoplankton growth, remineralisation, nutrient dynamics) are considered. While the full ecosystem scale models may have more recent versions with updated formulations, we give the original reference to the biogeochemical compartment of the ecosystem scale models. REM designates those models that include Remineralisation (Rem) marked with V is present and X is absent. Ratios shows if the stoichiometry in the model considers variable or fixed ratios of intracellular elements (C:N:Si:P:Fe). The Nutrients considered are given under Nutrients. If DIN is considered as both NH_4 and NO_3, N is shown as N^2. MEDUSA has Fe dependent Si:N ratios, which makes them fixed in the Arctic (fixed*).

Model	Reference	#param	Rem	ratios	Nutrients
		Culture scale			
EXT	This study	21^{*1}	V	variable	N^2, Si
G98	Geider et al., 1998	10^{*2}	X	variable	N
ANIM	Flynn, 1997	30	V	variable	N^2
SHANIM	Flynn and Fasham, 1997	23	X	variable	N^2
Flynn01	Flynn, 2001	54	X	variable	N^2, Si, P, Fe
		Ecosystem scale			
BFM	Vichi et al., 2007	54	V	variable	N^2, Si, P, Fe
REcoM-2	Hauck et al., 2013	28	X	variable	N, Si, Fe
MEDUSA	Yool and Popova, 2011	21	V	fixed*	N, Si, Fe
LANL	Moore et al., 2004	15	V	fixed	N^2, Si, P, Fe
NEMURO	Kishi et al., 2007	21	V	fixed	N^2, Si
NPZD	Gruber et al., 2006	9	V	fixed	N^2
SINMOD	Wassmann et al., 2006	12	X	fixed	N^2, Si

Degrees of freedom after constraints by the measured data are $^{*1}14$ and $^{*2}6$

Appendix

Tables

Table A1. State variables of the G98 model and the EXT model (marked with V if present and X if absent) with units and designation if these state variables had been measured in the experiment.

variable	Description	G98	EXT	Measured	Unit
DIN	Dissolved inorganic nitrogen	V	V	V	mgN m^{-3}
C	Particulate organic carbon	V	V	V	mgC m^{-3}
N	Particulate Nitrogen	V	V	V	mgN m^{-3}
Chl	Chlorophyll a	V	V	V	mgChl m^{-3}
Si_d	Dissolved Silicate	X	V	X	µmol L^{-1}
Si_p	Particulate/biogenic Silicon	X	V	V	mgSi m^{-3}
Bact	Bacteria cells	X	V	V	10^{r}. cells mL^{-1}
DONr	refractory dissolved organic nitrogen	X	V	V	mgN m^{-3}
DONl	labile dissolved organic nitrogen	X	V	X	mgN m^{-3}
NH4	Ammonium	X	V	V	µmol L^{-1}
NO3	Nitrate	X	V	V	µmol L^{-1}
Q	Particulate N : C ratio	X	V	X	gN gC^{-1}
θ^C	Chl to POC ratio	X	V	X	gChl gC^{-1}
θ^N	Chl : phytoplankton nitrogen ratio	X	V	X	gChl gN^{-1}

Table A2. parameters of the original G98 model and the model extension with associated units.

parameter		Unit
	G98	
ζ	cost of biosynthesis	gC gN^{-1}
R^C	The carbon-based maintenance metabolic rate	d^{-1}
θ^N_{max}	Maximum value of Chl:N ratio	gChl gN^{-1}
Q_{min}	Min. N:C ratio	gN gC^{-1}
Q_{max}	Max. N:C ratio	gN gC^{-1}
α^{Chl}	Chl-specific initial C assimilation rate	gC m^2 (gChl µmol photons)$^{-1}$
I	Incident scalar irradiance	µmol photons s^{-1} m^{-2}
n	Shape factor for V^N_{max} max photosynthesis	-
K_{no3}	Half saturation constant for nitrate uptake	µmol L^{-1}
P^C_{ref}	Value of max C specific rate of photosynthesis'	d^{-1}
	Extension	
x_f	Carbon excretion fraction	-
K_{si}	Half saturation constant for Si uptake	µmol L^{-1}
V_{max}	maximum Si uptake rate	mol Si d^{-1} mg C^{-1}
s_{min}	minimum Si required for uptake	µmol L^{-1}
rem	remineralisation rate of excreted don	$bact^{-1}$ d^{-1}
rem_d	remineralisation rate of refractory don	$bact^{-1}$ d^{-1}
μ_{bact}	bacteria growth rate	mio. cells mL^{-1} d^{-1}
$bact_{max}$	Carrying capacity for bacteria	mio. cells mL^{-1}
K_{nh4}	Half saturation constant for ammonium uptake	µmol L^{-1}
$nh4_{thres}$	threshold concentration for ammonium uptake	µmol L^{-1}
Si_{PS}	Fraction of photosynthesis possible after Si lim.	-

Table A3. Parameters of the original G98 model and the EXT model with initial values used in the model and the lower and upper value constraints used for model fitting, unless the parameter was already defined by the data (measured). The constraints are either based on G98 fits to other diatom species, to present experimental data, or to typical values found in the literature.

parameter	value	lower	upper	constrained by
G98				
ζ	1	1	2	G98
R^C	0.01	0.01	0.05	G98
θ^N_{max}	1.7	measured		Data
Q_{min}	0.05	measured		Data
Q_{max}	0.3	measured		Data
α^{Chl}	0.076	0.075	1	G98
I	100	measured		Data
n	3.45	1	4	G98
K_{no3}	2	1	10	G98
P^C_{ref}	0.8	0.5	3.5	G98
Extension				
x_f	0.06	0.01	0.3	Schartau et al., 2017
K_{si}	7.6	0.5	8	Werner 1978
V_{max}	0.1	0.05	0.9	Data
s_{min}	1.82	1.5	6	Werner 1978
rem	10	10	20	open (rem > rem_d)
rem_d	4.86	0.1	10	open (rem_d < rem)
μ_{bact}	0.04	0.01	0.79	Data
$bact_{max}$	0.015	0.005	0.1	Data
K_{nh4}	6.97	0.5	9.3	Eppley 1969
$nh4_{thres}$	1.19	0.1	10	open
Si_{PS}	0.2	0	0.5	Werner 1978

Table A4. Output of the sensitivity analysis (senFun of the FME package in R) with the value for each parameter and different sensitivity indices obtained after quantifying the effects of small perturbations of the parameters.on the output variables (POC, PON, Chl, DIN). The L1 and L2 norms are normalized sensitivity indices defined as $L1 = \sum \frac{|S_{i,j}|}{n}$ and $L2 = \sqrt{\frac{S_{i,j}^2}{n}}$ with $S_{i,j}$ being the the sensitivity of parameter i for model output j.

par	value	L1	L2	Mean	Min	Max
			G98			
ζ	1.00	0.10	0.19	-0.02	-0.15	0.98
R^C	0.07	0.04	0.05	-0.03	-0.08	0.14
θ^N_{max}	1.70	0.23	0.34	0.14	-1.00	0.58
Q_{min}	0.05	0.06	0.08	-0.04	-0.14	0.22
Q_{max}	0.30	0.34	0.47	-0.24	-1.90	0.28
α^{Chl}	0.08	0.20	0.29	-0.10	-1.10	0.20
I	100	0.20	0.29	-0.10	-1.10	0.20
n	3.40	0.33	0.75	0.03	-0.47	4.07
K_{no3}	2.00	0.01	0.02	0.00	-0.01	0.09
P^C_{ref}	0.80	0.82	1.48	0.16	-7.70	1.04
			EXT			
x_f	0.06	0.18	0.25	-0.10	-0.36	0.91
K_{si}	7.6	0.00	0.00	0.00	0.00	0.00
V_{max}	0.1	0.00	0.00	0.00	0.00	0.00
s_{min}	1.82	0.00	0.00	0.00	0.00	0.00
rem	10	0.00	0.00	0.00	0.00	0.00
rem_d	4.86	0.24	0.31	0.24	0.00	0.59
μ_{bact}	0.04	0.00	0.00	0.00	0.00	0.01
$bact_{max}$	0.015	0.00	0.00	0.00	0.00	0.01
K_{nh4}	6.97	0.08	0.11	-0.03	-0.25	0.43
$nh4_{thres}$	1.19	0.00	0.00	0.00	0.00	0.00
Si_{PS}	0.2	0.07	0.21	-0.01	-1.20	0.30

Table A5. Other parameters calculated and used in the model equations

parameter	Description	Unit
P^{C}_{phot}	C-specific rate of photosynthesis	d^{-1}
P^{C}_{max}	Maximum value of P^{C}_{phot} at temperature T	d^{-1}
R^{Chl}	Chl degradation rate constant	d^{-1}
R^{N}	N remineralization rate constant	d^{-1}
V^{C}_{nit}	Diatom carbon specific nitrate uptake rate	gN $(gC\ d)^{-1}$
V^{C}_{ref}	Value of V^{C}_{max} at temperature T	gN $(gC\ d)^{-1}$
p_{Chl}	Chl synthesis regulation term	-
μ	specific growth rate of algae	cells d^{-1}

Table A6. Model equations from G98 (Geider et al., 1998) corrected for typographical errors by Ross and Geider (2009) with extensions.

1)	Carbon synthesis (C originates from unmodelled excess pool of DIC)	$\frac{dC}{dt} = \left(P^C - \zeta V_N^C - R^C\right)C = \mu C$
2)	Chl synthesis	$\frac{dChl}{dt} = \left(\frac{\rho_{Chl} V_N^C}{\Theta^C} - R^{Chl}\right) Chl$
3)	Nitrogen uptake	$\frac{dN}{dt} = \left(\frac{V_N^C}{Q} - R^N\right) N$
4)	from Eq. (1) and (2)	$\frac{dQ}{dt} = V_N^C - \mu Q$
5)	from Eq. (1) and (2)	$\frac{d\Theta^C}{dt} = V_N^C \rho_{Chl} - \Theta^C \mu$
6)	Photosynthesis	$P^C = P_{max}^C \left[1 - exp\left(-\frac{I}{I_K}\right)\right]$
7)	Max. N uptake	$V_N^C = V_{ref}^C \left[\frac{Q_{max} - Q}{Q_{max} - Q_{min}}\right] \frac{DIN}{DIN + K_{no3}}$
8)	with	$\rho^{Chl} = \Theta_{max}^N \left[1 - exp\left(-\frac{I}{I_K}\right)\right]$
9)		$V_{ref}^C = P_{ref}^C Q_{max}$
10)		$P_{max}^C = P_{ref}^C \frac{Q - Q_{min}}{Q_{max} - Q_{min}}$
11)		$I_K = \frac{P_{max}^C}{\alpha^{Chl} \Theta^C}$

Table A7. Model equations of the EXT model based on G98

1a)	Carbon synthesis *(Reduced C synthesis under Si limitation after Werner 1978)*	$IF\ (Si_d < 2\ s_{min})$ $Si_{PS} = Si_{PS}$ $ELSE$ $Si_{PS} = 1$
1b)		$\frac{dC}{dt} = Si_{PS}\left(P^C - \zeta V_N^C - R^C - xf\right)C = \mu C$
2)	Chl synthesis *(Chl synthesis stops under Si limitation after Werner 1978)*	$IF\ (Si_d < 2\ s_{min})$ $\frac{dChl}{dt} = 0$ $ELSE$ $\frac{dChl}{dt} = \left(\frac{\rho_{Chl} V_N^C}{\Theta^C} - R_{Chl}\right) Chl$
3)	from Eq. (1 & 2)	$\frac{dQ}{dt} = V_N^C - \mu Q$
4)	from Eq. (1 & 2)	$\frac{d\Theta^C}{dt} = V_N^C \rho_{Chl} - \Theta^C \mu$
5)	Nitrogen uptake	$\frac{dN}{dt} = \left(\frac{V_N^C}{Q} - R^N - xf\right) N$
6)	Bacteria biomass production *(Logistic growth)*	$\frac{dBact}{dt} = Bact\ \mu_{Bact}\ (Bact_{max} - Bact)$

7a) Silicate uptake

(Monod kinetics after Spilling et al., 2010)

$$\frac{dSi_d}{dt} = V_S^C = \left(V_{max} Si_d \frac{Si_d - S_{min}}{K_{si}\, S_{min}}\right) C$$

7b)

$$\frac{dSi_p}{dt} = -\frac{dSi_d}{dt}\ 14$$

8) Ammonium uptake and production

(Threshhold after Tezuka 1989, and Gilpin 2004)

$$IF\ (\frac{C}{N} < 10)$$

$$\frac{dNH4}{dt} = \frac{-\left(\frac{V_{NH4}^C}{Q}\right) N + Bact\ xf\ N\ rem + Bact\ DON\ rem_d - \frac{Bact}{16})}{14\ 10^3}$$

$$ELSE$$

$$\frac{dNH4}{dt} = \frac{-\left(\frac{V_{NH4}^C}{Q}\right) N + Bact\ xf\ N\ rem - \frac{Bact}{16})}{14\ 10^3}$$

9) DON uptake and production

$$IF\ (\frac{C}{N} < 10)$$

$$\frac{dDON}{dt} = -\frac{Bact\ xf\ N\ rem + Bact\ DON\ rem_d + xf\ N}{14\ 10^3}$$

$$ELSE$$

$$\frac{dDON}{dt} = -\frac{Bact\ xf\ N\ rem + xf\ N}{14\ 10^3}$$

10) DIN uptake

$$IF\ (NH4 > nh4_{thresh})$$

$$\frac{dDIN}{dt} = \frac{-\left(\frac{V_{NO3}^C}{Q}\right) N - \frac{Bact}{16}}{14\ 10^3}$$

$$ELSE$$

$$\frac{dDIN}{dt} = \frac{-0.2\left(\frac{V_{NO3}^{C}}{Q}\right)N - \frac{Bact}{16}}{14\,10^{3}}$$

11) Photosynthesis

$$P^{C} = P_{max}^{C}\left[1 - exp\left(-\frac{I}{I_K}\right)\right]$$

12a) Max NO3 uptake

$$V_{NO3}^{C} = V_{ref}^{C}\left[\frac{Q_{max} - Q}{Q_{max} - Q_{min}}\right]\frac{NO3}{NO3 + K_{no3}}$$

12b) Max NH4 uptake

(based on SHANIM Eq4 by Flynn and Fasham, 1997)

$$V_{NH4}^{C} = (0.01\,Q)\,0.0021\,\frac{NH4}{NH4 + K_{nh4}}$$

13) Max N uptake

(Based on Flynn and Fasham, 1997 and Flynn, 1999 showing no total inhibition in cold water)

$$IF\ (NH4 > nh4_{thresh})$$

$$V_N^{C} = V_{NH4}^{C} + 0.2\,V_{NO3}^{C}$$

$$ELSE$$

$$V_N^{C} = V_{NH4}^{C} + V_{NO3}^{C}$$

14) with

$$\rho^{Chl} = \Theta_{max}^{N}\left[1 - exp\left(-\frac{I}{I_K}\right)\right]$$

15)

$$V_{ref}^{C} = P_{ref}^{C} Q_{max}$$

16)

$$P_{max}^{C} = P_{ref}^{C}\frac{Q - Q_{min}}{Q_{max} - Q_{min}}$$

17)

$$I_K = \frac{P_{max}^{C}}{\alpha^{Chl}\Theta^{C}}$$

Table A8. Output of the collinearity or parameter identifiability analysis using the collin function of the FME R package (Soetart et al., 2010b). A subset of any combinations of two parameter with a collinearity above 20, indicating non-identifiable parameter combinations is given (Brun et al., 2001).

ζ	R^C	θ^N_{max}	Q_{min}	Q_{max}	α^{Chl}	I	n	K_{no3}	P^C_{ref}	collinearity
1	0	1	0	0	0	0	0	0	0	31
1	0	0	0	1	0	0	0	0	0	59
1	0	0	0	0	1	0	0	0	0	42
1	0	0	0	0	0	1	0	0	0	42
1	0	0	0	0	0	0	1	0	0	74
0	1	0	0	0	0	0	0	0	1	22
0	0	1	0	1	0	0	0	0	0	32
0	0	1	0	0	1	0	0	0	0	26
0	0	1	0	0	0	1	0	0	0	26
0	0	1	0	0	0	0	1	0	0	41
0	0	0	0	1	1	0	0	0	0	49
0	0	0	0	1	0	1	0	0	0	49
0	0	0	0	1	0	0	1	0	0	81
0	0	0	0	0	1	1	0	0	0	1756319
0	0	0	0	0	1	0	1	0	0	60
0	0	0	0	0	0	1	1	0	0	60

Figure

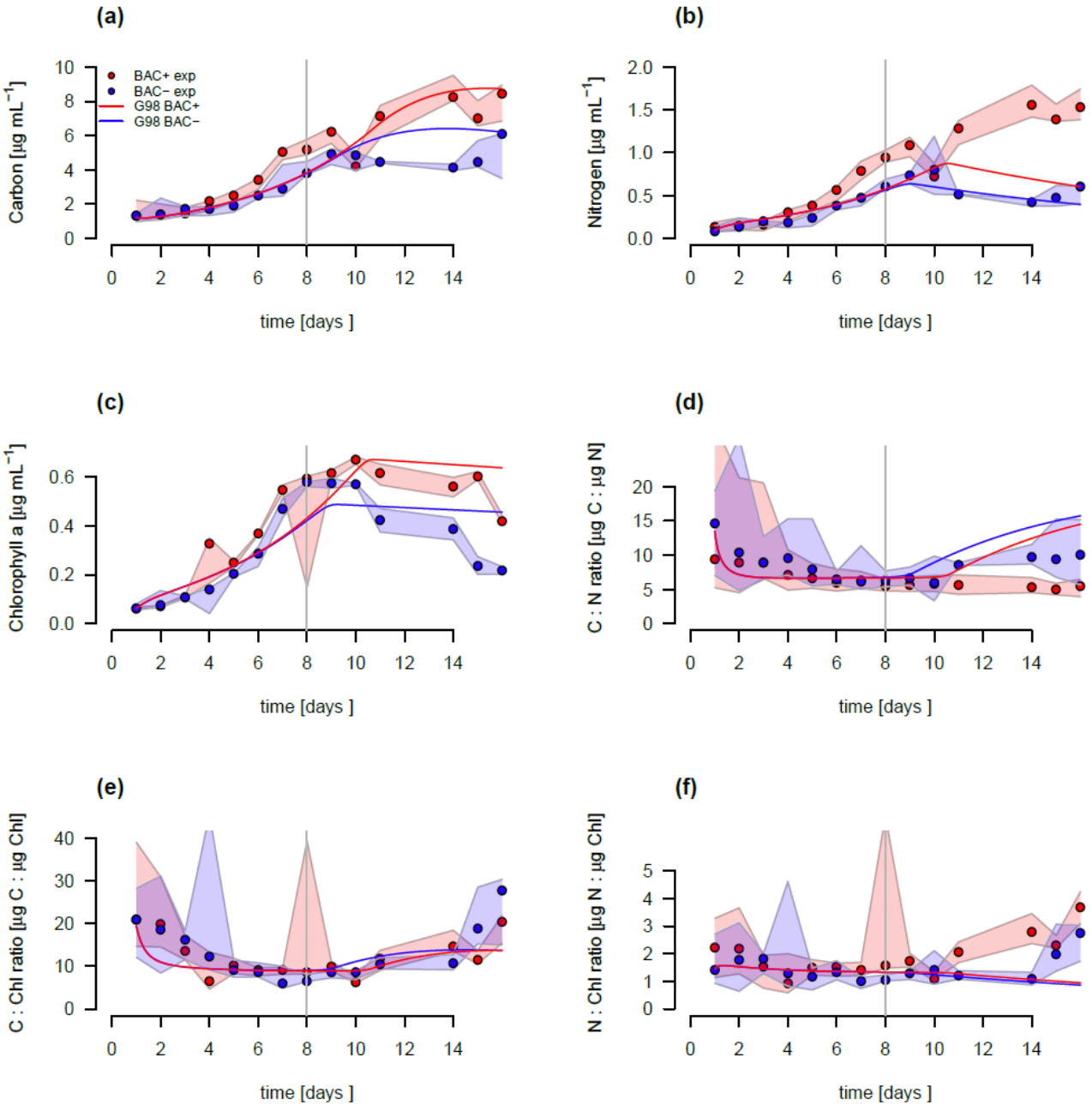

1070 Figure B1: Model fit of the G98 model to the BAC- (blue) and BAC+ (red) experiment. Circles show median values and the colored polygons show the minimum and maximum of the measured data (n=3). Solid lines show the model outputs of a) POC, b) PON, c) Chl (including outlier at day 8 in BAC+), d) C:N, e) C:Chl, and f) N:Chl.

Equations

Equation C1. F-ratio estimation in the cultivation experiments with the average PON concentrations at day 13 to 15 ($PON^{d13\text{-}15}$) for the BAC- and BAC+ treatments.

$$f-ratio = \frac{PON_{BAC-}^{d13-15}}{PON_{BAC-}^{d13-15} + PON_{BAC+}^{d13-15}}$$

Equation C2. normalized RMSE with i being the different variables (POC, PON, Chl, DIN), and j the different values of each state variable. Predicted values are given as P and observed values as O.

$$RMSE = \sqrt{\sum_{\substack{i=1 \\ j=1}}^{n,p} \frac{(P_{i,j} - O_{i,j})^2}{Var(O_i)}}$$

Subglacial upwelling in winter/spring increases under-ice primary production

Tobias Reiner Vonnahme[1], Emma Persson[1], Ulrike Dietrich[1], Eva Hejdukova[2], Christine Dybwad[1], Josef Elster[3], Melissa Chierici[4,5], Rolf Gradinger[1]

[1] Department of Arctic and Marine Biology, UiT – The Arctic University of Norway, Tromsø, Norway
[2] Department of Ecology, Faculty of Science, Charles University, Prague, Czech Republic
[3] University of South Bohemia, České Budějovice, and Institute of Botany ASCR, Třeboň, Czech Republic
[4] Institute of Marine Research, Tromsø, Norway
[5] University Centre in Svalbard (UNIS), Longyearbyen, Svalbard, Norway

Correspondence to: Tobias R. Vonnahme (Tobias.Vonnahme@uit.no)

Abstract. Subglacial upwelling of nutrient rich bottom water is known to sustain elevated summer primary production in tidewater glacier influenced fjord systems. However, during the winter/spring season, the importance of subglacial upwelling has not been considered yet. We hypothesized that subglacial upwelling under sea ice is present in winter/spring and sufficient to increase phytoplankton primary productivity. We evaluated the effects of the subglacial upwelling on primary production in a seasonally fast ice covered Svalbard fjord (Billefjorden) influenced by a tidewater outlet glacier in April/May 2019. We found clear evidence for subglacial upwelling. Although the estimated entrainment factor (1.6) and total fluxes were lower than in summer studies, we observed substantial impact on the fjord ecosystem and primary production. The subglacial meltwater leads to a salinity stratified surface layer and sea ice formation with low bulk salinity and permeability. The combination of the stratified surface layer, a two-fold higher under-ice irradiance, and higher N and Si concentrations at the glacier front supported two orders of magnitude higher primary production (42.6 mg C m^{-2} d^{-1}) compared to a marine reference site at the fast ice edge. The nutrient supply increased primary production by approximately 30 %. The brackish water sea ice at the glacier front with its low bulk salinity contained a reduced brine volume, limiting the inhabitable place and nutrient exchange with the underlying seawater compared to full marine sea ice. Microbial and algal communities were substantially different in subglacial influenced water and sea ice compared to the marine reference site, sharing taxa with the subglacial outflow water. We suggest that with climate change, the retreat of tidewater glaciers could lead to decreased under-ice phytoplankton primary production, while sea ice algae production and biomass may become increasingly important, unless sea ice disappears before, in which case spring phytoplankton primary production may increase.

1 Introduction

Tidewater glacier fronts have recently been recognized as hotspots for marine production including top trophic levels, such as marine mammals, birds and piscivorous fish (Lydersen et al., 2014, Meire et al., 2016b), but also primary producers (Meire et al., 2016b; Hopwood et al., 2020). During summer, large amounts of freshwater are released below the glacier and entrap nutrient rich bottom water, sediments and zooplankton during the rise to the surface (Meire et al., 2016a, b, Moon et al., 2018). Together with katabatic winds pushing the surface water out of the fjords, it creates a strong upwelling effect (Meire et al., 2016b). The biological response to this upwelling will depend on the characteristics of the upwelling water. Summer primary production is typically low in direct proximity to the glacier front due to high sediment loads of the plumes absorbing light, but potentially also due to lateral advection (Meire et al., 2016b, Halbach et al., 2019). The light absorbing effect of the plumes is highly dependent on the glacial bedrock (Halbach et al., 2019). However, the high nutrient concentrations supplied to the surface increase summer primary production at some distance from the initial upwelling event, once the sediments settled out (Meire et al., 2016, Halbach et al., 2019). These tidewater upwelling effects have been described in a variety of different Arctic fjords including deep glacier termini in western Greenland (Meire et al., 2016), eastern Greenland (Cape et al., 2019), and north-western Greenland (Kanna et al., 2018), but also in shallower fjords on Svalbard (Halbach et al., 2019). Studies of the effect of potential subglacial upwelling in winter/spring on sea ice and pelagic primary productivity are rare (e.g. Fransson et al., 2020, Schaffer et al., 2020), making quantification of subglacial outflow difficult.

In addition to subglacial discharge at the grounding line, tidewater glacier related upwelling mechanisms can also be caused by the melting of deep icebergs (Moon et al., 2018), or the melting of the glacier terminus in contact with warm seawater (Moon et al., 2018, Sutherland et al., 2019). A seasonal study within an East Greenland fjord showed high melt rates of icebergs throughout the year, while subglacial runoff had been detected as early as April, but with substantially higher freshwater inputs in summer (Moon et al., 2018). Glacier terminus melt rates are low compared to the subglacial outflow but can be present throughout the year (Chandler et al., 2013, Moon et al., 2018). In fact, Moon et al. (2018) found higher terminus melt rates below 200 m in winter than in summer, which may allow winter upwelling. Svalbard glaciers are typically shallower and deep terminus melt (below 200 m) and iceberg induced upwelling are less important (Dowdeswell, 1989). However, subglacial outflows can persist throughout winter and specifically in early spring through the release of subglacial meltwater stored from the previous melt season (Hodgkins, 1997), or through constant supply from groundwater, temperate parts of the glacier, geothermal heat, or frictional dissipation (Schoof et al., 2014). While studies on upwelling in winter and spring are limited to oceanographic observations, the biological effects on e.g. primary production have been neglected (Chandler et al., 2013, Moon et al., 2018). We hypothesize that even low rates of subglacial outflows can be sufficient to supply nutrients to the surface, while at the same time entrapping considerably less light absorbing sediments compared to the summer situation. We suggest, that in the absence of wind induced mixing due to the seasonal presence of a fast ice cover, upwelling of subglacial outflows could be a mechanism increasing primary production in tidewater fjords compared to similar fjords without these glaciers, especially towards the end of the ice algal/phytoplankton spring bloom when nutrients become limiting (Leu et al.

2015). With climate change, these dynamics are expected to change substantially (e.g. Błaszczyk et al., 2009, Holmes et al., 2019). Higher glacial melt rates and earlier runoffs may initially increase tidewater glacier induced upwelling, due to increased subglacial runoff (Amundson and Carroll, 2018). However, their retreat and transformation into shallower tidewater glacier termini may lead to less pronounced upwelling, unless the shallower grounding line is compensated by the increased runoff (Amundson and Carroll, 2018). Eventually, the tidewater glaciers transform into land terminated glaciers, where wind induced mixing is still possible, but subglacial upwelling is eliminated (Amundson and Carroll, 2018) – potentially reducing the primary production.

Due to high inputs of freshwater in the autumn preceding the onset of sea ice formation, tidewater glacier influenced fjords are often sea ice covered in spring, mainly by coastal fast ice. Within the sea ice, ice algae start growing, once sufficient light is penetrating the snow and ice layers with the onset varying between March and April, depending on latitude and local ice conditions (Leu et al., 2015). While the beginning of the ice algal blooms is typically related to light, the magnitude depends on the initial nutrient concentration and nutrient additions from the water column into the brine channel network (Gradinger, 2009). Thus, subglacial upwelling has the strong potential to extend the duration and increase the magnitude of the ice algal blooms. Similar control mechanisms apply to phytoplankton bloom formation and duration. Under-ice phytoplankton blooms are thought to be light limited if the ice is snow covered and substantial blooms have been described in areas with lack of snow cover (e.g. melt ponds, after rain events, Fortier et al., 2002, Arrigo et al., 2014) or at the ice edge related to ice edge induced upwelling (Mundy et al., 2009). On Svalbard, low precipitation rates and strong katabatic winds (Esau & Repina, 2012) often limit snow coverage also on the fast ice near glacier fronts (Braaten, 1997), potentially allowing enough light for under-ice phytoplankton blooms to occur. Once sufficient light reaches the water column, typically a diatom dominated bloom starts along the receding ice edge or even below the sea ice (e.g. Hodal et al., 2012; Lowry et al., 2017). Once silicate becomes limiting for diatom growth, other taxa like *Phaeocystis pouchetii* dominate the next stage of the seasonal succession (von Quillfeldt, 2000). This succession pattern can be significantly influenced by tidewater glacier related spring upwelling. Sea ice formed from brackish water has relatively low bulk salinity, low brine volume and low total ice algal biomass as observed e.g. in the Baltic Sea (Haecky & Andersson, 1999). Brackish ice conditions with low algal biomass will reduce light absorption allowing more light to reach the water column to potentially fuel under-ice phytoplankton blooms. We suggest that higher nutrient levels supplied via slow subglacial upwelling in the absence of wind mixing may enhance algal growth and cause different succession patterns for phytoplankton and sea ice algae.

We used the natural conditions in a Svalbard fjord as a model system contrasting the biological response at two glacier fronts with different freshwater inputs during the winter/spring transition period while a fast ice cover was present. The aim of the study was to investigate the effect of the glacier terminus, and subglacial outflow related upwelling on winter/spring primary productivity and algae community structures both in and under the sea ice. We hypothesized that; 1) subglacial upwelling throughout winter and spring supplies nutrient rich meltwater and bottom water to the surface, 2) subglacial upwelling increases primary production near the glacier front, 3) biomass of sea ice algae is lower at glacier fronts as a result of low permeability sea ice.

2 Methods

2.1 Field work and physical properties

Fieldwork was conducted on Svalbard in Billefjorden (Fig. 1) between 22nd of April and 5th of May 2019, when most samples were collected. For comparison, some samples had been already taken in April 2018 (subglacial outflow water for DNA analyses) and July 2018 (glacier ice and supraglacial runoff). Billefjorden is fed by a few streams, rivers and the tidewater glacier Nordenskiöldbreen and partly fast ice covered from January to June. Nordenskiöldbreen has an estimated grounding depth of 20 m at its southern margin (personal observation). Tidal currents are very slow with under 0.1 cm s^{-1}, which translates to advection below 22 m per tidal cycle (Kowalik et al., 2015). Katabatic winds can be strong due to several glaciers and valleys leading into the fjord system (Láska et al., 2012). Together with low precipitation, this leads to a thin snow depth on the sea ice. Bare sea ice spots are often present in the sea ice season (personal observations). The fjord is separated from Isfjorden, a larger fjord connected to the West Spitsbergen current, by a shallow approximately 30 to 40 m sill (Norwegian Polar Institute, 2020) making Billefjorden an Arctic fjord with limited impacts of Atlantic water inflows. This character is shown in water masses, circulation patterns and animal communities including the presence of polar cod (Maes, 2017, Skogseth et al., 2020).

Samples were taken at three stations 1) at the fast ice edge (IE) – a full marine reference station (78°39'09N, 16°34'01E); 2) at the southern site of the ocean terminated glacier terminus (SG) (approx. 20 m water depth) with freshwater outflow observed during the sampling period (78°39'03N, 16°56'44E) and; 3) at the northern site of the glacier terminus (NG) with no clear freshwater outflow observed and a mostly land-terminating glacier front (78°39'40N, 16°56'19E).

Snow depth and sea ice thickness around the sampling area were measured with a ruler. Sea ice and glacier ice samples were taken with a Mark II ice corer with an inner diameter of 9 cm (Kovacs Enterprise, Roseburg, OR, USA). Temperature of each ice core was measured immediately by inserting a temperature probe (TD20, VWR, Radnor, PA, USA) into 3 mm thick pre-drilled holes. For further measurements the ice cores were sectioned into the following sections: 0–3 cm, 3–10 cm and thereafter in 20 cm long pieces from the bottom to the top, packed in sterile bags (Whirl-Pak™, Madison, WI, USA) and left to melt at about 4–15 ˚C for about 24–48 h in the dark. Sections for chlorophyll *a* (Chl) measurements, DNA extractions, and algae and bacteria counts were melted in 50 % vol/vol sterile filtered (0.2 µm Sterivex filter, Sigma-Aldrich, St. Louis, MO, USA) seawater to avoid osmotic shock of cells (Garrison and Buck 1986), while no seawater was added to the sections for salinity and nutrient measurements. Salinity was measured immediately after melting using a conductivity sensor (YSI Pro 30, YSI, USA). Brine salinity and brine volume fractions were calculated after Cox et al. (1983) for sea ice temperatures below -2 °C and after Leppäranta and Manninen (1988) for sea ice temperatures above.

Samples of under-ice water were taken using a pooter (Southwood and Henderson, 2000) connected to a hand-held vacuum pump (PFL050010, Scientific & Chemical Supplies Ltd., UK). Deeper water at 1 m, 15 m, 25 m depths and bottom water at IE station were taken with a water sampler (Ruttner sampler, 2 L capacity, Hydro-Bios, Germany). Glacial outflow water was sampled in April 2018 close to SG station using sterile Whirl-Pak™ bags. No outflow water was found around NG station.

Cryoconite hole water (avoiding any sediment) was sampled in July 2018 with a pooter on sites known to differ in their biogeochemical settings (Nordenskiöldbreen main cryoconite site (NC), and Nordenskiöldbreen near Retrettøya (NR) sites characterized by Vonnahme et al., 2016). One metre long glacier surface ice samples were taken with the Mark II ice corer at the southern side of the glacier on the NC site.

CTD profiles were taken at each station by a CastAway™ (SonTek/-Xylem, San Diego, CA, USA). At the SG station an additional CTD profile was taken with a SAIV CTD SD208 (SAIV, Lakselv, Norway) including turbidity and fluorescence sensors. Unfortunately, readings at the other stations failed due to sensor freezing at low air temperatures. Surface light data were obtained from the photosynthetic active radiation (PAR) sensor of the ASW 1 weather station in Petuniabukta (23 m a.s.l), operated by the University of South Bohemia (Láska et al., 2012; Ambrožová and Láska, 2017).

During the sampling days, Billefjorden and Adventdalen were overcast. The light regime under the ice was calculated after Masicotte et al. (2018) with a snow albedo of 0.78, a snow attenuation coefficient of 15 m^{-1} (Mundy et al., 2005), ice attenuation coefficients of 5.6 m^{-1} for the upper 15 cm and 0.6 m^{-1} below (Perovich et al., 1998). For sea ice algae, an absorption coefficient of 0.0025 m^2 mg^{-1} Chl was used. The fraction of fjord water vs subglacial meltwater for the water samples was calculated assuming linear mixing of the two salinities (glacial meltwater salinity = 0 PSU, average seawater salinity at IE=34.7 ± 0.03 standard deviation), since no other water masses in regard to temperature or salinity signature were present (Table 1). The variabiltiy of the IE sea water salinity leads to a small (< 1%) uncertainty in the estimated value of the relative contributions of sea water vs subglaical meltwater.

2.2 Chemical properties

Nutrient samples of water and melted sea ice and glacier ice were sterile filtered as described above, stored in acid washed (rinsed in 5 % vol/vol HCl) and MQ rinsed 50 ml falcon tubes and kept at -20 °C until processing. Total alkalinity (TA), Dissolved inorganic carbon (DIC), and pH samples were sampled in 500 ml borosilicate glass bottles avoiding air contamination and fixed within 24 h with 2 % (fin. con.) $HgCl_2$ and stored at 4 °C until processing.

Nutrients were measured in triplicates using standard colorimetric methods with a nutrient autoanalyser (QuAAtro 39, SEAL Analytical, Germany) using the instrument protocols: Q-068-05 Rev. 12 for nitrate (detection limit = 0.02 µmol L^{-1}), Q-068-05 Rev. 12 for nitrite (detection limit = 0.02 µmol L^{-1}), Q-066-05 Rev. 5 for silicate (detection limit = 0.07 µmol L^{-1}), and Q-064-05 Rev. 8 for phosphate (detection limit = 0.01 µmol L^{-1}). The data were analysed using the software AACE v5.48.3 (SEAL Analytical, Germany). Reference seawater (Ocean Scientific International Ltd., United Kingdom) was used as blanks for calibrating the nutrient analyser. The maximum differences between the measured triplicates were 0.1 µmol L^{-1} for silicate and nitrate and 0.05 µmol L^{-1} for nitrite and phosphate. Concentrations of nitrate and nitrite (NO_X) were used to estimate the fraction of bottom water reaching the surface at SG assuming linear mixing of bottom water (at station IE) and surface water concentration using the NO_X concentration measured at IE (Table 1).

DIC and TA were analyzed within 6 months after sampling as described by Jones et al. (2019) and Dickson et al. (2007). DIC was measured on a Versatile Instrument for the Determination of Titration carbonate (VINDTA 3C, Marianda, Germany),

following acidification, gas extraction, coulometric titration, and photometry. TA was measured with potentiometric titration in a closed cell on VINDTA Versatile INstrument for the Determination of Titration Alkalinity, VINDTA 3S, Marianda, Germany). Precision and accuracy was ensured via measurements of Certified Reference Materials (CRM, obtained from Dickson, Scripps Institution of Oceanography, USA). Triplicate analyses on CRM samples showed mean standard deviations below ±1 μmol kg^{-1} for DIC and AT.

2.3 Biomass and communities

For determination of algal pigment concentrations about 500 ml sea water or melted sea ice were filtered onto GF/F filter (Whatman plc, Maidstone, UK) in triplicates using a vacuum pump (max 200 mbar vacuum) before storing the filter in the dark at -20 °C. Water and melted sea ice for DNA samples were filtered onto Sterivex filter (0.2 μm pore size) using a peristaltic pump and stored at -20 °C until extraction. Algae were sampled in two ways; 1) a phytoplankton net (10 μm mesh size) was pulled up from 25 m and the samples fixed in 2 % (final conc.) neutral Lugol and stored at 4 °C in brown borosilicate glass bottles before processing; and 2) water or melted sea ice was fixed and stored directly as described above. For later bacteria abundance estimation, 25 ml of water was fixed with 2 % (final con.) formaldehyde for 24–48 h at 4 °C before filtering onto 0.2 μm polycarbonate filters (Isopore™, Merck, US) and washing with filtered seawater and 100 % ethanol before freezing at -20 °C.

Algal pigments (Chl, phaeophytin) were extracted in 5 ml 96 % ethanol at 4 °C for 24 h in the dark. The extracts were measured on a Turner Trilogy AU-10 fluorometer (Turner Designs, 2019) before and after acidification with a drop of 5 % HCl. 96 % ethanol was used as a blank and the fluorometer was calibrated using a chlorophyll standard (Sigma S6144). For estimations of algae derived carbon a conversion factor of 30 g C $(g\ Chl)^{-1}$ was applied (Cloern et al., 1995). The maximum differences (max-min) between the measured triplicates were under 0.05 μg Chl L^{-1} unless stated otherwise.

DNA was isolated from the Sterivex filter cut out of the cartridge using sterile pliers and scalpels, using the DNeasy® PowerSoil® Kit following the kit instructions with a few modifications. Solution C1 was replaced with 600 μL Phenol:Chloroform:Isoamyl Alcohol 25:24:1 and washing with C2 and C3 was replaced with two washing steps using 850 μL chloroform. Before the last centrifugation step, the column was incubated at 55 °C for 5 min to increase the yield. For microbial community composition analysis, we amplified the V4 region of a ca. 292 bp fragment of the 16S rRNA gene using the primers (515F, GTGCCAGCMGCCGCGGTAA and 806R, GGACTACHVGGGTWTCTAAT, assessed by Parada et al., 2016). For eukaryotic community composition analyses, we amplified the V7 region of ca 100-110 bp fragments of the 18S rRNA gene using the primers (Forward 5'-TTTGTCTGSTTAATTSCG-3' and Reverse 5'-GCAATAACAGGTCTGTG-3', assessed by Guardiola et al., 2015). The Illumina MiSeq PE library was prepared after Wangensteen et al. (2018).

For qualitative counting of algal communities, the phytoplankton net and bottom sea-ice samples were counted under an inverted microscope (Zeiss Primovert, Carl Zeiss AG, Germany) with 10x40 magnification. For quantitative counts, 10-50 ml of the fixed water samples were settled in an Utermöhl chamber (Utermöhl, 1958) and counted. Algae were identified using identification literature by Tomas (1997), and Throndsen et al. (2007). For bacteria abundance estimates, bacteria on

polycarbonate filter samples were stained with DAPI (4,6-diamidino-2-phenylindole) as described by Porter and Feig (1980), incubating the filter in 30 µl DAPI (1 µg ml^{-1}) for 5 min in the dark before washing with MQ and ethanol and embedding in Citifluor:Vectashield (4:1) onto a microscopic slide. The stained bacteria were counted using an epifluorescence microscope (Leica DM LB2, Leica Microsystems, Germany) under UV light at 10x100 magnification. At least 10 grids or 200 cells were counted. The community structure of the phytoplankton net haul was used for estimating the contribution of sea ice algae to the settling community based on typical Arctic phytoplankton (Von Quillfeldt, 2000) and sea ice algal species (von Quillfeldt et al., 2003) described in literature.

2.4 In situ measurements and incubations

Vertical algal pigment fluxes were measured using custom made (Faculty of Science, Charles University, Prague, Czech Republic) short-term sediment traps (6.2 cm inner diameter, 44.5 cm height) at 1 m, 15 m, and 25 m under the sea ice anchored to the ice at SG and IE, as described by Wiedmann et al. (2016). Sediment traps were left for 24 h at the SG station and 37 h at the IE station. After recovery, samples for algal pigments were taken, fixed and analysed as described above.

Primary production (PP) was measured based on ^{14}C-DIC incorporation. Samples were incubated *in situ* in 100 ml polyethylene bottles attached to the rig of the sediment trap giving identical incubation times. Seawater or bottom sea ice melted in filtered seawater (ca 20 °C initial temperature to ensure fast ice melt) on site were incubated with ^{14}C sodium bicarbonate at final concentration of 1 µCi ml^{-1} (PerkinElmer Inc., Waltham, USA). PP samples were incubated in triplicates for each treatment with two dark controls for the same times as the sediment traps. Samples were filtered onto precombusted Whatman GF/F filters (max 200 mbar vacuum) and acidified with a drop of 37 % fuming HCl for 24 h for removing remaining inorganic carbon. The samples were measured in Ultima Gold™ Scintillation cocktail on a liquid scintillation counter (PerkinElmer Inc., Waltham, USA, Tri-Carb 2900TR) and PP was calculated after Parsons et al., (1984). Dark carbon fixation (DCF) rates were used to estimate bacterial biomass production using a conversion factor of 190 mol POC (mol CO_2)$^{-1}$ fixed (Molari et al., 2013).

A reciprocal transplant experiment was conducted in water from 1 m and 15 m depth under the sea ice to test for fertilizing effects of glacial front water at stations SG and IE. At each site, incubations were made where half of the initial water volume was replaced with sterile filtered (0.2 µm) seawater of either the same station or the other station, excluding physical effects (light, temperature, sediment load). These samples were incubated and processed together with the other PP incubations at the adequate depths as described above.

2.5 Statistics and bioinformatics

Silicate, phosphate and NO_X concentrations were plotted against salinities and correlation were tested via linear regression analysis using the lm function in R (R Core Team, Vienna, Austria). P values were corrected for multiple testing using the false discovery rate. Since the primary production estimates of the reciprocal transplant experiments were not normally distributed, came from a nested design, and had heterogeneous variance, a robust nested Analysis of variance (ANOVA) was

performed to test for significant treatment effects of incubation water with water depth as nested variable. The map was created in R using the PlotSvalbard v0.9.2 package (Vihtakari, 2020). The Svalbard basemap was retrieved from the Norwegian Polar institute (2020, CC BY 4.0 license), the pan-Arctic map was retrieved from Natural Earth (2020, CC Public domain license), and the bathymetric map was retrieved from the Norwegian mapping authority (Kartverket, 2020, CC BY 4.0 license).

16S sequences were analysed using a pipeline modified after Atienza et al. (2020) based on OBITools v1.01.22 (Boyer et al., 2014). The raw reads were demultiplexed and trimmed to a median phred quality score minimum of 40 and sequence lengths between 215bp and 299bp (16S rRNA) or between 90 and 150bp (18S rRNA) and merged. Chimaeras were removed using uchime with a minimum score of 0.9. The remaining merged sequences were clustered using swarm (Mahe et al., 2014). 16S swarms were classified using the RDP classifier (Wang et al., 2007) and 18S swarms using the sina aligner (Pruesse et al., 2012) with the silva SSU 138.1 database (Quast et al., 2012). Further multivariate analyses were done in R using the vegan package. The non-metric multidimensional scaling (NMDS) plots are based on Bray-Curtis dissimilarities and were used to visualize differences between groups (brackish water at SG – Fjord water, sea ice – seawater). Analysis of Similarities (ANOSIM) were done to test for differences of the communities between the groups (999 permutations, Bray-Curtis dissimilarities).

3 Results

3.1 Physical parameters

The physical conditions of sea ice (temperature T/bulk salinity S) and surface water (uppermost 4 m under the sea ice, T and S) at the freshwater inflow impacted site SG differed substantially from NG and IE. The sea ice and the upper 4 m under the sea ice were having consistently lower salinities (<8 PSU) and higher temperatures (-0.4 ˚C to -0.2 ˚C) at SG compared to NG and IE and also compared to the deeper water masses at SG (salinity > 34.6 PSU, temperature < -1.4 ˚C)(Fig. 2c,d). Sea ice melt was unlikely because the measured water temperatures and sea ice temperatures were below freezing point considering the sea ice bulk salinity. The water column at SG was highly stratified with a low salinity 4 m thick layer under the sea ice, separated by a sharp ca 1 m thick pycnocline (Fig. 2c,d). In contrast, the water column at IE was fully mixed and at NG only a minor salinity drop from 34.6 to 33.6 PSU occurred within the the upper 50 cm under the sea ice (Fig. 2c,d). Sea ice temperature and salinity showed similar variations between the three sites with SG ice having lower salinities and higher temperatures relative to sea ice at the other stations (Fig. 2a,b). At SG, bulk salinities were mostly below 0.7 PSU and calculated brine salinities below 14 PSU, except for the uppermost 40 cm where bulk salinities reached around 1.5 PSU and a brine salinity of 32 PSU (Fig. 2). This resulted in very low brine volume fractions below 5 %, except for the lowermost 10 cm with brine volume fractions up to 9 % (Supplementary table S1). At IE and NG, bulk salinities are mostly above 5 PSU (>40 PSU brine salinity) and temperatures were below -0.4 ˚C, which led to brine volume fractions above 6 % in all samples and above 10 % in the bottom 30 cm.

The homogenous temperature and salinity water column profiles at IE and NG stations indicate the presence of only one water mass (Local Arctic water, Skogseth et al., 2020). The only additional water mass was subglacial meltwater (salinity of 0 PSU) mixed into the surface layer of SG. Applying a simple mixing model based on the two salinities (IE= 34.6 PSU, Glacier= 0 PSU) provide an estimation of the fraction of glacially derived water in the surface layer of ca. 85 % in the uppermost 2 m under the sea ice, before decreasing to 0 % at 4 m under the sea ice below the strong halocline. The water sample taken 1 m under the sea ice had a fraction of 32 % glacial meltwater (Table 1). For NG, glacial derived water contributed only 3 % in the first 50 cm under the sea ice.

The SG station was 33 m deep and about 180 m away from the glacier front. The sea ice was 1.33 m thick and covered by 3 cm of snow. The ice appeared clear with some minor sediment and air bubble inclusions and missed a skeletal bottom layer. In the water column, a higher potential sediment load was observed as a turbidity peak at the halocline (Fig. 3). Direct evidence of subglacial outflow had been observed at the southern site of the glacier in form of icing and liquid water flowing onto the sea ice in April 2018, April 2019 and October 2019, but this form of subglacial outflow froze before reaching the fjord, which was additionally blocked by sea ice. The sea ice temperature was between -0.4 ˚C at the bottom and -1.7 ˚C at the top (Fig. 2b).

NG was 27 m deep and about 360 m away from the glacier front. The sea ice was thinner (0.92 m) and the snow cover thicker (6 cm) compared to SG. The ice had a well developed skeletal layer at the bottom with brown coloration due to algal biomass. The ice temperature ranged between -2 ˚C at the bottom to -2.7 ˚C at the top (Fig. 2b). The IE station was about 75 m deep and 50 m away from the ice edge. The sea ice was thinnest (0.79 m) and the snow cover thickest (10 cm). Sea ice temperatures were coldest ranging from -2.2 ˚C at the bottom to -3.1 ˚C on the top (Fig. 2b). Loosely floating ice algae aggregates were present in the water directly under the ice. The recorded surface PAR irradiance were similar during the primary production incubation times at SG and IE (SG: average=305 µE m^{-2} s^{-1}, min=13 µE m^{-2} s^{-1}, max=789 µE m^{-2} s^{-1}; IE: average=341 µE m^{-2} s^{-1}, min=37 µE m^{-2} s^{-1}, max=909 µE m^{-2} s^{-1}). Using published attenuation coefficients irradiance directly under the ice was 5 µE m^{-2} s^{-1} at IE and higher at SG with 9 µE m^{-2} s^{-1} due to the thinner snow cover.

3.2 Nutrient variability in sea ice and water

Overall, nutrient concentrations were highest in the bottom water (4.0- 4.5 µmol L^{-1} $Si(OH)_4$, 9.1- 9.6 µmol L^{-1} NO_X, 0.7-0.8 µmol L^{-1} PO_4) and depleted at the surface and in the sea ice with the exception of the under-ice water (UIW, 0- 1 cm under the sea ice) of SG, where NO_X (10 µmol L^{-1}) and silicate (19 µmol L^{-1}) levels were exceptionally high (Fig. 4). We cannot exclude anomalies or sampling artifacts to be responsible for the high values, and therefor used the values measured 1 m under the sea ice for further calculations in this manuscript as surface water reference. SG had overall higher levels of silicate and NO_X compared to the IE at both 1 m below the sea ice (factors of 3 for $Si(OH)_4$ and 2 for NO_X) and bottom ice (factor of 18 for $Si(OH)_4$ and 3 for NO_X compared to IE bottom ice) (Fig. 4). Silicate concentrations deeper in the water column were similar at all the stations with values of ca 4 µmol L^{-1} . Close to the surface silicate was reduced to 1.6 µmol L^{-1} at 1 m at the IE, while it stayed at 4.3 µmol L^{-1} at SG (Fig. 4a). In the water column, NO_X and phosphate gradients were similar between the sites.

However in sea ice, NO_X concentrations were more than two times higher at SG than at the IE. In the bottom 30 cm of sea ice all nutrients had higher concentrations at SG, except for phosphate, which was depleted in the bottom 3 cm of SG, but not in the bottom of IE sea ice. In the ice interior in 50- 70 cm distance from the ice bottom, also the other nutrients were depleted at SG, before rising slightly towards the surface of the ice. N:P ratios were generally highest at SG with values above 40, exceeding Redfield ratios in the surface water and sea ice. N:P ratios at the IE were below Redfield in the entire water column and bottom sea ice with values ranging from 10 to 13. A slight increase in NO_X was observed at the sea ice-atmosphere interface at NG and SG. Subglacial outflow water and glacial ice had relatively low nutrient levels (in glacial ice: $Si(OH)_4$ < 0.3 µmol L^{-1}, NO_X < 0.9 µmol L^{-1}, PO_4 < 0.75 µmol L^{-1}, in outflow: $Si(OH)_4$ <1.5- 2.0, NO_X 1.8- 2.3 µmol L^{-1}, PO_4 < 0.1 µmol L^{-1}), but the nutrient concentrations in subglacial outflow water were higher than in most sea ice samples and the depleted surface water (1 m under the sea ice) at the IE.

Nutrient versus salinity profiles can give indications of the endmembers (sources) of the nutrients (Fig. 5). In general, a linear correlation indicates conservative mixing. A positive correlation indicates higher concentrations of the nutrients of the saline Atlantic water endmember, while a negative correlation points to a higher concentrations in the fresh glacial meltwater endmember. Biological uptake and remineralisation could eliminate the correlation, indicating non-conservative mixing. In the water column at NG and IE silicate (R^2=0.66, p=0.008), NO_X (R^2=0.62, p=0.01) and phosphate (R^2=0.69, p=0.005) showed conservative positive mixing patterns with a higher contribution of Atlantic water (Fig. 5a-c). SG showed a negative correlation for silicate pointing to a higher contribution of glacial meltwater (R^2=0.86, p<0.0001) and no correlations for NO_X and PO_4 indicating non-conservative mixing (Fig. 5d-f). At SG, silicate concentrations were higher with lower salinities. The same pattern was observed in sea ice, scaled to brine salinities, with higher silicate and NO_X concentrations in the fresher SG ice, compared to NG and IE (Fig. 5g-i). However, the R^2 value were lower in particular for $Si(OH)_4$ (NO_X: R^2=0.18, p=0.059; $Si(OH)_4$: R^2=0.41, p=0.002).

The contribution of nutrients by upwelling as well as freshwater inflow from glacial meltwater was estimated by linear mixing calculations. At 1 m below the sea ice, about 32 % of the water was derived from glacial meltwater based on salinity-based mixing of glacial meltwater and local Arctic water (Table 1). The remaining 68 % came from either bottom water upwelling (25 m at SG as reference) or entrained surface water (IE values at 1 m under the sea ice as reference). Based on a similar estimation for inorganic nutrients, 58 % of NO_X and 48 % of PO_4 was provided by subglacial upwelling (Table 1). For silicate, higher concentrations were required in the bottom water of subglacial meltwater at the glacier front to explain the very high surface concentrations measured. Considering the estimated NO_X and PO_4 fractions, the overall fraction of nutrients derived from upwelling was about 53 %. The overall budget 1 m under the sea ice is was 32 % glacial meltwater, 53 % subglacial upwelling (deep water), and 15 % horizontal transport (surface water).

3.3 Carbon cycle

Net primary productivity (NPP) was overall one order of magnitude higher at SG than at IE, with the highest production value occurring within the brackish layer under the ice at SG (5.27 mg m^{-3} d^{-1}, Fig. 6, 7). Within this layer, also Chl values were

about two times higher compared to IE (21 mg m^{-3} at SG, 9.1 mg m^{-3} at IE), and also the Chl-specific productivity in this layer exceeded values at the other stations (Table 2). Within sea ice, a slightly different pattern emerged. While the primary productivity in the bottom sea ice (0–3 cm) was two times higher at SG compared to IE, Chl values were two order of magnitudes lower (Fig. 6). This indicates high Chl-specific production at SG (5.6 mg C mg Chl d^{-1} in the sea ice and 11.4 mg C mg Chl d^{-1} integrated over 25 m depth). At the IE, the contribution of released ice algae to algal biomass in the water column was higher and the overall vertical Chl flux was about 1.5 times higher than at SG at 25 m depth. Bacterial biomass was comparable at both stations with higher biomass concentrations within the ice than in the water column. Bacterial activity (based on DCF) was comparable in the bottom sea ice at the two sites; however, it was 63x higher in the brackish surface water of SG leading to very high growth rate estimates (Table 2) of 6 mg C m^{-3} d^{-1}.

Integrated Chl values over the uppermost 25 m of the water column were nearly identical for SG and IE with values of about 3.75 mg Chl m^{-2} (Table 2). The fraction of Chl was highest at IE (85 %) and lowest at the SG (30 %) (Table 2). The integrated NPP was considerably higher at SG (42.6 mg C m^{-2} d^{-1} at SG, 0.2 mg C m^{-2} d^{-1} at IE), while the vertical export of Chl was about three times higher at IE than SG. This leads to more (14 times) vertical export based on the sediment trap measurements than production at IE and considerably lower (5 %) export than production at SG (Table 2). Relative to the standing stock biomass of Chl at IE, 0.2 % of the Chl was renewed daily by NPP at IE and 3 % was vertically exported daily at IE, which would relate - assuming absence of grazing and advection – a daily loss of 3 % of the standing stock Chl. At SG, 38 % was renewed per day, while 2 % were exported. This leads to an accumulation of biomass of 38 % per day, and a doubling time of about 2.6 days. Bacterial growth doubling times were estimated to be between minutes (SG water) and days (IE water), but within hours in sea ice (Table 2).

Considering the N demand based on the carbon based PP measurement (16 mol C mol N^{-1} after Redfield, 1934), about 2 µmol N L^{-1} $month^{-1}$ (equivalent to 32 % of 1 m value for NO_X) was needed to sustain the PP measured at SG. Assuming constant PP and steady state nutrient conditions, 32 % of the surface water had to be replaced by subglacial upwelling per month to supply this N demand via upwelling. Since only 62 % of the upwelling water was entrained bottom water the actual vertical water replenishment rate would be 52 % per month. Assuming a 2 m freshwater layer under the ice, this translates to flux of about 1.1 m^3 m^{-2} $month^{-1}$. Considering the distance of 250 m to the glacier front and a width of 1.6 km of the SG bay, this translates to a minimum of about 422,000 m^3 $month^{-1}$.

The results from the reciprocal transplant experiment (Fig. 7) showed clearly that the higher NPP at SG, compared to NG was related to the nutrient concentrations (nested ANOVA, p=0.0038, F=10.88). In any combination, sterile filtered water from the SG had a fertilising effect, increasing PP of IE communities by approx. 30 %. SG communities of the most active fresh surface layer fixed twice as much CO_2 when incubated in the same water, compared to incubations in the IE water.

3.4 Bacterial, archaeal and eukaryotic communities

After bioinformatic processing 13,043 bacterial and archaeal (16S rRNA) OTUs, belonging to 1,208 genera with between 9,708 and 331,809 reads were retained. Differences between the bacterial 16S sequences of the various sample types indicated

that they can be used as potential markers for the origin of the water (Fig. 8). The first non-metric multidimensional scaling (NMDS1) axis separated sea ice from water communities (ANOSIM, p=0.004, R=0.35) with no overlapping samples (Fig. 8a). Generally IE and NG communities were very similar, while sea ice and under-ice water communities at SG were significantly different (ANOSIM, p=0.001, E=0.593) from the other fjord samples. The second NMDS2 axis separated communities along a gradient from subglacial communities towards fjord communities, with SG communities being in between fjord and subglacial communities (Fig. 8a). Bacterial communities at SG in the bottom layer of the sea ice and the brackish water layer were more similar to subglacial outflow communities than the other samples in both 2018 and 2019. Six OTUs were unique to the glacial outflow and SG surface (*Fluviimonas*, *Corynebacterineae*, *Micrococcinae*, *Hymenobacter*, *Dolosigranuum*), which are 6.6 % of their OTUs. The community structure of supraglacial ice samples was very different from any other sample. Also in the most abundant genera clear differences can be detected (Fig. S1). *Flavobacterium* sp. was most abundant in sea ice and UIW samples in both 2018 and 2019 at SG, but rare or absent in the other samples. *Aliiglaciecola* sp. was characteristic for NG sea ice and UIW samples. *Paraglaciecola* sp. was abundant in NG and IE sea ice and UIW samples, and *Colwellia* sp. was abundant in all sea ice and UIW samples. In sea water samples the genus *Amphritea* sp. was more abundant. *Pelagibacter* sp. was abundant in all samples. Glacial outflow water was dominated by *Sphingomonas* sp. and glacier ice by *Halomonas* sp., which were rare or absent in the other samples.

The eukaryotic community (18S rRNA) consisted of 4,711 OTUs, belonging to 535 genera, with between 2,204 and 15,862 reads. Overall, the same NMDS clustering has been found as for the 16S rRNA sequencing. We found distinctive communities in the sea ice and 1 m layer under the sea ice at SG being significantly different (ANOSIM, p=0.001, R=0.456) to the other samples (Fig. 8c). In fact, the SG surface communities were more similar to the outflow community (Fig. 8c). The clear differentiation between all sea ice and water column communities was also visible in the 18S rRNA samples (ANOSIM, p=0.005, R=0.192). As for the 16S communities, also the abundant genera differed between the groups (Fig. S2). The cryptophytes *Hemiselmis* sp. and Geminigeraceae were abundant at SG, but rare at the other sites. Dinophyceae, Imbricatea (*Thaumatomastix* sp.) and Bacillariophyceae were abundant in all samples with diatoms being mostly more abundant in sea ice or UIW. The Chytridiomycota family of Lobulomycetaceae were abundant in water samples from 2018, but not 2019. Subglacial outflow water was dominated by unclassified Cercozoa and *Bodomorpha* sp..

In total 22 different taxa were detected by microscopy. The communities composition was clearly separated between sea ice and water samples. Furthermore species composition at SG station differed from NG and IE (Fig. 8b). SG sea ice was completely dominated by unidentified flagellates (potentially *Hemiselmis* sp., Geminigeraceae, and *Thaumatomastix* sp. based on 18S sequences), with the exception of the 70–90 cm layer with high abundances of *Leptocylindrus minimus*. Sea ice samples at NG and IE were dominated by *Navicula* sp. and *Nitzschia frigida*. Water samples were more diverse with abundance of *Fragillariopsis* sp., *Coscinodiscus* sp., and *Chaetoceros* sp.. Overall, diatoms dominated most samples at NG and IE in sea ice and water samples.

4 Discussion

The hydrography, sea ice properties, water chemistry and bacterial communities at SG provide clear evidence for subglacial upwelling at a shallow tidewater outlet glacier under sea ice, a system previously not considered for subglacial upwelling processes. Briefly, our first hypothesis that subglacial upwelling persists also in winter/spring, supplying nutrient-rich glacial meltwater and upwelling of bottom fjord water to the surface has been confirmed as discussed in detail below.

4.1 Indications for subglacial upwelling

The physical properties at SG were distinctly different to stations NG and IE. In contrast to NG and IE, the marine terminating SG site had a brackish surface water layer of 4 m thickness under the sea ice and low sea ice bulk salinities below 1.5 PSU comparable to sea ice in the nearby tidewater glacier influenced Tempelfjorden (Fransson et al., 2020) and in brackish Baltic sea ice (Granskog et al., 2003). We excluded surface melt or river run off as freshwater sources for the following reasons. With air temperatures below freezing point during the sampling periods, surface runoff based on snowmelt was not possible and no melting was observed during field work. In addition, no major river flow into the main bay studied (Adolfbukta), as indicated by small catchment areas (Norsk Polarinstitutt, 2020). We did observe some subglacial runoff at the southern site of the glacier (close to SG), however this outflow water froze before it reached the fjord, which was additionally blocked by a 1.33 m thick sea ice cover. The sea ice cover would also block any inputs by atmospheric precipitation, considering the impermeable sea ice conditions especially at SG with brine volume fractions below 5 % (Golden et al., 1998; Fransson et al., 2020). Additional potential freshwater sources could be related to basal glacial ice melt of glacier fronts (Holmes et al., 2019; Sutherland et al., 2019) or icebergs (Moon et al., 2018). However, in the absence of Atlantic water inflow, which is blocked in Billefjorden by a shallow sill depth at the entrance of Billefjorden (Skogseth et al., 2020), water temperatures were consistently below freezing point (max -0.2 ˚C) and no Atlantic inflow water was detected at any station, which does not allow basal glacial ice to melt. Subglacial meltwater itself is unlikely to lead to basal ice melting due to its low salinity. However, basal ice melt is likely more important in systems with Atlantic water inflows, such as Greenland or Svalbard fjords without a shallow sill (e.g. Kongsfjorden and Tunabreen, Holmes et al., 2019). Sea ice may melt at lower temperatures compared to glacial ice, but the absence of typical sea ice algae in the water column at SG and the low salinity of the sea ice indicated that this was not the case. In fact, sea ice with a salinity of 1.5 PSU (measured at SG) would melt at -0.08 ˚C (Fofonoff et al., 1983), but the water and ice temperatures did not exceed -0.2 ˚C. Consistent with our study Fransson et al. (2020) also found substantial amount of freshwater in the sea ice in Tempelfjorden (approx. 50 % meteoric water fraction) in a year with large glacier meltwater contribution further supporting the presence of subglacial upwelling under sea ice. Fransson et al. (2020) suggested the combination of low salinities with high silicate concentrations as indicator for glacial meltwater, which was also the case in our study. In addition, the overall low sea ice salinity and sediment inclusions at SG cannot be explained by sea ice melt, but must originate from another source.

4.2 Potential magnitude of subglacial upwelling

Considering the slow tidal currents in our study area (<22 m per 6 h tidal period, Kowalik et al., 2015) and wind mixing blocked by sea ice, a potential source of the freshwater within Billefjorden may be remains from the previous melting season. Hence, the question of how much subglacial meltwater reaches the surface at SG is important. We estimated that the fresh surface water was most likely exchanged on time scales of days to weeks. Even slow vertical mixing would be capable to erode the halocline in over six months since the last melting season. The turbidity peak we observed at the halocline would also settle out in a short time (weeks), if not replenished by fresh inputs (Meslard et al., 2018). Vertical export flux was determined to account for approximately 4% of the Chl standing stock at 25 m. Considering that glacial sediment settles typically substantially faster than phytoplankton due its higher density this suggests that the turbidity peak would erode within days to weeks without fresh sediment input via upwelling (Meslard et al., 2018). Furthermore, the inorganic nitrogen demand for the measured primary productions would consume the present nutrients in a few (approx. 2) months. Assuming steady state, the nutrient uptake by phytoplankton primary production would require an upwelling driven water flux of at least 1.1 m^3 m^{-2} $month^{-1}$.

Microbial communities (16S rRNA and 18S rRNA) in SG UIW and sea ice were similar to the subglacial outflow water. Bacterial communities (16S rRNA) at SG shared 6.6 % of their OTUs with subglacial outflow communities, which is twice as much as NG and IE (3.6 %) shared with the outflow communities. Considering the estimated bacterial growth rates and biomass at SG the doubling time of the bacteria would be between 0.5 h and 7 h. However, the use of a conversion factor for biomass production based on sediment bacterial data is adding uncertainty to the estimation of the bacterial doubling time. Estimates reported from Kongsfjorden in April are indeed longer (3-10 days, Iversen & Seuthe, 2010), as are other Arctic bacterioplankton doubling time estimates ranging between 1.2 days (Rich et al., 1997), 2.8 days (de Kluijver et al., 2013) and weeks (2 weeks, Rich et al., 1997; 1 week, Kirchman et al., 2005).

Based on the growth in the range of hours to days, the distinctive community at SG would have changed to a more marine community on time scales of weeks, assuming only growth of marine OTUs at SG and settling out or grazing of inactive glacial bacteria taxa. Consequently, the presence of shared OTUs between SG and the glacial outflow indicates a constant supply of fresh inoculum to sustain these taxa. The clearest evidence for outflow comes from the visual observations of subglacial outflow exiting the southern part of the glacier in October 2019, April 2018 and April 2019 which we assume also occurred under the marine terminating front. In fact, subglacial outflows in spring have been observed at various other Svalbard glaciers with runoff originating from meltwater stored under the glacier from the last melt season and released by changes in hydrostatic pressure or glacier movements (Wadham et al., 2001). Active subglacial drainage systems in winter have also been described elsewhere, and can be sustained by geothermal heat or frictional dissipation, groundwater inputs, or temperate ice in the upper glacier (Wilson 2012; Schoof et al., 2014). This meltwater has also been found to be rich in silicate due to the long contact with the subglacial bedrock during its storage over winter (Wadham et al., 2001; Fransson et al., 2020). We therefore suggest

that winter and spring subglacial upwelling is not unique to Billefjorden, but likely occurs at all polythermal or warm based marine-terminating glaciers.

The amount of upwelling was estimated using hydrographic data. In our study, three water masses were distinguished; i) subglacial outflow (SGO) with low salinity (0 PSU) relatively high temperatures (>0 ˚C) and high silicate concentrations (Cape et al.,2019), (ii) deep local Arctic water (DLAW) with low temperatures (-1.7 ˚C) high salinities (34.6 PSU) and high nutrient concentrations (Skogseth et al., 2020), and iii) surface local Arctic water (SLAW) with the same temperature and salinity signature as the DLAW, but depleted in nutrients (Skogseth et al., 2020). Our mixing calculations estimate that 32 % of the SG water 1 m under the sea ice was derived by SGO, which pulled 1.6 times more (53 %) DLAW with it during upwelling. Fransson et al. (2020) found that 30-60 % of glacier derived meltwater was incorporated in the bottom sea ice at the glacier front of Tempelfjorden, again indicating that this is a widespread process at marine terminating glacier fronts.

4.3 Importance of subglacial upwelling under sea ice

Compared to the massive subglacial plumes of summer systems (250-500 $m^3\ s^{-1}$, Carroll et al., 2016), subglacial upwelling in spring is a small volume transport with only about >1.1 $m^3\ m^{-2}\ month^{-1}$ (approx. 2 $m^3\ s^{-1}$) upwelling needed to sustain measured surface primary production. This rough, but conservative estimate translates to a freshwater input for Billefjorden of at least 1.76 x 10^5 $m^3\ day^{-1}$, which is one order of magnitude lower than summer values at Kronebreen (2.7 × 10^6 $m^3\ day^{-1}$, Halbach et al., 2019), a Svalbard tidewater glacier of similar size. In our study, each volume of SGO water pulled about the same volume of DLAW with it to the surface (Entrainment factor of 1.6 – see above). This value is low compared to other entrainment factor estimates ranging mostly between 6 and 10 (Hopwood et al., 2020). The entrainment factor is mostly dependent on the depth of the glacier front (Carroll et al., 2016), which can explain the low rate at Nordenskiöldbreen in Billefjorden, with an estimated depth of 20 m at the terminus (based on CTD cast at terminus in April 2018, data not shown). Kronebreen with a glacier terminus depth of about 70 m and an entrainment factor of 3 is the most comparable tidewater glacier to Nordenskiöldbreen, where these fluxes were estimated. Although entrainment rate was low, it substantially increased summer primary production in Kongsfjorden (Halbach et al., 2019). In spite of the low discharge and entrainment rate of our study, subglacial upwelling appears to be the main mechanism to replenish bottom water with high nutrient concentrations to the surface and can substantially increase spring primary production due to; i) the absence of any other terrestrials inputs, ii) Atlantic water blocked by a shallow sill (Skogseth et al., 2020), iii) very weak tidal currents (Kowalik et al., 2015), and iv) wind mixing blocked by sea ice in Billefjorden.

4.4 Importance for under-ice phytoplankton

Our main finding was that i) higher irradiance, ii) a stratified surface layer, and iii) increased nutrient supply via subglacial upwelling allowed increased phytoplankton primary production at SG. Surprisingly, the ice edge station (IE) was light and nutrient limited and supported a lower phytoplankton primary production.

4.4.1 Increased light

Despite the substantial subglacial upwelling, the negative effect of light limitation with the massive sediment plumes in summer (Pavlov et al., 2019) were not observed in spring. We did measure a small turbidity peak under the SG sea ice, but the values were comparable to open fjord systems in summer (Meslard et al., 2018, Pavlov et al., 2019), where light is not considered limiting for photosynthesis. Under-ice phytoplankton blooms are typically limited by light, which is attenuated and reflected by the snow and sea ice cover (Fortier et al., 2002, Mundy et al., 2009, Ardyna et al., 2020). Some blooms have been observed, mostly under snow-free sea ice, such as after snow melt (Fortier et al., 2002), under melt ponds (Arrigo et al., 2012, Arrigo et al., 2014), after rain events (Fortier et al., 2002), or at the ice edge related to ice edge driven upwelling (Mundy et al., 2009). In our study however, light levels available for phytoplankton growth were low compared to other under-ice phytoplankton bloom studies (Mundy et al., 2009, Arrigo et al., 2012), but higher at SG than at IE. This can be explained through the combined effects of sea ice and snow properties at SG. Light attenuation in low salinity sea ice is typically lower due to a lower brine volume (Arst and Sipelgas, 2004). Also, lower sea ice algae biomass and thinner snow cover due to snow removal with katabatic winds (e.g. Braaten 1997; Laska et al., 2012) leads to less light attenuation and lower albedo. Our estimates showed that about twice as much light reached the water at SG compared to the IE, in spite of the thicker sea ice cover and the estimated light levels of 5 and 9 µE m^{-2} s^{-1} were above the minimum irradiance (1 µE m^{-2} s^{-1}) required for primary production (Mock & Gradinger, 1999). Hence, the increased light under the brackish sea ice at SG could be one factor explaining the under-ice phytoplankton bloom observed.

4.4.2 Stratified surface layer

The strong stratification at SG is another factor; allowing phytoplankton to stay close to the surface, where light is available, allowing a bloom to form. In fact, Lowry et al. (2017) found that convective mixing by brine expulsion in refreezing leads can inhibit phytoplankton blooms even in areas with sufficient under-ice light and nutrients. At the same time, they found moderate phytoplankton blooms under snow covered sea ice (1–3 mg Chl m^{-3}), which was, however, still an order of magnitude lower than the SG values. Our finding of a higher vertical flux at IE compared to SG shows that stronger stratification may indeed be a contributing factor for the higher phytoplankton biomass at SG due to lower loss rate. However, our reciprocal transplant experiment clearly showed, that location alone (light, stratification) could not explain the increased primary production, but that the water properties at SG had a fertilising effect on algal growth, most probable because of higher nutrient levels, which were limiting at IE.

4.4.3 Upwelling of nutrients

Algal growth at IE was co-limited by lower irradiance as well as nutrient concentrations. Dissolved inorganic nitrogen (DIN) to phosphate rations (N:P) at the IE were mostly below Redfield ratios (16:1), especially in sea ice with DIN concentrations below 1 µmol L^{-1}, indicating potential nitrogen limitations (Ptacnik et al., 2010), while the N:P ratio at SG was balanced and

close to Redfield. Silicate concentrations below 2 µmol L^{-1} are typically considered limiting for diatom growth (Egge & Aksnes, 1992) and this threshold had been reached at UIW and sea ice (concentration estimate in brine volume) at IE, but not at SG. This indicates that nitrate supplied by deep water upwelling and silicate by combined upwelling and additions from the glacial run off had a fertilising effect on the SG water.. High silicate values have been observed at glacier fronts in other areas such as the Greenland fjords (Azetsu-Scott and Syvitski, 1997) and Tempelfjorden (Fransson et al., 2015:2020). Iron has not been measured, but is an essential micronutrient, often enriched in subglacial meltwater (Bhatia et al., 2013, Hopwood et al., 2020). However, iron limitation is unlikely in these systems (Krisch et al., 2020). Besides the subglacial upwelling, nutrient concentrations may simply be higher due to the shallower water depth at SG compared to IE, facilitating vertical mixing down to the bottom. However, NG was slightly shallower than SG and algal growth was still limited by nutrients. Besides, silicate and nitrate showed negative correlations with salinity, when including SG samples. In fact, these nutrients only correlated positively with salinity at IE and NG, while at SG, the negative correlations or non-conservative mixing are indicative for subglacial upwelling (mainly N and Si) and/or meltwater input (for Si) (Hopwood et al., 2020). Biological nutrient uptake did not play a significant role, due to relatively low bacterial and primary production. The subglacial outflow water itself was poor in nitrate, but high in silicate due to the interaction with the bedrock and long residence time below the glacier (Wadham et al., 2001), which was also found in the Tempelfjorden (Fransson et al., 2015; 2020). Nordenskiöldbreen has a mix of metamorphic bedrock including silicon rich gneiss, amphibolite, and quartzite, but also carbonate rich marble (Strzelecki, 2011), which can partly contribute to the high silicate levels observed. The role of bedrock derived minerals and particles for composition of sea ice chemistry have been described in detail by Fransson et al. (2020). The values in subglacial outflow water were lower (<1.5 – 2 µmol L^{-1}) compared to estimates in Greenland (Meire et al., 2016a, Hawkings et al., 2017, Hatton et al., 2019), indicating that direct fertilisation in spring may be even more important in other tidewater glacier influenced fjords. Another potential source may be higher silicate concentrations in the sediments at SG (Hawkings et al., 2017). However, bottom water values were similar between SG and IE, showing a limited role of higher silicate inputs from sediment, presumably due to silicate-poor subglacial bedrock.

Another nitrogen source may be ammonium, which has been related to subglacial upwelling in Kongsfjorden (Halbach et al., 2019). Ammonium regeneration and subsequent nitrification (Christman et al., 2011), may explain the exceptionally high nitrate concentration of the UIW at SG, which can be part of the explanation for the high N:P ratios. In fact, bacterial activity was higher at SG potentially allowing higher ammonium recycling. Another explanation for the high N:P ratios and low phosphate concentrations can be related to phosphate scavenging by iron, as discussed by Cantoni et al. (2020). Atmospheric inputs of N have been shown in the Baltic Sea, but thinner sea ice and warm periods with increased sea ice permeability were needed for the N to reach the brine pockets or water column (Granskog et al., 2003). Our NO_X profiles show some evidence of atmospheric N deposition, but only at NG and SG, which may be related to precipitation or surface flooding. For under-ice phytoplankton, these atmospheric N inputs play no role, but may have benefitted the high algae biomass layer in the upper ice parts of SG. Overall, the clearest evidence of nutrient limitations and fertilisation by subglacial upwelling was demonstrated with the reciprocal transplant experiment, which showed an approx. 30 % increase in primary production related to SG water.

Overall, primary production at SG was an order of magnitude higher than at IE. This indicates that both fertilisation by subglacial upwelling and increased light play a role in increasing phytoplankton primary production.

4.4.4 Increased phytoplankton primary production

The integrated primary production to 25 m at SG was 42.6 mg C m^{-2} d^{-1} which is low compared to other marine terminating glacier influenced fjord systems in summer with integrated NPP of 480 ±403 mg C m^{-2} d^{-1} (Hopwood et al., 2020). Also studies in the same month (April) observed higher primary production rates in a marine-terminating glacier influenced fjord system, such as Kongsfjorden (405 mg C m^{-2} d^{-1}, Hopwood et al., 2020). However, none of these systems was sea ice covered during the studies and therefore not limited by light compared to our study. Under sea ice, phytoplankton communities have typically much lower NPP rates of 20–310 mg C m^{-2} d^{-1} with only about 10 % or less light transmission reaching the water column (Mundy et al., 2009). These values are more comparable to the SG values, despite the lower light transmission (3 %). In the central Arctic, higher under-ice NPP has been observed, but always related to high light transmission due to the absence of ice, or under melt ponds with light transmissions up to 59 % (Arrigo et al., 2012). However, in the sea ice area north of Svalbard, Assmy et al. (2017) found substantial spring PP below relatively thick sea ice caused by leads. This was also confirmed by large CO_2 decrease due to primary production under the sea ice (Fransson et al., 2017). Phytoplankton production under snow covered Arctic sea ice is often considered negligible compared to sea ice algae or summer production. This can be shown in low biomass, mostly consisting of settling sea ice algae (Leu et al., 2015), or very low NPP rates (e.g. Pabi et al., 2008). The same has been observed under Baltic sea ice with similar low light levels and primary production between 0.1–5 mg C m^{-2} d^{-1} under snow covered ice and about 30 mg C m^{-2} d^{-1} under snow-free sea ice (Haecky & Andersson, 1999). These values are comparable to the IE without subglacial meltwater influence, but an order of magnitude lower than the SG production. Moderate blooms of 1–3 mg Chl m^{-3} have been described under snow covered sea ice with equal (3 %) light transmission (Lowry et al., 2017). Lowry et al. (2017) argues that a stratified water column and sufficient nutrients allow moderate blooms even under these low light conditions. Our study found Chl values up to an order of magnitude higher than Lowry et al. (2017), showing that under-ice phytoplankton blooms are indeed important under snow covered sea ice and can be facilitated by subglacial upwelling.

Our study is the first to show that the combination of several factors (stratified water column, increased light and supply of fresh nutrients via tidewater glacier driven processes) can support a rather productive under-ice phytoplankton community, exceeding biomass and production of under-ice phytoplankton in systems with comparable light levels. Besides the increased and extended primary production fuelled by tidewater glacier, the active and abundant phytoplankton taxa in surface water with consistently replenished nutrients, may be a viable seed community for summer phytoplankton blooms, once the sea ice disappears and light levels increase (Hegseth et al., 2019). The significantly different community at SG may also contribute to a more diverse seed community available to the entire fjord, compared to fjords without spring subglacial upwelling.

4.5 Impact on sea ice algae

4.5.1 Impact on biomass and primary production

While phytoplankton biomass and production were clearly enhanced at SG, exceeding levels of other snow covered under-ice systems, sea ice algal biomass and activity had been differently affected. Our third hypothesis suggested lower sea ice algae biomass and production at SG due to the lower brine volume fractions. In agreement with our hypothesis, algal biomass was indeed an order of magnitude lower compared to the IE and NG. However, their production was two times higher, showing more efficient photosynthesis.

Compared to most other sea ice studies conducted at the same period of the year, typically representing the mid-bloom phase with 10–20 mg Chl m^{-2} (Leu et al., 2015), Chl biomass was very low at all stations of our study (<0.32 mg Chl m^{-2}). Only Greenland fjords (0.1-3.3 mg Chl m^{-2}) or pre- and post-bloom systems had comparably low biomass (Mikkelsen et al., 2008, Leu et al., 2015). The significantly different communities with high number of cryptophyte flagellates, a high proportion of phaeophytin (14–68 % in the bottom 3 cm), and the high contribution of sea ice algae in the water column indicate that we sampled indeed a post-bloom situation. Considering the low air, sea ice and water temperatures and the absence of a fresh UIW layer at the IE, the bloom was most likely not terminated by bottom ice erosion but limited by nutrients. In fact, SG bottom ice was deficient in phosphate (0.27 µmol (L brine)$^{-1}$), while the IE was deficient in silicate (1 µmol (L brine)$^{-1}$) and nitrogen (N:P = 1 mol N mol P^{-1}). This finding fits to earlier studies where phosphate limitations had been described as limiting for brackish sea ice algae at concentrations below 0.27 µmol L^{-1} (Haecky and Andersson, 1999), while N and Si limitations are typical for Arctic sea ice algae (Gradinger, 2009). The low concentrations of phosphate in the subglacial meltwater would partly explain the low concentration in SG sea ice. In addition, most studies summarized by Leu et al. (2015) were done 10 years or more prior our measurements. Hence, an earlier sea ice algae bloom and the earlier termination observed in our study may be related to thinner sea ice due to the warmer climate. In fact, the Greenland study by Mikkelsen et al. (2008) with comparable sea ice algae biomass had the thinnest sea ice cover of 0.5 m sampled in the warmest year (2006). During our study, the weather station in Longyearbyen measured a mean temperature of –3.9 °C in April 2019, which was 8.3 °C above average and the second warmest average April temperature recorded after April 2006 (0.1 °C), indicating that a warmer climate may explain the earlier bloom termination (yr.no).

Similar to algal biomass, primary production (approx. 0.01 mg C m^{-2} d^{-1} at SG and 0.005 mg C m^{-2} d^{-1} at IE, assuming 10 cm productive bottom layer) was considerably lower than in most studies of Arctic sea ice (0.8–55 mg C m^{-2} d^{-1} in the Barents Sea) mentioned by Leu et al.(2015). Only algal aggregates (Assmy et al., 2013) and Baltic sea ice (Haecky & Andersson, 1999) measured similarly low production rates indicating that the senescence of the bloom (aggregates) and brine volume fraction (Baltic Sea) were factors contributing to low primary production in sea ice.

4.5.2 Stressors in brackish sea ice

In addition to the post bloom status of the bloom, the lower biomass at SG can be partly explained by the lower brine salinity. Permeability of sea ice is typically related to salinity and temperature, which determine the brine volume. With a brine volume fraction below 5 %, or temperature below -5 °C and salinity below 5 PSU, sea ice is considered impermeable (Golden et al., 1998). At SG, temperatures were higher, but a brine volume fraction above 5 % was only found in bottom ice sections (7–9 %), indicating that the brine channels are weakly connected and algae had limited inhabitable place and nutrient supply (Granskog et al., 2003), especially in the upper layers of the sea ice. In more saline systems, such as the Chuckchi or Beaufort Sea a high flux of seawater through the ice (0.4–19 m^3 seawater m^{-2} sea ice) has been discussed as crucial to allow continuous primary production and accumulation of biomass (Gradinger, 2009). In impermeable ice, this flux is eliminated. However, the algal biomass at SG was very low, even compared to other brackish sea ice system, such as the Baltic Sea with similar or lower brine volume fractions and comparable light levels (Granskog et al., 2003: 3-6 mg Chl m^{-3}; Haecky & Andersson, 1999: 1.2 mg Chl m^{-2}), indicating that other stressors played a role at SG. Grazing is assumed to be a minor control on algae production and biomass in Arctic sea ice (Gradinger, 2002). However, grazing by heterotrophic flagellates on small primary producers has been described as important in the Baltic Sea, indicating that it might plays a role at SG as well (Haecky & Andersson, 1999). SG sea ice communities were indeed dominated by small flagellate algae (microscopy based) and a high proportion of potential grazers (18S rRNA data). Other stressors, such as phosphate limitation, viral lysis, or osmotic stress related to episodic outbursts of subglacial meltwater are likely additional factors explaining the low biomass.

DIC has also been described as potentially limiting for sea ice primary production, especially towards the end of the bloom (Haecky & Andersson, 1999) and may be supplied with the carbonate rich subglacial outflow (Fransson et al., 2020). Higher mortality due to factors mentioned above, together with the higher measured bacterial activity, allowing recycling of nutrients may be another factor explaining higher production with lower Chl biomass. Last, nutrients may have been replenished recently via advective processes when the brine volume fraction was higher.

At SG another layer of potentially high activity has been found in the upper sea ice. In this layer, depleted nutrient concentrations correspond with high *Leptocylindrus minimus* abundances indicating that these algae were actively taking up the nutrients, despite the impermeable sea ice. NO_X concentrations increased towards the surface and bottom indicating inputs from surface flooding above (Granskog et al., 2003) and seawater below. Silicate and phosphate were only supplied from the seawater below. The observed brine volume fractions below 5 % would not allow inputs of these nutrients, but episodes with higher temperatures and thereby higher brine volume fractions may be sufficient to supply the needed nutrients to this distinctive layer.

Overall, sea ice influenced by subglacial outflow was very similar to other brackish sea ice such as in the Baltic Sea in regard to structure, biomass and production (Haecky & Andersson, 1999, Granskog et al., 2005). Compared to Arctic sea ice the effect was negative on sea ice algae biomass due to low brine volume fractions, phosphate limitation and potentially higher mortality via grazing and possibly higher osmotic stress.

5 Outlook

Our study showed that even a shallow marine-terminating glacier can lead to increased under-ice phytoplankton production by locally enhanced light levels, stronger stratification and nutrient supply by subglacial upwelling, which are all factors expected to change due to climate change. While most of our evidence is circumstantial, the number of different evidence leading to the same conclusion makes our findings rather robust. We propose that our findings are applicable to other tidewater glaciers with a polythermal or warm base, as is common on Svalbard, but also on Greenland (Hagen et al., 1993; Irvine-Fynn et al., 2011). With a changing climate, tidewater glaciers will retreat and transform towards land terminating glaciers (Błaszczyk et al., 2009). In winter and spring, this would result in the lack of subglacial upwelling and systems more similar to the IE with less nutrients and light available for phytoplankton. The local effect would reduce primary production, biomass and bacterial production in the water column, but higher biomass of sea ice algae with the known Arctic taxa of pennate diatoms. The pelagic/sympagic benthic coupling would be stronger supporting the benthic food web. Winter and spring subglacial upwelling is most likely present at all polythermal or warm-based marine-terminating glaciers, which includes glacier termina with much deeper fronts, much higher entrainment rates of bottom water, and higher silicate concentrations in glacial meltwater (Hopwood et all., 2020). Thus, the effect of spring subglacial upwelling is likely more pronounced in other fjords. Additional effects of climate change include increased precipitation in the Arctic, which would reduce light levels below the sea ice. However, also land-terminating glaciers would allow snow removal by katabatic wind as discussed for Nordenskiöldbreen. Another impact of climate change will be the reduction of sea ice and Atlantification of fjords, leading to increased light, and wind mixing. In the ice free Kongsfjorden, higher primary production rates have been measured in the same month, indicating that the lack of sea ice may lead to increased overall primary production (Iversen & Seuthe, 2010). However, Kongsfjorden is still influenced by subglacial upwelling, supplying nutrients for the bloom (Halbach et al., 2017). In systems not affected by subglacial upwelling the additional light will most likely not lead to substantially higher primary production as indicated by lower measured rates in these type of fjords (Hopwood et al., 2020). Since the entrainment in our study occurs at only approximately 20 m depth, upwelling under sea ice-free conditions would have much less effect, since wind induced mixing plays a more important role and the fjord is likely more nitrate than silicate limited, due to the later stage of the spring bloom.

6 Acknowledgements

The field was funded by the individual Arctic field grants of the Svalbard Science forum for TV, UD, CD, and EH (project numbers: 282622 (TV, UD, CD), 282600 (TV), 296538 (EH), 281806 (UD)). Additional, funding for lab work and analyses was obtained by the ArcticSIZE - A research group on the productive Marginal Ice Zone at UiT (grant no. 01vm/h15). JE was also supported by the the Ministry of Education, Youth and Sports of the Czech Republic ECOPOLARIS, project No. CZ.02.1.01/0.0/0.0/16_013/0001708 and the Institute of Botany CAS (grant no. RVO 67985939). The publication charges for this article have been partly funded by a grant from the publication fund of UiT The Arctic University of Norway.

We also wish to thank Jan Pechar, Jiří Štojdl, and Marie Šabacká for field assistance; and Janne Søreide, Maja Hatlebekk, Christian Zoelly, Marek Brož, Stuart Thomson, and Tore Haukås for field work preparation help. We are also acknowledged to Melissa Brandner, Paul Dubourg, and Claire Mourgues for the help in the lab and Owen Wangensteen for the help with bioinformatics analyses. We are thankful for the meteorological data of Petuniabukta supplied by Kamil Laska.

7 Authors contributions

TRV designed the experiments, formulated the hypotheses and developed the sampling design with contributions of CD and UD, and RG. Fieldwork was conducted by TRV, UD, CD, EH, and JE with support by RG and EP for preparations. Lab analyses were done by TRV, UD, EP, CD, MC and EH. Computational analyses were performed by TRV. The manuscript has been prepared by TRV with contributions of all co-authors.

8 Data availability

Environmental data have been archived at Dataverse under the doi number https://doi.org/10.18710/MTPR9E. 18S and 16S rRNA sequences have been archived at the European Nucleotide archive under the project accession number PRJEB40294. The R and unix code for the statistical and bioinformatics analyses are available from the corresponding author upon request. More detailed reports of the fieldwork are available in the Research in Svalbard database under the RiS-ID 10889.

9 Competing interests

The authors declare that they have no conflict of interest.

References

Ambrožová, K., and Láska, K.: Air temperature variability in the vertical profile over the coastal area of Petuniabukta, central Spitsbergen, Polish Polar Research, 41-60, 2017.

Amundson, J. M., and Carroll, D.: Effect of topography on subglacial discharge and submarine melting during tidewater glacier retreat, Journal of Geophysical Research: Earth Surface, 123(1), 66-79, 2018.

Ardyna, M., Mundy, C. J., Mills, M. M., Oziel, L., Grondin, P. L., Lacour, L., Verin, G., Van Dijken, G., Ras, J., Alou-Font, E., Babin, M., Gosselin, M., Tremblay, J. É., Raimbault, P., Assmy, P., Nicolaus, M., Claustre, H. and Arrigo, K.R.: Environmental drivers of under-ice phytoplankton bloom dynamics in the Arctic Ocean, Elem Sci Anth, 8(1), 30, DOI: http://doi.org/10.1525/elementa.430, 2020.

Arrigo, K. R., Perovich, D. K., Pickart, R. S., Brown, Z. W., vanDijken, G. L., Lowry, K. E., Mills, M. M., Palmer, M. A., Balch,W. M., Bahr, F., Bates, N. R., Benitez-Nelson, C., Bowler, B.,Brownlee, E., Ehn, J. K., Frey, K. E., Garley, R.,

Laney, S.R., Lubelczyk, L., Mathis, J., Matsuoka, A., Mitchell, G. B.,Moore, G. W. K., Ortega-Retuerta, E., Pal, S., Polashenski, C.M., Reynolds, R. A., Schieber, B., Sosik, H. M., Stephens, M.,P., and Swift, J. H.: Massive phytoplankton blooms under Arctic sea ice, Science, 336, 1408, https://org/10.1126/science.1215065, 2012.

Arrigo, K. R., Arrigo, K. R., Perovich, D. K., Pickart, R. S., Brown, Z. W., van Dijken, G. L., Lowry, K. E., Mills, M. M., Palmer, M. A., Balch, W. M., Bates, N. R., Benitez-Nelson, C. R., Brownlee, E., Frey, K. E., Laney, S. R., Mathis, J., Matsuoka, A., Mitchell, B. G., Moore, G. W. K., Reynolds, R. A., Sosik, H. A., Swift, J. H.: Phytoplankton blooms beneath the sea ice in the Chukchi Sea, Deep Sea Res. Part II Top. Stud. Oceanogr., 105, 1-16, https://org/10.1016/j.dsr2.2014.03.018, 2014.

Arst, H., and Sipelgas, L.: In situ and satellite investigations of optical properties of the ice cover in the Baltic Sea region, in: Proceedings of the Estonian Academy of Sciences, Biology and Ecology, edited by: Aben, H., and Kurnitski, V., Estonian Academy of Sciences, Tallinn, 25-36, 2004.

Assmy, P., Ehn, J. K., Fernández-Méndez, M., Hop, H., Katlein, C., Sundfjord, A., Bluhm, K., Daaase, M., Engel, A., Fransson, A., Granskog, M. A., Hudson, S. R., Kristiansen, S., Nicolaus, M., Peeken, I., Renner, A. H. H., Spreen, G., Tatarek, A., and Wiktor, J.: Floating ice-algal aggregates below melting Arctic sea ice, PLoS ONE, 8(10), e76599, https://org/10.1371/journal.pone.0076599, 2013.

Assmy, P., M. Fernández-Méndez, P. Duarte, A. Meyer, A. Randelhoff, C. J. Mundy, L. M. Olsen, H. M. Kauko, A. Bailey,and Chierici, M.: Leads in Arctic pack ice enable early phytoplankton blooms below snow-covered sea ice,Scientific reports, 7, 40850, 2017.

Atienza, S., Guardiola, M., Præbel, K., Antich, A., Turon, X., and Wangensteen, O. S.: DNA Metabarcoding of Deep-Sea Sediment Communities Using COI: Community Assessment, Spatio-Temporal Patterns and Comparison with 18S rDNA, Diversity, 12(4), 123, https://org/10.3390/d12040123, 2020.

Azetsu-Scott, K., and Syvitski, J. P. M.: Influence of melting icebergs on distribution, characteristics and transport of marine particles in an East Greenland fjord, Journal of Geophysical Research 104 (C3), 5321–5328, 1999.

Bhatia, M. P., Kujawinski, E. B., Das, S. B., Breier, C. F., Henderson, P. B., and Charette, M. A.: Greenland meltwater as a significant and potentially bioavailable source of iron to the ocean, Nat Geosci, 6(4), 274-278, https://org/10.1038/ngeo1746, 2013.

Błaszczyk, M., Jania, J. A., and Hagen, J. O.: Tidewater glaciers of Svalbard: Recent changes and estimates of calving fluxes, Pol Polar Res, 2, 85-142, 2009.

Boyer, F., Mercier, C., Bonin, A., Le Bras, Y., Taberlet, P., and Coissac, E.: obitools: A unix-inspired software package for DNA metabarcoding, Mol Ecol Resour, 16(1), 176-182, https://org/10.1111/1755-0998.12428, 2016.

Braaten, D. A.: A detailed assessment of snow accumulation in katabatic wind areas on the Ross Ice Shelf, Antarctica, J Geophys Res Atmos, 102(D25), 30047-30058, https://org/10.1029/97JD02337, 1997.

Cantoni, C., Hopwood, M. J., Clarke, J. S., Chiggiato, J., Achterberg, E. P., and Cozzi, S.: Glacial drivers of marine biogeochemistry indicate a future shift to more corrosive conditions in an Arctic fjord, Journal of Geophysical Research: Biogeosciences, e2020JG005633, https://doi.org/https://doi.org/10.1029/2020JG005633, 2020.

Carroll, D., Sutherland, D. A., Hudson, B., Moon, T., Catania, G. A., Shroyer, E. L., Nash, J. D., Bartholomaus, T. C., Felikson, D., Stearns, L. A., Noël, B. P. Y., and van den Broeke, M. R.: The impact of glacier geometry on meltwater plume structure and submarine melt in Greenland fjords, Geophys. Res. Lett., 43, 9739–9748, https://doi.org/10.1002/2016GL070170, 2016.

Chandler, D. M., Wadham, J. L., Lis, G. P., Cowton, T., Sole, A., Bartholomew, I., Telling, J., Nienow, P., Bagshaw, E.B., Mair, D., Vinen, S., and Hubbard A.: Evolution of the subglacial drainage system beneath the Greenland Ice Sheet revealed by tracers, Nat Geosci, 6(3), 195-198, https://org/10.1038/ngeo1737, 2013.

Christman, G. D., Cottrell, M. T., Popp, B. N., Gier, E., and Kirchman, D. L.: Abundance, diversity, and activity of ammonia-oxidizing prokaryotes in the coastal Arctic Ocean in summer and winter, Appl. Environ. Microbiol., 77(6), 2026-2034, https://org/10.1128/AEM.01907-10, 2011

Cloern, J. E., Grenz, C., and Vidergar-Lucas, L.: An empirical model of the phytoplankton chlorophyll: carbon ratio-the conversion factor between productivity and growth rate, Limnol. Oceanogr., 40(7), 1313-1321, https://org/10.4319/lo.1995.40.7.1313, 1995.

Cox, G. F., and Weeks, W. F.: Equations for determining the gas and brine volumes in sea-ice samples, J Glaciol, 29(102), 306-316, https://org/10.3189/S0022143000008364, 1983.

De Kluijver, A., Soetaert, K., Czerny, J., Schulz, K. G., Boxhammer, T., Riebesell, U., and Middelburg, J. J.: A 13C labelling study on carbon fluxes in Arctic plankton communities under elevated CO2 levels, Biogeosciences, 10(3), 1425-1440, 2013.

Dickson, A. G., Sabine, C. L., and Christian, J. R.: Guide to best practices for ocean CO2 measurements, PICES Special Publication 3, 2007.

Dowdeswell, J. A.: On the nature of Svalbard icebergs, J Glaciol, 35(120), 224-234, https://org/10.3189/S002214300000455X, 1989.

Egge, J. K., and Aksnes, D.L.: Silicate as regulating nutrient in phytoplankton competition, Mar Ecol Prog ser. Oldendorf, 83, 281-289, https://org/10.3354/meps083281, 1992.

Esau, I., and Repina, I.: Wind climate in Kongsfjorden, Svalbard, and attribution of leading wind driving mechanisms through turbulence-resolving simulations, Advances in Meteorology, https://org/10.1155/2012/568454, 2012.

Fransson, A., Chierci, M., Nomura, D., Granskog, M. A., Kristiansen, S., Martma, T., and Nehrke, G.: Influence of glacialwater and carbonate minerals on wintertime sea-ice biogeochemistry and the CO2 system in an Arctic fjord in Svalbard, Annals of Glaciology, 1–21, https://doi.org/10.1017/aog.2020.52, 2020.

Fransson, A., Chierici, M., Skjelvan, I., Olsen, A., Assmy, P., Peterson, A., Spreen, G., and Ward, B.: Effect of sea-ice and biogeochemical processes and storms on under-ice water fCO2 during the winter-spring transition in thehigh Arctic Ocean: implications for sea-air CO2 fluxes, J. Geophys. Res. Oceans, 122, 5566–5587, doi: 10.1002/2016JC012478, 2017.

Fofonoff, P., and Millard R. C.: Algorithms for computation of fundamental properties of seawater, Unesco Technical Papers in Marine Science, 44, 53, http://hdl.handle.net/11329/109, 1983.

Fortier, M., Fortier, L., Michel, C., and Legendre, L.: Climatic and biological forcing of the vertical flux of biogenic particles under seasonal Arctic sea ice, Mar. Ecol. Prog. Ser., 225, 1-16, https://org/10.3354/meps225001, 2002.

Garrison, D. L., and Buck, K. R.: Organism losses during ice melting: a serious bias in sea ice community studies, Polar Biol 6:237-239, 1986.

Golden, K. M., Ackley, S. F., and Lytle, V. I.: The percolation phase transition in sea ice, Science, 282(5397), 2238-2241, https://org/10.1126/science.282.5397.2238, 1998.

Gradinger, R.: Sea ice microorganisms, Encyclopedia of environmental microbiology, Wiley, https://org/10.1002/0471263397.env310, 2003.

Gradinger, R.: Sea-ice algae: Major contributors to primary production and algal biomass in the Chukchi and Beaufort Seas during May/June 2002, Deep Sea Res. Part II Top. Stud. Oceanogr., 56(17), 1201-1212, https://org/10.1016/j.dsr2.2008.10.016, 2009.

Granskog, M. A., Kaartokallio, H., and Shirasawa, K.: Nutrient status of Baltic Sea ice: Evidence for control by snow-ice formation, ice permeability, and ice algae, J Geophys Res Oceans, 108(C8), https://org/10.1029/2002JC001386, 2003.

Guardiola, M., Uriz, M. J., Taberlet, P., Coissac, E., Wangensteen, O. S., and Turon, X.: Deep-sea, deep-sequencing: metabarcoding extracellular DNA from sediments of marine canyons, PloS one, 10(10), e0139633, 2015.

Haecky, P., and Andersson, A.: Primary and bacterial production in sea ice in the northern Baltic Sea, Aquat Microb Ecol, 20(2), 107-118, https://org/10.3354/ame020107, 1999.

Hagen, J. O., Liestøl, O., Roland, E., and Jørgensen, T.: Glacier Atlas of Svalbard and Jan Mayen, Oslo: Norwegian Polar Institute, 1993.

Halbach, L., Vihtakari, M., Duarte, P., Everett, A., Granskog, M. A., Hop, H., Kauko, H. M., Kristiansen, S., Myhre, P. I., Pavlov, A. K., Pramanik, A., Tatarek, A., Torsvik, T., Wiktor, J. M., Wold, A., Wulff, A., Steen, H., Assmy, P.: Tidewater glaciers and bedrock characteristics control the phytoplankton growth environment in a fjord in the arctic, Front Mar Sci, 6, 254, https://org/10.3389/fmars.2019.00254, 2019.

Hatton, J. E., Hendry, K. R., Hawkings, J. R., Wadham, J. L., Kohler, T. J., Stibal, M., Beaton, A. D., Bagshaw, E. A., and Telling, J.: Investigation of subglacial weathering under the Greenland Ice Sheet using silicon isotopes, Geochim Cosmochim Acta, 247, 191-206, https://org/10.1016/j.gca.2018.12.033, 2019.

Hawkings, J. R., Wadham, J. L., Benning, L. G., Hendry, K. R., Tranter, M., Tedstone, A., Nienow, P., and Raiswell, R.: Ice sheets as a missing source of silica to the polar oceans, Nat. Commun, 8(1), 1-10, https://org/10.1038/ncomms14198, 2017.

Hegseth, E. N., Assmy, P., Wiktor, J. M., Wiktor, J., Kristiansen, S., Leu, E., Tverberg, V., Gabrielsen, T. M., Skogseth, R., and Cottier, F.: Phytoplankton seasonal dynamics in Kongsfjorden, Svalbard and the adjacent shelf, in: The Ecosystem of Kongsfjorden, Svalbard, edited by: Hop, H., and Wiencke, C., Springer, Cham., 173-227, 2019.

Hodal, H., Falk-Petersen, S., Hop, H., Kristiansen, S., and Reigstad, M.: Spring bloom dynamics in Kongsfjorden, Svalbard: nutrients, phytoplankton, protozoans and primary production, Polar Biol 35, 191–203, https://doi.org/10.1007/s00300-011-1053-7, 2012.

Hodgkins, R.: Glacier hydrology in Svalbard, Norwegian high arctic, Quat Sci Rev, 16(9), 957-973, https://org/10.1016/S0277-3791(97)00032-2, 1997.

Holmes, F. A., Kirchner, N., Kuttenkeuler, J., Krützfeldt, J., and Noormets, R.: Relating ocean temperatures to frontal ablation rates at Svalbard tidewater glaciers: Insights from glacier proximal datasets, Sci. Rep, 9(1), 1-11, https://org/10.1038/s41598-019-45077-3, 2019.

Hopwood, M. J., Carroll, D., Dunse, T., Hodson, A., Holding, J. M., Iriarte, J. L., Ribeiro, S., Achterberg, E. P., Cantoni, C., Carlson, D. F., Chierici, M., Clarke, J. S., Cozzi, S., Fransson, A., Juul-Pedersen, T., Winding, M. S. and Meire, L.: How does glacier discharge affect marine biogeochemistry and primary production in the Arctic?, Cryosphere, 14, 1347-1383, https://org/10.5194/tc-14-1347-2020, 2020.

Irvine-Fynn, T. D., Hodson, A. J., Moorman, B. J., Vatne, G., & Hubbard, A. L.: Polythermal glacier hydrology: A review, Reviews of Geophysics, 49(4), 2011.

Iversen, K. R., and Seuthe, L.: Seasonal microbial processes in a high-latitude fjord (Kongsfjorden, Svalbard): I. Heterotrophic bacteria, picoplankton and nanoflagellates, Polar Biol, 34(5), 731-749, https://org/10.1007/s00300-010-0929-2, 2011.

Jones, E., Chierici, M., Skjelvan, I., Norli, M., Børsheim, K. Y., Lødemel, H. H., Sørensen, K., King, A. L., Lauvset, S., Jackson, K., de Lange, T., Johannsessen, T., and Mourgues, C.: Monitoring ocean acidification in Norwegian seas in 2018, Miljødirektoratet, M-1417|2019, 2019.

Kanna, N., Sugiyama, S., Ohashi, Y., Sakakibara, D., Fukamachi, Y., and Nomura, D.: Upwelling of macronutrients and dissolved inorganic carbon by a subglacial freshwater driven plume in Bowdoin Fjord, northwestern Greenland, J Geophys Res Biogeosci, 123(5), 1666-1682, https://org/10.1029/2017JG004248, 2018.

Kartverket, https://kartkatalog.geonorge.no/metadata/kartverket/dybdedata/2751aacf-5472-4850-a208-3532a51c529a, last access: 10 August 2020.

Kirchman, D. L., Malmstrom, R. R., and Cottrell, M. T.: Control of bacterial growth by temperature and organic matter in the Western Arctic, Deep Sea Research Part II: Topical Studies in Oceanography, 52(24-26), 3386-3395, 2005.

Kowalik, Z., Marchenko, A., Brazhnikov, D., and Marchenko, N.: Tidal currents in the western Svalbard Fjords, Oceanologia, 57(4), 318-327, https://org/10.1016/j.oceano.2015.06.003, 2015.

Krisch, S., Browning, T. J., Graeve, M., Ludwichowski, K.U., Lodeiro, P., Hopwood, M. J., Roig, S., Yong, J. C., Kanzow, T., and Achterberg, E. P.: The Influence of Arctic Fe and Atlantic Fixed N on Summertime Primary Production in Fram Strait, North Greenland Sea, Sci. Rep, 10 (1), 15230, https://doi.org/10.1038/s41598-020-72100-9, 2020.

Leppäranta, M., and Manninen, T.: The brine and gas content of sea ice with attention to low salinities and high temperatures, Finnish Institute of Marine Research Internal Report, 2, 1-15, 1988.

Láska, K., Witoszová, D., and Prošek, P.: Weather patterns of the coastal zone of Petuniabukta, central Spitsbergen in the period 2008–2010, Polish Polar Research, 297-318, 2012.

Leu, E., Mundy, C. J., Assmy, P., Campbell, K., Gabrielsen, T. M., Gosselin, M., Juul-Pedersen, T., and Gradinger, R.: Arctic spring awakening–Steering principles behind the phenology of vernal ice algal blooms, Prog Oceanogr, 139, 151-170, https://org/10.1016/j.pocean.2015.07.012, 2015.

Lowry, K. E., Pickart, R. S., Selz, V., Mills, M. M., Pacini, A., Lewis, K. M., Joy-Warren, H., Nobre, C., van Dijken, G. L., Grondin, P., Ferland, J., and Arrigo, K. R.: Under-ice phytoplankton blooms inhibited by spring convective mixing in refreezing leads, J Geophys Res Oceans, 123(1), 90-109, https://org/10.1002/2016JC012575, 2018.

Lydersen, C., Assmy, P., Falk-Petersen, S., Kohler, J., Kovacs, K. M., Reigstad, M., Stehen, H., Strøm, H., Sundfjord, A., Varpe, Ø., Walczowski, W., Weslawski, K. M., and Zajaczkowski, M.: The importance of tidewater glaciers for marine mammals and seabirds in Svalbard, Norway, J Marine Sys, 129, 452-471, https://org/10.1016/j.jmarsys.2013.09.006, 2014.

Maes, S.: Polar cod population structure: connectivity in a changing ecosystem, Ph.D. thesis, KU Leuven, Leuven, Belgium, 2017.

Mahé, F., Rognes, T., Quince, C., de Vargas, C., and Dunthorn, M.: Swarm: robust and fast clustering method for amplicon-based studies, PeerJ, 2, e593, https://org/10.7717/peerj.593, 2014

Massicotte, P., Bécu, G., Lambert-Girard, S., Leymarie, E., and Babin, M.: Estimating underwater light regime under spatially heterogeneous sea ice in the Arctic, Appl. Sci., 8(12), 2693, https://org/10.3390/app8122693, 2018.

Meire, L., Meire, P., Struyf, E., Krawczyk, D. W., Arendt, K. E., Yde, J. C., Juul Pedersen, T., Hopwood, M. J., Rysgaard, S., and Meysman, F. J. R.: High export of dissolved silica from the Greenland Ice Sheet, Geophys. Res. Lett., 43, 9173–9182, https://doi.org/10.1002/2016GL070191, 2016a.

Meire, L., Mortensen, J., Rysgaard, S., Bendtsen, J., Boone, W., Meire, P., and Meysman, F. J.: Spring bloom dynamics in a subarctic fjord influenced by tidewater outlet glaciers (Godthåbsfjord, SW Greenland), J Geophys Res Biogeosci, 121(6), 1581-1592, https://org/10.1002/2015JG003240, 2016b.

Meslard, F., Bourrin, F., Many, G., and Kerhervé, P.: Suspended particle dynamics and fluxes in an Arctic fjord (Kongsfjorden, Svalbard), Estuarine, Estuar Coast Shelf S, 204, 212-224, https://org/10.1016/j.ecss.2018.02.020, 2018.

Mock, T., and Gradinger, R.: Determination of Arctic ice algal production with a new in situ incubation technique, Mar. Ecol. Prog. Ser., 177, 15-26, https://org/10.3354/meps177015, 1999.

Molari, M., Manini, E., and Dell'Anno, A.: Dark inorganic carbon fixation sustains the functioning of benthic deep-sea ecosystems, Global Biogeochem Cycles, 27(1), 212-221, https://org/10.1002/gbc.20030, 2013.

Moon, T., Sutherland, D. A., Carroll, D., Felikson, D., Kehrl, L., and Straneo, F.: Subsurface iceberg melt key to Greenland fjord freshwater budget, Nat Geosci, 11(1), 49-54, https://org/10.1038/s41561-017-0018-z, 2018.

Mundy, C. J., Barber, D. G., and Michel, C.: Variability of snow and ice thermal, physical and optical properties pertinent to sea ice algae biomass during spring, J Marine Sys, 58(3-4), 107-120, https://org/10.1016/j.jmarsys.2005.07.003, 2005.

Mundy, C. J., Gosselin, M., Ehn, J., Gratton, Y., Rossnagel, A., Barber, D. G., Martin, J., Tremblay, J., Palmer, M., Arrigo, K. R., Darnis, G., Fortier, L., Else, B., Papakyriokou, T.: Contribution of under-ice primary production to an ice-edge upwelling phytoplankton bloom in the Canadian Beaufort Sea, Geophys. Res. Lett, 36(17), https://org/10.1029/2009GL038837, 2009.

Natural Earth, http://www.naturalearthdata.com/, last access: 10 August 2020.

Norwegian Polar institute, Toposvalbard, https://toposvalbard.npolar.no, last access: 16 Septemper 2020.

Pabi, S., van Dijken, G. L., and Arrigo, K. R.: Primary production in the Arctic Ocean, 1998–2006, J Geophys Res Oceans, 113(C8), https://org/10.1029/2007JC004578, 2008.

Parada, A. E., Needham, D. M., and Fuhrman, J. A.: Every base matters: assessing small subunit rRNA primers for marine microbiomes with mock communities, time series and global field samples, Environ. Microbiol, 18(5), 1403-1414, https://org/10.1111/1462-2920.13023, 2016.

Parsons, T. R., Maita, Y. and Lalli, C. M. (Eds.): A Manual of Chemical and Biological Methods for Seawater Analysis. Pergamon Press, Toronto, 1984.

Pavlov, A. K., Leu, E., Hanelt, D., Bartsch, I., Karsten, U., Hudson, S. R., Gallet, J., Cottier, F., Cohen, J. H., Berge, J., Johnsen, G., Maturilli, M., Kowalczuk, P., Sagan, S., Meler, J., and Granskog, M. A.: The underwater light climate in Kongsfjorden and its ecological implications, in: The Ecosystem of Kongsfjorden, Svalbard, edited by: Hop, H., and Wiencke, C., Springer, Cham., 137-170, 2019.

Perovich, D. K., Roesler, C. S., and Pegau, W. S.: Variability in Arctic sea ice optical properties, J Geophys Res Oceans, 103(C1), 1193-1208, https://org/10.1029/97JC01614, 1998.

Porter, K. G., and Feig, Y. S.: The use of DAPI for identifying and counting aquatic microflora1, Limnol Oceanogr, 25, 943–948, https://wiley.com/10.4319/lo.1980.25.5.0943, 1980.

Pruesse, E., Peplies, J., and Glöckner, F. O.: SINA: accurate high-throughput multiple sequence alignment of ribosomal RNA genes, Bioinformatics, 28(14), 1823-1829, 2012.

Ptacnik, R., Andersen, T., and Tamminen, T.: Performance of the Redfield ratio and a family of nutrient limitation indicators as thresholds for phytoplankton N vs. P limitation, Ecosystems, 13(8), 1201-1214, https://org/10.1007/s10021-010-9380-z, 2010.

Quast, C., Pruesse, E., Yilmaz, P., Gerken, J., Schweer, T., Yarza, P., Replies, J., and Glöckner, F. O.: The SILVA ribosomal RNA gene database project: improved data processing and web-based tools. Nucleic acids research, 41(D1), D590-D596, 2012.

Redfield, A. C.: On the proportions of organic derivatives in sea water and their relation to the composition of plankton, In James Johnstone Memorial Volume, 176–192. Liverpool University Press, 1934.

Rich, J., Gosselin, M., Sherr, E., Sherr, B., and Kirchman, D. L.: High bacterial production, uptake and concentrations of dissolved organic matter in the Central Arctic Ocean, Deep Sea Research Part II: Topical Studies in Oceanography, 44(8), 1645-1663, 1997.

Sager, J. C., and Mc Farlane, J. C.: Radiation, in: Plant growth chamber handbook, edited by: Langhans, R. W., and Tibbits, T. W., Iowa Agr. Home Econ. Expt. Sta. Special Rpt, 99, 1-29, 1997.

Schaffer, J., and Kanzow, T.: von Appen, W. J.; von Albedyll, L.; Arndt, J. E.; Roberts, D. H. Bathymetry Constrains Ocean Heat Supply to Greenland's Largest Glacier Tongue, Nat. Geosci, 13(3), 227-231, https://doi.org/10.1038/s41561-019-0529-x, 2020.

Schoof, C., Rada, C. A., Wilson, N. J., Flowers, G. E., and Haseloff, M.: Oscillatory subglacial drainage in the absence of surface melt, The Cryosphere, 8(3), 959-976, 2014.

Skogseth, R., Olivier, L. L., Nilsen, F., Falck, E., Fraser, N., Tverberg, V., Ledang, A. B., Vader, A., Jonassen, M. O., Søreide, J., Cottier, F., Berge, J., Ivanov, B. V., and Falk-Petersen, S.: Variability and decadal trends in the Isfjorden (Svalbard) ocean climate and circulation-an indicator for climate change in the European Arctic, Prog Oceanogr, 187, 102394, https://org/10.1016/j.pocean.2020.102394, 2020.

Southwood, T. R. E. and Henderson, P. A. (Eds.): Ecological methods, John Wiley and Sons, 269, 2000.

Strzelecki, M. C.: Schmidt hammer tests across a recently deglacierized rocky coastal zone in Spitsbergen-is there a "coastal amplification" of rock weathering in polar climates?, Pol Polar Res, 239-252, https://org/10.2478/v10183−011−0017−5, 2011.

Sutherland, D. A., Pickart, R. S., Peter Jones, E., Azetsu-Scott, K., Jane Eert, A., and Ólafsson, J.: Freshwater composition of the waters off southeast Greenland and their link to the Arctic Ocean, J Geophys Res Oceans, 114(C5), https://org/10.1029/2008JC004808, 2009.

Throndsen, J., Hasle, G. R., & Tangen, K. (Eds.): Phytoplankton of Norwegian coastal waters, Almater Forlag AS, 2007.

Tomas, C. R. (Ed.): Identifying Marine Phytoplankton, Elsevier, San Diego, 1997.

Utermöhl, H.: Methods of collecting plankton for various purposes are discussed, SIL Commun 1953-1996. 9, 1–38, https://doi.org/10.1080/05384680.1958.11904091, 1958.

Vihtakari, M.: PlotSvalbard: PlotSvalbard - Plot research data from Svalbard on maps. R package version 0.9.2, https://github.com/MikkoVihtakari/PlotSvalbard, 2020.

von Quillfeldt, C. H.: Common diatom species in Arctic spring blooms: their distribution and abundance, Bot Mar, 43(6), 499-516, https://org/10.1515/BOT.2000.050, 2000.

von Quillfeldt, C. H., Ambrose, W. G., and Clough, L. M.: High number of diatom species in first-year ice from the Chukchi Sea, Polar Biol, 26(12), 806-818, https://org/10.1007/s00300-003-0549-1, 2003.

Vonnahme, T. R., Devetter, M., Žárský, J. D., Šabacká, M., and Elster, J.: Controls on microalgal community structures in cryoconite holes upon high Arctic glaciers, Svalbard, Biogeosciences, 13, 659-674, https://org/10.5194/bg-13-659-2016, 2016.

Wadham, J. L., Hodgkins, R., Cooper, R. J., and Tranter, M.: Evidence for seasonal subglacial outburst events at a polythermal glacier, Finsterwalderbreen, Svalbard, Hydrol. Process., 15(12), 2259-2280, https://org/10.1002/hyp.178, 2001.

Wang, Q., Garrity, G. M., Tiedje, J. M., and Cole, J. R.: Naive Bayesian Classifier for Rapid Assignment of rRNA Sequences into the New Bacterial Taxonomy, Appl Environ Microbiol. 73(16), 5261-7, https://org/ 10.1128/AEM.00062-07, 2007.

Wangensteen, O. S., Palacín, C., Guardiola, M., and Turon, X.: DNA metabarcoding of littoral hard-bottom communities: high diversity and database gaps revealed by two molecular markers, PeerJ, 6, e4705, https://org/10.7717/peerj.4705, 2018.

Wiedmann, I., Reigstad, M., Marquardt, M., Vader, A., and Gabrielsen, T. M.: Seasonality of vertical flux and sinking particle characteristics in an ice-free high arctic fjord—Different from subarctic fjords?, J Marine Sys, 154, 192-205, https://org/10.1016/j.jmarsys.2015.10.003, 2016.

Wilson, N.: Characterization and interpretation of polythermal structure in two subarctic glaciers, Doctoral dissertation, Science: Department of Earth Sciences, 2012.

yr.no, Longyearbyen – historikk, https://www.yr.no/nb/historikk/graf/1-2759929/Norge/Svalbard/Svalbard/Longyearbyen?q=2019-04, last access: 24 July 2020.

Figures

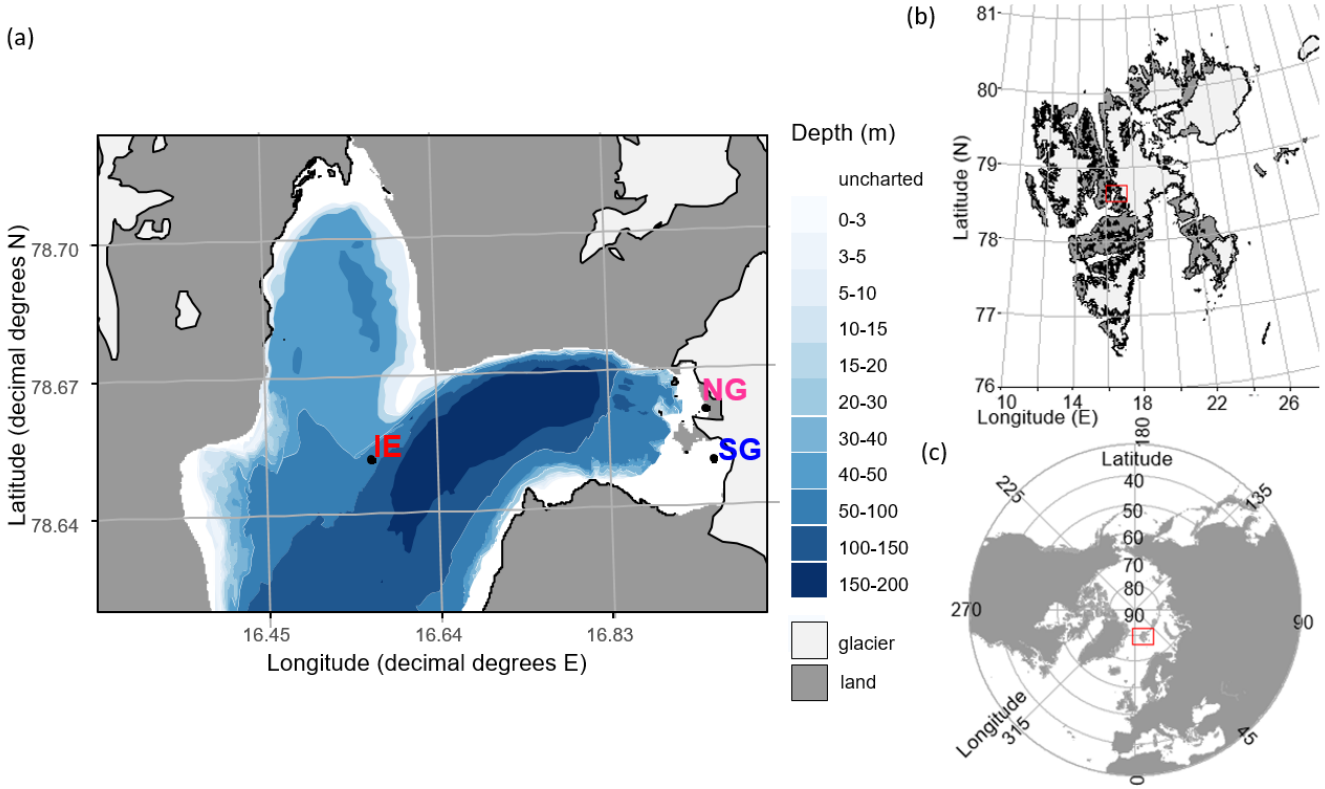

Fig 1. Sampling sites in Billefjorden: a) detailed Billefjorden map showing the stations at the ice edge (IE), north glacier (NG) and south glacier (SG) on the underlying bathymetric map. White areas are uncharted with water depths of about 30 m at NG and SG. The insets to the right show the location of b) Billefjorden on a Svalbard map and of c) Svalbard on a pan-Arctic map, marked with red boxes. Land is shown as dark grey, ocean as white, and glaciers as light grey. All maps were created using the PlotSvalbard R package (Vithakari, 2019). The Svalbard basemap is retrieved from the Norwegian Polar institute (2020, CC BY 4.0 license), the pan-Arctic map is retrieved from Natural Earth (2020, CC Public domain license), and the bathymetric map is retrieved from the Norwegian mapping authority (Kartverket, 2020, CC BY 4.0 license).

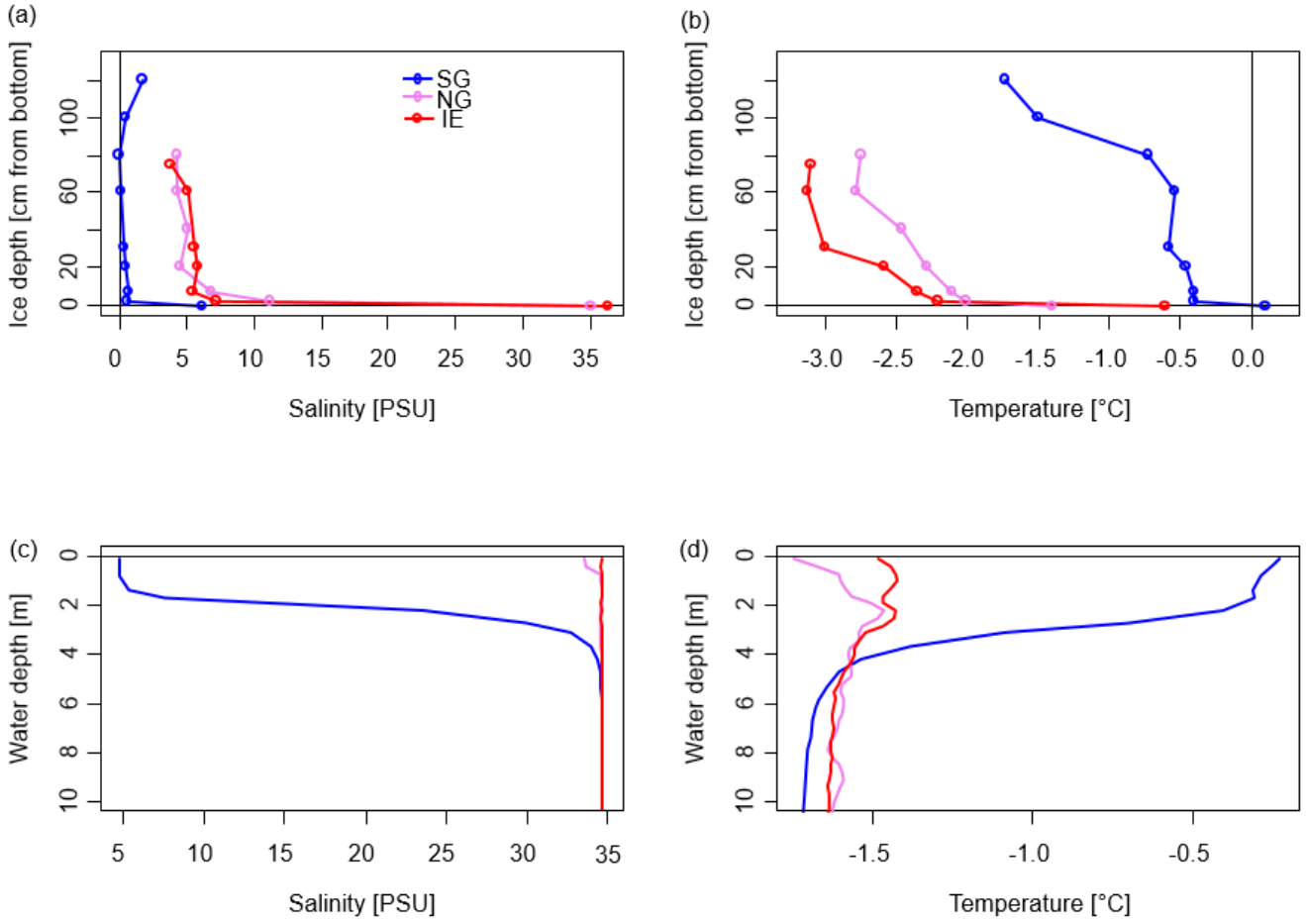

Fig 2. Bulk salinity and temperature profiles in a,b) sea ice cores (0 cm at the bottom) and c,d) the water column down to 10 m, of the three stations.

985

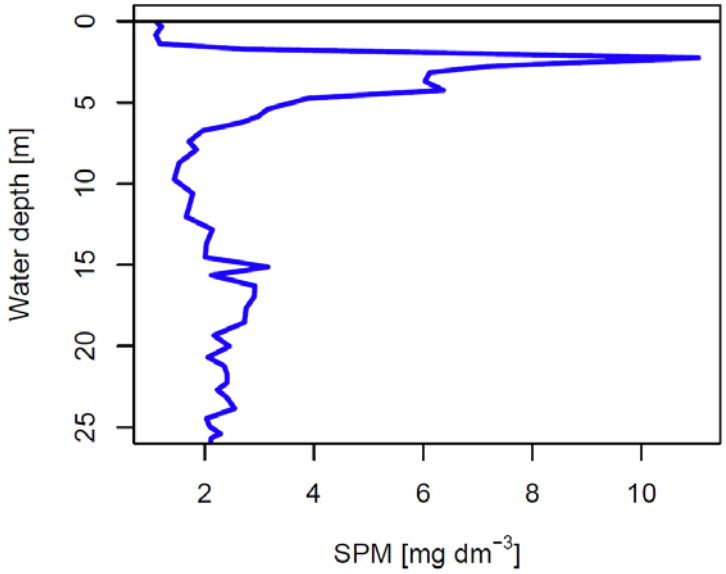

Fig 3. Turbidity profile of the SG station converted to suspended particles

990

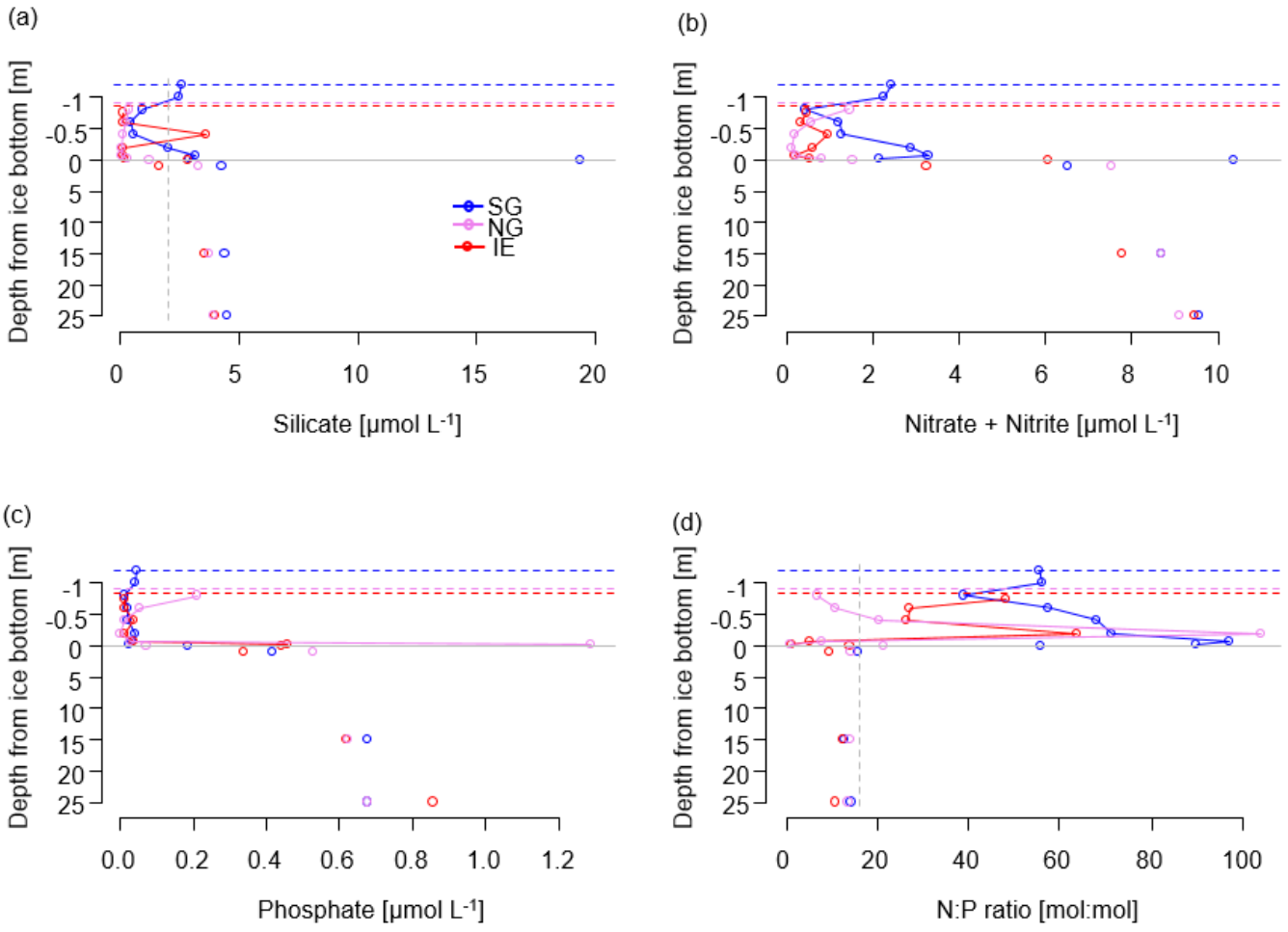

995 Fig 4. Nutrients in the water column (below grey line) and in sea ice (above the grey line) of a) silicate with a suggested threshold for limitation marked as dashed grey line, b) NO_X as nitrate and nitrite, c) phosphate and d) molar N:P ratios with the Redfield threshold of N:P 16:1 marked as dashed grey line indicating potential N limitation. Dashed lines indicate the position of the ice surface, while solid lines show the measured data.

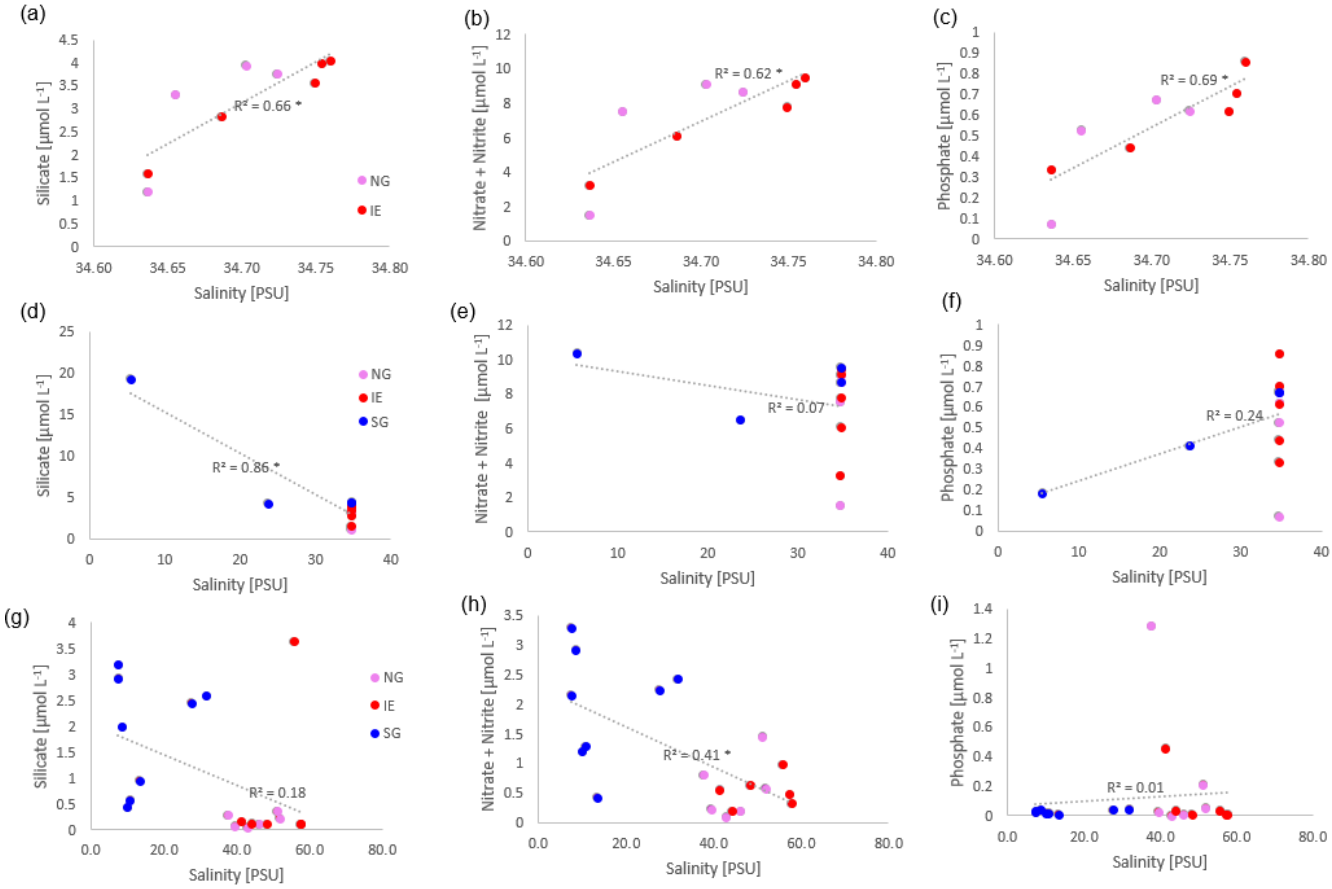

Fig 5. Linear salinity-nutrient correlations of NG and IE water samples (a–c), NG, IE, and SG water stations (d–f) and sea ice samples of NG, IE and SG (g–i). A higher concentration in saline Atlantic water is shown as a positive correlation, a higher concentration in glacial meltwater as a negative correlation. Significant correlations ($p<0.05$) are asterisk marked behind the R^2 value.

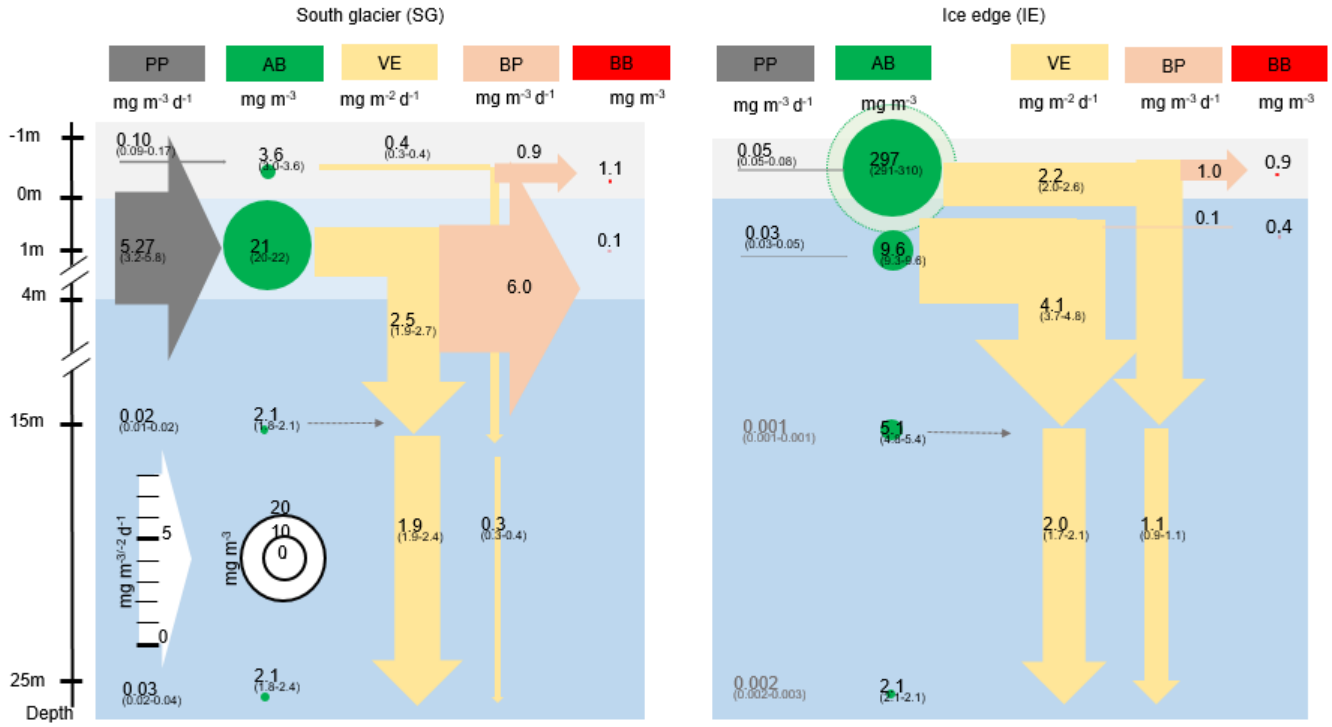

Fig 6. Schematic representation of the C cycle at SG and IE stations. All units are in mg C with the median given in the circles and arrows and the minimum and maximum in brackets below. 0 m depth is at the sea ice water interface. Grey arrows indicate net primary production (PP) with its height scaled to the uptake rates. Green circles show standing stock algae biomass (AB) converted from Chl to C (conversion factor = 30 gC $gChl^{-1}$, Cloern et al., 1995) with its diameter scaled to the concentrations, except sea ice at IE with the light green circle scaled one order of magnitude higher. Yellow arrows indicate vertical export (VE) of chlorophyll converted to C (conversion factor = 30 gC $gChl^{-1}$, Cloern et al., 1995) with the contribution of sea ice algae and phytoplankton estimated by the fraction of typical sea ice algae in phytoplankton net hauls and the width of the arrows scaled to the fluxes. Orange arrows indicate bacterial biomass production (BP) based on dark carbon fixation (conversion factor = 129 gC $gDIC^{-1}$, Molari et al., 2013) with the arrows scaled to the values. Red circles to the right are bacteria biomass (BB) assuming 20 fg C $cell^{-1}$ in the bottom sea ice and UIW. The grey area represents sea ice, the light blue area a brackish water layer and the darker blue area deeper saline water layers.

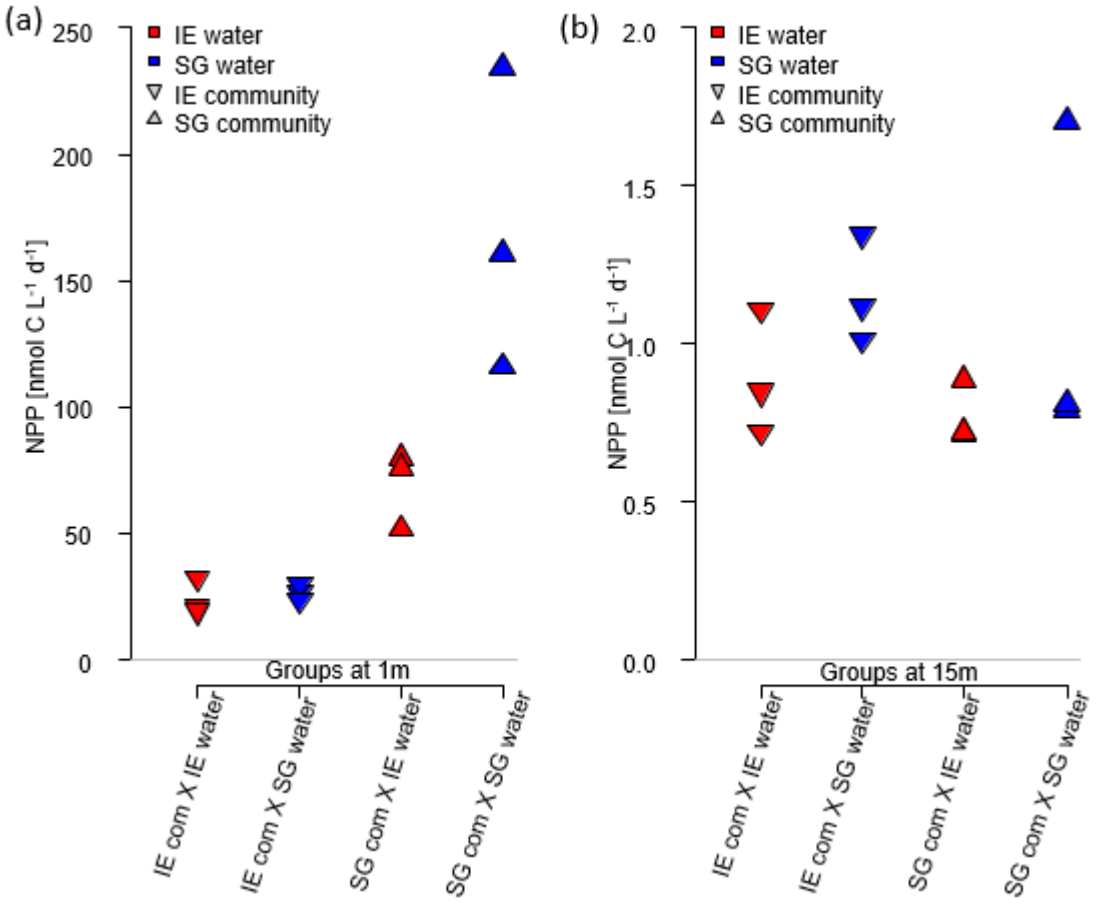

Fig 7. Impact of water source on primary production assessed via a reciprocal transplant experiment. Primary production of IE and SG communities incubated in sterile filtered water originated from either station at a) 1 m and b) 15 m depth. The symbols show the source of the community and the colors indicate the source of the sterile filtered incubation water. The type of incubation water (color) explains the variation in a nested ANOVA with community (symbol) and depth as nested constrained variables and water source (color) as explanatory variable (p=0.0038, F=10.88).

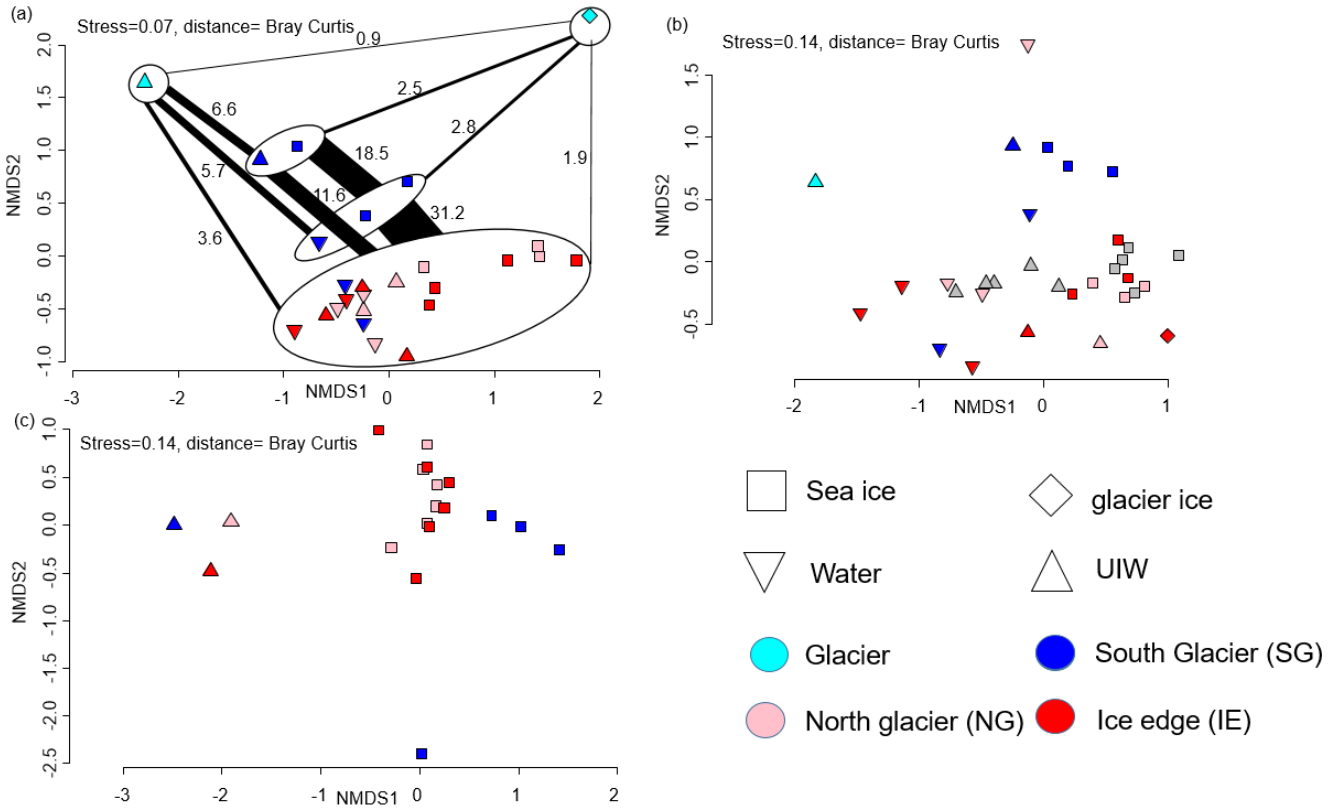

Fig 8. a) NMDS plot of microbial community structure based on 16S data, including samples from April 2018. Groups highlighted in eclipses: glacier ice (top right), glacial outflow (top left), station SG 2019 (top blue), station SG 2018 (bottom blue) and others (bottom). The fraction of shared OTUs (in %) are shown as lines scaled to the fraction [%] of shared OTUs. b) NMDS plot of community structure based on 18S data, including samples from April 2018, c) NMDS plot based on algae abundances in sea ice and UIW based on light microscopic counts.

Tables

Table 1. Properties of the three identified water masses and SG surface water and the estimated contributions of the different water masses based on salinity and different nutrients.

	Surface water		Bottom water		Meltwater		SG 1 m
Salinity [PSU]	34.7		34.7		0	32 %	23.6
Temperature [°C]	-1.4		-1.4		0		-0.4
Silicate [µmol L^{-1}]	1.59	0 %	4.46	84 %	1.79	32 %	4.30
NO_X [µmol L^{-1}]	3.27	10 %	9.57	58 %	2.06	32 %	6.52
Phosphate [µmol L^{-1}]	0.34	20 %	0.67	48 %	0.09	32 %	0.42

Table 2. Integrated standing stock biomass of Chl and fluxes of Chl and C, fractions of the different fluxes and standing stocks, and bacterial production based on dark carbon fixation (DCF).

Variable	SG	IE	Unit
Chl int. in sea ice	0.02	0.40	mg m^{-2}
NPP in bottom sea ice	0.10	0.05	mg C m^{-3} d^{-1}
Chl int. in 25 m water column	3.74	3.75	mg m^{-2}
Vertical Chl flux to 25 m	0.07	0.11	mg Chl m^{-2} d^{-1}
NPP at 1 m	5.27	0.03	mg C m^{-3} d^{-1}
C based NPP int. over 25 m	42.6	0.2	mg C m^{-2} d^{-1}
Estimated Chl production int. over 25 m	1.4	0.0	mg C m^{-2} d^{-1}
mg C fixed per mg Chl	11.4	0.1	mg C mg Chl d^{-1}
NPP as fraction of Chl standing stock	38 %	0.2 %	% Chl renewal d^{-1}
Doubling time	2.63	500	days
Vertical Chl flux as % of Chl standing stock	2 %	3 %	% export of Chl d^{-1}
Vertical Chl flux as % of NPP based Chl prod.	5 %	1375 %	% export of NPP d^{-1}
Loss of Chl from 15 to 25 m	12 %	19 %	Δexp 15m to 25m
Average Chl fraction of (Chl + Phaeo) in 0-3 cm ice	30%	85%	% Chl
Average Chl fraction of (Chl + Phaeo) in water	47 %	50 %	% Chl
Bacteria DCF ice	7.0	7.6	µg C m^{-3} d^{-1}
Bacteria Biomass prod (DCF based) ice	0.9	1.0	mg C m^{-3} d^{-1}
Doubling time	1.2	0.9	days
Bacteria DCF 1 m	46.9	1.1	µg DIC m^{-3} d^{-1}
Bacteria Biomass prod (DCF based) 1m	6.0	0.1	mg C m^{-3} d^{-1}
Doubling time	0.02	2.9	days

Appendix

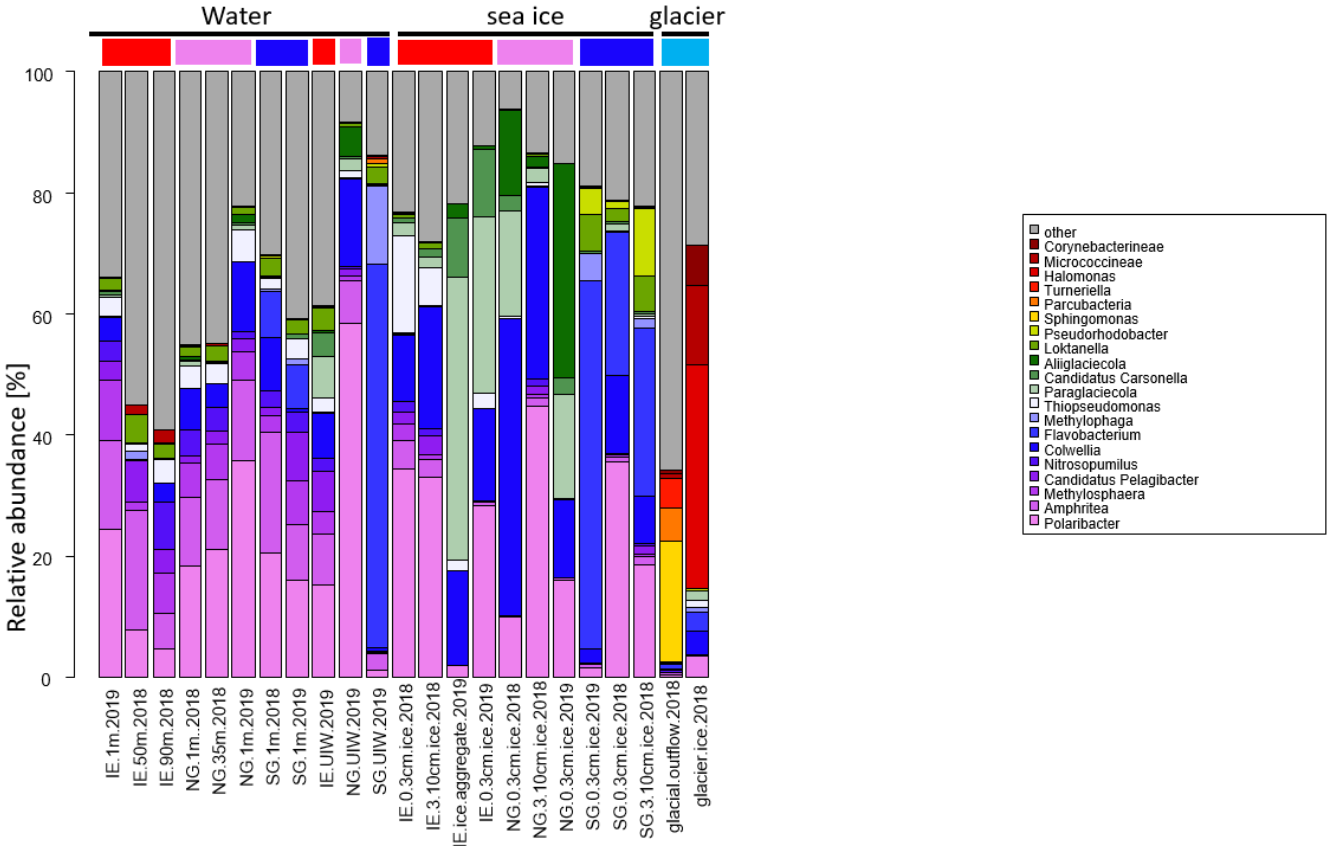

Fig. A1. Community composition of the most abundant genera based on 16S rRNA sequencing data.

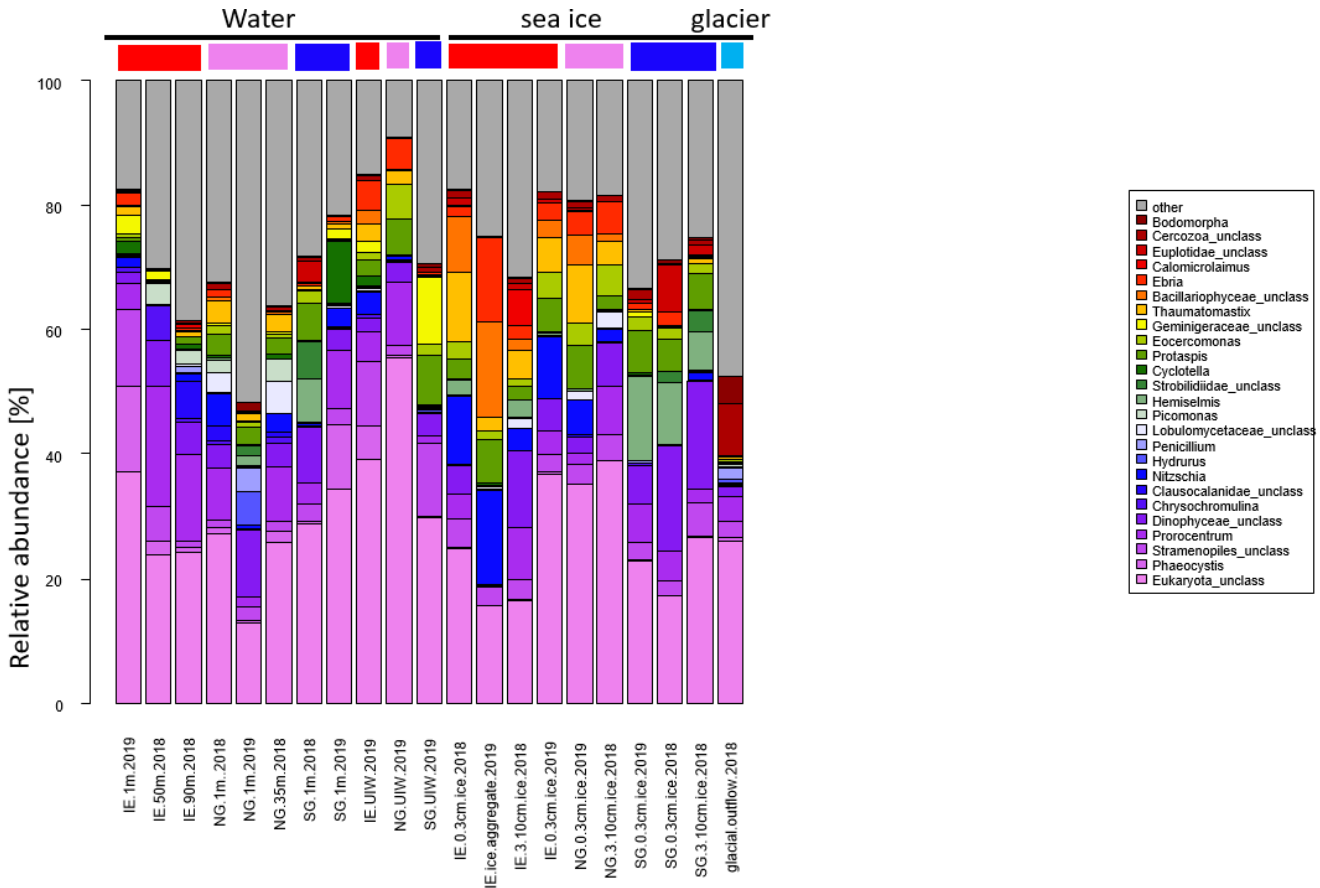

Fig. A2. Community composition based on 18S rRNA sequencing data of the most abundant genera or highest taxonomic level if no related genus has been found.

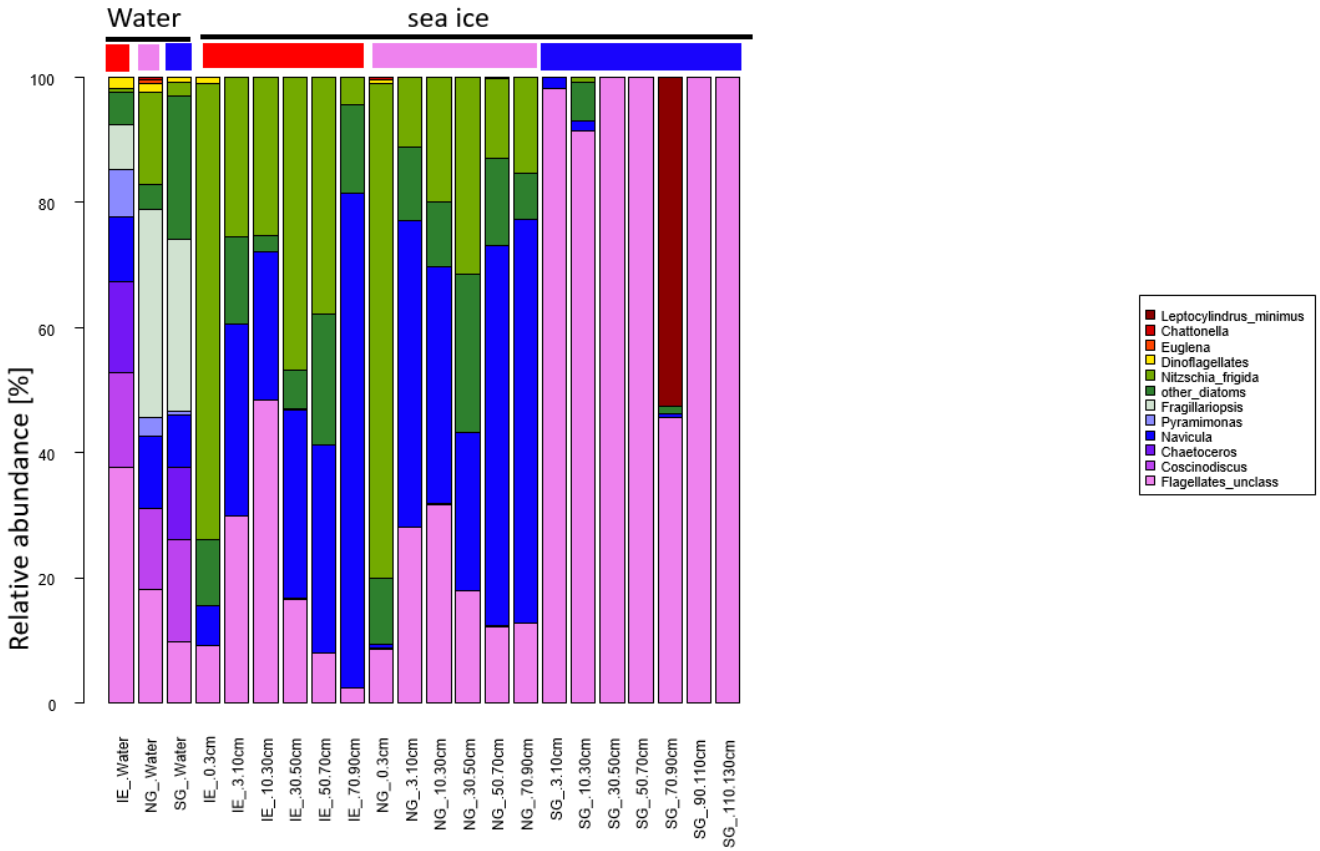

Fig. A3. Sea ice algae and UIW algae community composition of the most abundant taxonomic groups based on light microscopy.

Table B1. Sea ice properties and conversions from bulk salinity and temperature to brine salinity, densities, and brine volume fractions.

Station	Ice core section [cm]	Temp [°C]	Brine Sal [PSU]	Ice density [kg m^{-3}]	Brine density [kg m^{-3}]	Brine volume fraction
SG	0 to 3	-0.4	7.4	917.1	1005.9	7 %
	3 to 10	-0.4	7.4	917.1	1005.9	9 %
	10 to 30	-0.5	8.5	917.1	1006.8	5 %
	30 to 50	-0.6	10.7	917.1	1008.6	3 %
	50 to 70	-0.5	10.0	917.1	1008.0	1 %
	70 to 90	-0.7	13.3	917.1	1010.6	0 %
	90 to 100	-1.5	27.6	917.2	1022.0	1 %
	110 to 130	-1.7	31.7	917.2	1025.4	5 %
NG	0 to 3	-2.0	37.6	917.3	1030.0	28 %
	3 to 10	-2.1	39.4	917.3	1031.6	16 %
	10 to 30	-2.3	42.8	917.3	1034.2	10 %
	30 to 50	-2.5	46.1	917.3	1036.9	10 %
	50 to 70	-2.8	51.8	917.4	1041.4	8 %
	70 to 92	-2.7	51.1	917.4	1040.9	8 %
IE	0 to 3	-2.2	41.3	917.3	1033.1	16 %
	3 to 10	-2.4	44.1	917.3	1035.3	11 %
	10 to 30	-2.6	48.3	917.4	1038.6	11 %
	30 to 50	-3.0	55.6	917.4	1044.5	9 %
	50 to 70	-3.1	57.7	917.4	1046.2	8 %
	70 to 80	-3.1	57.3	917.4	1045.9	6 %

Table B2. Geographic metadata and nutrient concentrations in μmol L^{-1} related to Billefjorden.

Depth	Station	Latitude (N)	Longitude (E)	type	Depth [m]	$Si(OH)_4$ [μmol L^{-1}]	NO_X [μmol L^{-1}]	PO_4 [μmol L^{-1}]	N:P [mol mol^{-1}]
UIW	SG	78°39'03	16°56'44	water	0.01	19.3	10.4	0.19	55.8
1 m	SG	78°39'03	16°56'44	water	1	4.3	6.5	0.42	15.7
15 m	SG	78°39'03	16°56'44	water	15	4.4	8.7	0.68	12.9
25 m	SG	78°39'03	16°56'44	water	25	4.5	9.6	0.67	14.2
UIW	NG	78°39'40	16°56'19	water	0.01	1.2	1.5	0.07	21.4
1 m	NG	78°39'40	16°56'19	water	1	3.3	7.6	0.53	14.3
15 m	NG	78°39'40	16°56'19	water	15	3.8	8.7	0.62	14.0
25 m	NG	78°39'40	16°56'19	water	25	4.0	9.1	0.68	13.5
UIW	IE	78°39'09	16°34'01	water	0.01	2.8	6.1	0.44	13.8
1 m	IE	78°39'09	16°34'01	water	1	1.6	3.3	0.34	9.7
15 m	IE	78°39'09	16°34'01	water	15	3.6	7.8	0.62	12.6
25 m	IE	78°39'09	16°34'01	water	25	4.0	9.5	0.86	11.1
Bot	IE	78°39'09	16°34'01	water	57	4.0	9.1	0.70	13.0
0-3 cm	IE	78°39'09	16°34'01	Sea ice	-1.5	0.2	0.6	0.46	1.2
3-10 cm	IE	78°39'09	16°34'01	Sea ice	-6.50	0.1	0.2	0.04	5.1
10-30 cm	IE	78°39'09	16°34'01	Sea ice	-20	0.1	0.6	0.01	63.5
30-50 cm	IE	78°39'09	16°34'01	Sea ice	-40	3.6	1.0	0.04	26.6
50-70 cm	IE	78°39'09	16°34'01	Sea ice	-60	0.1	0.3	0.01	27.1
70-80 cm	IE	78°39'09	16°34'01	Sea ice	-75	0.1	0.5	0.01	48.1
0-3 cm	NG	78°39'40	16°56'19	Sea ice	-1.5	0.3	0.8	1.29	0.6
3-10 cm	NG	78°39'40	16°56'19	Sea ice	-6.50	0.1	0.2	0.03	7.9
10-30 cm	NG	78°39'40	16°56'19	Sea ice	-20	0.0	0.1	0.00	104.0
30-50 cm	NG	78°39'40	16°56'19	Sea ice	-40	0.1	0.2	0.01	20.3
50-70 cm	NG	78°39'40	16°56'19	Sea ice	-60	0.2	0.6	0.05	10.9
70-90 cm	NG	78°39'40	16°56'19	Sea ice	-80	0.4	1.5	0.21	6.9
0-3 cm	SG	78°39'03	16°56'44	Sea ice	-1.5	2.9	2.2	0.02	89.8
3-10 cm	SG	78°39'03	16°56'44	Sea ice	-6.50	3.2	3.3	0.03	97.1
10-30 cm	SG	78°39'03	16°56'44	Sea ice	-20	2.0	2.9	0.04	71.2
30-50 cm	SG	78°39'03	16°56'44	Sea ice	-40	0.6	1.3	0.02	68.1
50-70 cm	SG	78°39'03	16°56'44	Sea ice	-60	0.4	1.2	0.02	57.6
70-90 cm	SG	78°39'03	16°56'44	Sea ice	-80	0.9	0.4	0.01	38.9
90-110 cm	SG	78°39'03	16°56'44	Sea ice	-100	2.4	2.3	0.04	56.3
110-130 cm	SG	78°39'03	16°56'44	Sea ice	-120	2.6	2.4	0.04	55.4

Table B3. Geographic metadata and nutrient concentrations related to Nordenskiöldbreen.

Date	Stat	Lat (N)	Lon (E)	type	Silicate [µmol L^{-1}]	NO_X [µmol L^{-1}]	Phosphate [µmol L^{-1}]	Nitrite [µmol L^{-1}]	Nitrate [µmol L^{-1}]
09.07.2018	NC	78°38'3	16°59'4	Cryoconite	0.18	0.741	0.597	0.133	0.608
09.07.2018	NC	78°38'3	16°59'4	Cryoconite	0.179	0.555	0.75	0.084	0.471
09.07.2018	NC	78°38'3	16°59'4	Cryoconite	0.066	0.732	0.332	0.069	0.663
09.07.2018	NC	78°38'3	16°59'4	Cryoconite	0.157	0.674	1.281	0.067	0.607
09.07.2018	NC	78°38'3	16°59'4	Cryoconite	0.044	0.681	0.163	0.052	0.629
09.07.2018	NR	78°39'3	16°56'5	Cryoconite	0.323	0.537	0.611	0.311	0.226
09.07.2018	NR	78°39'3	16°56'5	Cryoconite	0.073	0.671	0.201	0.07	0.601
09.07.2018	NR	78°39'3	16°56'5	Cryoconite	0.062	0.361	0.383	0.077	0.284
09.07.2018	NR	78°39'3	16°56'5	Cryoconite	0.146	0.609	0.222	0.113	0.496
09.07.2018	NR	78°39'3	16°56'5	Cryoconite	0.049	0.53	0.26	0.065	0.465
25.04.2018	Out	78°38'2	16°75'2	outflow	1.535	2.304	0.083	0.009	2.295
25.04.2018	Out	78°38'2	16°75'2	outflow	2.047	1.814	0.096	0.013	1.801
25.04.2018	NC	78°38'3	16°59'4	glacier ice	0.085	0.928	0.038	0.008	0.92